UNIVERSITA' DEGLI STUDI DI PADOVA

Sede Amministrativa: Università degli Studi di Padova

Dipartimento di Principi e Impianti di Ingegneria Chimica "I. Sorgato"

SCUOLA DI DOTTORATO DI RICERCA IN BIOLOGIA E MEDICINA DELLA RIGENERAZIONE

INDIRIZZO INGEGNERIA DEI TESSUTI E DEI TRAPIANTI

CICLO XXI

MICROSCALE TISSUE ENGINEERING OF HUMAN SKELETAL AND CARDIAC MUSCLES FOR *IN VITRO* APPLICATIONS

Direttore della Scuola: Ch.mo Prof. Pier Paolo Parnigotto

Supervisore:Ch.mo Prof. Piergiorgio Gamba

Co-supervisore: Prof. Nicola Elvassore

Prof. Gordana Vunjak-Novakovic

Dottorando: Elena Serena

2 Febbraio 2009

Table of contents

Sommario

L'utilizzo di tessuti ingegnerizzati come modelli *in vitro* è recentemente emerso come applicazione alternativa al loro tradizionale impianto *in vivo*. Lo sviluppo di nuovi farmaci e terapie, nel caso di malattie quali la Distrofia Muscolare di Duchenne (DMD) o l'infarto miocardico (HF), sono infatti fortemente limitati e rallentati della mancanza di adeguati modelli *in vitro*: rappresentativi del tessuto umano e delle sue proprietà funzionali, di semplice utilizzo ed accessibili economicamente. Prerequisiti necessari all'ottenimento di un modello che risponda a tali esigenze sono: l'utilizzo di una fonte cellulare umana primaria; l'impiego di tecniche micrometriche, in primo luogo per il fine controllo del microambiente e del conseguente differenziamento cellulare in tessuto funzionale e per la riduzione dei costi di ricerca. Lo sviluppo su microscala permette inoltre di effettuare sperimentazioni multiparametriche, essenziali per patologie multifattoriali quali DMD e HF, con un elevato numero di dati in uscita. Infine, l'utilizzo di metodologie e tecniche semplici permette il trasferimento tra laboratori e ricercatori di diversa formazione. Lo scopo di questa tesi è stato quindi l'ottenimento di tessuti umani funzionali di muscolo scheletrico e cardiaco mediante l'utilizzo di tecniche di microscala, al fine di soddisfare le attuali esigenze di ricerca. È stato utilizzato un approccio biomimetico e multidisciplinare: un'accurata ingegnerizzazione del microambiente cellulare ha permesso di riprodurre *in vitro* i principali stimoli che *in vivo* guidano la differenziazione cellulare, così da ottenere un tessuto funzionale e rappresentativo del tessuto naturale. Le metodologie classiche dell'ingegneria dei tessuti sono state accoppiate ad innovative tecnologie di microscala, precedentemente sviluppate dagli ingegneri del laboratorio, per il preciso controllo dell'ambiente cellulare a livello micrometrico. In particolare sono state ottimizzate le proprietà chimico-fisiche del substrato, l'organizzazione topologica delle colture e l'applicazione di stimolazione elettrica esogena. Tali sistemi sono stati utilizzati con colture di particolare interesse quali mioblasti umani distrofici e cellule staminali embrionali umane (hESC). L'analisi funzionale del tessuto scheletrico umano così ottenuto, sia distrofico che sano, ha evidenziato come i sistemi sviluppati siano in grado di indurre un processo differenziativo più rapido rispetto ai tradizionali metodi di coltura. È stato valutato l'effetto di stimolazioni elettriche esogene sul differenziamento cardiomiocitario di hESC ed è stato sviluppato un array di cardiomiociti umani contrattili. Tali risultati aprono promettenti prospettive per lo sviluppo di modelli *in vitro* che permettano lo screening preclinico di nuovi farmaci o nuove terapie per la cura delle patologie a carico della muscolatura scheletrica e cardiaca.

Introduzione

Le malattie a carico dell'apparto muscolare, sia scheletrico che cardiaco, sono numerose e in molti casi prima invalidanti e successivamente letali.
Nel caso della Distrofia Muscolare di Duchenne, una malattia genetica con elevata incidenza, la degenerazione muscolare causata dall'assenza della distrofina costringe i pazienti sulla sedia a rotelle attorno ai 10 anni e progressivamente alla morte attorno ai 20. Nonostante la causa molecolare sia conosciuta e studiata da tempo, non esiste ancora una terapia efficace; la somministrazione di corticosteroidi permette solo il rallentamento del decorso della patologia.
Le malattie cardiovascolari sono la principale causa di morte della società occidentale. In seguito ad un infarto, il miocardio subisce un danno più o meno esteso con conseguente morte dei cardiomiociti e formazione di tessuto fibroso, determinando una parziale perdita di funzionalità del muscolo cardiaco. Il graduale assottigliamento della parete muscolare causa l'insorgenza di un'insufficienza cardiaca cronica, che attualmente è curata in modo efficace solo tramite trapianto.
Il ritardo nello sviluppo di farmaci e terapie efficaci è da imputarsi in parte alla complessità del tessuto muscolare striato e al carattere multifattoriale di simili patologie ed in parte agli elevati costi di tali processi di ricerca. Attualmente, infatti, gli unici modelli disponibili sono colture cellulari *in vitro* e modelli animali *in vivo*. Le prime sono un modello semplice, economico e che permette di avere risposte immediate, ma sono poco rappresentativi del complesso ambiente cellulare *in vivo*. I secondi sono una buona approssimazione delle risposte di un organismo complesso, ma non rappresentano fedelmente la fisio-patologia umana e la loro gestione richiede tempi e costi elevati.
In questo contesto, lo sviluppo di nuovi modelli di studio *in vitro* è un bisogno urgente per il progresso scientifico negli ambiti farmaceutico e clinico. L'obiettivo da perseguire è l'ottenimento di una modello che coniughi la semplicità e rapidità delle colture cellulari *in vitro* e sia rappresentativo della fisiopatologia di un organismo complesso, al pari dei modelli animali *in vivo*. Le metodologie sviluppate dall'ingegneria dei tessuti costituiscono la base ottimale per l'ottenimento di un tale modello *in vitro*, in quanto l'obiettivo di tale disciplina è la riproduzione fedele del tessuto nativo. Ad esse, è necessario abbinare due prerequisiti: il modello deve essere rappresentativo della fisiologia umana, quindi il materiale di partenza deve essere tale, e la scala di sviluppo deve essere micrometrica, così da abbattere costi e

tempi di ricerca. Da queste necessità nasce l'ingegneria dei tessuti su microscala, approccio utilizzato in questo lavoro di tesi, con l'obiettivo di sviluppare tessuto muscolare scheletrico e cardiaco funzionale che possa fungere da modello *in vitro*. Obiettivo che è stato perseguito attraverso la riproduzione *in vitro* dei principali stimoli che *in vivo* guidano il differenziamento in tessuto muscolare striato.

Tale lavoro ha carattere estremamente multidisciplinare: lo studio è stato infatti svolto con la stretta collaborazione di ingegneri, i quali hanno sviluppato innovative tecnologie per la coltura cellulare, in seguito accoppiate alla coltura di cellule umane di alto valore clinico, quali mioblasti umani primari distrofici e cellule staminali embrionali umane.

Obiettivi specifici sono stati: 1) lo sviluppo di miotubi (l'unità fondamentale del muscolo scheletrico) umani sani e distrofici con proprietà funzionali rappresentative del muscolo scheletrico ed esprimenti la proteina coinvolta nelle distrofie muscolari, la distrofina; 2) l'ottenimento di cardiomiociti (il tipo cellulare responsabile della contrazione cardiaca) umani funzionali da cellule staminali embrionali umane, una delle poche fonti cellulari disponibili e la più promettente per un efficace utilizzo clinico; 3) la valutazione della possibilità di accoppiare i tessuti ingegnerizzati ai punti (1) e (2) a tecniche microfluidiche per lo sviluppo di una piattaforma per screening farmacologici o lo sviluppo di nuove terapie.

La tesi quindi si articola su due argomenti principali: lo sviluppo *in vitro* di muscolo scheletrico e di muscolo cardiaco. Ha come corollario 5 articoli riportati come appendici, che costituiscono il principale risultato di questo lavoro di dottorato.

La progressione del lavoro è stato schematizzato in figura 1, per il muscolo scheletrico, e in figura 2, per quanto concerne il muscolo cardiaco. Nelle figure 1 e 2 sono stati marcati in nero gli obiettivi effettivamente ottenuti nel corso di questa tesi, in grigio chiaro sono invece state indicate le prospettive future individuate nel corso del lavoro di ricerca.

Le fasi che compongono l'ottenimento di un modello *in vitro* di muscolo scheletrico sono: l'espansione di mioblasti umani primari; il loro successivo differenziamento in tessuto bidimensionale (2D); lo sviluppo di proprietà funzionali, quali la contrattilità e il signaling del calcio; lo sviluppo del tessuto in tre dimensioni (3D) e quindi l'ottenimento di un modello *in vitro*.

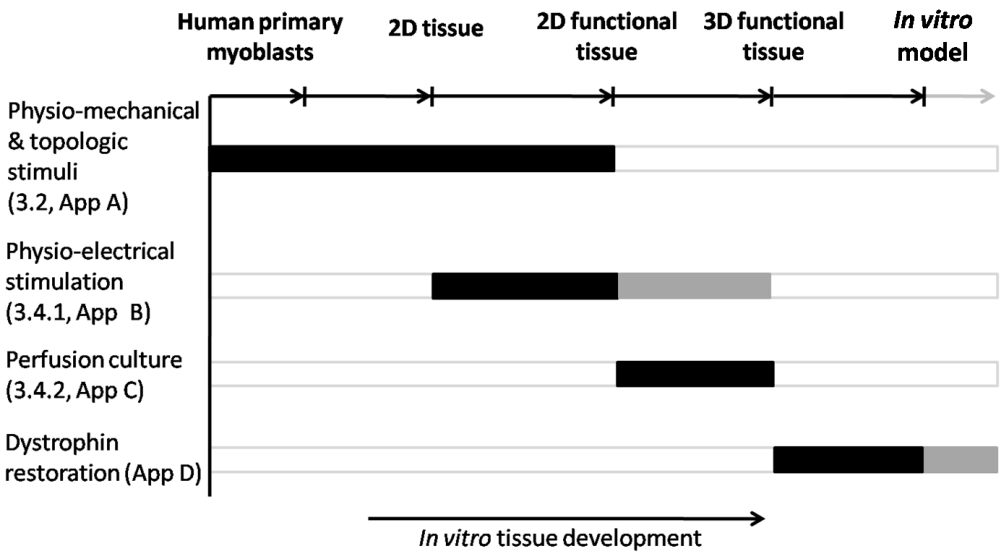

Figure 1. Rappresentazione schematica delle fasi seguite in questo lavoro di tesi per lo sviluppo *in vitro* di muscolo scheletrico umano. In nero sono riportati i risultati effettivamente ottenuti, mentre in grigio le prospettive future individuate nel corso del lavoro.

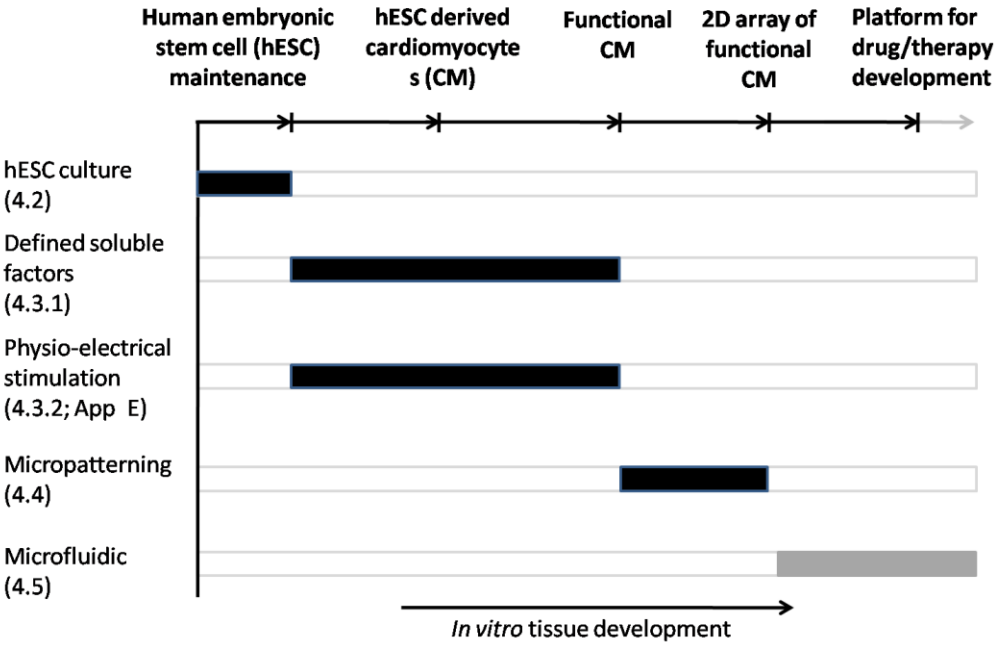

Figure 2. Rappresentazione schematica delle fasi seguite in questo lavoro di tesi per lo sviluppo *in vitro* di muscolo cardiaco umano. In nero sono riportati i risultati effettivamente ottenuti, mentre in grigio le prospettive future individuate nel corso del lavoro.

La fase primaria per lo sviluppo di muscolo cardiaco è la coltura e l'espansione di cellule staminali embrionali umane, che sono state scelte come fonte cellulare per la loro elevata capacità proliferativa e differenziativa. Successivamente, cardiomiociti

con proprietà funzionali (contrattili) sono stati impiegati nello sviluppo di un array bidimensionale, che possa essere facilmente accoppiato ad una piattaforma microfluidica per screening farmacologici e di nuove terapie.

Questa tesi di dottorato è quindi organizzata come segue:
Il Capitolo 1 descrive le limitazioni degli attuali modelli di studio *in vitro* per muscolo scheletrico e cardiaco e i possibili vantaggi derivanti dall'utilizzo dei metodi dell'ingegneria tissutale su scala micrometrica.

Il Capitolo 2 è incentrato sulla descrizione dell'approccio biomimetico utilizzato nel guidare il differenziamento cellulare. Tale approccio è fondato sull'applicazione di tecniche di microscala, di cui viene illustrato brevemente lo stato dell'arte e le metodologie utilizzate. Le metodologie dettagliate sono riportate nelle appendici A, B, E.

Il Capitolo 3 presenta i risultati conseguiti nell'ingegnerizzazione di muscolo scheletrico umano, sano e affetto da Distrofia Muscolare di Duchenne. Sono brevemente illustrate le principali caratteristiche morfologiche, strutturali e fisiologiche di tale tessuto *in vivo*. Sulla base delle proprietà funzionali e morfologiche del tessuto ottenuto *in vitro* viene discusso il suo possibile utilizzo come modello per screening farmacologici e sviluppo di nuove terapie cliniche. Vengono inoltre illustrate alcune strategie per promuoverne ulteriormente il differenziamento funzionale, tecniche già state utilizzate con successo su cellule muscolari non umane e i cui risultati sono riportati nelle appendici A-C.

Il Capitolo 4 tratta i risultati ottenuti in merito allo sviluppo di muscolo cardiaco. Sono brevemente illustrate le principali caratteristiche morfologiche, strutturali e fisiologiche del miocardio umano *in vivo* e le possibili strategie rigenerative. I risultati ottenuti nella coltura, espansione e differenziazione in senso cardiomiocitario di cellule staminali embrionali umane, la più promettente fonte di cardiomiociti umani, sono descritte. Inoltre sono illustrati i risultati ottenuti nello sviluppo di un array di cardiomiociti contrattili umani *in vitro*. In appendice E è riportato il testo completo riguardante il controllo differenziativo tramite stimolazione elettrica; mentre in appendice F si riporta uno spaccato sull'utilizzo di staminali embrionali umane nel contesto italiano.

Il Capitolo 5 riassume le conclusioni e delinea le prospettive di sviluppo della ricerca a breve e lungo termine.

Summary

Recently, engineered tissues have found an alternative application as *in vitro* models. They will never be implanted directly into patients, but will instead be used to transform the way we study human tissue physiology and pathophysiology *in vitro*. The development of new drugs and therapies for diseases such as Duchenne Muscular Dystrophy or myocardium failure is greatly slowed and hindered by the lack of adequate *in vitro* models, which should be functional, representative of human tissue, easy to use and economic. Therefore the requirements are the use of a human cell source; working at the microscale, in order to reproduce with high precision the cell microenvironment and to guide cell differentiation correctly. The microscale gives the additional possibility of developing micrometric array of cells which can be coupled to microfluidic platforms for highthroughput experiments, which are fundamental for multifactorial diseases such as DMD and HF. Moreover the use of easy methodologies and simple techniques allowed the use of the model by researchers with different background and skills. In this scenario, the aim of this thesis is the obtainment of human functional skeletal and cardiac tissues, through the application of innovative microscale techniques to standard cell culture devices. The strategy employed is biomimetic and multidisciplinary: the cell culture microenvironment has been engineered in order to reproduce *in vitro* the major stimuli that guide muscle cell differentiation *in vivo*. The coupling of tools and methodologies of the tissue engineering with innovative microscale technologies developed by engineers of the laboratory has led to a precise control of the cell microenvironment. In particular, the chemical-physical properties of the substrates, the topologic organization of cells and the application of exogenous electrical stimuli were optimized during this work. The developed devices were used with cell culture of particular interest, such as human primary dystrophic myoblasts and human embryonic stem cells (hESC). The functional analysis of the obtained skeletal muscle tissue, both dystrophic and healthy, highlighted a more rapid differentiation process of myoblasts cultured with the innovative techniques in comparison to standard cell culture systems. Electrical stimulation was applied to hESC in order to favor the cardiac differentiation pathway and an array of human beating cardiomyocytes has been developed.Taken together these results open new promising prospective for the development of *in vitro* model for preclinical trials of drugs or therapies for the treatment of pathologies of skeletal and cardiac muscles.

Foreword

Suring this thesis, I could apply engineering tools to my educational biological background, thus having the possibility to explore new and exciting frontiers. Being an industrial biotechnologist, I believe I found the suitable multidisciplinary laboratory for my educational training. I would like to thank here my supervisor Prof. Gamba, and co-supervisors, Prof. Elvassore, for giving me this chance while always believing in me, and Prof. Vunjak-Novakovic, for the experience abroad.

The author is grateful to Ministero Italiana dell'Università e della Ricerca (MIUR), Università di Padova, Regione Veneto for Azione Biotech II and III, Città della Speranza and Telethon for the financial support to the research activity and to Columbia University for the financial support of the research activity abroad.

During of the period of the PhD program the following publications have been produced:

1. E. Cimetta, S. Pizzato, E. Serena, S. Bollini, P. De Coppi, N. Elvassore. "Production of arrays of cardiac and skeletal muscle myofibers by micropatterning techniques on a soft substrate". Biomed Microdevices. 2008 Nov 6. DOI 10.1007/s10544-008-9245-9.

2. E. Cimetta, M. Flaibani, M. Mella, E. Serena, L. Boldrin, P. De Coppi, N. Elvassore. "Enhancement of viability of muscle precursor cells on 3D scaffols in a perfusion bioreactor". Int J Artif Organs, 2007, 30(4):220-26.

3. E. Serena, M. Flaibani, S. Carnio, L. Boldrin, L. Vitello, P. De Coppi, N. Elvassore. "Electrophysiological stimulation improves myogenic potential of muscle precursor cells grown in a 3D collagen scaffold". Neurological Research, 2008, 30 (2): 207-214.

4. E. Serena, E. Figallo, N. Tandon, S. Gerecht-Nir, C. Cannizzaro, N. Elvassore, G. Vunjak-Novakovic. "Electrical stimulation and cardiac differentiation of human Embryonic Stem Cells" (to be submitted).

5. E. Serena, E. Cimetta and M. Zagallo. "Financing for research on embryonic stem cells: The situation in Italy and its origins" Report on 3rd Italian National Congress of the Group of Italian Researchers on Embryonic Stem Cells (IES Group) Rome, 1st July 2008. Notizie di Politeia. Rivista di Etica e Scelte Pubbliche" Vol. 91/Anno XXIV, 2008, pp. 110-113.

Numerous abstracts were submitted to several international conferences during the PhD program, including: Biomedical Engineering Society (BMES), Tissue & Cell Engineering Society (TERMIS-EU), International Society for Stem Cell Research (ISSCR).

Introduction

Skeletal and cardiac muscles suffer from a variety of pathologies, which are invalidating or, in the worst case scenario, lethal.

The Duchenne Muscular Dystrophy (DMD) is a genetic disease with high incidence, causing muscle degeneration due to the absence of dystrophin. Patients are limited to wheelchair mobility by 9–12 y of age, and death by the late teens or 20s. Although the molecular defect causing DMD has been identified decades ago, an efficient therapy doesn't exist yet; the administration of corticosteroids has the mere effect of delaying the progression of the disease. Cardiovascular diseases are the major cause of death of the western society. When heart muscle is damaged by injury such as a heart failure (HF), heart muscle cells, known as cardiomyocytes, die. The following instauration of an inflammatory state leads to the remodeling of functional contracting tissue, which is replaced with nonfunctional scar tissues. This process diminishes the heart pumping ability and is efficaciously treated only by heart transplantation.

The delay in developing new drugs and therapies is in part due to the high complexity of striated muscles and the multifactorial nature of these diseases and in part to the elevated cost and time incurred in the development processes. In fact, the actual available models for these processes are *in vitro* cell culture and animal models for *in vivo* studies. The former are an easy, rapid and economic model, but they are not representative of *in vivo* complex network of signaling and stimuli. The latter are a good approximation of the response of a complex organism, but they are not representative of the human pato-physiology. In addition, the *in vivo* experimentation is highly time and money demanding and requires the operators to be trained. In this scenario, the development of new *in vitro* models is an emerging issue for the scientific progress both in pharmaceutical and clinical fields.

The required model should couple the simplicity and rapidity of *in vitro* cell culture and the correct representation of a complex organism, such *in vivo* models do. The tools and methodologies developed by tissue engineering constitute optimal landmarks for the development of such a model, since this field always aimed at reproducing *in vitro* the *in vivo* complexity of a tissue. Two additional prerequisites

are required: the cell source should be human, in order to be representative of the human biology, and the developed tissue should be micrometric and highthroughput, in order to lower costs and time respectively.
From these needs developed the concept of "microscale tissue engineering", which is the approach used in this thesis for the development of human skeletal and cardiac tissues *in vitro*. The culture substrate have been engineered reproducing the main stimuli that *in vivo* guide the formation of striated muscles.
This thesis has a highly multidisciplinary nature: the tight collaboration with engineers of the laboratory, whose designed and developed the miscroscale technologies used in this thesis, allowed the application of innovative devices to the culture of relevant cells, such as human primary dystrophic myoblasts and human embryonic stem cells.
Specific aims of this thesis are: 1) the development of human functional myotubes (the fundamental unit of skeletal muscles), both healthy and dystrophic, representative of the human tissue and expressing the key protein of muscular dystrophies, dystrophin; 2) the derivation of functional cardiomyocytes (the cells of the myocardium) from human embryonic stem cells, which is the most promising cell source in sight of clinical applications; 3) exploring the feasibility of coupling the engineered skeletal and cardiac tissues with microfluidics techniques for the development of pharmacological screening and new therapies.
Two are the main themes of the thesis: the in vitro development of skeletal and cardiac muscles. The thesis is based on 5 papers, which constitute the main outcome of the Ph.D. study and are reported in Appendix.
The progression of the work is represented in the schematic figure 1, for skeletal muscle, and figure 2, for cardiac muscle. In these figures, the results obtained are marked in black, while light grey indicates the identified future perspectives.
The main steps for the obtainment of a skeletal muscle *in vitro* are: the expansion of human primary myoblasts; their differentiation in a bi-dimensional (2D) tissue; the following acquisition of functional properties, such as contractility and calcium release and uptake; the development of a three-dimensional (3D) tissue and the obtainment of an *in vitro* model (Fig. 1).
Concerning the development of cardiac muscle (Fig. 2), the first critical step is the culture and expansion of human embryonic stem cells (hESC), chosen as cell source for their high proliferation and differentiation capacity. The following phase is the control over hESC differentiation towards the cardiac lineage and the obtainment of human functional cardiomyocytes. The final stage is the

development of a bi-dimensional array of cardiomyocytes, easily coupled with microfluidic platform for the development of drug screenings and new therapies.

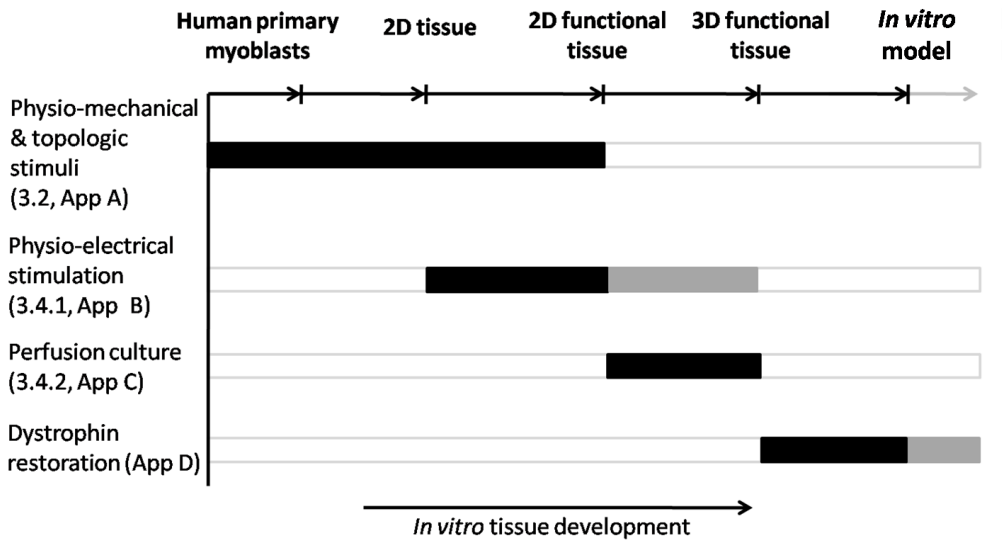

Figure 1. Schematic representation of the main phases of this PhD research, for the development of an *in vitro* model of human skeletal muscle Black bars show the results obtained in this work, while the light grey gives the future perspectives.

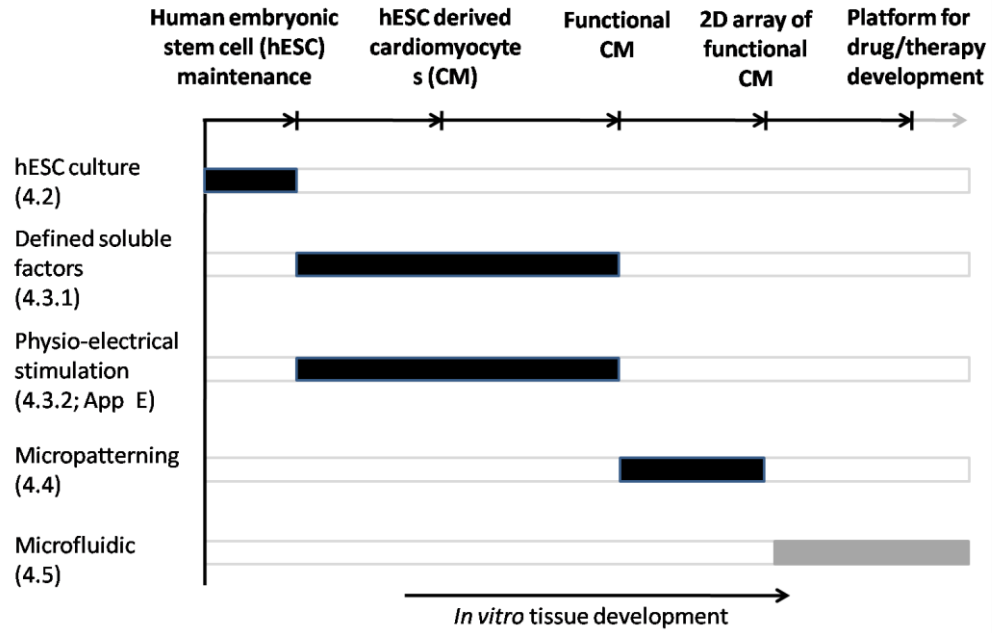

Figure 2. Schematic representation of the main phases of this PhD research, for the development of an *in vitro* model of human cardiac muscle. Black bars show the results obtained in this work, while the light grey gives the future perspectives.

The thesis is organized as follows:
Chapter 1 reviews the actual *in vitro* models available and their limitations. It introduces the concept of microscale tissue engineering and its contribution to the development of new *in vitro* model.

Chapter 2 focuses on the description of the biomimetic approach used in the development of skeletal and cardiac muscles. The state of the art and methodologies of the microscale techniques applied are reported. Complete and detailed protocols are reported in appendix A-C

Chapter 3 illustrates the results obtained in the engineering of human skeletal muscle, both healthy and affected by Duchenne Muscular Dystrophy. The morphological and physiological properties of the obtained tissue are showed and the possibility of using it as an *in vitro* model for drug screening and new therapy development is discussed. In addition, some possible strategies for improving its differentiation degree are introduced. Such strategies were already applied to murine muscle cells and this results are reported in appendix A-C.

Chapter 4 deals with the results obtained with cardiac muscle. A brief introduction on myocardium morphology and physiology and its regeneration is given. Follows an introduction on human embryonic stem cells (hESC) and two methodologies applied for the induction of their differentiation in cardiomyocytes. Such cells are then used for the development of a bi-dimensional array of human beating cardiomyocytes. In appendix D is reported the complete manuscript describing the effects of electrical stimulation on cardiomyogenesis of hESC; and in appendix E is reported the point of view of Italians researchers working on hESC.

Chapter 5 presents the conclusions of the thesis project and discusses the future perspective and the vast possibilities opened by the application of engineering tools to cell biology.

Chapter 1

Tissue engineering for the development of *in vitro* models

This chapter introduces the concept of microscale tissue engineering, outlining on the clinical and scientific motivations of the present work. The state of the art of skeletal and cardiac muscle tissue engineering are reported, since they constitute the basis of this work. Alternative and innovative approaches for the development of *in vitro* skeletal and cardiac functional tissues are presented.

1.1 Skeletal and cardiac muscle diseases

Skeletal muscles represent the largest tissue mass in the body and are responsible for its voluntary movements. Cardiac muscle tissue plays the most important role in heart contractions and rhythmical beating, causing the circulation of the blood throughout the body. Both these tissues, holding fundamental functions, are subjected to several pathological conditions or external events that cause the loss of their functionality. Skeletal muscles may be injured by exposure to myotoxic agents (bupivacaine or lidocaine), sharp or blunt trauma (punctures or contusions). Traumatic injury, aggressive tumor ablation and prolonged denervation are common clinical situations that often result in significant loss of skeletal muscle tissue requiring subsequent surgical reconstruction[1]. This tissue is also affected by several primary myopathies, which are characterized by a progressive wasting of the tissue

that leads to deterioration of movements and, in the most severe cases, such as in Duchenne's Muscular Dystrophy (DMD), to complete paralysis and death. Concerning cardiac tissue, cardiovascular diseases (CVD) is a major health problem and the leading cause of death in the Western world[2]. Mortality data for 2006 show that CVD accounted for 1 of every 2.9 deaths in the United States[3]. In Europe, the estimated frequency of Heart Failure (HF) patients range between 6–10% in the population >65 years of age[4]. HF is responsible for a large number of prolonged and recurrent hospitalizations, representing 1–2% of global health care costs[5]. In general, when heart muscle is damaged by injury, cardiomyocytes (the cell of cardiac muscle) die and functional contracting tissue is replaced with nonfunctional scar tissues, diminishing heart pumping ability.

Referring in particular to DMD and HF, no effective therapies are available at present. DMD patients are essentially treated with anti-inflammatory molecules, such as corticosteroids[6] and deflazacort[7], which have the only benefit to delay the disease. Possible alternative treatment are gene- and cell-therapies[8]: several vectors (plasmid DNA and DNA–RNA chimeric oligonucleotides[9], adenoviral vectors[10], adeno-associated viral vectors[11]) and cell types (multipotent adult progenitors[12], mesoangioblasts[13], muscle-derived stem cells[14] human embryonic stem cells[15]) has been tested for restoring dystrophin expression in DMD patients with some promising results. Heart transplantation is the only successful and definitive treatment for heart failure, but it is hampered by a severe shortage of organs donors and rejection[16]. Alternative treatments are pharmacological therapies[17], cell-based myocardial regeneration[2,18], or the use of mechanical cardiac support[19]. The pharmacological therapies for HF (diuretics, inotropes, vasolidators, ACE inhibitors, β-blockers and antiarrythmic drugs) have demonstrated to reduce the patient mortality, relieving and stabilizing symptoms and preventing the progression of myocardial dysfunction[20]. Myocardial regeneration with cell-based therapies has been largely investigated using numerous cell types, delivery systems, and strategies, but many obstacles (attaining sufficient distribution and fusion of donor cells with host tissue, extending the donor cardiomyocytes survival period after transplantation, and eliminating the immune response) must be overcome before it

becomes a suitable therapeutic approach. Mechanical circulatory support devices, such as left ventricular assist devices, are currently used as a bridge to cardiac transplantation, but thromobogenicity, device size and weight, and power transmission are current limitations of these support devices[19].

1.2 Current limitations: needs for new models

Despite the intense research conducted over the last decades on the development of an effective therapy for DMD or an alternative treatment to cardiac transplantation, a clinically relevant result has not been obtained yet. Besides, as discussed above, the existing therapies have the only effect of delaying the disease progression or are merely used as a bridge to organ transplantation. For instance, two decades have past since the identification of the molecular defect involved in DMD, but there are still no effective cures to significantly alter the relentless progression of the disease. On the other hand, costs and time for the development of new drugs and therapies is exponentially increased over the last few years[21] (~US$1 billion per-compound cost of developing new drugs)[22].

Another consideration to take in account is that the development of therapeutic strategies, effective in blocking the progressive and multifactorial nature of disease such as muscular dystrophy and myocardial degeneration, may only be achieved through a combination of different approaches. Such studies, assessing the potential beneficial impact of multiple strategies combined into a single preclinical trial, can be an enormous challenge if pursuit with the actual standard methodology and technology available: assay based on human cell model and disease animal models. The former, human cell−based testing, has proven to be a valuable tool to quickly explore toxic and non functional compounds. The low−cost and high−speed testing of compounds in cell culture, and the obvious advantages of using intact cells as a first representation of the living patients, would make the cell−based testing a key component on therapy discovery programs. However, many individuals in the industry and academic community would argue that cell models may give unsatisfactory, misleading and non−predictive data for the actual response of a

complex functional tissue. The principal component of this failure is the quality of the cell culture conditions *in vitro*, such as the lack of structural and topological cues, the different mechanical and chemical properties of the substrate used *in vitro* or the unpredictable spatio−temporal combination of different soluble factors in conventional cell culture systems[23,24]. It has thus been argued that we need a new generation of *in vitro* culture systems that would be "something between a Petri dish and a mouse," to authentically represent a cell's environment in a living organism and be more predictive of *in vivo* systems[25].

On the other hand, animal model based assays show three main limitations. First, animal models cannot reliably predict human biology; even if a model can be predictive of human target biology, it cannot predict human drug biology or therapy response. Second, therapies that looked promising in animal models have repeatedly yielded disappointing results in clinical trials[26]. Third, *in vivo* experimentations require elevated operative time and costs for animal care.

In this scenario, there is a great need for new and alternative models for *in vitro* studies and research, suitable for conducting low cost pre-clinical trials and more representative of the human cell behavior. It would be of paramount importance to develop a human *in vitro* tissue which should: 1) provide robust and reproducible biological and physiological functional data representative of human skeletal and cardiac muscles; 2) be integrated with technological platforms for highthroughput screenings and development of new therapeutic strategies at large scale; 3) be easily transferable to research laboratory for facilitating the therapy development process in reduced time and at lower cost.

Recently, *in vitro* engineered tissues have found new roles as models for fundamental research, studies of disease, testing of drugs, and many other applications[23,27]. In Europe, human skin engineered *in vitro*[28] has replaced animals in the regulatory approval process for testing drugs and other agents for their skin corrosiveness[29]. Therefore, engineered constructs, which reproduces with high fidelity the native tissue, could also serve as physiologically relevant yet controllable models for basic studies on tissue development and cell function in response to genetic alterations, drugs, hypoxia and physical stimuli[23]. The development of tissue and quasi-organ *in*

vitro models that are based on human cells would provide a potential bridge for the gap between animal models and human studies, to help understand the basic mechanisms of human disease[22].

Tissue engineering can be the starting point for the development of new *in vitro* models.

1.3 Tissue engineering of skeletal and cardiac muscle

Tissue engineering has been defined first as "an interdisciplinary field that applies the principles of engineering and the life sciences toward the development of biological substitutes that restore, maintain, or improve tissue function"[30]. Another definition is "understanding the principles of tissue growth, and applying this to produce functional replacement tissue for clinical use"[31]. Thus, tissue engineering has always been driven by the need to provide functional equivalents of native tissues that can be used for *in vivo* implantation[30,32] in order to restore, maintain, or enhance tissue and organ physiology[33]. To engineer living tissues, cultured cells are coaxed to grow on bioactive degradable scaffolds that provide the physical and chemical cues to guide their differentiation and assembly into two- or three-dimensional tissues[34]. Skeletal and cardiac tissue engineering focuses on the reconstruction of skeletal and heart muscle, developing three main areas of research: cell source, scaffold design and bioreactor development.

1.3.1 Cell Sources

Adult cells, such as skeletal myoblasts, were able to differentiate into skeletal myotubes *in vitro* and to improve cardiac functions *in vivo*[35]. Satellite cells and muscle side population cells were both able to restore dystrophin expression in *mdx* mice, but the level of restoration was not significant[36]. However, the most promising cell sources for tissue engineering are human stem cells, capable of differentiation toward cardiac and myoblast lineage, such as: human embryonic stem cells (hESC)[15,37], induced Pluripotent Stem Cells (iPS)[36], Cardiac Stem Cell[35], Bone Marrow Stem Cells, Fetal Amniotic Stem Cell, Stem Cell derived from adipose

tissue[38], multipotent adult progenitors[12], mesoangioblasts[13], and muscle-derived stem cells[14].

Mesenchimal stem cells seem have great potential as source for cell therapy, because they can differentiate *in vitro* into nerve cells, skeletal muscle cells, vascular endothelial cells[39], and into cells with cardiomyocyte features[40]. Furthermore, after differentiation, these cells are positive for specific cardiac protein, such as β-myosin heavy chain, cardiac troponin T and α-cardiac actin, they prove functionality with Ca^{2+} transients[41], and respond to α and β adrenergic stimulation with an increase in contractility[42]. Nevertheless, some improvements in cardiac performance were observed after cell transplantation in patients, but the cardiomyogenic efficiency of these cells is still very limited (0.02%)[43].

In general, human embryonic stem cells, derived from the inner cell mass of the blastocyst[44] and Cardiac Stem Cell, harvested from endomyocardial biopsy of patients[45], seem to be the best sources for cardiac regeneration therapy because they differentiate into beating cells with a cardiomyocyte phenotype and they can also be expanded *in vitro* to generate large quantities of cells. In particular, Embryonic stem cells (ESC) can spontaneously organize, after differentiation, into a functional syncitium with action potential propagation. Injection of mesangioblasts into skeletal muscle resulted in extensive and widespread engraftment, accompanied by functional improvement[46]. Darabi and colleagues developed an embryonic stem cell line overexpressing Pax3, which were then sorted for PDGFαR and absence of Flk-1. These subset of cells generated an homogenous monolayer of myogenic progenitors expressing Pax3 and Myf5 as well as CD44, CD29, M-cadherin, CXCR4 and syndecam-4, markers associated with satellite cells or with the migration and differentiation of myogenic progenitors. When this population was injected locally or systemically into *mdx* mice, there was a significant restoration of dystrophin levels and improvement in the contractile strength of treated muscles[47].

1.3.2 Biomaterials

Scaffolds are used to provide structural support during the initial stages of tissue formation (initial attachment and remodeling) but then the cells slowly begin to

generate their own ECM components. Due to the contraction/relaxation cycle, typical of the muscle tissue, the governing factors for the choice of a scaffold are not only the biodegradability and biocompatibility of matrices, but also the mechanical properties, above all elasticity and strength. Natural and synthetic scaffolds have both been used for cardiac and skeletal muscle tissue engineering[48]. Synthetic polymers have the advantages of having chemical and physical properties well defined but they can induce inflammatory response, whereas natural scaffold are biocompatible and facilitate cell adhesion even though their production is more difficult. Several strategies have been described by the literature for engineering cardiac tissue *in vitro*: utilizing polymeric scaffolding material as a support matrix[2,49]; incorporating cardiac myocytes within biodegradable gels[50]; or utilizing overlapping of cellular contractile sheets[51]. Christman and Lee summarized the most used polymers in cardiac field, to date aliphatic polyesters such as polyglycolic acid (PGA), polylactic acid (PLLA), their copolymers (e.g. PLGA) and polycaprolactone (PCL) are used as solid scaffold whereas naturally derived protein (collagen, fibronectin) or carbohydrate polymers have been used as both solid or liquid scaffolds [52].

An important characteristic of biomaterials for skeletal muscle engineering is the cell orientation, since myofibers need to be packed parallel to each other to generate sufficient force for contraction. Thus, microstructured scaffolds, giving the right orientation to myoblasts, have been used[53]. Boldrin et al[54] showed that myogenic progenitor cells seeded onto bi-dimensional PLA-PLGA scaffolds could induce muscle regeneration *in vivo*, suggesting a new strategy to perform cell transplantation.

1.3.3 Bioreactors

Bioreactors are generally defined as devices in which biological processes (such as cell expansion, differentiation, or tissue formation on 3D scaffolds) occur under tightly controlled environmental conditions (such as exchange of oxygen, nutrients, and metabolites, and application of molecular and physical regulatory factors)[55]. Bioreactors have the purpose of enabling the culture of cells in sterile, physiological and controlled conditions while ensuring, through the dynamic regime, a more

efficient mass transfer of nutrient and gases between the cellularized scaffold and the culture medium and removal of debris. Such devices are indispensable when cells are cultured in 3D scaffolds to achieve tissue uniformity and avoid widespread necrosis in the inner regions of the construct. Many different devices has been developed, including: rotating vessels[56], spinner flasks[57] and perfusion bioreactors[58]. Several studies have involved the 3D culture of muscle cells in a bioreactor. Some of these works are focused on cell differentiation under mechanical stimuli using myoblasts seeded on microcarrier beads[59], on the improvement of the architecture of engineered cardiac tissues[60] or on smooth muscle cells cultured on stretched scaffolds[61].

1.4 Microscale tissue engineering

Cells respond to and remodel their immediate microenvironment, via homotypic or heterotypic interactions with neighboring cells, and with the tissue matrix. The microenvironment in which cells reside provides key signals that direct the cells, in particular stem cells, to proliferate, differentiate, or remain dormant; these factors include soluble molecules, the extracellular matrix, neighboring cells, and physical stimuli (Fig. 1.1). it is evident that such a complex cell context is not mimicked in the laboratory under standard 2D culture conditions[27].

Tissue structure and function are known to be highly inter-related and the correct organization at micrometric level is also essential for the emergent properties of the multicellular networks, the macrometric tissue. The sarcomere is the basic unit of a functional muscle, which allow muscle contraction: multi-protein complexes and microfilaments, such as myosin heavy chain and actinin, interact at a micrometric level and their architecture is highly organized in space. The characteristic scale of the sarcomere is micrometric: it's entire length is 2-3 μm and the dimension of the band of thick filaments is around 1.5 μm[62].

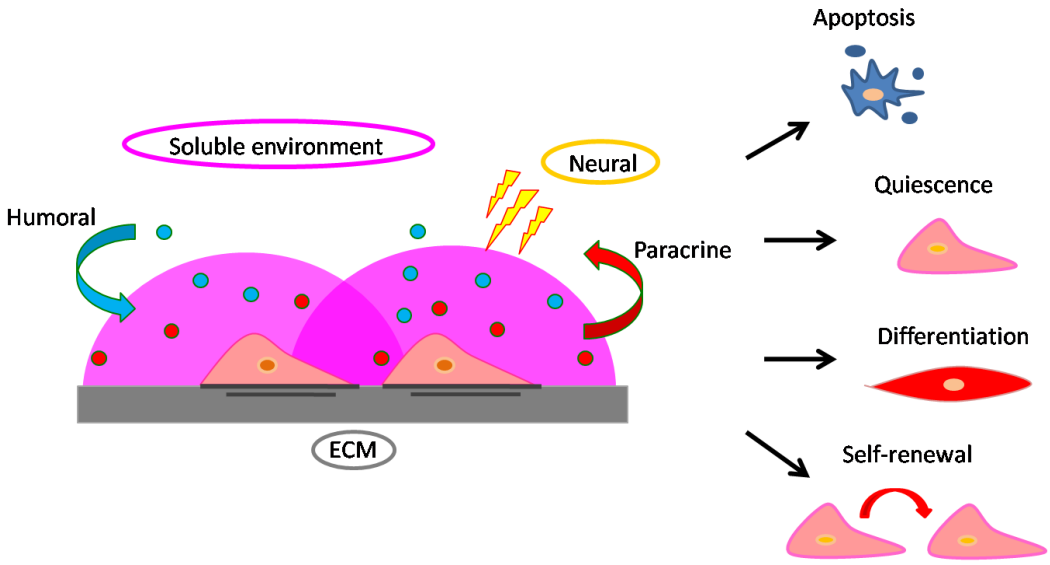

Figure 1.1. Cell microenvironment. The interaction with soluble factors, ECM, external nervous stimulation, and biophysical forces synergize to influence the cell fate, directing towards self-renewal, differentiation, quiescence, or apoptosis.

The whole muscle structure develops upon and within the sarcomere: sarcomeres assemble in myofibrils; which in turn are organized in myofibers, which are then packed in muscle fibers. Such a fine organization, starting from the micro-level of the sarcomere, allow the formation of a functional tissue which is able to contract and generate force (Fig. 1.2).

The requirements are, thus, to provide the cells with the appropriate cues and to control the conditions in the cell microenvironment: to direct cells to differentiate at the right time, in the right place, and into the right phenotype, one needs to recreate the right microenvironment, with biology and engineering interacting at multiple levels. The concept of "microscale tissue engineering" originate from this need: new microfabrication technologies are coupled to the tools and knowledge developed by classic tissue engineering in order to reproduce the appropriate micro-stimuli and micro-interaction leading to the correct tissue formation. Microfabricated cell cultures will offer unique opportunities to study key features of the microenvironment on relevant length scales. The increasingly intimate combination of engineering and biology give the possibility of development of sophisticated physiological *in vitro* models of many different human tissues.

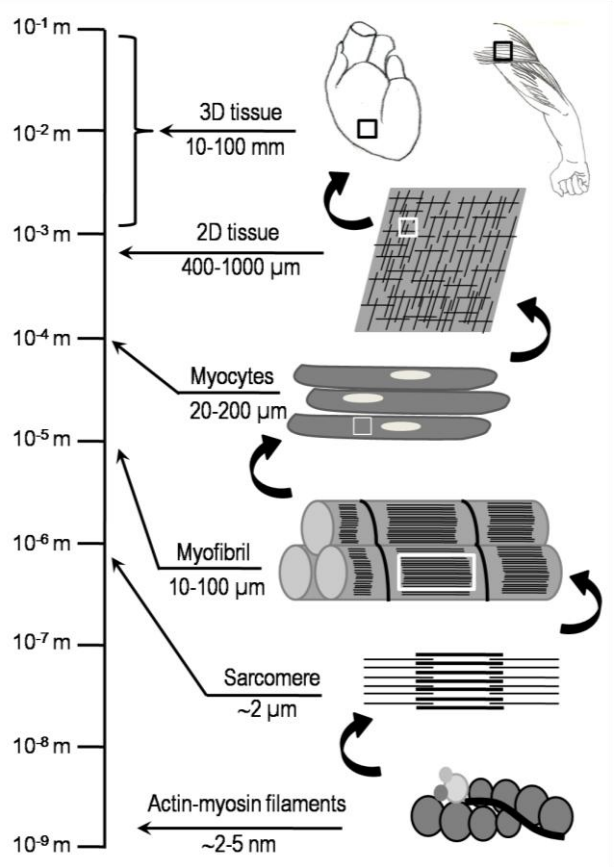

Figure 1.2. Scaling of cardiac and skeletal muscles. The assembly of these muscles represents a multiscale issue, that spans several orders of spatial magnitude from the alignment of actin-myosin complexes within a sarcomere, their alignment in myofibrils, the organization of myofibrils in a myocyte, and the coupling between myocytes in laminar muscle. 2D and 3D indicate two- and three-dimensional, respectively.

Besides the classic aim of tissue engineering, to create functional grafts suitable for implantation and repair of failing tissues, microscale tissue engineering thus opens several exciting possibilities: (i) to study stem cell behavior and developmental processes in the context of controllable models of engineered tissues, and (ii) to utilize engineered tissues as models for studies of physiology and disease. In addition, the microscaling of culture systems offers unique advantages when it comes to the reduction of operative costs, the highthroughput of the outcomes and analyses and to the development of multi-parametric experiments screening an high number of variables at a single time.

1.5 Aim of the thesis

The aim of this PhD thesis is the development of engineered human skeletal muscle myotubes and human cardiomyocytes, which could be possibly used as *in vitro* model for drug and therapy development and for physiological studies.

To this end, one of the specific aim of this work, is the application of biologically inspired micro-techniques, able to reproduce *in vitro* the major physiological stimuli that guide human cell differentiation and physiology maintenance of striated muscles *in vivo* .

In addition, both skeletal and cardiac human muscles were engineered as cell array (aligned and independent array of myotubes and cardiomyocytes dots), in order to make them suitable for the following coupling with a microfluidic platform, developed by engineers of the laboratory[63]. The coupling would ultimately allow the development of highthroughput drug and therapy screenings.

1.6 References

1 McCully, K. K. and Faulkner, J. A. , Injury to skeletal muscle fibers of mice following lengthening contractions. *Journal of Applied Physiology* **59** (1), 119 (1985); Bach, A.D., Beier, J.P., Stern-Staeter, J., and Horch, R.E., Skeletal muscle tissue engineering. *Journal of Cell. Mol. Med* **8** (4), 413 (2004).

2 Jawad, H. et al., Myocardial tissue engineering: a review. *J. Tissue Eng. Regen. Med.* **1** (5), 327 (2007).

3 Lloyd-Jones, D. et al., Heart Disease and Stroke Statistics 2009 Update. A Report From the American Heart Association Statistics Committee and Stroke Statistics Subcommittee. *Circulation* **119**, e1 (2009).

4 Kaye, D. M. and Krum , H., Drug discovery for heart failure: a new era or the end of the pipeline? *Nature Review Drug Discovery* **6** (2), 127 (2007).

5 Roman-Sanchez, P., P. Conthe, et al. , Factors influencing medical treatment of heart failure patients in Spanish internal medicine departments: a national survey. *QJM* **98** (2), 127 (2005).

6 Campbell, C. and Jacob, P., Deflazacort for the treatment of Duchenne dystrophy: a systematic review. *BMC Neurology* **3** (7) (2003).

7 Anderson, J. E. and Vargas, C. , Correlated NOS-Imu and myf5 expression by satellite cells in mdx mouse muscle regeneration during NOS manipulation and deflazacort treatment. *Neuromuscul. Disord.* **13**, 388 (2003).

8 Chakkalakal, J. V., Thompson, J., Parks, R. J., and Jasmin, B. J., Molecular, cellular, and pharmacological therapies for Duchenne/Becker muscular dystrophies. *FASEB J.* **19**, 880 (2005).

9 Van Deutekom, J.C.T. and Van Ommen, G. J., Advances in Duchenne Muscular Dystrophy gene therapy. *Nat. Rev. Genet.* **4**, 774 (2003).

10 Dello Russo, C. et al. , Functional correction of adult mdx mouse muscle using gutted adenoviral vectors expressing full-length dystrophin. *Proc. Natl. Acad. Sci. U. S. A.* **99**, 12979 (2002).

11 Harper, S.Q. et al. , Modular flexibility of dystrophin: implications for gene therapy of Duchenne muscular dystrophy. *Nature Medicine* **8**, 253 (2002).

[12] Reyes, M. and al., et, Purification and ex vivo expansion of postnatal human marrow mesodermal progenitor cells. *Blood* **98**, 2615 (2001).

[13] Minasi, M.G. and al., et, The meso-angioblast: a multipotent, selfrenewing cell that originates from the dorsal aorta and differentiates into most mesodermal tissues. *Development* **129**, 2773 (2002); Galvez, B. G. et al., Complete repair of dystrophic skeletal muscle by mesoangioblasts with enhanced migration ability. *The Journal of Cell Biology* **174** (2), 231 (2006).

[14] Cao, B. and al., et, Muscle stem cells differentiate into hematopoietic lineages but retain myogenic potential. *Nat. Cell Biol.* **5**, 640 (2003).

[15] Barberi, T. et al., Derivation of engraftable skeletal myoblasts from human embryonic stem cells. *Nature Medicine* **13** (7), 642 (2007).

[16] Stevenson, L.W., Warner, S.L. , and al., et, The impending crisis awaiting cardiac transplantation. Modeling a solution based on selection. *Circulation* **89** (1), 450 (1994); Miniati, D.N. and Robbins, R.C. , Heart Transplantation: A Thirty-Year Perspective. *Annual Review of Medicine* **53** (1), 189 (2002).

[17] Goldstein, M. S., Heart Failure Therapy at the Turn of the Century. *Heart Failure Reviews* **6**, 7 (2000).

[18] Ortak, J. et al., Stem cell use for cardiac diseases as of 2008. *Transfusion and Apheresis Science* **38**, 253 (2008); Zimmermann, W et al., Heart muscle engineering: An update on cardiac muscle replacement therapy. *Cardiovascular Research* (2006).

[19] Stevenson, L. W. and Kormos, R. L. , Mechanical Cardiac Support 2000: Current applications and future trial design. *J Thorac Cardiovasc Surg* **121** (3), 418 (2001).

[20] Zimmermann, W.H. and Eschenhagen, T., Cardiac Tissue Engineering for Replacement Therapy. *Heart Failure Reviews* **8**, 259 (2003).

[21] Grabowski, H., Follow-on biologics: data exclusivity and the balance between innovation and competition. *Nature Reviews Drug Discovery* **7**, 479 (2008).

[22] Griffith, L. G. and Swartz, M. A., Capturing complex 3D tissue physiology in vitro. *Nat. Rev. Mol. Cell Biol.* **7** (3), 211 (2006).

[23] Gerecht-Nir, S. et al., Biophysical regulation during cardiac development and application to tissue engineering. *Int. J. Dev. Biol.* **50**, 233 (2006).

[24] Kaplan, D. L., Moon, R. T., and Vunjak-Novakovic, G., It takes a village to growth a tissue. *Nature Biotechnology* **23** (10), 1237 (2005).

[25] Zhang, S. , Beyond the Petri dish. *Nature Biotechnology* **22**, 151 (2004).

[26] Collins, C.A. and Morgan, J.E. , Duchenne's muscular dystrophy: animal models used to investigate pathogenesis and develop therapeutic strategies. *International Journal of Experimental Pathology* **84**, 165 (2003).

[27] Burdick, J. A. and Vunjak-Novakovic, G., Engineered Microenvironments for Controlled Stem Cell Differentiation. *Tissue engineering: Part A* **14** (00), 1 (2008).

[28] Bernhofer, L. P. , Seiberg, M. , and Martin, K. M. . *Toxicology In Vitro* **13**, 219 (1999).

[29] Interagency Coordinating Committee on the Validation of Alternative Methods, Available at http://iccvam.niehs.nih.gov (2001).

[30] Langer, R. and Vacanti, J. P., Tissue Engineering. *Science* **260**, 920 (1993).

[31] MacArthur, B. D. and Oreffo, R. O. C., Bridging the gap. *Nature* **433** (7021), 19 (2005).

[32] Lysaght, M. J. and Reyes, J. . *Tissue Engineering* **7,485** (2001).

[33] Griffith, L. G. and Naughton, G., Tissue Engineering: Current Challenges and Expanding Opportunities. *Science* **295** (1009-1016) (202).

[34] Strain, A. J. and Neuberger, J. M. . *Science* **295, 1005** (2002).

[35] Passier, R., van Laake, L. V., and Mummery, C. L., Stem-cell-based therapy and lessons from the heart. *Nature* **453** (322-329) (2008).

[36] Darabi, R., Santos, F. N. C., and Perlingeiro, R. C. R. , The Therapeutic Potential of Embryonic and Adult Stem Cells for Skeletal Muscle Regeneration. *Stem Cell Review* **4**, 217 (2008).

[37] Goh, G. et al., Molecular and phenotypic analyses of human embryonic stem cell-derived cardiomyocytes Opportunities and challenges for clinical translation. *Thrombosis and haemostasis* **94**, 728.737 (2005).

[38] Fukuda, K. and Yuasa, S., Stem Cells as a Source of Regenerative Cardiomyocytes. *Circ Res* **98** (8), 1002 (2006).

[39] Jiang, Y., Jahagirdar, B. N. , and ()., et al., Pluripotency of mesenchymal stem cells derived from adult marrow. *Nature* **418** (6893), 41 (2002).

[40] Rangappa, S., Entwistle, J. W. C. , and al., et, Cardiomyocyte-mediated contact programs human mesenchymal stem cells to express cardiogenic phenotype. *J Thorac Cardiovasc Surg* **126** (1), 124 (2003).

[41] Pittenger, M. F. and Martin, B. J. , Mesenchymal Stem Cells and Their Potential as Cardiac Therapeutics. *Circ Res* **95** (1), 9 (2004).

[42] Li, X. , Yu, X., and al., et, Bone marrow mesenchymal stem cells differentiate into functional cardiac phenotypes by cardiac microenvironment. *Journal of Molecular and Cellular Cardiology* **42** (2), 295 (2007).

[43] Haider, H. K. and Ashraf, M., Bone marrow stem cell transplantation for cardiac repair. *American Journal of Physiology Heart Circulation Physiology* **288** (6), H2557 (2005).

[44] Thomson, J. A. et al., Embryonic Stem Cell Lines Derived from Human Blastocysts. *Science* **282**, 1145 (1998).

[45] Messina, E., De Angelis, L., and al., et, Isolation and Expansion of Adult Cardiac Stem Cells From Human and Murine Heart. *Circ Res* **95** (9), 911 (2004).

[46] Sampaolesi, M. et al., Mesoangioblast stem cells ameliorate muscle function in dystrophic dogs. *Nature*, 1 (2006).

[47] Darabi, R. et al., Functional skeletal muscle regeneration from differentiating embryonic stem cells. *Nature Medicine* **14**, 134 (2008).

[48] Bach, A. D., Beier, J. P., Stern-Staeter, J., and Horch, R. E., Skeletal muscle tissue engineering. *J. Cell. Mol. Med.* **8** (4), 413 (2004).

[49] Engelmayr, G. C. et al., Accordion-like honeycombs for tissue engineering of cardiac anisotropy. *Nature Materials* (2008).

[50] Eschenhagen, T., Fink, C., and al., et, Three-dimensional reconstitution of embryonic cardiomyocytes in a collagen matrix: a new heart muscle model system. *FASEB J.* **11** (8), 683 (1997).

[51] Ishii, O., Shin, M., and al., et, In vitro tissue engineering of a cardiac graft using a degradable scaffold with an extracellular matrix-like topography. *Journal of Thoracic and Cardiovascular Surgery* **130** (5), 1358 (2005).

[52] Christman, K. L. and Lee, R. J. , Biomaterials for the treatment of myocardial infarction. *J Am Coll Cardiol.* **48** (5), 907 (2006).

[53] Choi, J. S. et al., The influence of electrospun aligned poly(3-caprolactone)/collagen nanofiber meshes on the formation of self-aligned skeletal muscle myotubes. *Biomaterials* **29**, 2899 (2008); Riboldi, S. A. et al., Skeletal myogenesis on highly orientated microfibrous

polyesterurethane scaffolds. *Journal of Biomedical Materials Research Part A* **84**, 1094 (2008); Engler, A. J. et al., Myotubes differentiate optimally on substrates with tissue-like stiffness: pathological implications for soft or stiff microenvironments. *Journal of Cell Biology* **166** (6), 877 (2004).

54 Boldrin, Luisa et al., Satellite Cells Delivered by Micro-Patterned Scaffolds: A New Strategy for Cell Transplantation in Muscle Diseases. *Tissue Engineering* **13** (2), 253 (2007).

55 Freshney, I. et al., in *Principles of Tissue Engineering*, edited by R. Langer R. Lanza, and J. Vacanti (2007), pp. 155.

56 Freed, L. E., Hollander, A. P. , and al., et, Chondrogenesis in a Cell-Polymer-Bioreactor System. *Exp Cell Res* **240** (1), 58 (1998).

57 Vunjak-Novakovic, G., Obradovic, B., and al., et, Dynamic Cell Seeding of Polymer Scaffolds for Cartilage Tissue Engineering. *Biotechnology Progress* **14** (2), 193 (1998).

58 Bancroft, G. N., Sikavitsas, V. I. , and et, al. , Design of a Flow Perfusion Bioreactor System for Bone Tissue-Engineering Applications. *Tissue Engineering* **9** (3), 549 (2003).

59 Torgan, C., Burge, S., and al., et, Differentiation of mammalian skeletal muscle cells cultured on microcarrier beads in a rotating cell culture system. *Med Biol Eng Comput* **38** (5), 583 (2000).

60 Carrier, R., Rupnick, M., and al., et, Perfusion Improves Tissue Architecture of Engineered Cardiac Muscle. *Tissue Engineering* **8** (2), 175 (2002); Radisic, M. et al., High density seeding of myocyte cells for tissue engineering. *Biotechnology Bioengineering* **82**, 403 (2003); Radisic, M. et al., Cardiac tissue engineering using perfusion bioreactor systems. *Nature Protocols* **3** (4), 719 (2008).

61 Cha, J. M., Park, S. N., and al., et, Construction of Functional Soft Tissues From Premodulated Smooth Muscle Cells Using a Bioreactor System. *Artificial Organs* **30** (9), 704 (2006).

62 Sanger, J. W. et al., Myofibrillogenesis in Skeletal Muscle Cells. *Clinical orthophaedics and related research* **403S**, 153 (2002).

63 Cimetta, E., Design and development of microscale technologies and microfluidic platforms for the in vitro culture of stem cells. PhD Thesis, University of Padova, 2009.

Chapter 2

Microscale technologies

This chapter describes the microscale technologies used for mimicking *in vitro* the key feature of skeletal and cardiac muscles: 1) the mechanical properties of muscle tissue have been replicated using an hydrogel as substrate for cell culture; 2) in order to reproduce the highly organized architecture of muscle tissues, microcontact printing of adhesion proteins onto the hydrogel surface has been used for imposing a precise topology to the culture; 3) the application of exogenous electrical stimulation mimicked part of the neuronal; 4) preliminary studies with microfluidic channels have been performed, in sight of integrating the micro-patterned substrate with a microfluidic platform for highthroughput studies. The state of the art of each technology is followed by the description of the methodologies and, briefly, the obtained results.

2.1 Engineering the cell culture microenvironment

Three main features characterized skeletal and cardiac muscles *in vivo*:

1- They are soft tissues: considering stiffness, muscles resides between the brain[1], considerably softer than muscle[2], and bones, much harder[3]. Rigid polystyrene (as Petri dish) are far from reproducing the physiological mechanical stimuli and cell-substrate interactions of myoblasts or cardiomyocytes microenvironment.

2- They have an highly organized architecture: striated muscles have a periodic structure composed of parallel fibers, formed in turns of ordered myofibers, which basic unit are sarcomeres: a defined network of thin and thick filaments (see § 3.1). In standard substrates, the lack of topological stimuli, able to guide

cell adhesion and the formation of the correct tissue architecture, greatly hinder the differentiation potential of muscle cells and the development of a functional construct.

3- They are electrically excitable tissues: skeletal muscles are innervated and stimulated via neuromuscular junctions; cardiac contraction is driven by waves of electrical excitation generated by pacing cells. Electrical stimulation is therefore a key component of muscle physiology and development.

The recent development of microscale techniques and their application to cell culture biology, have lead to the possibility of generating new and innovative *in vitro* cell culture systems, able to reproduce the relevant cues of the *in vivo* microenvironment. Microfabrication-based tools allowed the engineering of cell culture surfaces, offering control over cell–Extra Cellular Matrix (ECM) and cell–cell interactions with micrometer precision. Tunable synthetic hydrogels, which have a high water content and mechanical properties similar to those of native tissues, have been used for the creation of three-dimensional tissues. Controlled microfluidic platforms and bioreactors have been developed in order to generate or mitigate gradients of stimuli, facilitate nutrient delivery and promote automation and scale up[4].

The strategy applied during this Ph.D thesis has been *"biologically inspired"*[5]: the key features of skeletal and cardiac muscles, mentioned above, have been reproduced *in vitro* in order to guide the correct cell differentiation and to obtain functional engineered tissues. In addition, for the development of an high-throughput device for *in vitro* screenings of drug and new therapies, the coupling with a microfluidics system, able to generate several patterns of stimulation on the same batch of cells, is required. In particular: a) human myoblasts and cardiomyocytes have been cultured onto an hydrogel with tissue-like mechanical properties, which have been tuned in order to understand the relationship between muscle differentiation/functionality and substrate stiffness; b) the hydrogel surface has been functionalized through micro-contact printing: several ECM proteins have been adsorbed onto the surface with a desired geometry, in order to give the correct biochemical stimuli and to impose a highly defined topology to the culture; c) exogenous electrical stimulation

has been applied to the culture, with the aim of giving a neuro-physiological cue; d) a microfluidic device has been used for studying the effect of medium flow over endothelial cells. This study have been performed in order to verify the biocompatibility of the materials and viability of cells, in sight of coupling the engineered skeletal and cardiac tissues with a microfluidic platform for the development of an *in vitro* highthroughput screening assay (Table 2.1).

Table 2.1: *In vivo* key features for skeletal (SkM) and cardiac (CaM) muscles functionality. Such characteristics have been reproduced *in vitro*, via microscale technologies, for the obtainment of functional engineered tissues.

In vivo **SkM and CaM**	***In vitro*** **required features**	***In vitro*** **strategy**	
Soft tissues	Substrates with tissue-like mechanical properties	Hydrogel	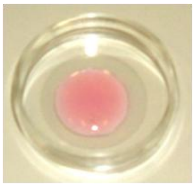 Described in paragraph 2.1
Highly organized tissues	Cell culture topology	Micropatterning	 Described in paragraph 2.2
Electrically excitable tissues	Neuro-physiological stimuli	Electrical stimulation	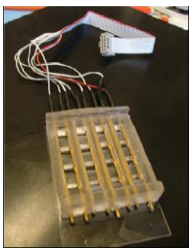 Described in paragraph 2.3
Additional requirement for the development of an highthroughput assay		Microfluidics	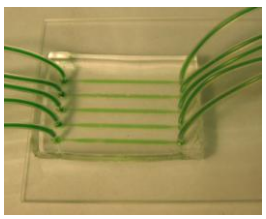 Described in paragraph 2.4

2.2 Cell-substrate interaction

Recent works have highlightened the role of extracellular matrix and substrate stiffness in several cellular processes[6]. In skeletal and cardiac muscles, the extracellular matrix not only displays adhesive ligands important for cell anchorage but also presents a number of influential physical properties responsible for the acquisition of the contractile phenotype in skeletal muscles[2] and for the maintenance of the correct beating rate in cardiac tissue[7]. One such property, matrix stiffness, has a key role in myoblasts differentiation, which process is highly regulated in a spatial and temporal way by the expression of different muscle specific proteins[8] and by not yet fully characterized cell-matrix interactions[3]. Previous work by Engler and colleagues[2] clearly show how mouse myoblast differentiate optimally on soft substrates with stiffness similar to that of natural tissue, achieving a level of differentiation that is not reachable using rigid substrates such as the conventional glass or plastic surface. An additional evidence of the key role of tissue elasticity is that the association of several pathologies with alteration of this properties. Dystrophinopathies induce the formation of fibrosis, due to the overexpression of ECM molecules (most notably collagen type I and type III), whose accumulate in the interstitial space[9]. Following a myocardial infarction, beating cardiomyocytes are replaced by a fibrotic scar, that is several-fold stiffer than normal myocardium[7].

The choice of the substrate is thus a key step in tissue engineering.

2.2.1 Hydrogels

Several biomaterials and scaffolds have been developed and tested for tissue engineering (see § 1.1.3). The ECM matrix has a fluid character, thus it's not surprising that hydrogels have found important roles in medicine, biology, tissue engineering, artificial organs, and other implantable devices[10]. Hydrogels are defined as three-dimensional (3-D) polymer networks that swell, but do not dissolve in water[11]. Their biocompatibility, high water content, and elastic properties, resembling those of native tissues, make them suitable for reproducing the correct

cell microenvironment, referring in particular to the mechanical stimuli. Besides, hydrogel transparency is a key issue for cell culture because it allows the visualization of living cells, optical image analyses and studies on the dynamics of interfacial processes, such as protein-surface interactions, using inverted microscopes (frequently used in cell biology)[12]. Hydrogels can be prepared with several polymers, including alginate, pluronics, chitosan, fibrin glue and poly-acrylamide[13] and in recent years many kinds of hydrogels, especially poly(ethylene glycol) (PEG) and derivatives[14], have been widely used for encapsulating living cells or as substrates for cell culture. A wide variety of copolymers, composed of a synthetic backbone and grafted biomolecules (or vice versa) such as fibrinogen[15] and hyaluronic acid[16] or short peptides sequences such as RGD[17], was proposed and tested to develop substrates with the biological cues required for cell attachment.
In this study, a poly-acrylamide (PA) hydrogel has been chosen because its elastic properties can be controlled and easily modulated by changing the proportion between the polymer and crosslinker, thus obtaining stiff or soft gels[2,18]. PA hydrogels are typically used in molecular biology as an analytical tool for separating proteins and oligonucleotides[11]. They are easy to fabricate, inexpensive and can be produced as a thin film and covalently bonded to a functionalized glass slide showing long term stability in culture. Moreover, PA hydrogels have a non fouling surface, which allow to perform micropatterning of adhesion proteins on its surface (see § 2.2).

2.2.1.1 Poly-acrylamide hydrogel preparation

PA hydrogels are prepared as homogeneous films with a circular shape (16 mm in diameter and an average thickness of 50 μm) over a microscope slide or coverslip. Briefly, the glass surface was chemically modified with surface plasma treatment for creating a hydrophobic layer to ensure covalent binding of the hydrogel films. The prepolymer solution Acrylamide/bisacrylamide 29:1 was diluted in phosphate-buffered saline (PBS) to the final desided concentrations (generally 10%). The photoinitiator was initially dissolved in methanol (200 mg/ml) and then added to the acrylamide/bis-acrylamide solution in order to obtain a final concentration of 20

mg/ml, and mixed thoroughly. 20 µl of the prepolymer solution were dropped over the functionalized glass surface. Hydrogel polymerization occurred by exposing the prepolymer solution to UV light for 3 min. Selective photo-polymerization of acrylamide solutions on the glass surface has been achieved by interposing a photomask with the desired geometry between the light source and the glass slide (Fig. 2.1A). Non-polymerized acrylamide was removed using distilled water. Glass slides with covalently bound hydrogel films were immersed in ultra-pure distilled water for 48 h to ensure complete removal of the un-reacted monomeric units or photoinitiator. After rinsing with ultra-pure distilled water, hydrogels were allowed to dry completely overnight. Final sterilization occurred after exposure to UV light under a sterile hood. For a detailed protocol see Appendix A.

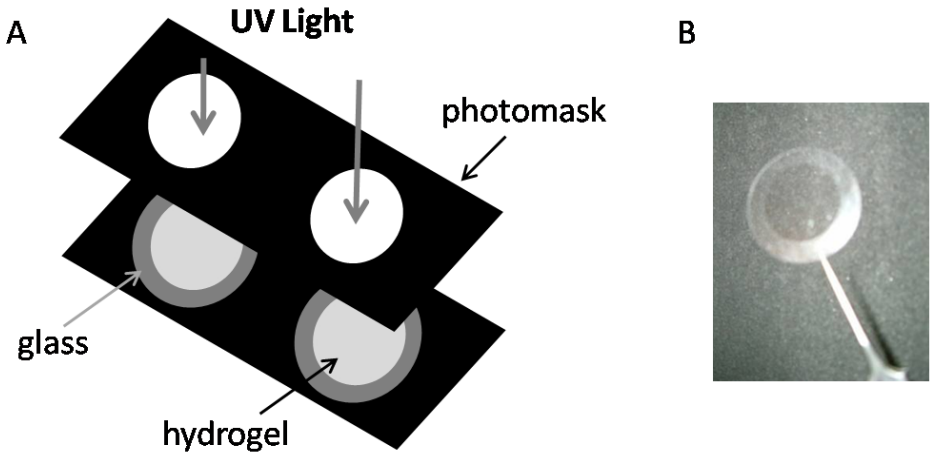

Figure 2.1. Hydrogel preparation. A: A layer of acrylamide/bis-acrilamyde solution is deposed over a glass coverslip (25 mm in diameter). The hydrogel is polymerized with UV light through a photomask. B: Picture of a polymerized hydrogel.

2.2.1.2 Mechanical properties of poly-acrylamide hydrogel

In order to understand the role of substrate stiffness on muscle differentiation and functionality and in sight of the development of an *in vitro* model of myocardial infarction or dystrophic muscles (which remodel induce the fibrous formation, increasing muscle stiffness), PA hydrogels with different mechanical properties were prepared tuning the prepolymer composition. The elastic properties were then quantitatively measured through standard compression tests, determining the bulk Young's modulus (E). Figure 2.2 shows the result of mechanical tests performed on

hydrogel samples taking in account four different concentrations of polymer in the prepolymer solution (5%, 10%, 15% and 20% v/v of acrylamide/bis-acrylamide 29:1 mixture).

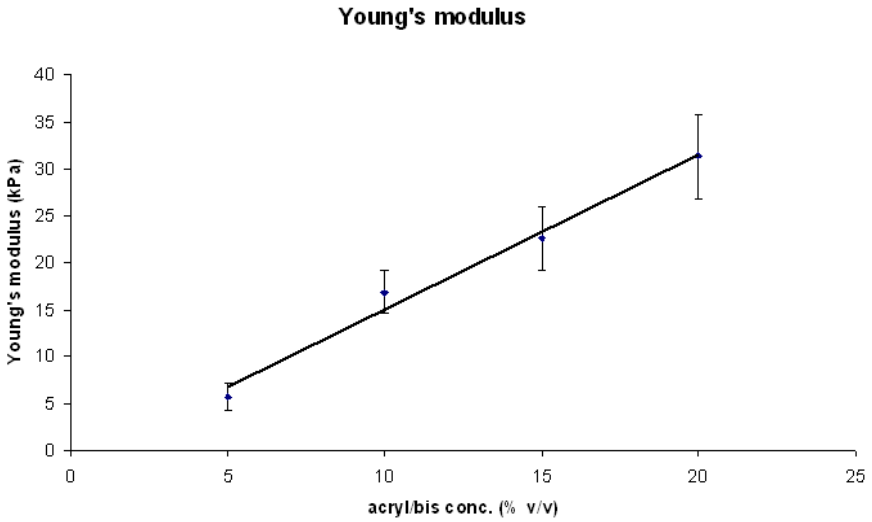

Figure 2.2. Young's modulus of PA hydrogel. Elastic moduli were quantitatively measured through standard compression tests for four different hydrogel compositions, i.e. 5-10-15-20% (v/v) acrylamide/bis-acrylamide 29:1 mixture in the prepolymer solution.

Hydrogels prepared with concentration of prepolymer solution below 5% were too soft, and not homogeneously polymerized; on the contrary, hydrogels with a concentration higher than 20% resulted in a tight network and the adsorption of proteins on its surface was not optimal, thus compromising cell adhesion.

As shown in figure 2.2, Young's modulus increased as the acrylamide/bis-acrylamide concentration increases. A linear interpolation of the data was used to determine the optimal hydrogel compositions, which fairly approximate the elastic modulus of skeletal and cardiac muscles. For instance, hydrogels with a composition of ≈8.2±2.5% (v/v) of acrylamide/bis-acrylamide may reproduce the values of the elastic modulus of normal murine skeletal muscles (E≈12±4 kPa) whereas hydrogels with ≈12.0±3.7% reproduce that of *mdx* muscles (E≈18±6 kPa)[2]. Considering cardiac muscles, Engler and colleagues verified that the substrate elasticity that maximizes cardiomyocytes (derived by quail) work is E≈11-17 kPa, while an infarcted heart could have an elastic modulus of E≈35-70 kPa[19].

2.3 Topologic control over the cell culture

The *in vivo* architecture of skeletal muscles is composed of aligned and parallel myofibes and is justified by the need of generating sufficient force of contraction: muscle myofibers are packed parallel to each other and cooperate in the same direction during muscle contraction. The topologic organization of cell is thus extremely important for skeletal myoblast. In addition, myoblast differentiation into myotubes is favored by their alignment. Indeed myoblasts cultured *in vitro* have the innate tendency to align before fusing. When myoblasts are cultured *in vitro*, in a standard culture substrate (Petri dish or glass), they adhere with random distribution and result in a disorganized network of myotubes without a preferential orientation; which do not resemble physiological muscle architecture. The optimal configuration in space for myoblasts is thus the culture in parallel lanes.

Concerning cardiac muscle, the topology is not such a crucial parameter for differentiation, but become an important factor when cardiomyocytes start beating: the most stable conformation for contracting cardiomyocytes is the aggregation in circular spots because mechanical stress due to contractions is minimized and equal in all the directions. Consequently, the risk of detachment is greatly reduced when these cells are cultured as circular dots.

For both skeletal and cardiac muscle, the topology of cell culture is relevant in sight of the development of an *in vitro* highthroughput assay: the generation of independent and ordered fascicles of myotubes or spots of cardiomyocytes is necessary in order to couple them to a microfluidic platform (see § 2.3) and to stimulate them with different medium, drugs, electrical stimuli or cytochines myotubes or cardio-dots obtained from the same batch of cells.

The topologic control over cell culture can be achieved through the use of microstructured substrates[20] or micropatterning of adhesion proteins.

In the first case, the substrates (generally synthetic polymeric membranes) are produced by soft-lithography technique and the geometry is directly impressed in its structure (Fig. 2.3). In this case, the cells can adhere to the entire surface, to both

the polymeric membrane and to the dish or glass underneath, thus the topology is partially controlled.

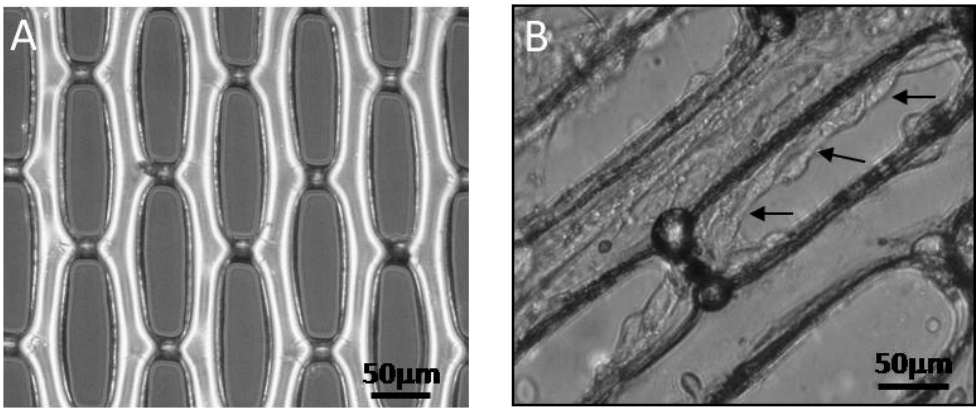

Figure 2.3. A:Example of a microstructured membrane of poly-(L-lactic acid) (PLA). B: Cells cultured onto it adhere following the structure (arrows), but the adhesion is not hindered in the surrounding area.

Micropatterned substrates have several advantages: adhesion proteins are printed with the desired topology onto a cell repellent surface. this technique is a simple and versatile method to pattern adhesion proteins with a resolution of ~1 µm, the immobilization on the surface occurs through physical adsorption and allows proteins to maintain their activity without suffering from major denaturation phenomena, and patterning proteins on hydrogel films enables microscope observations on the same focal plane of the substrate.

2.3.1 Micro-contact printing

Micro-contact printing, first described by the Whitesides group in 1993[21], is the technique for micropatterned substrates production, and consists in using an elastomeric stamp with bas relief features to transfer an 'inked' material (adhesion proteins in the case of cell culture) onto a substrate (PA hydrogel)[22]. Originally developed for creating patterns for microelectronics applications[21], micro-contact printing was soon adapted to produce substrates for cellular patterning[23]. Since that time there have been numerous publications on biological applications and many useful methodological developments were introduced. The popularity of the technique originates from its simplicity, cost-effectiveness and flexibility, with

regards to both the choice of the substrate and the protein to be transferred during imprinting[12]. The process of micro-contact printing as used in the majority of cell-patterning applications is illustrated in Figure 2.5. First (Fig. 2.4A), an elastomeric stamp is formed by casting a liquid-phase polymer (e.g., silicon) over a microstructured master. After hardening, the stamp is removed from the master. The next step (Fig. 2.4B) is the "inking" of the stamp into the protein solution, which is followed by the actual stamping procedure upon which the protein is transferred to the substrate. Several surfaces have been patterned successfully, such as gold, silver, various metal or metal–oxide surfaces, glass, and different plastic[22].

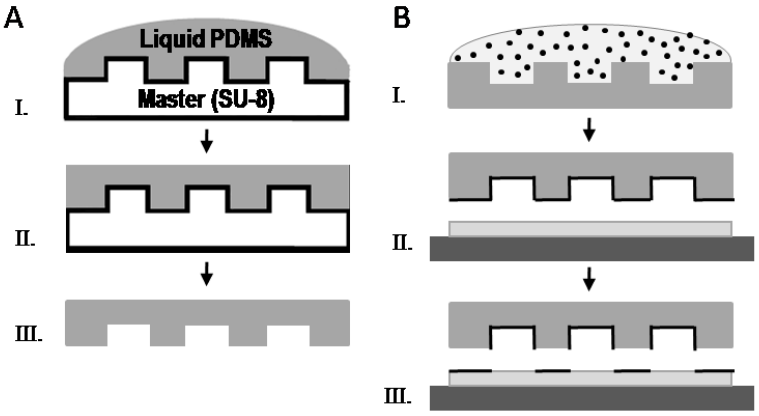

Figure 2.4. Schematic representation of the micro-contact printing technique. (A) Procedure of creating the PDMS mold with the desired geometry. Liquid PDMS is cast on the structured master surface (I.) After curing (II.) the elastomeric stamp is ready for use (III.) (B) The stamp is inked with the solution containing the protein to be printed (I.). The protein is transferred by printing onto the PA hydrogel (II.). Following the removal of the stamp (III.), the patterned hydrogel is ready. [dark grey: glass coverslip; light grey: PA hydrogel; black: ECM protein]

For a detailed description of the protocol see appendix A.

2.3.1.1 Creating the masters and PDMS mold

The first step, creating the master and the poly(dimethyl)-siloxane (PDMS) mold (Fig. 2.4A), has been optimized and performed by chemical engineers of the laboratory. The master is obtained using a soft-lithography technique. The name "soft lithography" cover a group of techniques with the common feature that at some stage of the process an elastomeric ("soft") material is used to create the chemical structures. Two related techniques of this family are micro-contact printing

and microfluidic (see § 2.4)[12]. Briefly, a master made of photoresistant resin (SU-8) with the desired geometry was created by spin coating a uniform layer of SU-8 onto silicon wafers. After thermal treatment, the resin was selectively cross-linked by exposing the SU-8-coated wafer to UV light through a patterned mask. After exposure, a treatment with the developer 1-methoxy-2-propanol acetate allowed to obtain the final mold. Subsequently, a PDMS mold is prepared by pouring and curing the liquid precursor onto the patterned SU-8. The molds are generally produced using PDMS because they must be soft enough to enable conformal contact with the hydrogel, in order to efficiently transfer the protein, which means that it must adapt elastically without leaving voids created by the natural roughness of the substrate. Once formed the PDMS mold, with the desired geometry, can be used several times, with particular attention to washing it with PBS and autoclaving it after each use. It can be reproduced by replica molding. The chosen geometries are: parallel lanes for human skeletal myoblasts 75 μm wide and 100 μm spaced, and circular dots for human cardiomyocytes 300 μm in diameter and 700 μm center to center spaced. The patterned area generally covers 4 mm^2.

2.3.1.2 Direct patterning

The second step is the effective patterning (Fig. 2.4B). The PDMS mold is inked into the protein solution for a few seconds and then the excess solution removed with the vacuum pump. Conformal contact between the dry hydrogel surface and the stamp is achieved by applying a gentle pressure, thus transferring the desired protein micropattern onto the substrate surface.

The list of applicable adhesion promoting molecules is long, several different ECM proteins or synthetic peptide constructs with ECM binding sites have been successfully printed (Fig. 2.5). The type of the printed ECM molecules needs to be matched to the cellular system used in the experiments.

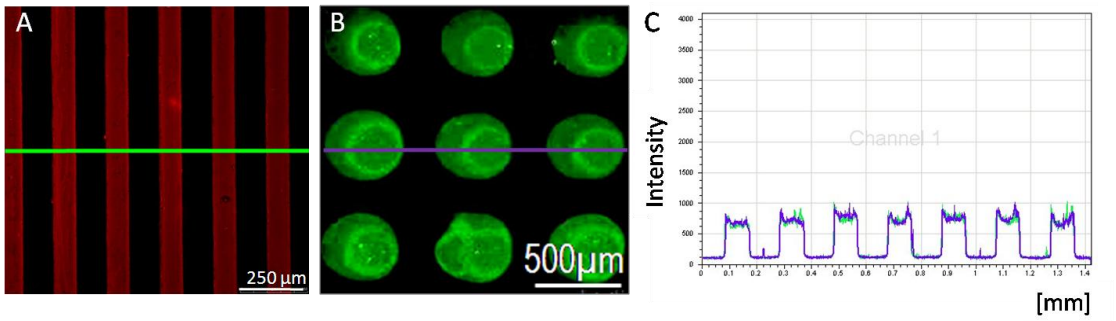

Figure 2.5. Examples of patterned geometry and transfer efficiency. A: Matrigel patterning in parallel lanes, revealed with immunofluorescence against laminin. B: FITC-conjugated Bovine Serum Albumin (BSA-FITC) patterning in circular dots. C: graph reporting the intensity of fluorescence along the green and purple line drawn in A and B respectively.

The printed molecules are only physisorbed on the surface; thus, exchange and degradation processes are likely to occur when the substrate is in contact with the cell-culture medium components. We observed degradation of the pattern with culture time, anyway the cultures were maintained successfully for up to 12 days. The transfer efficiency is likely to be below 100% and may show large variations from one different experiment to the other. For this reason a precise protocol for printing and several protein concentrations have been tested and optimized. In particular, the best transfer efficiency was not achieved by inking the PDMS mold into the protein solution, but by dropping with a micropipette 50 µL of the protein solution over the mold. The excess was then removed as described above. Laminin, fibronectin and matrigel were successfully patterned with this technique; while the micro-contact printing of collagen didn't result in an homogeneous pattern. Collagen in fact has a gelatinous consistency and it didn't adsorb onto the hydrogel, but it formed a layer of gel over it, which easily peeled off during cell culture.

Several protein concentrations have been tested (25 µg/ml, 50 µg/ml and 100 µg/ml for laminin and fibronectin; 2.5%, 5% and 10% for matrigel). The analysis of transfer efficiency, homogeneity of the pattern (Fig. 2.6) and stability in culture demonstrated that the optimal concentrations were: 100 µg/ml for laminin and fibronectin; 2.5% matrigel.

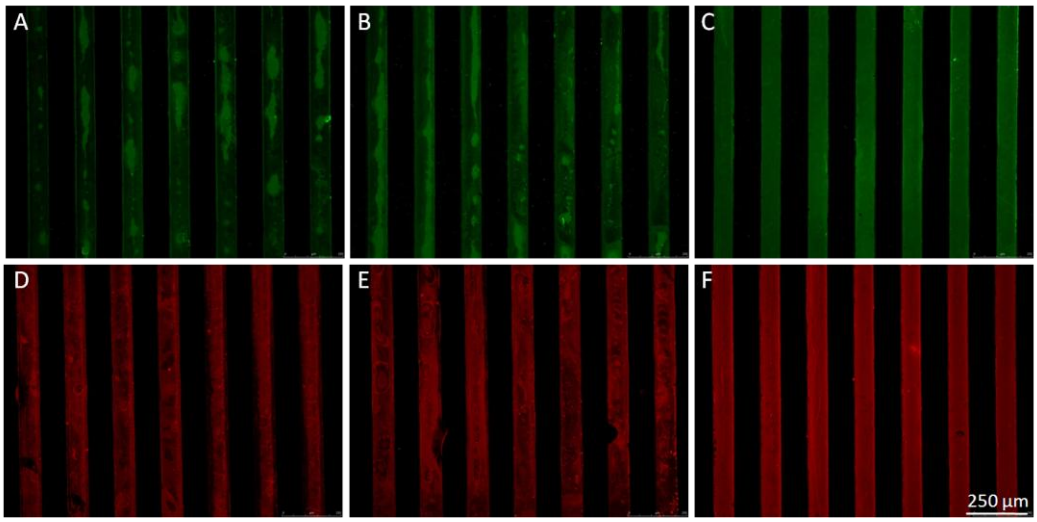

Figure 2.6. Micropattern of BSA-FITC (upper lane) and matrigel (lower lane). Three different concentration have been tested: (A) 25 µg/ml, (B) 50 µg/ml and (C) 100 µg/ml for BSA and (D) 0.5% (v/v) in DMEM, (E) 1.5% (v/v) in DMEM, (F) 2.5% (v/v) in DMEM. The higher protein concentration gave the best pattern.

2.3.2 Cell seeding onto patterned hydrogels

Once the hydrogel surface is patterned, the cells can be seeded and let attach to the patterned area (Fig. 2.7). 200-300 µL of cell suspension were dropped over the hydrogel, forming a bubble-like structure. The seeding cell density depends on the cell type: human myoblasts were seeded at a cell density of 1,5 $\times 10^4$ cells/cm^2, while cardiomyocytes at 6,2 $\times 10^4$ cells/cm^2.

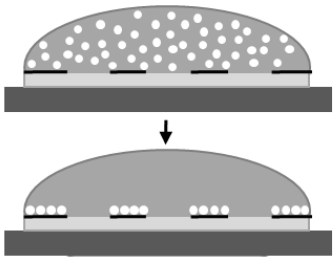

Figure 2.7. Schematic representation of cell seeding onto a patterned surface. The cell suspension is dropped on to the hydrogel. After 3-4 hours cells have adhered only to the micropatterned surface with micrometric precision.

As shown in figures 2.5 and 2.6, the pattern obtained is extremely precise and reproduce with high fidelity the mold geometry. Such a precision is then respected in directing cell adhesion. In figure 2.8, a time course of adhesion of myoblasts and cardiomyocytes is reported.

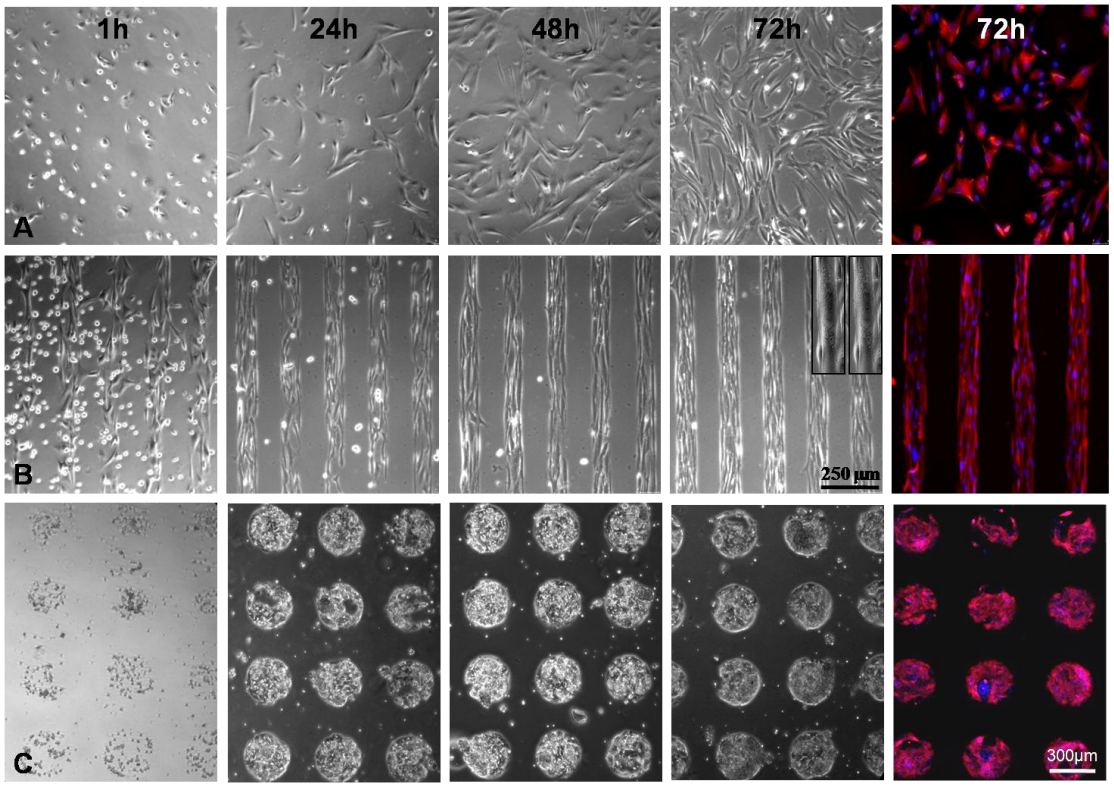

Figure 2.8. Time course of cell adhesion on standard Petri dish (A) and patterned PA hydrogel (B, C). A: on a regular Petri dish, human myoblasts start to align 48 hours after the seeding, 72h later they are still far from the confluence. B: on patterned hydrogel, 24 hours after seeding myoblats are perfectly aligned. After 48 hours they reach confluence and start fusing, 72 hours later they show few myotubes (magnification). C: human cardiomyocytes on patterned hydrogel, showing the same time course of patterned myoblasts. Last column: immunostaining on desmin for myoblasts and cardiac Troponin T for cardiomyocytes, nuclei are stained with DAPI.

In conclusion, micropatterning allow to print protein with micrometric precision, and thus to gain a micrometric control over cell culture. This level of accuracy gives the unique opportunity of closely controlling structures at the microscale, conditioning and guiding the geometry and spatial organization of the cultured systems.

2.4 Electro-physiological stimulation

Since Galvani's very first experiments demonstrating the existence of "animal electricity" in the mid-1700s[24], the knowledge on bioelectricity has greatly increased and nowadays we know that electric fields play a key role in several biological processes: endogenous direct-current (DC) electric field (EF) are present in

developing and regenerating animal tissues and wound healing (Fig. 2.9B), they guide cell movement and growth[25]. Electrical stimulation has also found several clinical applications: the ability of electrical stimulation protocols to improve skeletal muscle performance in healthy and dysfunctional muscle is widely accepted and routinely demonstrated[26]. Electrical activation of skeletal muscle has important clinical applications. These principles are applied in the treatment of respiratory paralysis (stimulation of the diaphragm, or more directly of the phrenic nerve), in the correction of scoliosis (stimulation of paravertebral muscles), in the treatment of paraplegia (stimulation of the lower limb muscles), and in orthopaedics (rehabilitation of muscular masses after prolonged inactivity). In cardiology, functional electrostimulation of skeletal muscles has been used to assist ventricular function by way of surgical procedures which generally involve the use of autologous muscle in the form of a latissimus dorsi muscle flap wrapped around the ventricles and electrostimulated in a rhythmic fashion during systole[27].

In general, skeletal and cardiac muscles are excitable tissues, characterized by the propagation of action potential along axons that innervate them and gradients of ions across their membranes. For example, the cardiomyocyte (CM) is the most physically energetic cell in the body, contracting more than three billion times in an average human lifespan, and pumping over 7000 L of blood per day along 160000 km of blood vessels[28]. Its contractile apparatus of sarcomeres and high metabolic activity are supported by the high density of mitochondria. Electrical signal propagation is provided by specialized intercellular connections, gap junctions[29]. The control of heart contractions is almost entirely self-contained, and can be attributed to a groups of specialized cardiomyocytes (pacemakers). Contraction of the cardiac muscle is driven by the waves of electrical excitation generated by pacing cells that spread rapidly along the membranes of adjoining CMs and trigger release of calcium, which in turn stimulates contraction of the myofibrils. Electromechanical coupling of the myocytes is crucial for their synchronous response to electrical pacing signals[30]. Thus, in line with the propose of mimicking the *in vivo* physiological conditions, exogenous electrical stimulation need to be taken in account for muscle engineering.

The exposure of cell culture to neuro-physiological stimulation can be achieved either through co-culture with neuronal tissue or through the generation of an electric field between two electrodes immersed in the medium culture. Co-cultivation of primary myoblasts with neuronal spinal cord slices results in the formation of contracting myofibers with a high level of differentiation, suggesting that innervation of skeletal muscle tissue *in vitro* and the exchange of signals between muscle and nerve cells is essential for the development of mature tissue[31]. The drawbacks of this strategy are, from the experimental point of view, the requirement of *in vitro* culture of a sensitive cell type and, in sight of a clinical application, the lack of availability of human neuronal tissue. The use of specifically designed devices (electrodes + a support + waves generator) for electrical stimulation is greatly easier and allow the fine control of crucial parameters, such as amplitude, duration and frequency of the imposed pulse. It was demonstrated that *in vitro* exposure to electric field is beneficial to primary rat cardiomyocytes cultured as monolayer and as engineered construct, inducing cell alignment and coupling, increasing the amplitude of synchronous construct contractions by a factor of 7, and resulting in a remarkable level of ultrastructural organization[32]. Moreover, exogenous electric field enhances the differentiation toward cardiac lineage of mouse embryonic stem cells[33]. Concerning skeletal muscles, the use of chronic electrical stimulation to imitate neuronal activity during myogenesis influence the expression of a myosin heavy chain (MHC)[34] and myogenic transcription factors[35]. Satellite cell proliferation increased in electrically stimulated cell cultures[20,36].

2.4.1 Principles of electrical stimulation and devices for cell culture stimulation

One of the simplest of electrical circuits is formed by a resistor connected to the two terminals of a voltage source, or battery, by conducting wires (Fig. 2.9A). Current is normally carried in the conductive wires by electrons. In a physiological solution such as the cytoplasm or the fluids of the extracellular spaces, there are no free electrons to carry charge so current is carried by charged ions such as Na^+ and Cl^- instead. If there is a voltage difference between any two points in a conductive

medium, current will flow. Inevitably then the existence of an EF and the flow of current are interdependent and inseparable events. Importantly, the EF and the current density are vectors, with both magnitude and direction. It is this directional quality of an EF that makes it a candidate spatial organizer, because it can impose directional movement on chemicals in the extracellular environment, on receptor molecules, on cells, and on tissues[25].

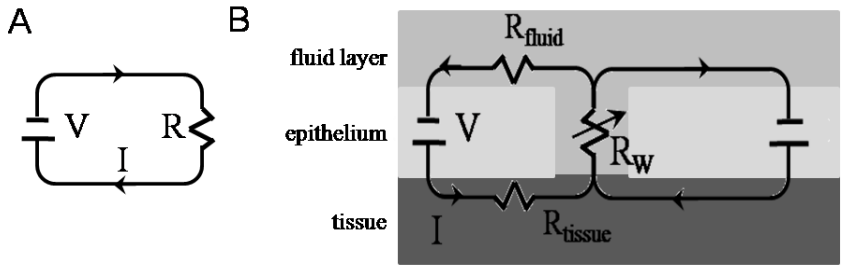

Figure 2.9. A: a simple, non biological electric circuit. Wires connect a battery (V) to a resistor (R). Electrons, which are negatively charged, carry the current (I, arrows) within the wire. B: in an ion-transporting epithelium, the transepithelial potential difference (TEP) of several tens of millivolts acts as a "skin battery" (V). Injury to the epithelium produces a low resistance path by which ions leak out through the wound. The resistance of the wound (R_w) is variable; R_w is higher if the wound is allowed to dry out than if the wound has a moist dressing. In frog skin and corneal epithelium, in which the outer layer of the epithelium is constantly bathed in a conductive fluid, the resistance of the return path of the current (R_{fluid}) is low compared with that within the tissue (R_{tissue}). As a result, most of the lateral potential drop is within the subepidermal tissue layer; therefore, a lateral electric field exists in the region near the wound. Because the direction of current flow is taken to be the direction of flow of positive ions (arrows), the wound is more negative than distal regions within the tissue. The wound therefore represents the cathode of the naturally occurring subepidermal electric field [modified from McCaig et al. Physiol Rev. 2005[25]].

Mimicking the EF in tissue or organ culture involves culturing cells in specially designed chambers, where two electrodes are placed in the medium (electrolyte) and connected to a DC power supply. There are important design features of the experimental set-up that should be taken in account: 1) the culture chambers should be of defined geometry. This allows the EF to be calculated easily and its vector to be controlled; 2) the electrodes material should be biocompatible, so it should not induce a toxic or necrotic response in the adjacent cells, and mechanically stable[37]; 3) the complete device should be autoclavable, in order to ensure the culture sterility; 4) preferentially, it should be easy to use and manipulate, to facilitate operation in the cell culture hood and maintain sterile conditions.

During this Ph.D thesis, two different devices for electric stimulation were developed by chemical engineers of the laboratory and used by the author for: improving the differentiation process of murine muscle precursor cells (MPCs) seeded onto a 3D collagen scaffold (Figure 2.10) (Appendix B); and enhancing the cardiac differentiation of human embryonic stem cells (hESC) (Figure 2.11) (Appendix D).

Electrical stimulation of MPCs seeded onto a 3D collagen scaffold. The apparatus for electric stimulation (Figure 2.10A) was composed of two stainless steel electrodes, 0.8 cm in height and 1 cm in length, which were placed at 14 mm distance. A PDMS holder was specifically designed to fit a 35 mm Petri dish and to keep the electrodes in a position perpendicular to the collagen scaffold immersed in the culture medium. The holder had a central hole of 26×6×6 mm, which allowed to keep the scaffold in a position parallel to the electrical field. The electrodes were connected to a LabView software, programmed to produce a square wave with a 0 V baseline and impulses of 70 mV/cm for 3 ms with frequency of 33.3 mHz. Electrical stimuli were applied starting 3 days after cell seeding on collagen scaffold, and maintained for additional 4 days.

Electrical stimulation did not affect cell viability and increased by 65.6% the release rate of NO_x, an early molecular activator of satellite cells (adult stem cells of skeletal muscles)[38] *in vivo*. Importantly, electrical stimulation increased the expression of two myogenic markers, MyoD and desmin[39]. The complete manuscript is reported in Appendix B.

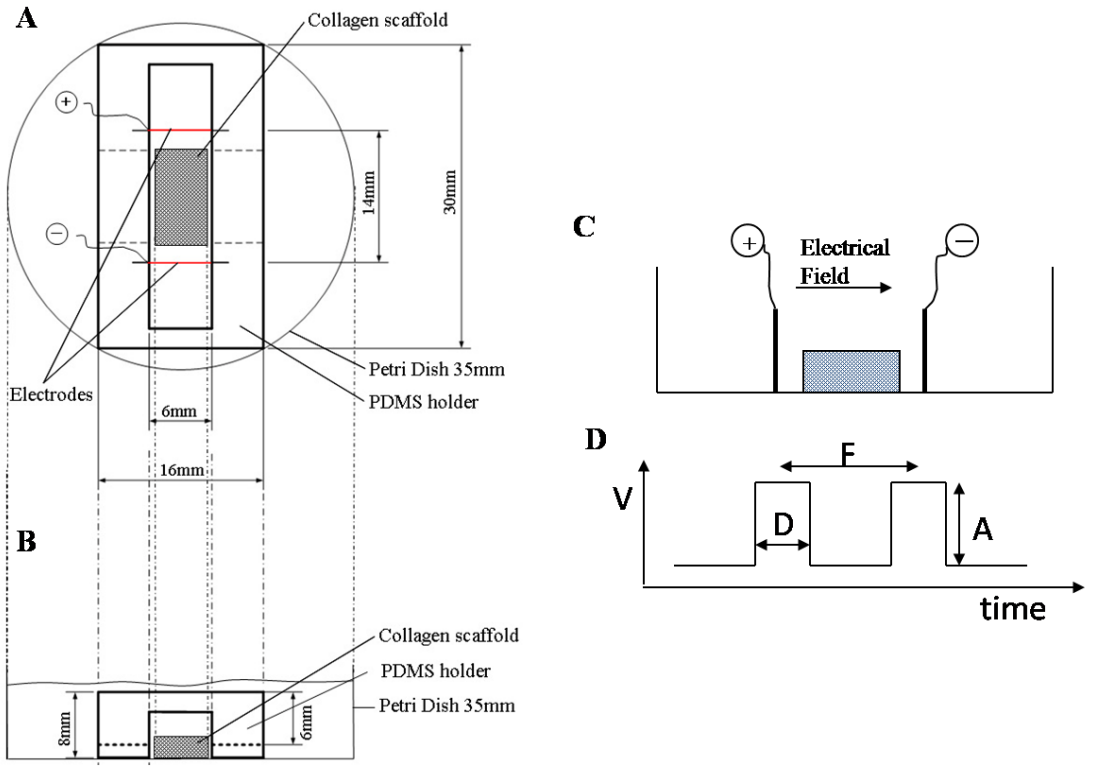

Figure 2.10. Schematic of the experimental set-up used for electrophysiological stimulation of MPCs. (A and B) Top and front view of electrical stimulation apparatus: 35 mm Petri dish, PDMS holder, stainless steel parallel plate electrodes placed at 14 mm separation distance and collagen scaffold. Symbols '+' and '–' show connections to the electric field function generator. (C) Schematic view of lateral prospective of 3D scaffold between two electrodes. (D) Square pulsed electric potential (V) applied to the cells within 3D scaffold: A: amplitude = 70 mV/cm; D: duration = 3 ms; F: 1/frequency = 33.3 mHz.

Electrical stimulation of hESC. When cultured in suspension, hESC form aggregates termed embryoid bodies (EBs) (see chapter 4 for detailed description). EBs have the ability to differentiate spontaneously *in vitro* into beating areas containing cardiomyocytes, but the yield is relatively low. The electrical stimulation apparatus was built in PDMS. It was characterized by an array of 4 by 4 wells. Electrodes of 1.3 mm of diameter were inserted in both sides of each row. Independent stimulation of each chamber was guaranteed by the PDMS insulation between different rows. The PDMS bioreactor was attached directly to a 75×25 mm glass slide via plasma treatment (Fig. 2.11). The optical transparency of the glass slide allowed the EB observation during the stimulation. EBs were suspended in the central area of the well (gray area in Figure 2.11A) in a low ionic content "pulsing

buffer" which contained 255 mM sucrose, 1 mM CaCl2, 1 mM MgCl2, and 5 mM HEPES (pH 7.2) and had a conductivity of 500 μS/cm. The electrodes were connected to electrical stimulator generating square-wave electric pulses. A single electrical field pulse with a field strength of 1 V/mm and duration of 1 and 90 s was applied to EBs.

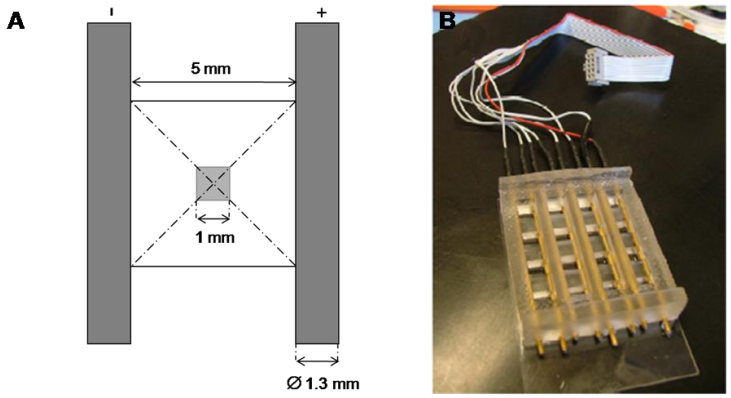

Figure 2.11. Bioreactor for electrical stimulation. A: Schematic representation of a single chamber of stimulation (25mm^2). The electrodes are 5 mm spaced and the EB placed in the gray area (1mm^2). C: Image of the bioreactor.

The electric field applied lead to the generation of intracellular Reactive Oxygen Species (ROS). Cardiac differentiation of stimulated EBs was confirmed by the expression of cardiac troponin T, through immunoflourescence. Part of this work was performed in the lab of Prof. Vunjak-Novakovic, at Columbia University, and a detail description of the results is reported in Chapter 4, while the detailed protocol and bioreactor description is reported in appendix D.

2.5 Microfluidic control of culture conditions

Standard culture methods involving cell culture in Petri dishes cannot be representative of the real state of physiologic systems and therefore often result in unrealistic and uncontrollable biological readouts. Standard cell culture on a Petri dish or multiwell could be considered "batch culture": the medium is changed periodically to the entire culture, thus not allowing for the generation and control of precise patterns of stimulation in space and time. Standard culture systems such as

Petri dishes, can be compared to batch reactors in which conditions are precisely defined only at time zero, and then continuously vary until next medium exchange. Batch processes have unpredictable time scales and, most important, are intrinsically uncontrollable. This strong limitation can be overcome by the use of perfusion as perfused systems offers the advantage of working under well defined and stable steady-state conditions.

2.5.1 Microfluidics devices for cell culture

Taking advantage of the soft-lithography technique (2.2.1), microfluidics is the design and development of miniaturized fluidic devices that manipulate samples at micro- and nano-liter volumes. Due to its extremely small-scale and low cost of production, microfluidics can revolutionize our ability to perform procedures such as highthroughput drug screening, biological and chemical sensing, and genetic analysis[40]. This technique is a beneficial experimental basis for systems biology because: micro-scale fluid flow enables precise and high-resolution microenvironment control; microfluidic devices are generally compatible with imaging and microscopy techniques; the ability to upscale and array microfluidic devices facilitates highthroughput experimentation. Microfluidics have been adapted to many different applications; bioseparation processes[41], cell-based assays[42], and cell culture devices for applications ranging from studies at a single cell level[43] to the recreation of more complex 3D tissues[44] and the development of diagnostics platforms[45]. Upon shrinking to the microscale, the dominant forces of physical phenomena change and three characteristics of physics at the micro-scale are particular relevant: laminar flow, diffusion, surface area to volume ratio. Due to the miniscule characteristic lengths of microfluidic channels (down to the order of 1 mm), microfluidic flow is generally laminar.

Laminar flow allows for the precise calculation of mass transport (i.e. the time required for the delivery of metabolite and catabolite removal) as a function of time and fluid streamlines remain constant over time, thus mixing of microfluidic streams occurs primarily by diffusion. The time it takes a particle to travel, one-dimensionally, over a distance is directly proportional to the square of that distance.

Consequently, for large distances, diffusive motion occurs on a high enough timescale to generally be negligible. When operating on the microscale, however, diffusion can account for a significant portion of mass transport. When moving to the microscale, the relative amount of surface area exposure experienced by a volume of fluid greatly increases. These first two properties (laminar flow and controlled diffusion) enable the creation of unique experimental platforms using microfluidics. Laminar flow allows barrier-free adjacent perfusion of different reagents, which can be used for localized treatment of cells (Fig. 2.12B,C). Controlled diffusion and laminar flow in combination can be used to construct chemical gradients with sub-cellular resolution[40].

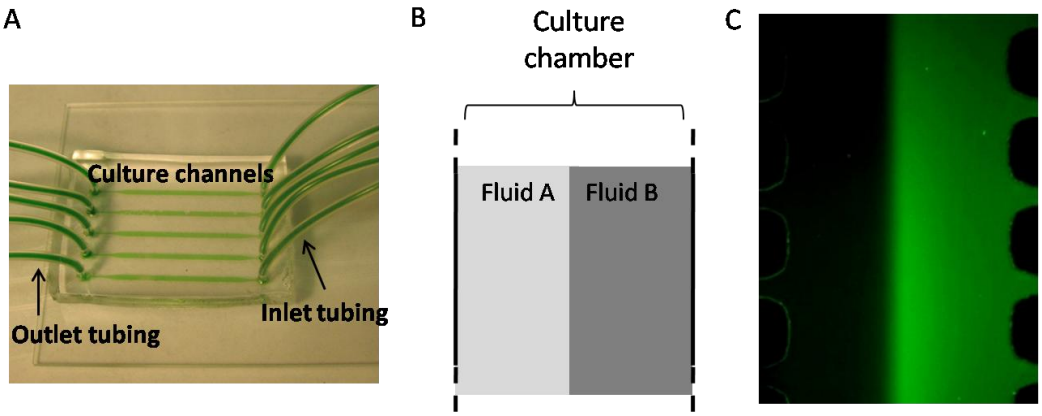

Figure 2.12. Microfluidics channel. A: Image of the microfluidic channels, connected to inlet and outlet tubing and filled with a green solution; B: schematic representation of a microfluidic culture channel where two fluids A and B flow side by side. C: real image of adjacent perfusion of two different fluids in a single channel.

During this Ph.D thesis, a microfluidic device was used for the culture of primary mouse aorta endothelial cells (PMAEC) and the analysis of synergic application of medium flow and glucose concentration on their morphology. This work was performed in order to test microfluidic systems with cell culture, verify their biocompatibility and cellular response.

Hyperglychemia is the main initiating factor for diabetic microvascular disease. High blood levels of glucose promote the formation of Advanced Glycation End Products (AGEs), which are modifications of proteins or lipids due to an hyperglycemic environment, on blood vessel walls, which in turn perturb the

structure and function of vascular cells. To mimic the diabetic physiology *in vitro*, murine endothelial cells harvested from aorta (PMAEC) were cultured inside microfluidic channels (Fig. 2.12A) with increasing glucose concentration (0.5 mM, 5 mM and 15mM) and cultured both in static and perfused condition (no flow or 0.2 μl/min), in order to subject cells to shear stress. The master of this particular microfluidics device was designed and developed with the same technique described in § 2.2.1.1, and in figure 2.13A the schematic is reported. The device was then produced via replica molding, by pouring 35 ml of PDMS over a master placed in a 150 mm Petri dish. The ports for fluidic connections (inlet and outlets) were punched through a biopsy punch with a 21-gauge. The PDMS was irreversibly bonded to the glass with plasma treatment. After coating the bottom surface of each lane with 20 μg/ml fibronectin, 15×10^3 cells/channel cells were seeded and cultured in static conditions (medium change daily) for up to 7 days or in dynamic conditions for up to 2 days. In dynamic culture, the constant medium flow was controlled by a syringe pump and set at 0.2 μl/min.

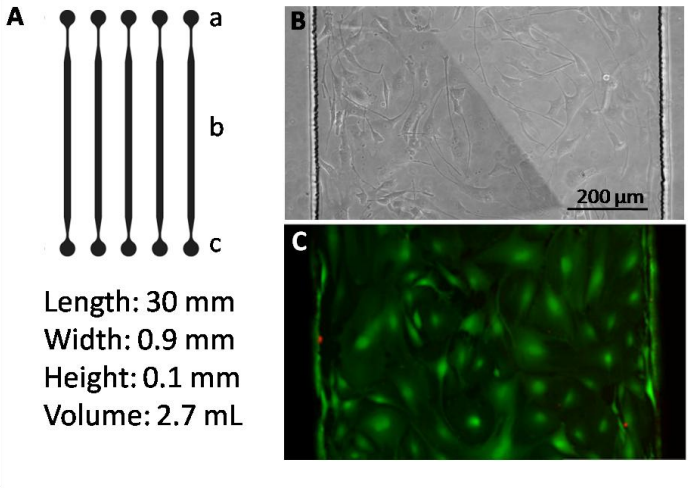

Figure 2.13. Culture of PMAEC cells in the microfluidic channels. **A**: schematic representation of the channels and dimensions. Bright field (**B**) and live and dead assay (**C**) of PMAEC after 2 days of culture in the channels. In C: live cells are stained in green, dead cells in red.

Changes in cell shape and morphology were observed in high glucose concentration culture (Fig. 2.14).

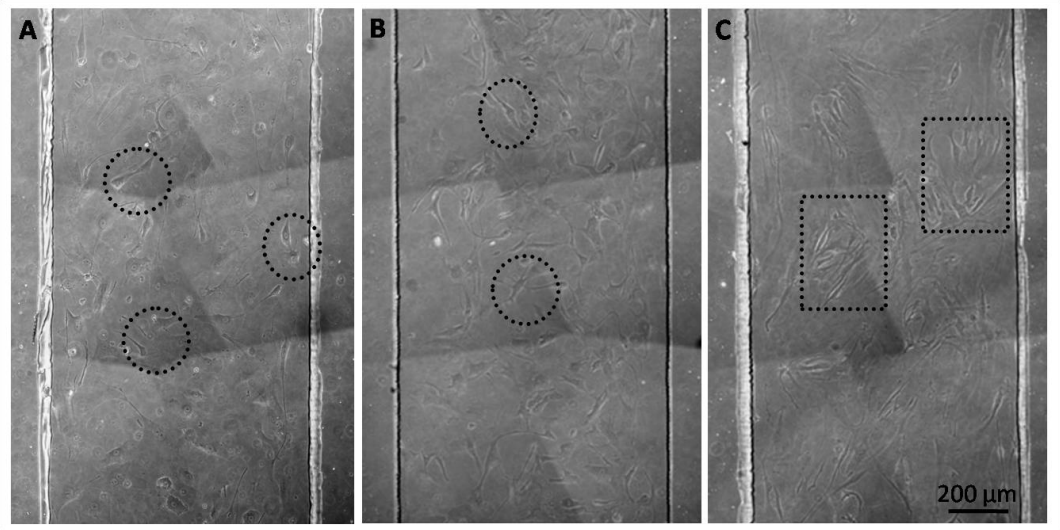

Figure 2.14. PMAEC morphology after 10 days of culture in Control (A), Low-glucose (B) and High glucose (C). Black circles and boxes highlight the cell morphology.

In particular, actin immunostaining revealed that PMAECs cultured in high glucose had enhanced cell spreading and protrusions, in comparison to control and Low-Glucose (Fig. 2.15). In addition, high glucose concentration resulted in increased generation of AGEs (detected through ELISA assay) and the simultaneous application of medium perfusion further increased the generation of AGEs (Fig. 2.16).

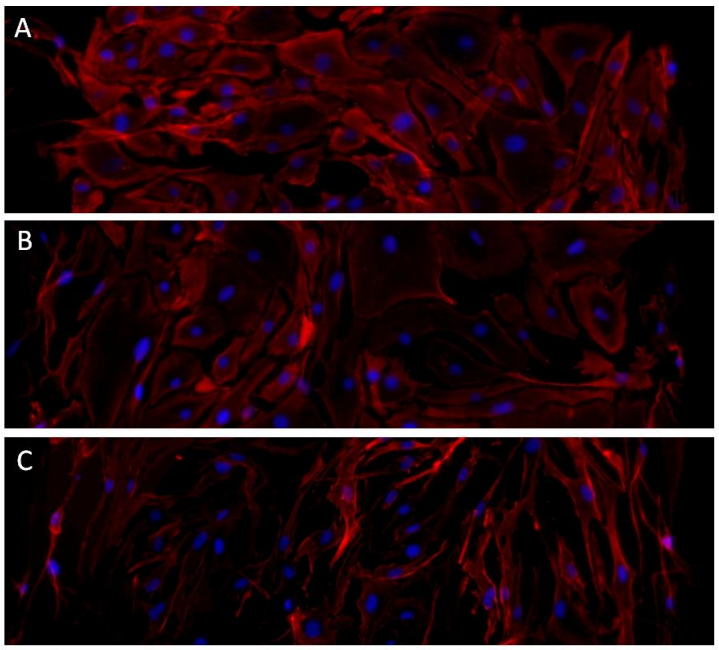

Figure 2.15. Actin immunostaining of PMAEC after 10 days of culture in Control (A), Low-glucose (B) and High glucose (C). Nuclei were counterstained with DAPI. Magnification=100X.

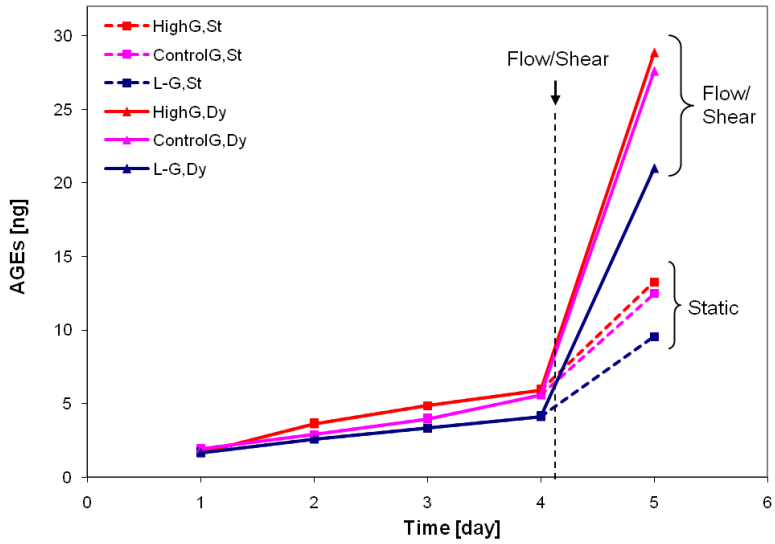

Figure 2.16. The graph reports the concentration of AGEs (in ng) released in the culture medium in function of time (in days) of culture. The medium perfusion started at day 4. Dotted lines represent static culture (st), while continuous lines report the perdused culture (Dy). HighG= high glucose concentration, L-G=Low-Glucose and ControlG=control glucose concentration.

This work has been done in the prospective of coupling the engineered tissues (both skeletal and cardiac muscles) to a microfluidic platform. Indeed, the feasibility of cell culture into microfluidic channels and the biocompatibility of the materials used were proved. It allowed the optimization of the methodologies for microfluidic device manipulation in order to maintain the culture sterility and the cell survival after exposure to medium perfusion.

This work verified the feasibility of coupling the engineered tissues (both skeletal and cardiac muscle) to a microfluidic platform in order to develop an highthroughput device for drug screening and therapy development.

2.6 References

1 Flanagan, L.A. et al., Neurite branching on deformable substrates. *Neuroreport* **13** (18), 2411 (2002).

2 Engler, A. J. et al., Myotubes differentiate optimally on substrates with tissue-like stiffness: pathological implications for soft or stiff microenvironments. *Journal of Cell Biology* **166** (6), 877 (2004).

3 Engler, A. J., Sen, S., Sweeney, H. L., and Discher, D. E., Matrix Elasticity Directs Stem Cell Lineage Specification. *Cell* **126** (4), 677 (2006).

4 Khetani, S. R. and Bhatia, S. N., Engineering tissues for in vitro applications. *Current Opinion in Biotechnology* **17** (5), 524 (2006).

5 Burdick, J. A. and Vunjak-Novakovic, G., Engineered Microenvironments for Controlled Stem Cell Differentiation. *Tissue Engineering: Part A* **14** (00), 1 (2008).

6 Daley, W. D., Peters, S. B., and Larsen, M., Extracellular matrix dynamics in development and regenerative medicine. *Journal of Cell Science* **121**, 255 (2007).

7 Engler, A. J. et al., Embryonic cardiomyocytes beat best on a matrix with heart-like elasticity: scar-like rigidity inhibits beating. *Journal of Cell Science* **121** (22), 3794 (2008).

8 Chargé, S. B. P. and Rudnicki, M. A., Cellular and Molecular Regulation of Muscle Regeneration. *Physiological Reviews* **84** (1), 209 (2004).

9 Alexakis, C., Partridge, T., and Bou-Gharios, G., Implication of the satellite cell in dystrophic muscle fibrosis: a self-perpetuating mechanism of collagen overproduction. *American Journal of Physiology-Cell Physiology* **293** (2), C661 (2007).

10 Chan, G. and Mooney, D. J., New materials for tissue engineering: towards greater control over the biological response. *Trends in Biotechnology* **26** (7), 382 (2008); Khademhosseini, A. and Langer, R., Microengineered hydrogels for tissue engineering. *Biomaterials* **28** (34), 5087 (2007); Lutolf, M. P. and Hubbell, J. A . Synthetic biomaterials as instructive extracellular microenvironments for morphogenesis in tissue engineering *Nature Biotechnology* **23** (1), 47 (2005).

11 Burnham, M. R., Turner, J. N., Szarowski, D., and Martin, D. L., Biological functionalization and surface micropatterning of polyacrylamide hydrogels. *Biomaterials* **27** (35), 5883 (2006).

12 Falconnet, D., Csucsb, G., Grandina, H. M., and Textora, M., Surface engineering approaches to micropattern surfaces for cell-based assays. *Biomaterials* **27** (16), 3044 (2006).

13 Elisseeff, J., Puleo, C., Yang, F., and B., Sharma, Advances in skeletal tissue engineering with hydrogels. *Orthodontics & Craniofacial Research* **8** (3), 150 (2005).

14 Burdick, J. A., Khademhosseini, A., and Langer, R., Fabrication of gradient hydrogels using a microfluidics/photopolymerization process. *Langmuir* **20** (13), 5153 (2004).

15 Almany, L. and Seliktar, D., Biosynthetic hydrogel scaffolds made from fibrinogen and polyethylene glycol for 3D cell cultures. *Biomaterials* **26** (15), 2467 (2005).

16 Leach, J. B. and Schmidt, C. E., Characterization of protein release from photocrosslinkable hyaluronic acid-polyethylene glycol hydrogel tissue engineering scaffolds. *Biomaterials* **26** (2), 125 (2005).

17 Hern, D. L. and Hubbell, J. A., Incorporation of adhesion peptides into nonadhesive hydrogels useful for tissue resurfacing. *Journal of Biomedical Materials Research* **39** (2), 266 (1998).

18 Peyton, S. R. and Putnam, A. J., Extracellular matrix rigidity governs smooth muscle cell motility in a biphasic fashion. *J. Cell. Physiol* **204**, 198 (2005).

19 Berry, M. F. et al., Mesenchymal stem cell injection after myocardial infarction improves myocardial compliance. *American Journal of Physiology-Heart and Circulatory Physiology* **290** (6), H2196 (2006).

20 Flaibani, M. et al., Muscle differentiation and myotubes alignment is influenced by micro-patterned surfaces and exogenous electrical stimulatio. *Tissue Engineering* **in press.** (2009).

21 Kumar, A. and Whitesides, G.M. , Features of gold having micrometer to centimeter dimensions can be formed through a combination of stamping with an elastomeric stamp and an alkanethiol ink followed by chemical etching. *Applied Physics Letters* **63** (14), 2002 (1993).

22 Ruizab, S. A. and Chen, C. S., Microcontact printing: a tool to pattern. *Soft Matter* **3** (2), 168 (2007).

23 Singhvi, R. et al., Engineering cell shape and function. *Science* **264** (5159), 696 (1994).

24 Geddes, L. A. and Hoff, H.E., The discovery of bioelectricity and current electricity. The Galvani-Volta controversy. *IEEE Spectrum* **8**, 38 (1971).

25 McCaing, C. D., Rajnicek, A. M., Song, B., and Zhao, M., Controlling Cell Behavior Electrically: Current Views and Future Potential. *Physiological Reviews* **85** (3), 943 (2005).

26 Kern, H. et al., Standing up with denervated muscles in humans using functional electrical stimulation. *Artificial Organs* **23** (5), 447 (1999); Stein, R. B., Chong, S. L., James, K. B., and , et al. . , Electrical stimulation for therapy and mobility after spinal cord injury. *Progress in Brain Research* **137**, 27 (2002).

27 Chachques, Juan C. et al., Cardiomyoplasty for refractory heart failure. *The Asia Pacific Heart Journal* **5** (2), 81 (1996).

28 Radisic, M. et al., Biomimetic approach to cardiac tissue engineering. *Philosophical Transactions of the Royal Society B-Biological Sciences* **362** (1484), 1357 (2007).

29 Brilla, C. G. et al., Pharmacological modulation of cardiac fibroblast function. *Herz* **20** (2), 127 (1995).

30 Severs, N. J. , The cardiac muscle cell *Bioessays* **22** (2), 188 (2000).

31 Guettier-Sigrist, S. et al., Muscle could be the therapeutic target in SMA treatment. *Journal of Neuroscience Research* **53** (6), 663 (1998); Bach, A. D. , Beier, J. P. , and Stark, G. B. , Expression of Trisk 51, agrin and nicotinic-acetycholine receptor e-subunit during muscle development in a novel three-dimensional muscle-neuronal co-culture system. *Cell and Tissue Research* **314** (2), 263 (2003); Askanas, V. et al., De novo neuromuscular junction formation on human muscle fibres cultured in monolayer and innervated by foetal rat spinal cord: ultrastructural and ultrastructural-cytochemical studies. *Journal of Neurocytology* **16** (4), 523 (1987).

32 Radisic, M. et al., Functional assembly of engineered myocardium by electrical stimulation of cardiac myocytes cultured on scaffolds. *Proceedings of the National Academy of Sciences of the United States of America* **101** (52), 18129 (2004).

33 Sauer, H., Rahimi, G., Hescheler, J., and Wartenberg, M., Effects of Electrical Fields on Cardiomyocyte Differentiation of Embryonic Stem Cells. *Journal of Cellular Biochemistry* **75** (4), 710 (1999).

34 Pette, D. et al., Partial fast-to-slow conversion of regenerating rat fast-twitch muscle by chronic low-frequency stimulation. *Journal of Muscle Research and Cell Motility* **23** (3), 215 (2002).

35 Neville, C. M., Schmidt, M., and Schmidt, J. , Response of myogenic determination factors to cessation and resumption of electrical activity in skeletal muscle: a possible role for myogenin in denervation supersensitivity. *Cellular and Molecular Neurobiology* **12** (6), 511 (1992); Buonanno, A. et al., The MyoD family of myogenic factors is regulated by electrical activity: isolation and characterization of a mouse Myf-5 cDNA. *Nucleic Acids Research* **20** (3), 539 (1992); Putman, C. T., Dusterhoft, S., and Pette, D. , Satellite cell proliferation in low frequency-stimulated fast muscle of hypothyroid rat. *American Journal of Physiology-Cell Physiology* **279** (3), C682 (2000).

36 Pedrotty, D. M. et al., Engineering skeletal myoblasts: roles of three-dimensional culture and electrical stimulation. *American Journal of Physiology-Heart and Circulatory Physiology* **288** (4), H1620 (2005).

37 Merrill, D. R., Bikson, M., and Jefferys, J. G. R., Electrical stimulation of excitable tissue: design of efficacious and safe protocols. *Journal of Neuroscience Methods* **141** (2), 171 (2005).

[38] Mauro, A. , Satellite cell of skeletal muscle fibers. *The Journal of Biophysical and Biochemical Cytology* **9**, 493 (1961).

[39] Serena, E. et al., Electrophysiologic stimulation improves myogenic potential of muscle precursor cells grown in a 3D collagen scaffold. *Neurological Research* **30** (2), 207 (2008).

[40] Breslauer, D. N., Lee, P. J., and Lee, L. P., Microfluidics-based systems biology. *Molecular BioSystems* **2** (2), 97 (2006).

[41] Zhang, X., Cooper, J. M. , Monaghan, P. B. , and Haswell, S. J. , Continuous flow separation of particles within an asymmetric microfluidic device. *Lab on a Chip* **6** (4), 561 (2006).

[42] McClain, M. A. et al., Microfluidic devices for the high-throughput chemical analysis of cells. *Analytical Chemistry* **75** (21), 5646 (2003); El-Ali, J. , Sorger, P. K. , and Jensen, K. F. , Cells on chips. *Nature* **442** (7101), 403 (2006).

[43] DiCarlo, D., Wu, L.Y. , and Lee, L.P., Dynamic single cell culture array. *Lab on a Chip* **6** (11), 1445 (2006).

[44] Hui, E.E. and Bhatia, S.N. , Micromechanical control of cell-cell interactions. *Proceedings of the National Academy of Sciences of the United States of America* **104** (14), 5722 (2007).

[45] Toner, M. and Irimia, D. , Blood-on-a-chip. *Annual Review of Biomedical Engineering* **7** 77 (2005).

CHAPTER 3

Microscale tissue engineering of human skeletal muscle

This chapter describes the human functional and dystrophic skeletal myotubes obtained through the microscale technologies described in Chapter 2. In particular, the key role of cell micropatterning and mechanical properties of the substrate in human myoblasts differentiation is highlighted and the improvements obtained in comparison to standard culture methodologies are shown. In addition, the potential use of the engineered tissue as an *in vitro* model for Duchenne Muscular Dystrophy is discussed. The future prospective and the implementation of the obtained tissue are presented, based on the author knowledge developed during this PhD.

3.1 Skeletal muscle physiology

Skeletal muscle represents the largest tissue mass in the body, constituting 40% to 45% of total body weight. Skeletal muscles are responsible for maintenance of structural contours of the body and create voluntary movement, by applying force to bones and joints via contraction. They generally contract voluntarily (via somatic nerve stimulation), although they can contract involuntarily through reflexes. The process of myogenesis during *in vivo* development results in a well-organized, hierarchically structured tissue, where fibers are arranged in highly dense

unidirectional assemblages, allowing the generation of a large vectorial muscular power[1] (Fig. 3.1). Topology is thus a key propertie of skeletal muscles.

The basic structural element of this tissue is the muscle fiber or myofiber (Fig. 3.1C). Its cytoplasm, called the sarcoplasm, contains a cellular matrix and several organelles, including the Golgi apparatus, mitochondria, sarcoplasmic reticulum, lipid droplets, glycogen, and myoglobin. The muscle fiber is a syncytium derived from the fusion of multiple myoblasts (myogenic precursor cells). Briefly, the myoblasts fuse to form long, cylindrical, multinucleated myotubes that exhibit central nucleation. Once the myonuclei shift from a central position to a subsarcolemmal position, the muscle cells are usually termed myofibers. The fiber arrangement, which is an important determinant of the functional and contractile properties of the skeletal muscle, may be parallel or oblique to the long axis of the muscle. The basal lamina or the basement membrane constitutes the 100 to 200-nm-thick external connective-tissue layer[2]. It contains a number of proteins, including collagen, fibronectin, laminin, and many glycoproteins. Separate cells called satellite cells are located between the basal lamina and plasma membrane and play a key role in the muscle regeneration process[3]. Satellite cells proliferate following muscle trauma and their. progeny (myoblasts) begin to fuse and form multinucleated myotubes after a few cell divisions. The functional unit of muscle contraction in both skeletal and cardiac muscles is the sarcomere (Fig 3.1 D-F), whose tandem repetitions give rise to the typical striations of striated muscles. The sarcomere is divided into four major compartments: the Z-disc, I band, A band and M-line, with one sarcomere being defined as stretching from one Z-disc to the next (Fig. 3.1 D,F). The Z-band anchors the thin (actin) filaments of the I-band, the M-line the thick (myosin) filaments of the A band. Despite the major protein components of the sarcomere having been known for many decades, novel sarcomeric proteins continue to be identified (Fig 3.1F)[4,5].

Skeletal muscle function is under the control of a nerve that enters the muscle at its motor point. Each nerve-cell axon branches many times, and each myofiber is contacted by one nerve terminal. The point of contact between the myofiber and the nerve is called the motor end plate of the neuromuscular junction. In general,

the initial step in muscle contraction involves the release of acetylcholine by the presynaptic axons.

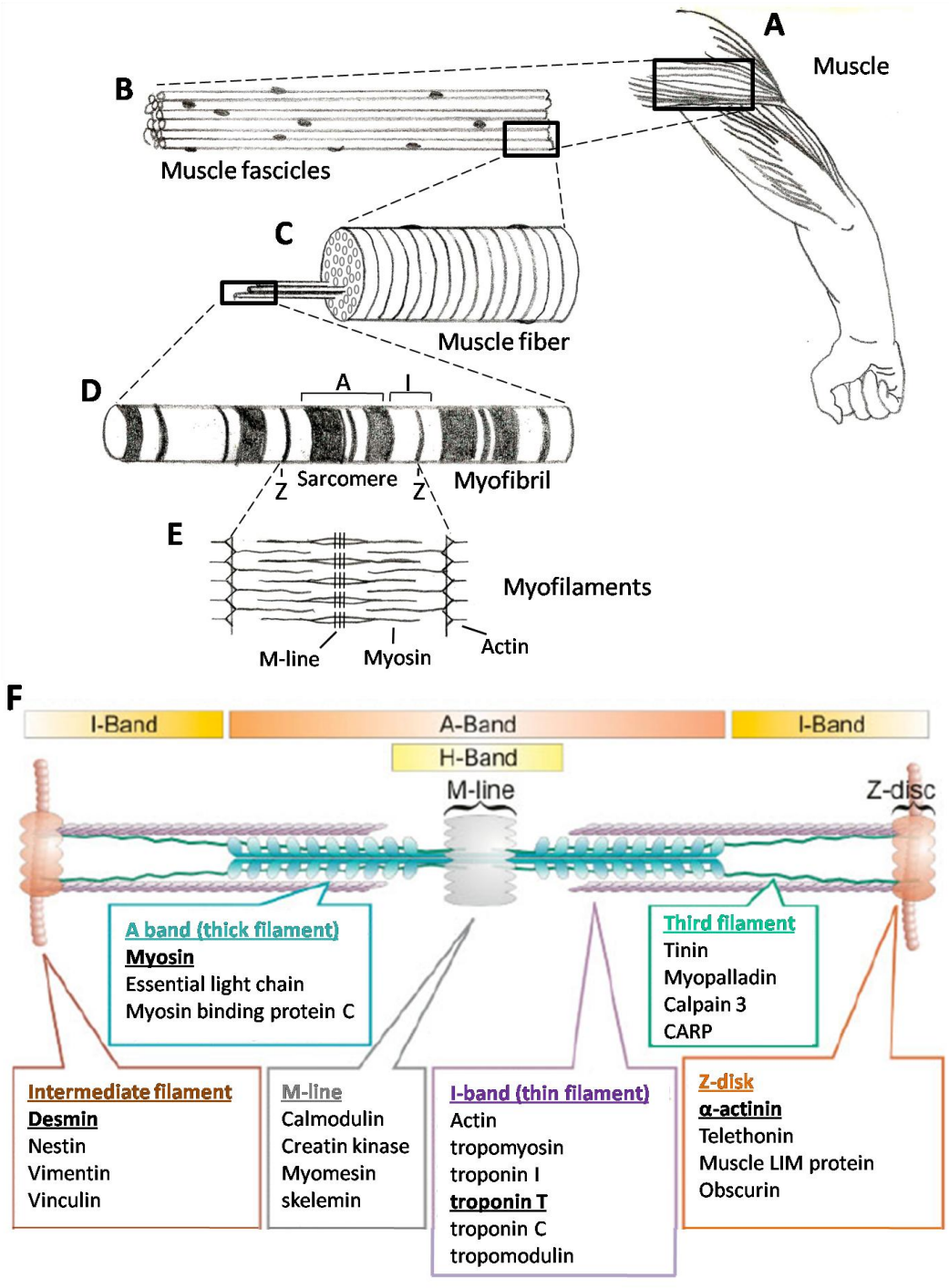

Figure 3.1. Schematic representation of skeletal muscle architecture: from the entire muscle (A) down to the sarcomere (E). (F): schematic diagram showing the major compartments of the sarcomere. Proteins known for each compartment are listed, and in bold are highlighted the proteins analyzed in this work (modified from Laing and Nowak, BioEssays, 2005[4]).

The acetylcholine released binds to the acetylcholine receptors of the myofibers (postsynaptic area) and consequently depolarizes the cell. The depolarization triggers an action potential that passes along the length of the myofibers, resulting in the release of ionic calcium from the sarcoplasmic reticulum. The calcium that is released causes the contractile proteins (actin and myosin) to interact and to generate force in a stepwise manner. Indeed, calcium causes a conformational change of troponin, allowing the interaction between actin and myosin and consequently resulting in muscle contraction (Fig. 3.1E,F). Finally, the acetylcholine is deactivated by the enzyme acetylcholinesterase (or by other less specific cholinesterases), muscle relaxation occurs, the intracellular calcium is transported in the transverse tubules within the myofiber, and the troponin prevents the interaction between the actin and myosin molecules[2].

Besides the highly organized architecture and the topology of skeletal muscle, one of the key feature is the extra cellular matrix (ECM). Although the various components have been commonly assumed to provide a mere passive space-filling substrate to maintain the structural integrity of the muscle, recent works are enlightening its role in several cellular processes[6]. In particular, the mechanical properties of ECM have a key role in muscle differentiation[7,8]. Engler and colleagues demonstrated the existence of an optimum value of substrate stiffness for *in vitro* differentiation of a murine muscle cell line, C2C12, and mouse primary myoblasts. The mechanical properties (thus the stiffness as well) of a substrate can be evaluate measuring the elastic modulus, E. Engler's lab demonstrated that the physiological elastic modulus of a mouse skeletal muscle is $E \approx 12 \pm 4$ kPa, and they showed that a substrate with such a physiological E value leads to an optimum differentiation of skeletal myoblasts[7]. Moreover, the importance of this parameter is also demonstrated by the active role of ECM stiffness in the pathogenesis of Duchenne Muscular Dystrophy (DMD)[9]. The most notable change in dystrophic muscles is the intense generation of fibrous tissue in the interstitial space due to the chronic inflammation of the muscle[10] and the biosynthesis of ECM molecules, especially collagens type I and type III, whose accumulate in the interstitial space, originating a tissue with increased stiffness[11] ($E \approx 18 \pm 6$ kPa [7]).

3.2 Human Duchenne Muscular Dystrophy engineered *in vitro*

DMD is the most common, lethal, inherited disease of childhood, affecting 1 of 3500 boys born worldwide[12]. This disease results from mutations in the dystrophin gene that lead to either a complete loss or loss of critical functional domains of the membrane associated protein, dystrophin[13]. Loss of dystrophin from the cell membrane results in a mechanically weaker membrane that is more easily damaged during muscle contraction. Muscle inflammation, necrosis, and fibrosis occur as direct or indirect consequences of dystrophin deficiency so that DMD patients experience severe and progressive loss of muscle mass and function[14]. Typically, DMD patients are limited to wheelchair mobility by 9–12 y of age, and die by the late teens or 20s, often because of complications that are secondary to respiratory muscle wasting[15]. Twenty years ago the genetic defect underlying DMD was mapped to chromosome Xp21 in humans. This gene is the largest identified to date[16] and can accommodate production of several dystrophin isoforms through alternative promoter usage and splicing of pre-mRNA. The predominant dystrophin isoform found in skeletal and cardiac muscles is an ~427 kDa cytoskeletal protein predicted to contain 3685 amino acids[14]. In skeletal muscle fibers, full-length dystrophin accumulates predominantly at the cytoplasmic face of the sarcolemma[17]. The distribution of dystrophin along muscle fibers is rather homogeneous, thereby creating a submembranous mesh of dystrophin molecules. Mutations and/or deletions in the dystrophin gene, as seen in DMD patients, prevent the production of dystrophin and lead to its absence in muscle fibers[18]. At the sarcolemma, dystrophin is part of a macromolecular group of proteins collectively referred to as the dystrophin-associated protein complex (DAP)[19]. Several key components of this complex have been well studied in recent years, and their interaction patterns and organization support the notion that dystrophin serves to link the intracellular microfilament network of actin to the extracellular matrix[19,20]. The absence of dystrophin ensues the loss of DAPs at the sarcolemma. Consequently, the absence of this physical link between the interior and exterior of the muscle cell renders the sarcolemma fragile, making muscle fibers susceptible to degeneration during

repeated cycles of muscle contraction and relaxation. The satellite cell response to the ongoing trauma is to replenish injured skeletal muscle with myofibers lacking dystrophin, resulting in multiple cycles of muscle degeneration and regeneration. Ultimately, this exhausts the satellite cell population[21].

Besides, nonstructural roles were described for dystrophin, making it a multifunctional protein. The localization of dystrophin and its associated components at the sarcolemma places them at an appropriate position to serve as a signaling scaffold that is responsive to extracellular stressors[22]. The mounting evidence pointing to a role for the dystrophin complex in localizing signaling mediators argues in favor of the notion that this function may be important in stimulating appropriate downstream cascades in response to various extracellular stimuli. Naturally, these signaling events would not function correctly in a dystrophin-deficient muscle, which likely contributes to the disease pathology.

Two decades have past since the identification of the molecular defect involved in DMD, but there are still no effective cures to significantly alter the relentless progression of the disease. Moreover, due to its multifactorial nature, it is likely that DMD could be treated only by a combination of different approaches. On the other hand, costs and time for the development of new drugs or therapies is exponentially increased over the last years (§ 1.2 and 1.3). In this scenario, the development of an *in vitro* model would be of paramount importance. It would represent an intermediate step between *in vitro* cell culture and *in vivo* experimentation; it would allow to control many of the independent variables that can lead to the variability of responses *in vivo*; if developed at the microscale, it would be cost-effective enough to permit highthroughput screening and to speed-up the processes of drug and therapy development (§ 1.4).

In this work, human functional dystrophic myotubes were obtained from human primary myoblasts of healthy and DMD affected donors. The cell culture substrate was engineered through the microscale technologies described in chapter 2, in order to reproduce the major physiological stimuli of the native skeletal muscle, cell topology and mechanical stimuli, which optimally direct myoblasts differentiation *in vivo* (Table 3.1).

Table 3.1: Key features of skeletal muscle (skM) *in vivo* are illustrated. In parallel the microscale technologies applied *in vitro* are reported, in order to reproduce the key features of the native tissue.

In vivo **skM**	***In vitro*** **required features**	***In vitro*** **strategy**	**Improvement obtained**
Highly organized tissue	Topology control over the cell culture	Micropatterning	Myoblasts alignment improved their differentiation in myotubes (§ 3.2.2; appendix A)
Soft tissue	Soft substrate with tissue-like mechanical properties	Hydrogel	Substrates with tissue-like stiffness allowed the formation of the sarcomeric structure of skeletal muscle (§ 3.2.3; appendix A)
Excitable tissue	Electrical stimulation	Electrical stimulation	Improved myoblasts differentiation(§ 3.4; appendix B)

3.2.1 Characterization of human primary myoblasts

A human cell source has been chosen for the development of a skeletal muscle tissue, representative of the human physiology. Primary myoblasts were derived from biopsies of both healthy and DMD affected donors, for a total of five individuals (Table 3.2). The biopsies were provided by Thelethon BioBank service (Istituto Nazionale Neurologico "Carlo Besta", Milano).

Results showed in the following sections were obtained with biopsies number 7475 ad 9208. They were then confirmed with other biopsies.

Table 3.2: Biopsy characteristics. Biopsy identification number, age, sex, and percentage of desmin and MyoD positive cells are reported.

	Biopsy number	Sex	Age	Desmin$^+$ cells (%)	MyoD$^+$ cells (%)
DMD	7475	M	2	89	90
	9374	M	2	88	95
Healthy	9208	M	2	92	92
	9347	F	3	93	91
	9420	M	7	85	91

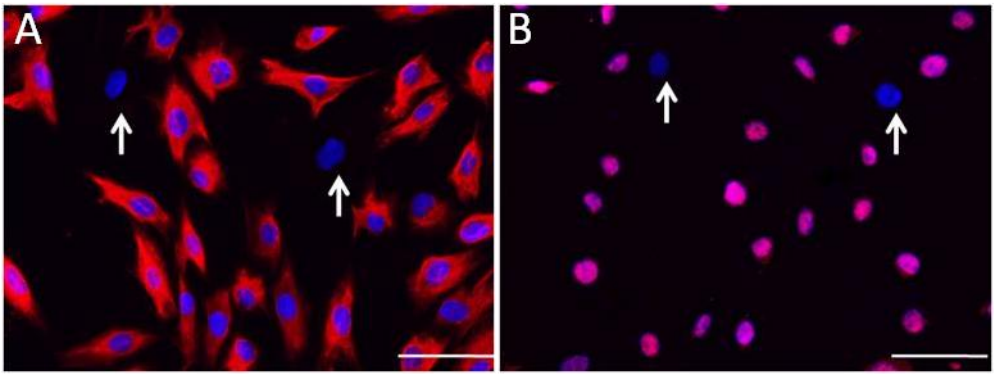

Figure 3.2. Human primary myoblasts characterization. A: Desmin immunoflourescence; B: MyoD immunoflourescence. Arrows indicate negative cells. Nuclei are countestained with DAPI. Scale bar = 75 μm.

The culture had high myogenic potential within early passages *in vitro*: >84% desmin positive cells, >90% MyoD positive cells and a fusion index, highly biopsy related, ranging from an average of 50% for healthy myoblasts to 20% for DMD myoblasts (Fig. 3.2).

3.2.2 Control over myoblast and myotube topology

Human myoblast adhesion was guided through the micropattening of adhesion proteins on the hydrogel surface (described in § 2.2). Based on the literature[23], which reports that muscle differentiation is improved especially in the presence of laminin, collagen[24] and matrigel[25], and the knowledge developed with primary mouse myoblasts (Appendix A), four adhesion proteins were tested: collagen type I,

laminin, fibronectin and matrigel. Collagen micropatterning was not achieved successfully: due to its gelatinous nature, it has been hypothesized that it creates a gel layer over the hydrogel surface, instead of adsorbing on it. Thus collagen pattern easily peeled off, especially when myoblasts started exerting force, resulting in an instable culture, which detached after a couple of days after seeding. Pattern of laminin and fibronectin were performed successfully with a protein concentration of 100 μg/ml (in PBS), while the optimal concentration for matrigel was 2.5 % (in DMEM).

As shown in figure 3.3, myoblasts seeded onto a smooth substrate (glass or Petri dish) adhered in all directions, without any preferential orientation (Fig. 3.3, upper panel). On the contrary, myoblasts on patterned hydrogel were guided in cell adhesion with micrometric precision, as shown in the lower panel of figure 3.3 (§ 2.2). The topological alignment of myoblasts induced the spontaneous fusion into myotubes as soon as 72 hours after seeding (magnification in Fig. 3.3). In some cases, myotubes were observed even before switching to a differentiation medium.

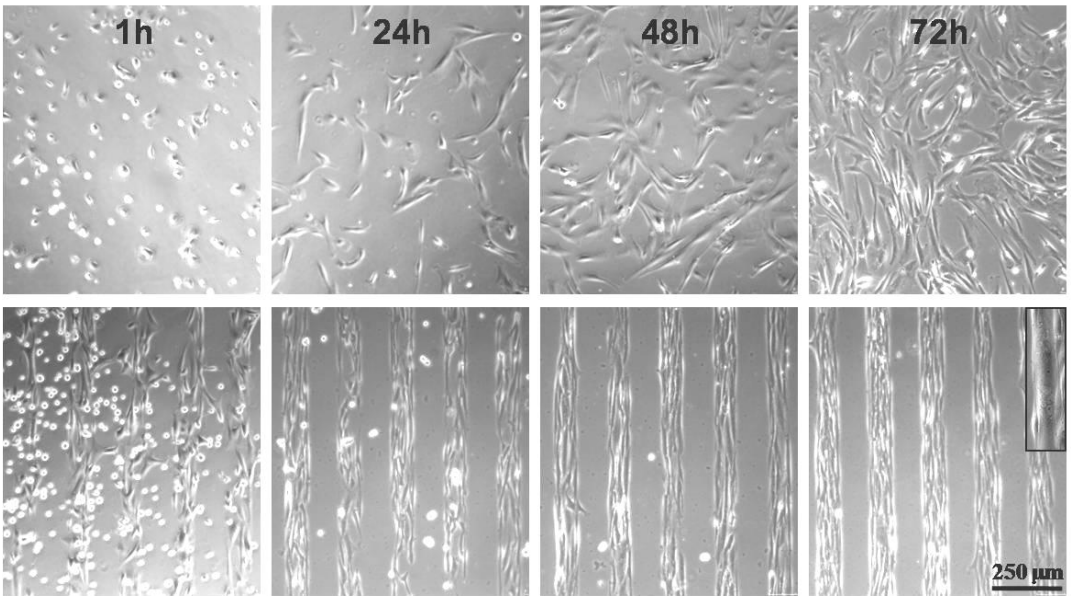

Figure 3.3. Time course of adhesion of human dystrophic myoblasts on glass (upper panel) and on patterned PA hydrogel (lower panel). Upper panel: when cultured on a standard Petri dish, human myoblasts started to align 48 hours after seeding, but 72 hours later they were still far from the confluence. Lower panel: on patterned hydrogel, 24 hours after seeding myoblats were perfectly aligned. After 48 hours they reached confluence and started fusing. The topological alignment of myoblasts induced the spontaneous fusion into myotubes as soon as 72 hours after (see magnification).

For the quantification of myoblasts alignment, the values of tangent to the myotubes in the range [-90, +90] were reported in a polar graph (Figure 3.4 C, D). In the patterned hydrogel, the direction of the pattern was chosen as the preferential direction, in the glass a random direction was selected.

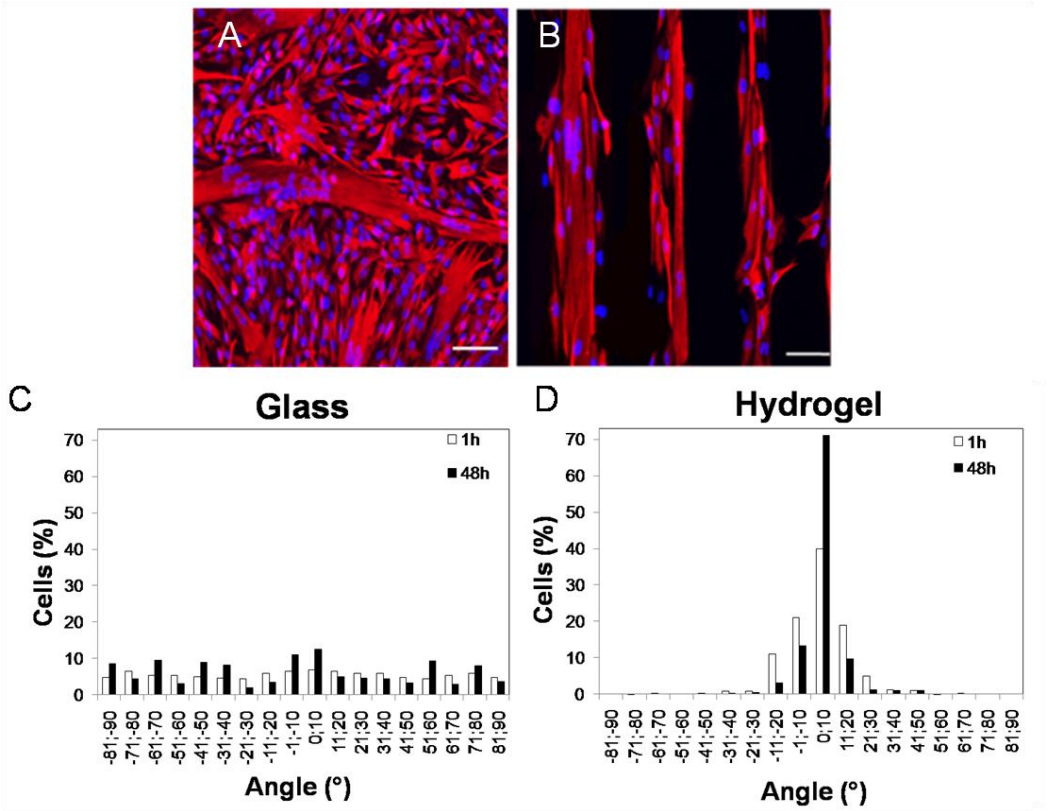

Figure 3.4. Myotubes orientation. A-B: Desmin immunoflourescence of human myotubes on glass (A) and patterned hydrogels (B). Nuclei were counterstained with DAPI. Scale bar = 75 μm C-D: polar graph of tangent values of myotubes on glass (C) and patterned hydrogel (D).

Myotubes, cultured on a substrate without topological cues, developed in a network lacking of a preferential orientation (Fig. 3.4A), as confirmed by the polar graph which show an uniform occurrence frequency in all the directions (Fig. 3.4C). On the contrary, the micropatterned hydrogel leaded to the formation of parallel myotubes (Fig. 3.4B), oriented along the direction of the pattern (Fig. 3.4D).

3.2.3 Sarcomere formation is driven by substrate mechanical properties

Skeletal muscle is a complex and well organized tissue that in normal conditions show little turnover of cells. The process of "myofibrillogenesis", the assembly of proteins into myofibrils, requires the formation of several different types of filaments, the association of additional proteins with the filamentous proteins, and the arrangement of the filaments into the sarcomeric subunits of myofibrils[26]. Recently the extracellular matrix and substrate stiffness, *in vivo* and *in vitro* respectively, was included among the critical variables influencing this process and, in general, the differentiation of striated muscles[7]. In order to investigate this aspect, the differentiation process of human myoblasts was analyzed both on stiff substrates (glass or polystyrene) and PA hydrogels with tissue like mechanical properties. Based on data reported in literature and on experimental measurements (§ 2.1.1.2), the hydrogel composition which better reproduced the elastic properties of skeletal muscle tissue is 10% of acrylamide/bis-acrylamide. The formation of the sarcomere, the fundamental unit of skeletal muscle functionality, has been investigated (Fig. 3.5). In particular, the spatial organization of myosin heavy chain (MHC) and α-actinin was investigated.

After 7 days of culture, myotubes grown on rigid substrates (both glass and plastic) didn't show sarcomeric structures; diffuse and not organized cytoplasmic immunostaining for MHC and α-actinin was observed (Fig. 3.5). Few sarcomeric striations was detected, covering only partially the length of the myotubes, but they mainly occurred when myotubes grown over a layer of myoblasts. These data are supported by Engler and colleagues: they reported that murine myotubes cultured on glass showed visible striations only when grown on top of a cell layer[7]. On the contrary, after 7 days of culture on PA hydrogels (10% PA, corresponding to an elastic modulus E≈15kPa) the majority of myotubes showed the typical sarcomeric striations of Z-disk (α-actinin) and A band (MHC) for the entire length of the myotubes (Fig. 3.5 E,F).

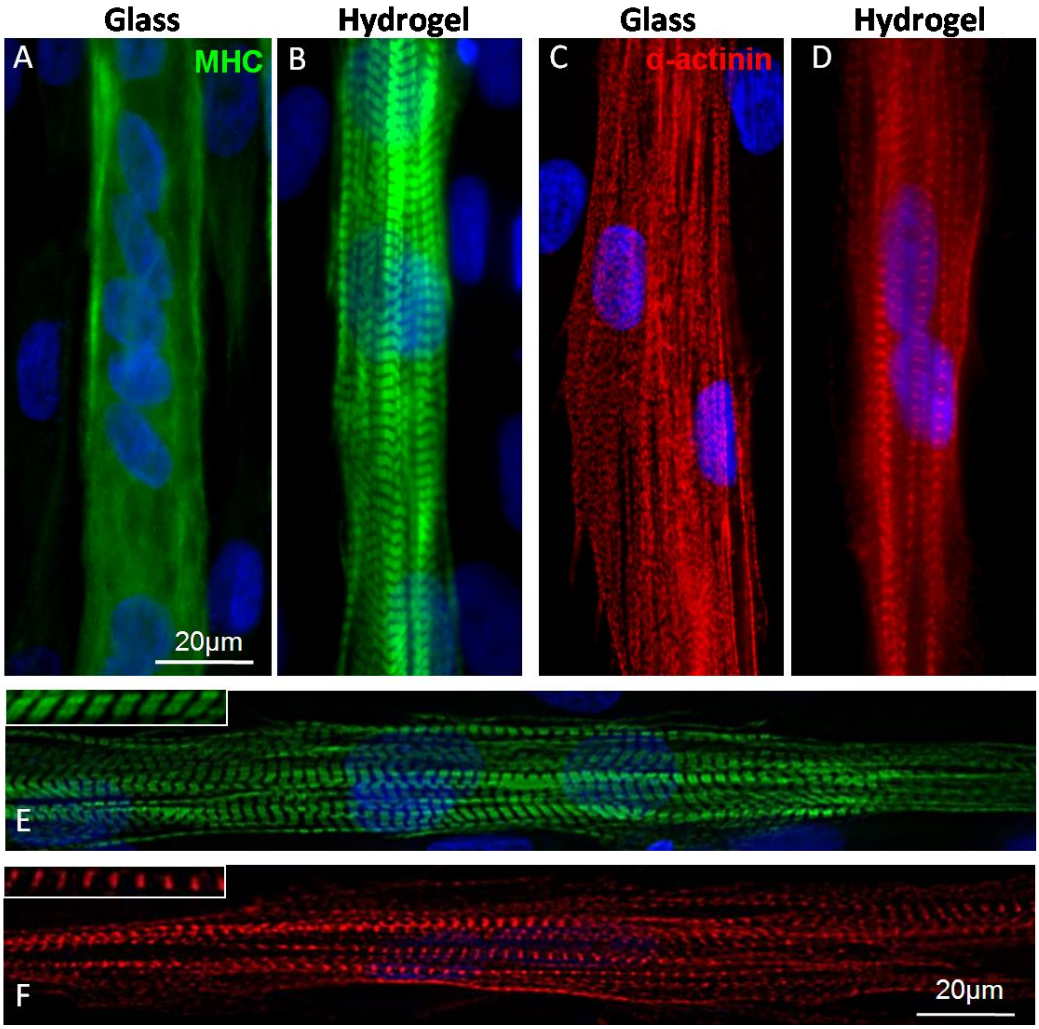

Figure 3.5. Sarcomere formation on human dystrophic myotubes. Immunostaining of α-actinin (C,D,F) and MHC (A,B,E) after 7 days of culture. Myotubes on glass showed a diffuse distribution of these sarcomeric proteins; while MHC and α-actinin revealed a defined sarcomeric organization of myotubes cultured on hydrogel. Nuclei are counterstained with DAPI. Magnification in E and F = 63X.

The dimensions of the entire sarcomere and the A-band corresponded to data reported in literature: 2-2.5 µm between Z-lines and A-band of 1.2 µm[26]. These results reveal that substrates with tissue-like mechanical properties (E≈15kPa) induced a rapid and spontaneous myoblast differentiation in functional myotubes, thus confirming the key role of mechanical properties of the substrate in human skeletal myoblasts differentiation.

The mechanical properties of a PA hydrogel can be easily tuned by varying the composition of the prepolymer solution, as described in paragraph 2.2.1.2. Thus, PA hydrogels with increasing stiffness (Young's modulus), resulting from increasing

concentration of acrylamide/bis-acrylamide, were prepared (Table 3.3) and the influence of this parameter in the formation of sarcomere was evaluate.

Table 3.3: Percentage of acrylamide/bis-acrylamide in the prepolymer solution and elastic modulus of the corresponding hydrogel, obtained by linear correlation of the data reported in paragraph 2.2.1.2.

Acrylamide/bis-acrylamide (%)	**Young's modulus (kPa)**
8	12
10	15
12	18
14	21

Besides substrate stiffness, the influence of biochemical interactions was evaluated, through the patterning of fibronectin, laminin and matrigel. As shown in figure 3.6A, the percentage of striated myotubes was strongly dependent on substrates stiffness. At 7 days the trend of striated myotubes was extremely conserved, regardless of the protein used: the maximum value of striated myotubes was reached with PA hydrogel of physiologic stiffness (E≈15kPa) and the minimum with PA hydrogel of E≈21kPa. The highest value of striated myotubes (60.31±3.78%) was obtained on hydrogel with physiological stiffness combined with a patterning of matrigel 2.5%. Considering the time in culture, as expected, the percentage of striated myotubes was proportional to time, independently to protein and stiffness (Fig. 3.6 B-D). These results confirm the data obtained from Engler and colleagues[7].

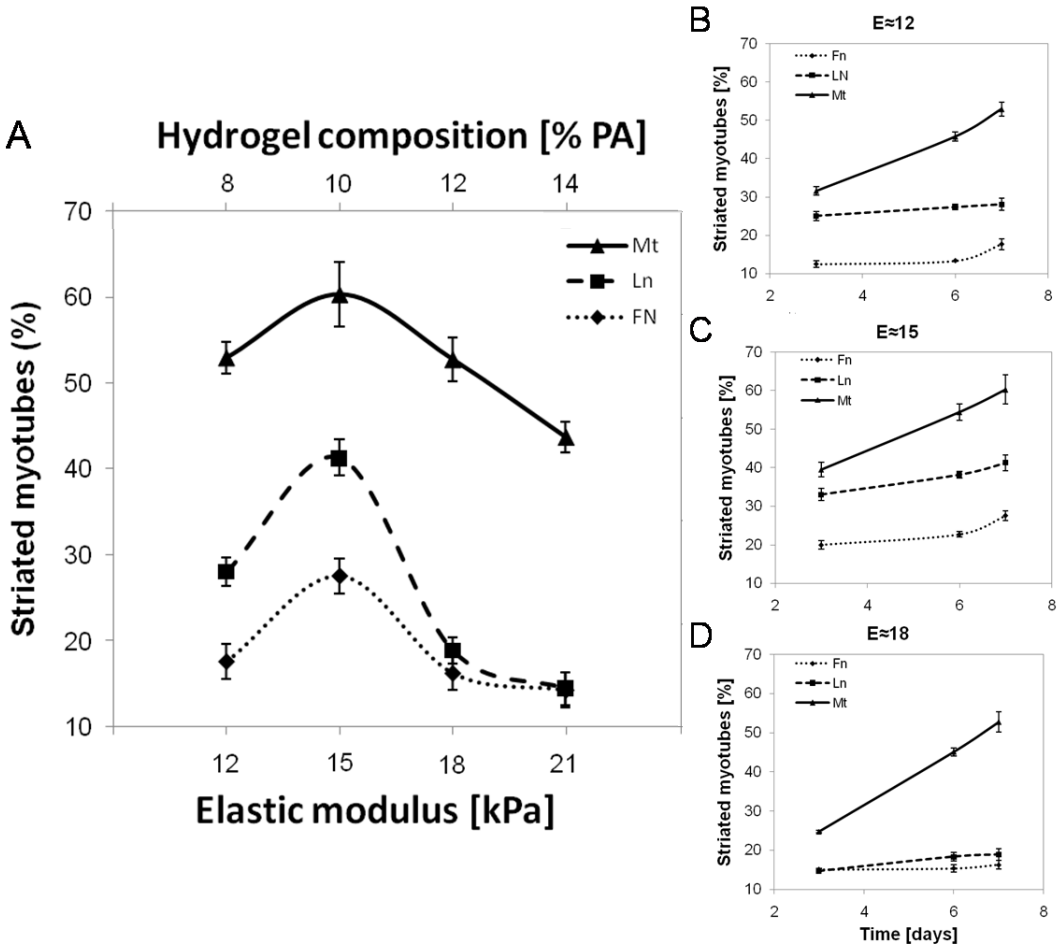

Figure 3.6. Optimum substrate modulus for myoblasts differentiation. A: The percentage of striated myotubes exhibits a strong dependency on the substrate's elastic modulus. The percentage of total cells (n>10 for each sample) exhibiting actin-myosin striation showed an optimum hydrogel modulus of E≈15 kPa, regardless of the adhesion protein used. B-D: Striation of myotubes is directly proportional to the time. The percentage of striated myotubes are shown in function of the days from seeding for hydrogel of stiffness E≈12 kPa (B), E≈15 kPa (C) and E≈18 kPa (D).

Taken together these data show that the use of a substrate with tissue-like mechanical properties and strict topological organization greatly improve the differentiation process of human dystrophic myoblasts cultured *in vitro*, in comparison to the actual standard methodologies, mainly in terms of timing and degree of myotubes maturation.

3.3 *In vitro* model of human DMD skeletal muscle

Several specific characteristics of an ideal *in vitro* model were identified: (1) being easy and simple, in order to be used by researchers with different background (biologists, biotechnologists, engineers,…); (2) being economic and rapid, in order to speed-up the processes of therapy and drug development; and (3) having micrometric dimensions, in sight of lowering the research costs and using low amount of precious reagents and materials, such as human cells. Referring in particular to the DMD, an *in vitro* model of this disease, to be effective and to have experimental advantages while remaining as close as possible to the physiological reality, should have physiological properties that make it predictive of the human response to therapy: (4) the cell source must be human, for being representative of human physio-pathology; (5): the *in vitro* developed tissue should have functional properties consistent with the natural tissue (morphology matching with that one of the adult tissue, functional calcium signaling, induced or spontaneous contractions, an adequate force of contraction) in order to determine, for example, if a specific drug or a therapy can restore the tissue functionality; (6) the model should guarantee the expression of the key protein causing the disease: dystrophin. In fact, most of the strategies for DMD healing focus on the restoration of dystrophin. In case of an *in vitro* trial of a specific cell- or gene-therapy or drug, the model should address the following questions: for cell therapy, "Are the tested cells effective in dystrophic myotubes treatment? Do they fuse with myotubes of the model? Do they induce the restoration of dystrophin? Do they recreate a pool of PAX7-positive stem cell?"; for gene therapy: "Is the transfection efficient? Do the investigated vectors induce the restoration of dystrophin? Do they restore alternative proteins (such as utrophin)"; for pharmacological therapy: "Does the new drug reduce the inflammatory state?".

The human skeletal myotubes engineered in this work respect the first three points mentioned above: the row materials are cheap and easily procured; the methodologies for hydrogel preparation and protein patterning are simple and do not require specific skills; the tissue was developed at the microscale and the maximum area covered by the human myotubes is 9 mm^2. It is representative of the human biology, since it was developed with human primary myoblasts. Concerning

physiology, requirement number five, functional studies of calcium signals were performed in collaboration with Prof. Reggiani (Department of Human Anatomy and Physiology, University of Padova). The calcium sensitive dye Fluo-4 was used in 7 days old myotubes plated on patterned hydrogel to study calcium signals of excitation contraction coupling in human myotubes. Several myotubes (derived by both DMD and healthy donors) were responsive and showed strong calcium transients as a result of exogenous electric excitation (Fig. 3.7). Isometric contractions of electrically stimulated myotubes were observed.

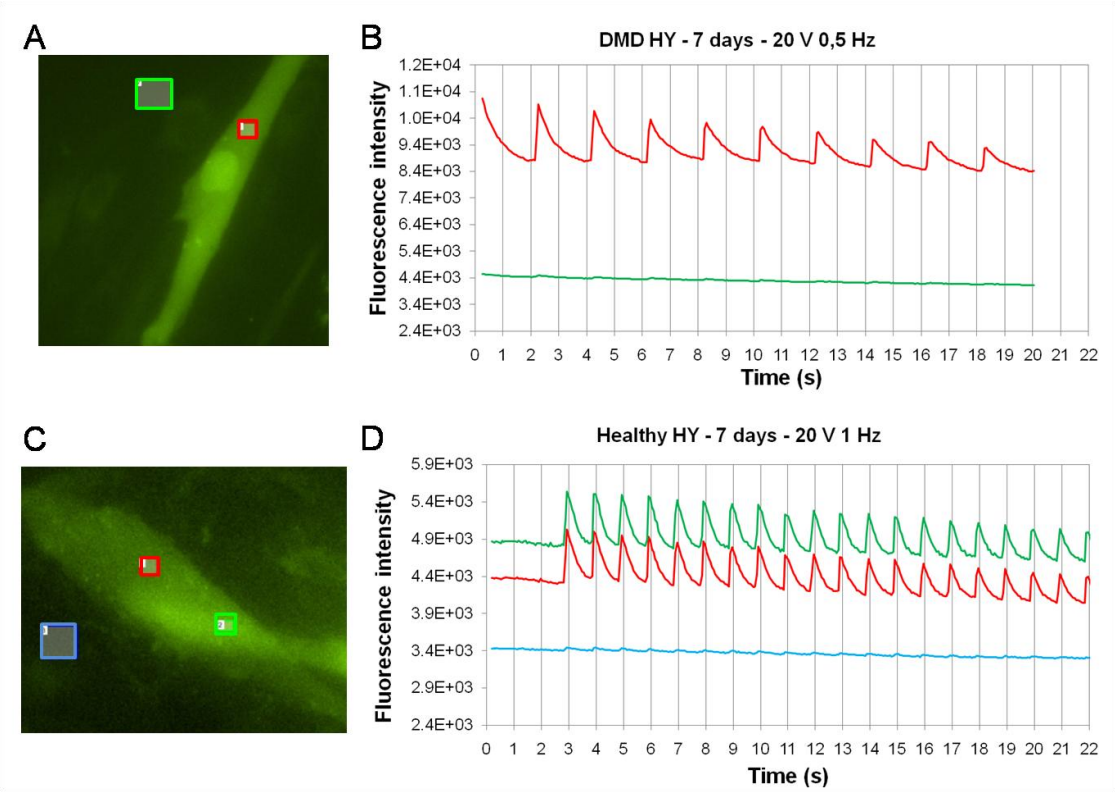

Figure 3.7. Functional studies of calcium signals. A, C: Images of the DMD (A) and healthy (C) myotubes loaded with Fluo-4. Analyzed areas are highlighted with colored square. The graphs report the fluorescence intensity of the dye, thus the intracellular calcium concentration in function of time in DMD (B) and healthy (D) myotubes.

A key point for an *in vitro* model of the DMD is the achievement of a high degree of differentiation of the myotubes, in order to detect the protein causing the disease: dystrophin (requirement number six). Such prospect was tested on the engineered tissue: myotubes obtained from healthy myoblasts, cultured for 11 days on PA hydrogel with physiologic stiffness, were analyzed for the expression of dystrophin. Immunofluorescence analysis confirmed the expression of such a crucial marker, as

shown in figure 3.8. The analysis with confocal microscope revealed a specific expression on the membrane of the myotube (Fig. 3.8 F).

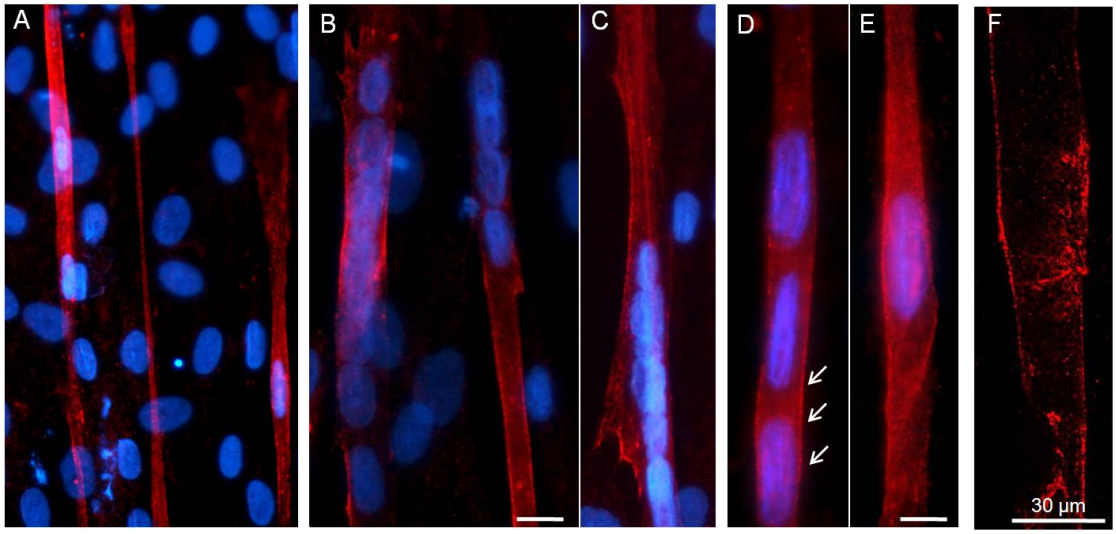

Figure 3.8. Dystrophin expression on healthy myotubes after 11 days of culture on PA hydrogel. Nuclei are counterstained with DAPI. Images taken at higher magnification (arrows in D and image in E) and at confocal microscope (F) show that dystrophin is expressed on the myotube membrane. Scale bar = 30 µm.

Such a remarkable expression of dystrophin, open the perspective of using the developed myotubes for testing the feasibility of cell- or gene-therapy *in vitro*. Preliminary tests on therapies or drugs could be performed *in vitro* before moving into *in vivo* trials, which require long time points and a considerable amount of work.

3.4 Conclusions and future perspective

Although the mechanisms underneath myoblast differentiation on a soft substrate, like the hydrogel, need further molecular investigations, the promising results obtained with such a sensitive cell source (human and dystrophic primary myoblasts) and the improvements in myotube differentiation, in comparison to standard culture systems, highlight the role of cell culture microenvironment and emphasize the prospective for new and innovative cell culture systems. In particular, engineering the substrate with a biologically inspired design offers great control over cell culture and cell fate, such as myoblasts topology and differentiation in the presented work.

The skeletal muscle myotubes here engineered represents a high-quality, but still partial biomimesis of the human *in vivo* tissue. Some key features are missing, such as innervation, vascularization and three dimensional architecture of the tissue, which represent real challenges for all tissue engineers and are the future prospective of this study.

3.4.1 Electrical stimulation mimicking innervation

Muscle innervation is the key factor controlling the main function of this tissue: the contractility. The ability of engineered muscle tissues to rapidly connect to the host neuromuscular system is expected to further facilitate their functional integration into the host environment and accelerate the functional recovery of the host muscle[27]. On the other hand, engineering an *in vitro* skeletal muscle tissue with functional contractile properties can be achieved by the application of an exogenous stimulus mimicking, at least in part, the neuronal activity of skeletal muscle *in vivo* (§ 2.4). A previous study showed that electrical stimulation of murine muscle precursor cells, cultured into a 3D collagen scaffold, improved the myogenic potential of these cells. In particular, the application of electrical stimulation enhanced the total amount of NO_x released in the culture medium (Fig. 3.9A), which is known to mediates satellite cells injury-induced activation *in vivo* and *in vitro*[28]. In addition, semiquantitative Western blot analysis of MyoD, desmin and myosin heavy chain revealed that mouse satellite cells cultured in electrically stimulated scaffold had a higher expression of MyoD and desmin, while myosin heavy chain expression was not significantly affected by electrical stimulation (Fig. 3.9B). The entire manuscript can be found in appendix B.

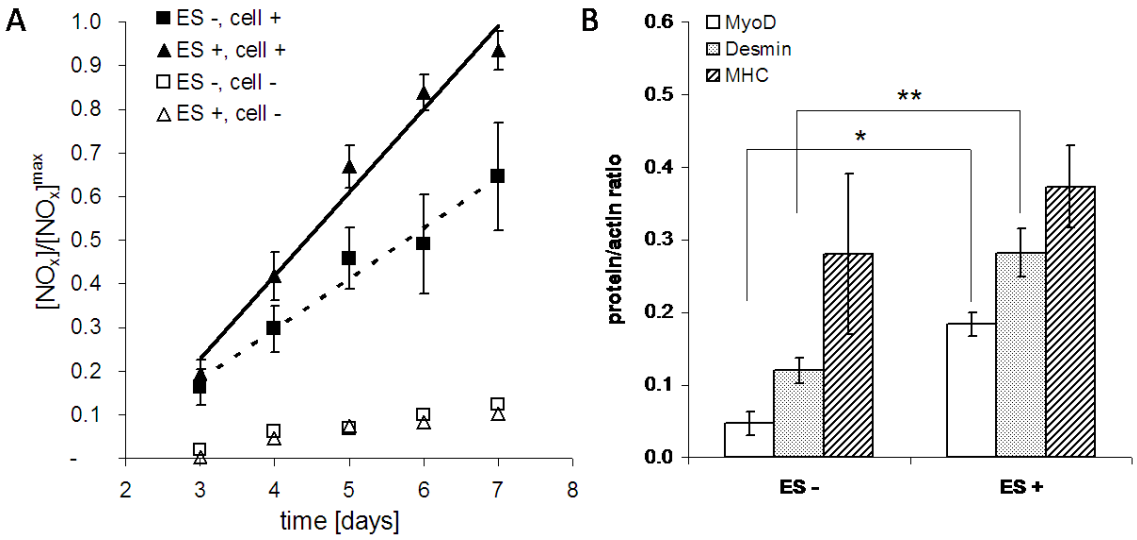

Figure 3.9. Effects of electrical stimulation on myogenic markers expression of mouse muscle precursors cells. A: NO_x release in the culture medium at different time points for electrically stimulated 3D culture (ES+, cell+) and non-electrically stimulated 3D culture (ES-, cell+). Negative controls are represented by not-seeded 3D scaffold (ES±, cell-). The graph shows the NO_x release in the culture medium normalized by the maximum value measured: full symbols refer to 3D cell culture, open symbols are negative control. Electrical stimulation (ES) starts at day 3. B: Western blot analysis on MyoD, desmin and myosin heavy chain (MHC) of non-electrically stimulated scaffold (ES-) and electrically stimulated scaffold (ES+). Actin was used as internal standard. *$p<0.01$; **$p<0.05$.

Among the future prospective, the application of exogenous electrical field to the human engineered myotubes should have the same beneficial impact on the differentiation process and should increase their functional maturation degree.

3.4.2 Three dimensional tissue and culture in a bioreactor

The *in vivo* microenvironment of a cell in a living organism has a three dimensional (3D) architecture: cells are surrounded by other cells and they are held in a complex network of ECM fibers that allows the establishment of various local microenvironment (chemical ad molecular gradients)[29]. On the contrary, the culture in a 2D environment could greatly influence cell behavior (metabolism and gene expression can be altered). The natural step forward for the *in vitro* myotubes developed in this work is the scale up to a 3D environment: a 3D hydrogel should be designed and developed with a structural template of parallel pores, mimicking the structure of parallel myofibers. Besides, moving into a 3D scaffold brings other

important considerations: efficient delivery of nutrient and metabolite removal to the cells and homogeneous of cell density along the scaffold. Both these problems can be overcome by the use of a bioreactor[30], which in part mimic the role played *in vivo* by vascularization: it enables efficient nutrient uptake and catabolite removal, and improve cell distribution throughout the whole scaffold. The author has already cultured muscle precursor cells with a 3D configuration in a perfusion bioreactor (appendix C). The viability of the murine cell line C2C12 was higher after seven days of culture in perfused conditions, in comparison to the static culture (Fig. 3.10).

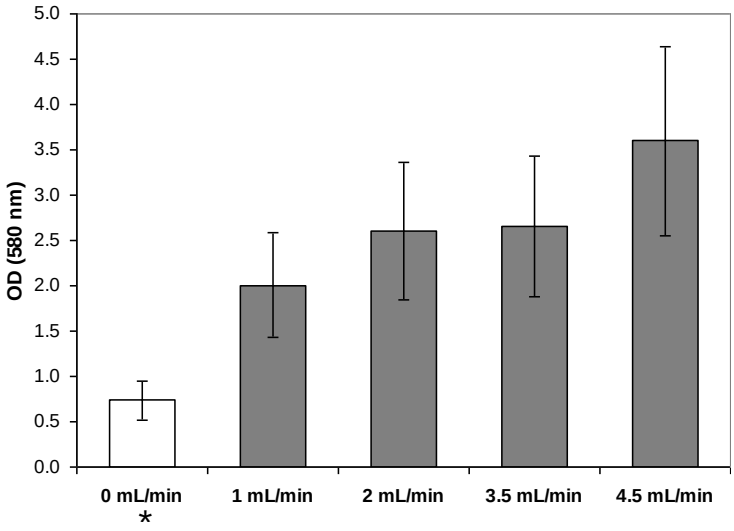

Figure 3.10. Influence of medium flow rate ranging between 1 ml/min and 4.5 ml/min on C2C12 viability, measured after 7 days of continuous culture in the bioreactor. (*) The column labelled "0ml/min" is an internal control which shows the viability of C2C12 cell statically cultured in 3D collagen sponges in standard Petri dishes.

Concerning cell distribution along the scaffold, culture in static conditions resulted in a thick, high density layer of cells on the seeded surface while few cells were in the core and bottom sections of the collagen sponge; on the contrary, histologies related to dynamic culture showed a uniform, high density cell distribution covering the entire 3D structure of the scaffold (see appendix C).

3.5 References

1 Riboldi, S.A. et al., Skeletal myogenesis on highly orientated microfibrous polyesterurethane scaffolds. *Journal of Biomedical Materials Research Part A* **84A** (4), 1094 (2008).

2 Garrett, W.E. Jr. and Best, T.M. , in *Orthopaedic basic science*, edited by Simon SR (American Academy of Orthopaedic Surgeons, Rosemont, 1994), pp. 89.

3 Bischoff, R. , in *Myology. Basic and clinical.*, edited by A.G. Engel and C. Franzini-Armstrong (New York:McGraw-Hill, 1994), pp. 97; Hurme, T. and Kalimo, H. , Activation of myogenic precursor cells after muscle injury. *Medicine and Science in Sports and Exercise* **24** (2), 197 (1992); Mauro, A. , Satellite cell of skeletal muscle fibers. . *The Journal of Biophysical and Biochemical Cytology* **9**, 493 (1961).

4 Laing, N.G. and Nowak, K.J., When contractile proteins go bad: the sarcomere and skeletal muscle disease. *BioEssays* **27** (8), 809 (2005).

5 Clark, K.A., McElhinny, A.S., Beckerle, M.C., and Gregorio, C.C., Striated muscle cytoarchitecture: An Intricate Web of Form and Function. *Annual Review of Cell and Developmental Biology* **18**, 637 (2002).

6 Raeber, G.P., Mayer, J., and Hubbell, J. A. , Part I: A novel in-vitro system for simultaneous mechanical stimulation and time-lapse microscopy in 3D. *Biomechanics and Modeling in Mechanobiology* **7** (3), 203 (2008); Lutolf, M. P. and Hubbell, J. A . Synthetic biomaterials as instructive extracellular microenvironments for morphogenesis in tissue engineering *Nature Biotechnology* **23** (1), 47 (2005).

7 Engler, A. J. et al., Myotubes differentiate optimally on substrates with tissue-like stiffness: pathological implications for soft or stiff microenvironments. *Journal of Cell Biology* **166** (6), 877 (2004).

8 Engler, A. J., Sen, S., Sweeney, H. L., and Discher, D. E., Matrix Elasticity Directs Stem Cell Lineage Specification. *Cell* **126** (4), 677 (2006).

9 Alexakis, C., Partridge, T., and Bou-Gharios, G., Implication of the satellite cell in dystrophic muscle fibrosis: a self-perpetuating mechanism of collagen overproduction. *American Journal of Physiology-Cell Physiology* **293** (2), C661 (2007).

10 Stedman, H.H. et al., The mdx mouse diaphragm reproduces the degenerative changes of Duchenne muscle dystrophy. *Nature* **352** (6335), 536 (1991).

11 Huebner, K.D. et al., Functional resolution of fibrosis in mdx mouse dystrophic heart and skeletal muscle by halofuginone. *American Journal of Physiology-Heart and Circulatory Physiology* **294** (1), H1550 (2008).

12 Emery, Alan E. H., Population frequencies of inherited neuromuscular diseases--A world survey. *Neuromuscular Disorders* **1** (1), 19 (1991).

13 Emery, A.E., Population frequencies of inherited neuromuscular diseases-a world survey. *Neuromuscular Disorders: NMD* **1** (1), 19 (1991).

14 Chakkalakal, J. V., Thompson, J., Parks, R. J., and Jasmin, B. J., Molecular, cellular, and pharmacological therapies for Duchenne/Becker muscular dystrophies. *FASEB Journal* **19** (8), 880 (2005).

15 Dubowitz, V. , Neuromuscular disorders in childhood. Old dogmas, new concepts. *Archives of Disease in Childhood* **50** (5), 335 (1975).

16 Hoffman, E. P. , Brown, R. H., and Kunkel, L. M., Dystrophin: The Protein Product of the Duchenne Muscular Dystrophy Locus. *Cell* **51**, 919 (1987).

17 Zubrzycka-Gaarn, E.E. et al., The Duchenne muscular dystrophy gene product is localized in sarcolemma of human skeletal muscle. *Nature (London)* **333** (6172), 466 (1988).

[18] Hoffman, E. P. , Brown, R. H., and Kunkel, L. M., Dystrophin: The Protein Product of the Duchenne Muscular Dystrophy Locus. *Cell* **51** (6), 919 (1987).

[19] Ervasti, J.M. and Campbell, K.P., Membrane organization of the dystrophin-glycoprotein complex. *Cell* **66** (6), 1121 (1991).

[20] Ervasti, J.M. and Campbell, K.P. , A role for the dystrophin-glycoprotein complex as a transmembrane linker between laminin and actin. *Journal of Cell Biology* **122** (4), 809 (1993).

[21] Jejurikar, S. S. and Kuzon, W. M., Satellite cell depletion in degenerative skeletal muscle. *Apoptosis* **8** (6), 573 (2003).

[22] Oak, S.A., Zhou, Y.W., and Jarrett, H.W., Skeletal muscle signaling pathway through the dystrophin glycoprotein complex and Rac1. *Journal of Biological Chemistry* **278** (41), 39287 (2003).

[23] Gawlitta, D. et al., The Influence of Serum-Free Culture Conditions on Skeletal Muscle Differentiation in a Tissue-Engineered Model *Tissue Engineering: Part A* **14** (1), 161 (2008).

[24] Lawson, M. A. and Purslow, P. P. , Differentiation of myoblasts in serum-free media: effects of modified media are cell linespecific. *Cells Tissues Organs* **167** (2-3), 130 (2000); Dennis, R.G., Kosnik, P.E., Gilbert, M.E., and Faulkner, J.A., Excitability and contractility of skeletal muscle engineered from primary cultures and cell lines. *American Journal of Physiology-Cell Physiology* **280** (2), C288 (2001).

[25] Maley, M. A., Davies, M. J., and Grounds, M. D., Extracellular matrix, growth factors, genetics: their influence on cell proliferation and myotube formation in primary cultures of adult mouse skeletal muscle. *Experimental Cell Research* **219** (1), 169 (1995).

[26] Sanger, J. W. et al., How to build a myofibril. *Journal of Muscle Research and Cell Motility* **26** (6-8), 343 (2005).

[27] Bian, W. N. and Bursac, N., Tissue engineering of functional skeletal muscle: challenges and recent advances. *Ieee Engineering in Medicine and Biology Magazine* **27** (5), 109 (2008).

[28] Kuang, S., Gillespie, M. A., and Rudnicki, M. A., Niche regulation of muscle satellite cell self-renewal and differentiation. *Cell Stem Cell* **2** (1), 22 (2008).

[29] Zhang, S, Gelain, F, and Zhao, X, Designer self-assembling peptide nanofiber scaffolds for 3D tissue cultures. *Seminars in Cancer Biology* **15** (15), 413 (2005).

[30] Martin, Y. and Vermette, P., Bioreactors for tissue mass culture: Design, characterization, and recent advances. *Biomaterials* **26** (35), 7481 (2005).

CHAPTER 4

Microscale tissue engineering of human cardiac muscle

This chapter illustrates the results obtained with the *in vitro* development of human cardiac tissue. After a brief introduction on morphology and physiology of the myocardium, two different methodologies for cardiomyocytes (the cells of miocardium) differentiation from human embryonic stem cells are presented. The first is based onto the stimulation with a defined temporal sequence of soluble factors; while the second induces hESC cardiomyogenesis with the application of electrical stimulation. The derived cardiomyocytes have been used for the development of an array or contracting cardiomyocytes dots, through the application of microscale technologies described in chapter 3, which could finally be integrated in a platform for drug screening and therapy development.

4.1 Myocardium physiology and its regeneration challenge

The essential function of the heart is to pump blood throughput the entire body. The mammalian heart has four chambers: right and left atria (upper) and right and left ventricles (lower). The two atria act as collecting reservoirs for blood returning to the heart, while the two ventricles act as pumps to eject the blood to the body. Cardiac muscle is a type of highly oxidative involuntary striated muscle found in the walls of the heart, specifically the myocardium. This tissue is adapted to be highly

resistant to fatigue: it has a large number of mitochondria, enabling continuous aerobic respiration and a good blood supply, which provides nutrients and oxygen. The heart is so tuned to aerobic metabolism that it is unable to pump sufficiently in ischaemic conditions. The myocardium is composed of cardiomyocytes and fibroblasts with a dense supporting vasculature (consisting of endothelial cells) and collagen-based extracellular matrix (ECM). Generally, the myocardium has an elastic modulus (E) of about 10 kPa[1]. The cardiomyocytes form a three-dimensional synctium that enables propagation of electrical signals across specialized intracellular junctions to generate coordinated mechanical contractions that pump blood forward. Only 20-40% of the cells in the heart are cardiomyocytes but they occupy 80-90% of the heart volume. Morphologically, intact cardiac myocytes have an elongated, rod shaped appearance. Their coordinated contraction in the heart propel blood from the atria and ventricles to the blood vessels of the circulatory system. The contractile apparatus of cardiomyocytes consists of sarcomeres arranged in parallel (such as in skeletal muscle, § 3.1). Metabolic requirements of the cardiomyocytes are supported by the high density of mitochondria, while electrical signal propagation is provided by specialized intercellular connections, gap junctions[2]. The control of heart contractions is almost entirely self-contained. Groups of specialized cardiomyocytes (pacemakers) drive periodic contractions of the heart through the generation of a wave of electrical excitation, which spread to neighboring cells causing a coordinated atrial-ventricular rhythmic contraction[3]. The majority of the cells in the myocardium are non-pacemaker cells and they respond to the electrical stimuli generated by pacemaker cells. Excitation of each cardiomyocyte is followed by an increase in the amount of cytoplasmic calcium that triggers mechanical contractions. The propagation of the electrical excitation through the tissue by ion currents in the extracellular and intracellular spaces results in synchronous contractions. The biochemical basis of muscle activity is related to the enzymatic and physical properties of actin, myosin, and the accessory proteins (troponin and tropomyosin) that constitute the thin and thick filaments in the cardiomyocyte cytoplasm and is highly similar to skeletal myotubes contraction (see § 3.1). Briefly, in a rested, non-contracting muscle, a myocardial cell has a negative

membrane potential. When the muscles is excited above a threshold value, the voltage-gated ion channels opens with a flood of cations into the cell [depolarization]. When the cytosolic calcium increases, the myosin binding sites on actin become available, an actomyosin complex is formed. These events are accompanied by simultaneous translocation of the attached thin filament toward the sarcomere, that gives the contraction. After a delay (the absolute refractory period), potassium channels reopen and the resulting flow of K^+ out of the cell causes repolarization to the resting state.

The heart is one of the least regenerative organs in the body[4] and, consequently, any major insult (due to ischemia, viral infection, or other pathologies) causing significant heart cell loss can result in the progression to irreversible heart failure. Congestive heart failure is a growing epidemic, and is already the most common cause of hospitalization in US citizens over 65[5]. Moreover, due to the poor prognosis of patients with advanced heart failure and the shortage in donor organs for heart transplantation, a search for new therapeutic paradigms for heart failure has become imperative[6]. Stem cells offer the possibility of repairing damaged organs like the heart from their component parts, and there is an intensive effort to develop stem cell–based strategies for cardiac repair (as discussed in chapter 1). Both adult and embryonic stem cells are being studied in preclinical models, and at least four types of autologous cells (skeletal myoblasts, bone marrow mononuclear cells, mesenchymal stem cells and endothelial progenitor cells) are being tested in early-stage clinical trials[7,8]. Apparently, several of these cell types do not transform to generate significant amounts of new myocardium[7,9]. This indicates that non-contractile mechanisms such as alteration of the infarct remodeling process, enhancement of angiogenesis, or augmentation of an endogenous repair mechanism probably underlie most of the benefit seen to date with cell transplantation. This has led to the investigation of groups of cells that may have the promise for true re-muscularization of the infarcted heart. At present the two most intensely studied cell sources for this task are human embryonic stem cells (hESC) and resident cardiac progenitor cells. hESC are an attractive population for cardiac repair because they can be maintained by well-established protocols, can be greatly expanded in culture

and be differentiated into definitive cardiomyocytes[10]. Initial studies with hESC–derived cardiomyocytes showed their capacity to form new myocardium in the uninjured heart[11]. One encouraging feature of these cells is that they appear capable of achieving at least some degree of electrical integration with surrounding host myocardium in such models, unlike skeletal myoblast grafts, which appear to remain electrically insulated[12]. In addition, hESC–derived cardiomyocytes (hESC-CM) have robust proliferative capacity both *in vitro* and after implantation, implying that their delivery into damaged tissue could be a promising clinical therapy[4].

This research field would great benefits from the development of an *in vitro* tissue representative of the *in vivo* cardiac tissue, which could be easily used for *in vitro* development and testing of new clinical strategies (Fig. 4.1). This is the philosophy underneath the work presented in this chapter.

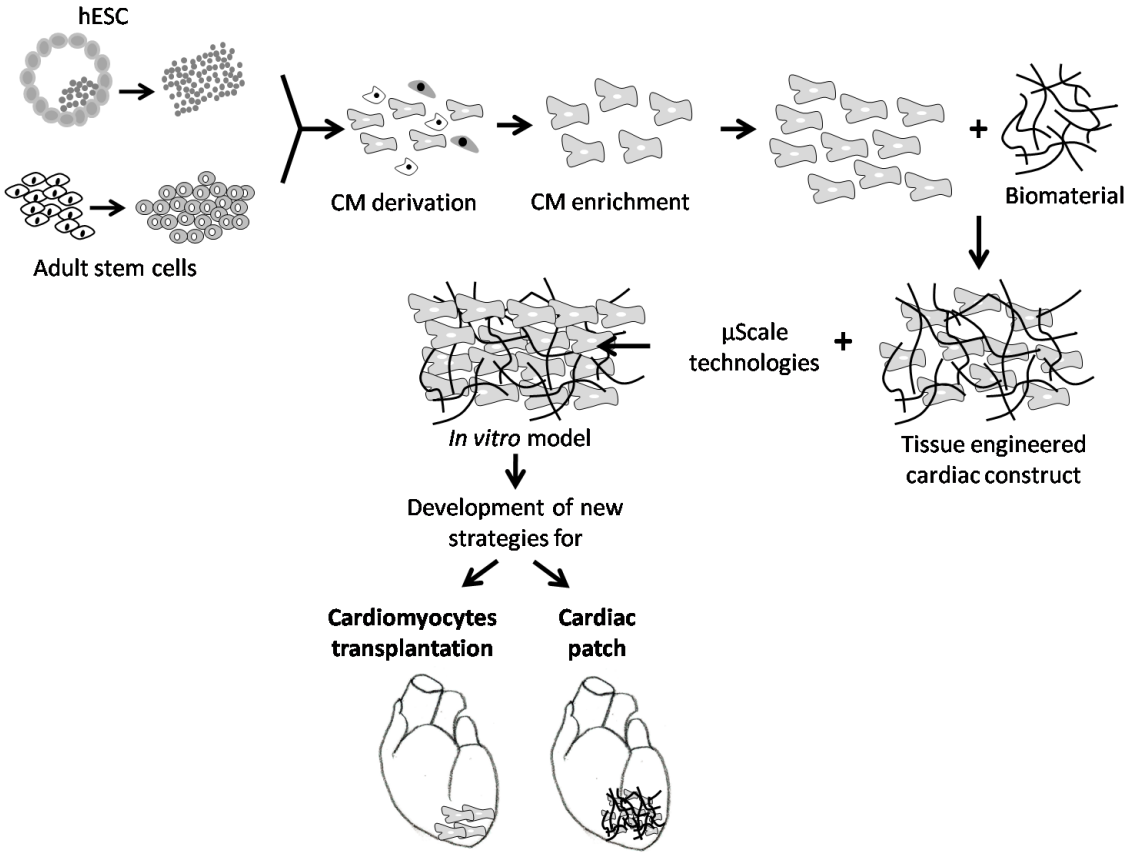

Figure 4.1. Generation of hESC lines and isolation of adult stem cells and road map for their clinical utilization. The hESC or adult stem cells can be propagated in their undifferentiated or stem state and then differentiated into cardiomyocytes (hESC-CM). The hESC-CMs could be isolated, enriched to increase the culture purity and used for the development of an *in vitro* model of cardiac tissue. In turns, this tissue could be used for in vitro studies of new clinical strategies.

4.2 Human embryonic stem cell

Embryonic stem cells (ESC) are pluripotent stem cell that have the potential to give rise to virtually every cell type in the body. The derivation of mouse ESC (mESC) was first reported in 1981[13]. It was not until 1998, however, that the derivation of similar human ESC (hESC) lines was first reported; initially by Thomson et al.[10] and later by Reubinoff and colleagues[14]. These human cell lines were derived from the inner cell mass (ICM) of human blastocysts of fresh or frozen human embryos, produced by *in vitro* fertilization (IVF) for clinical purposes, and donated by individuals after informed consent and after institutional review board approval[10]. The cellular origin of the ESCs, the ICM, exists for only a short period in the developing mammalian embryo. At this stage, the blastocyst is comprised of an outer layer of cells (the trophoectoderm) that will become supporting embryonal tissues and from the ICM cells that will give rise, through specialized progenitor cells, to all tissue types in the developing embryo. During the derivation of ESC, the trophectoderm layer is removed by immunosurgery, the ICM cells are isolated, and plated on a mitotically inactivated mouse embryonic fibroblast (MEF) feeder layer where they form colonies, which are then selected, passaged, and expanded (Fig. 4.2).

Thomson and colleagues proposed that the essential characteristics of primate embryonic stem (ES) cells should include (i) derivation from the preimplantation, (ii) prolonged undifferentiated proliferation, and (iii) stable developmental potential to form derivatives of all three embryonic germ layers even after prolonged culture[15]. More recently, the definition included that hESC: (iv) maintain a normal euploid karyotype over extended culture, (vi) express high level of Oct4, (v) show telomerase activity[16].

In fact, when cultured on a MEF feeder layer, conditioned media, or cocktails of specific growth factors, the hESC could be propagated continuously in the undifferentiated state.

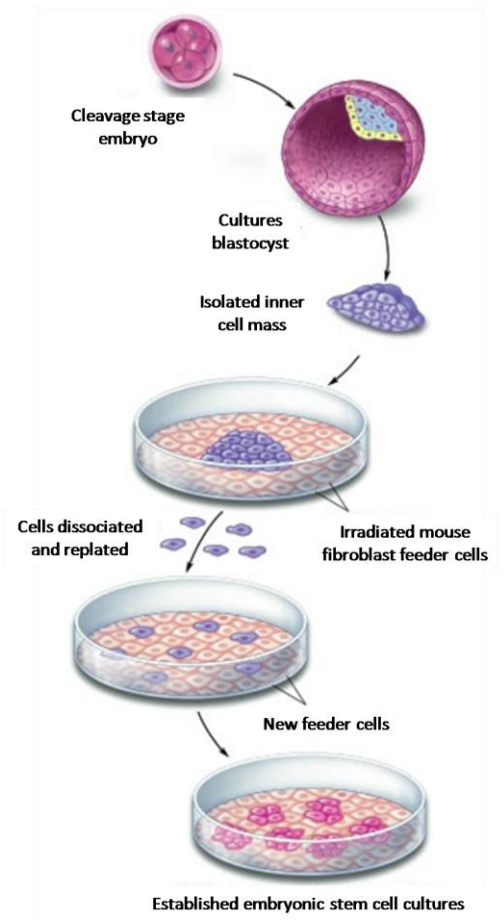

Figure 4.2. Techniques for generating embryonic stem cell cultures. [modified from http://stemcells.nih.gov/info/scireport/appendixC.as]

The undifferentiated hESCs and their clonal derivatives were shown to retain a normal diploid karyotype and to continue to display a high level of telomerase activity during long-term propagation in culture. Pluripotencey of the hESC was confirmed by injection into immunocompromised mice to produce teratomas containing differentiated derivatives of all three germ layers[17]. Pluripotency was also demonstrated *in-vitro*. When removed from the MEF feeder layer and cultivated in suspension, the hESC tend to spontaneously form three-dimensional differentiating cell clusters termed embryoid bodies (EBs), which contain cell derivatives of endoderm, mesoderm, and ectoderm origin[18]. The latter property has captured the imagination of both scientists, clinicians, and the public. If hESC can be coaxed to differentiate into specific cell lineages, then they may bring a unique value to several scientific fields such as developmental biology, functional genomics, patho-physiological studies, and drug screening and development. Furthermore, since many of the diseases that place the greatest burden on society (heart failure,

neurodegenerative disorders, diabetes, etc.) result from cellular deficiency or dysfunction, having the ability to generate inexhaustible numbers of defined cell populations may allow the development of future cell replacement strategies for the treatment of these devastating disorders[6]. Since the first hESC lines were reported in 1981, a numerous genetically diverse cell lines were derived from human blastocysts and cultured with several techniques from laboratory to laboratory. In order to assess the similarities and differences in the expression of commonly used markers of hESC and to identify a set of well-validated markers to establish hESC identity of newly derived lines, the International Stem Cell Initiative (ISCI)[19] was established by the International Stem Cell Forum (http://www.stemcellforum.org.uk) to carry out a comparative study of a large and diverse set of hESC lines[20]. Such a study, revealed that the most commonly expressed markers are the glycolipid antigens SSEA3 and SSEA4, the keratan sulfate antigens TRA-1-60, TRA-1-81, GCTM2 and GCT343, and the protein antigens CD9, Thy1 (also known as CD90), tissue-nonspecific alkaline phosphatase and class 1 HLA, as well as the strongly developmentally regulated genes NANOG, POU5F1 (formerly known as OCT4), TDGF1, DNMT3B, GABRB3 and GDF3. While markers of the differentiate state are: SSAE1, CD30, GT_3, GD_2, GD_3, Desmin, FoxA2, Cdx2 and Brachyury[21].

4.2.1 Human Embryonic stem cell culture

hESC are sensitive and fragile cells, which spontaneous differentiation is frequently observed during routine expansion[22]. These cells are especially sensitive to chemical reagents. Such characteristic implicates that (a) hESC medium preferentially does not contain any antibiotics, and their manipulation should be done with particular attention to the maintenance of culture sterility; (b) cell passaging should be performed by mechanical disaggregation, although enzymatic treatment can be done carefully. In addition, hESC have a high metabolism and they fast deplete the medium nutrients, thus (c) the medium should be chanced daily. It results that hESC culture, propagation and expansion are laborious and time demanding processes.

The culture occurs on six multiwells, which are pre-coated with 0.1% gelatin (in water) for the adhesion of the feeder layer cells: inactive MEF. The feeder layer provides certain currently unknown factors, which support undifferentiated growth of hES cells[23]. Several other feeders have been tested: alternative human cells[20] or synthetic matrix, such as matrigel[24]. MEF need to be mitotically inactivated to be used as feeders to prevent their continued growth. These cells can be inactivated chemically with Mitomycin-C or through γ-irradiation and cultured in DMEM with 10% (v/v) heat inactivate fetal bovine serum and 1% (v/v) non-essential amino acids. Once plated, MEF can be used for hESC culture within 14 days maximum, thus the coordination between the preparation of MEF and hESC culture is the first critical step to consider. The medium for hESC culture is composed of 80% KnockOut dulbecco's modified eagle's medium (KnockOut D-MEM) supplemented with 20% (v/v) KnockOut serum replacement (Knock-Out SR), 4 ng/ml basic fibroblast growth factor (bFGF), 1mM L-glutamine, 0.1mM b-mercaptoethanol, and 1% stock solution of non-essential amino acids. The protocol for hESC maintenance is reported in appendix D. hESC grow in colonies, with defined and regular edges, as shown in figure 4.3.

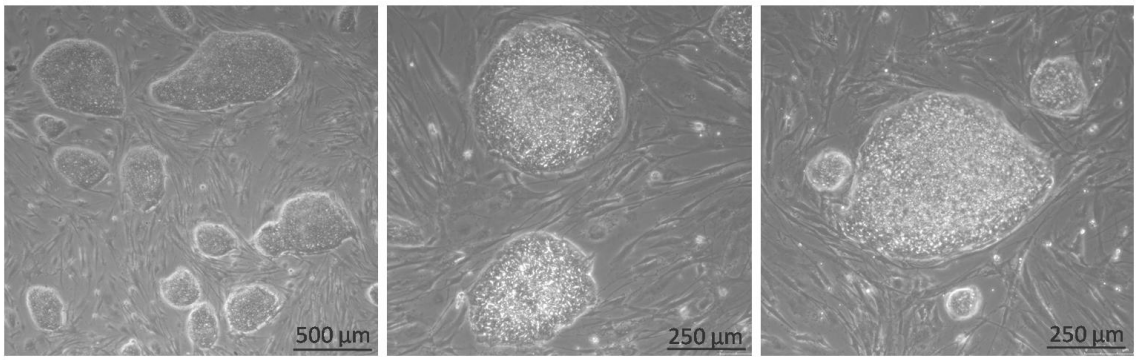

Figure 4.3. Bright field images of H13 colonies cultured on top of MEF. Undifferentiated colonies have defined and bright edge and a regular shape. The dimension of the colonies are very different from colony to colony.

Cell splitting and expansion generally occurs when MEF feeder layer is two weeks old or when colonies are too dense or too large. The passaging can be done both mechanically and enzimatically; the first should be preferred, because of hESC sensitivity. The mechanical separation of colonies is done with the use of a stereomicroscope to dissect the undifferentiated colonies into several pieces using a

cutting pipette. These selected pieces then are replated individually onto dishes containing fresh MEF feeders. The enzymatic treatment consist of 5 minutes of incubation with 1 mg/mL collagenase (in Knock Out DMEM) at 37°C, followed by scraping the cells off the surface of the plate, using a glass 5ml pipet. hESC culture should be checked daily for both medium changing and maintenance of the undifferentiated state. These cells in fact show spontaneous differentiation in culture when culture conditions are suboptimal (i.e. when permitted to reach over-confluence). MEF has a key role in maintaining hESC undifferentiated. Timing and density are essential: MEF should not be used after 14 days post inactivation and the optimal seeding density is $1,6\text{-}1,8\times10^4$ cells/cm^2. The differentiation of hESC occurs mainly through three mechanisms. When center differentiation occurs, a lighter region forms in the middle of colony, which looks like a "hole" in the colony (Fig. 4.4A). When the colony has poorly defined borders with flat cells, it has edge differentiation (Fig. 4.4B). In some cases, colonies have piled cells in the center (Fig. 4.4C). The piled cells tend to die first and may be differentiated and generally indicate that the cells are not being broken up enough during passaging.

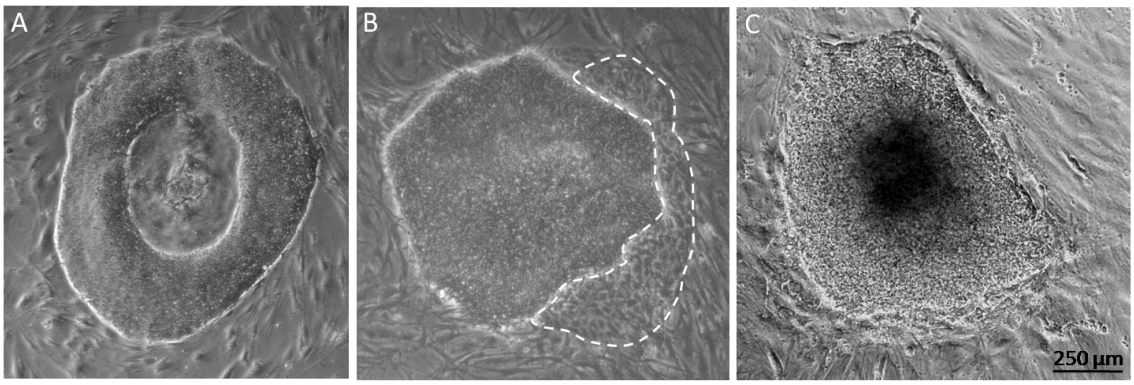

Figure 4.4. hESC differentiation. Center differentiation (A); edge differentiation (B, the area marked with a white dotted line show visibly differentiated cells); center differentiation (C).

All these situations should be avoided in culture and differentiated cells should be removed as soon as they form. Depending on the amount of differentiated colonies in the culture the methodologies for cell expansion are: "picking to remove" or "picking to keep". If there are mostly undifferentiated colonies on the plate with only a few differentiated single cells and colonies, the picking to remove is preferred: the differentiated cells are picked, removed, and discarded.

Undifferentiated colonies are kept on the plate until they are ready to passage. If there are only a few undifferentiated colonies on the plate with a large number of differentiated cells and colonies, the picking to keep methodology is used. The undifferentiated colonies are picked, plated, and propagated. The differentiated cells are left on the plate and discarded.

Two hESC lines, H13 and H9 from WiCell, were successfully cultured and the correct maintenance in culture was verified by the expression of Oct 4 and SSEA3 with immunoflourescence (Fig 4.5).

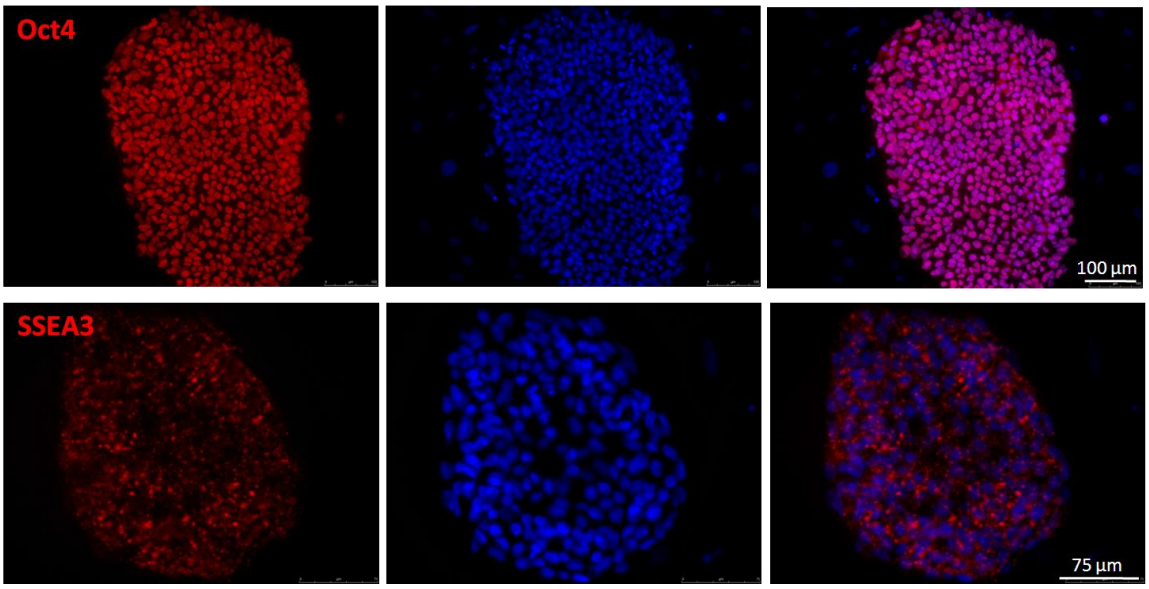

Figure 4.5. Oct4 (upper panel) and SSEA3 (lower panel) expression in H13 cell line. Nuclei are counterstained with DAPI.

hESC can be induced to enter a program of *in vitro* differentiation through the primary germ layers via the formation of embryoid bodies (EBs)[25]. The basic principle for EB production is the induction of cell aggregation by seeding hESC into bacteriological-grade Petri dishes, to which these cells are non-adherent (for a detailed protocol see in appendix D); or through the hanging-drop technique. Figure 4.6 shows a time-course of EB formation, in culture they increase in size and dimensions.

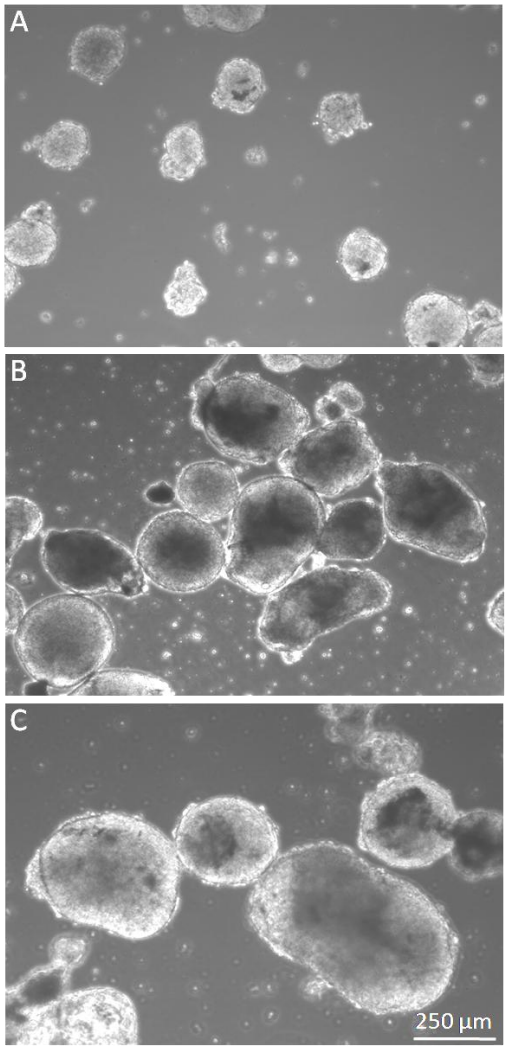

Figure 4.6. Time course of EB development: EB morphology after 7 (A), 14 (B) and 20 (C) days of culture.

The differentiation of hES cells in EBs has been shown to reproduce aspects of early embryogenesis, and occurs in sequential stages[25,26]. Therefore the EB system offers opportunities for the *in vitro* investigation of cellular interactions normally occurring during early embryonic development, and of mechanisms of lineage determination.

Another methodology for demonstrating the pluripotency of hESC is the formation of teratomas *in vivo*. For mES cell lines, pluripotency is validated in utero, in embryo reconstitution experiments, but such manipulations are obviously prohibited for hESC lines. The raising of teratomas following hESC implantation in immunosuppressed mice is the method of choice for producing from hESC a full range of differentiated cell phenotypes. The detection of derivatives of the three

primary germ layers in teratomas is prerequisite to ascribing the characteristic of pluripotency to any novel hESC line[27]. Such a characteristic of hESC, present a safety concern for their use in clinical application, because of their potential to form tumors. Currently, the only way to ensure that teratomas do not form is to differentiate the hESC in advance, enrich for the desired cell type, and screen for the presence of undifferentiated cells[28]. When such procedures were rigorously followed, teratomas were not observed in over 200 animals transplanted with human ESC-derived cardiomyocytes[4]. Thus, a major focus of research is to define procedures for directing hESC differentiation towards a single cell fate. The true utility of hESC will only be realized when they can be safely differentiated into cell lines of clinical importance[28].

4.3 Cardiomyogenesis of human embryonic stem cell

Production of hESC-derived cardiomyocytes (hESC-CMs) *in vitro* was demonstrated by several groups[6,29-31]. Few days after formation (8 days generally) EBs display easily identifiable, rhythmically contracting outgrowths[32]. The methodologies to derive hESC-CMs reported in literature are mainly based on the use of a cocktail of growth factors[33] or coculture[30].

In this PhD work two "biologically inspired" methodologies were learned: a) defined temporal sequence of growth factors, mimicking the development of cardiac tissue in the embryo; b) application of exogenous electrical stimulation, based on the excitability of cardiac tissue (see § 2.4)

4.3.1 Soluble factors acting during embryogenesis

At the moment, the more efficient protocol for cardiomyocytes derivation from hESC was established by Professor Keller, Toronto University[31]. In general, the most successful human ESC differentiation strategies are those that recapitulate normal development[28]. In line with this principle, the methodology developed by Keller's laboratory reproduces *in vitro* the signaling effecting cardiac differentiation during embryogenesis, and is based on the addition to EB culture medium of

specific soluble factors in a precise temporal sequence. These factors are cytokines known to have a key role during cardiogenesis of a developing embryo.

One of the most important events during embryogenesis is the generation of the three primary germ layers: ectoderm, mesoderm, and endoderm during the process of gastrulation. Cardiac cells derive from the mesoderm germ layer (Fig. 4.7).

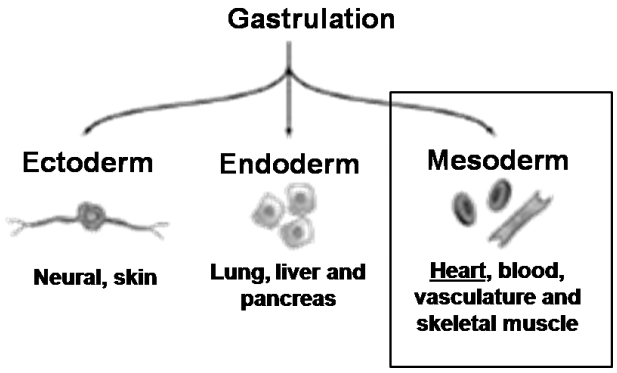

Figure 4.7. Gastrulation and germ layer formation. The derivatives of the three primary germ layers, ectoderm, mesoderm and endoderm, generated during gastrulation. Heart cells derive from mesoderm (box).

The beginning of gastrulation is marked by the formation of a transient structure known as the primitive streak (PS)[34]. Mapping studies have shown that the specification of distinct subpopulations from the PS is not random but rather appears to be controlled both temporally and spatially. Although the precise regulation of PS formation and germ layer induction is not fully understood, expression analyses and gene-targeting studies showed that members of the TGFβ family including bone morphogenetic protein 4 (BMP4) and Nodal (Activin A) as well as members of the Wnt family are essential for these developmental steps[28].

For the establishment of their protocol, Keller and colleagues used ESC as model system for studying mammalian development and lineage commitment, since they recapitulate *in vitro* the developmental stage of embryo *in vivo*. They first studied mESC, demonstrating the existence of a cardiovascular progenitor arising from a population of cells expressing the vascular endothelial growth factor receptor 2 (Flk-1, also known as kinase insert domain protein receptor, Kdr). This population represents one of the earliest stages in mesoderm specification to the cardiovascular lineages[35]. When cultured with cytokines known to function during cardiogenesis, vascular endothelial growth factor (VEGF), basic fibroblast growth factor (bFGF), BMP4 and dickkopf homolog 1 (DKK1, the Wnt inhibitor), these progenitors generated colonies that displayed cardiomyocyte, endothelial, and vascular smooth

muscle (VSM) potential. Subsequently, Keller and colleagues moved to hESC, in order to find the same cardiovascular progenitor in humans. In particular, to direct the differentiation of hESC to the cardiac lineage, they designed a staged protocol of 20 days (Fig. 4.8) that involved the formation of a primitive-streak-like population (stage 1), the induction and specification of cardiac mesoderm (stage 2) and the expansion of the cardiovascular lineages (stage 3).

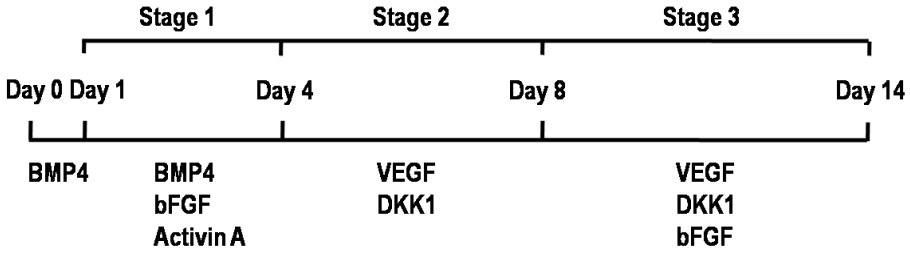

Figure 4.8. Specification of the cardiac lineage from hESC. An outline of the protocol developed by Keller and colleagues for the differentiation of human ESCs to the cardiac lineage.

They demonstrated that, after induction with combinations of activin A, BMP4, bFGF, VEGF and DKK1 in serum-free media, hESC-derived embryoid bodies generate a KDR^{low}/C-KIT$(CD117)^{neg}$ population that displays cardiac, endothelial and vascular smooth muscle potential *in vitro* and, after transplantation, *in vivo*. When plated in monolayer cultures, these KDR^{low}/C-KIT^{neg} cells differentiate to generate populations consisting of greater than 50% contracting cardiomyocytes[31].

Keller and colleagues, applied the same strategies for the regulation of primitive streak formation, primary germ layer induction, and tissue specification (hematopoietic, vascular, pancreatic) from differentiated mouse ESCs. A schematic of the methodology is reported in figure 4.9, for a detailed review see Murry and Keller, 2008[28].

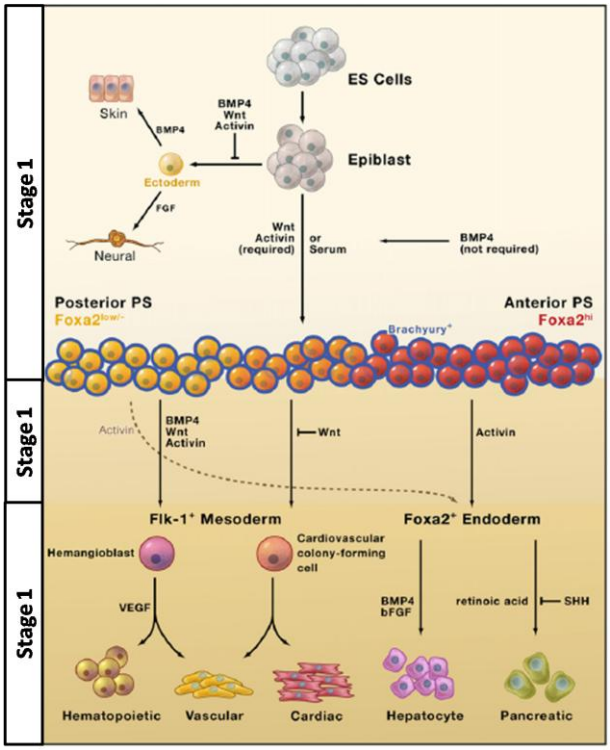

Figure 4.9. ESC Differentiation in culture towards several lineages and cell types[Modified from Murry et al, Cell, 2008[28]].

The protocol for cardiomyocyte differentiation has been acquired during the period spent in the laboratory of Professor Keller. For the study presented in this chapter (§ 4.4), EBs at day 21 were sent from Keller's Laboratory. Upon arrival, the EB contractility was verified and EBs were dissociated in order to obtain single cell suspension (§ 4.4). Figure 4.10 shows the expression of cardiac Troponin T and Connexin43 in a cardiomyocytes monolayer derived after dissociation of EBs.

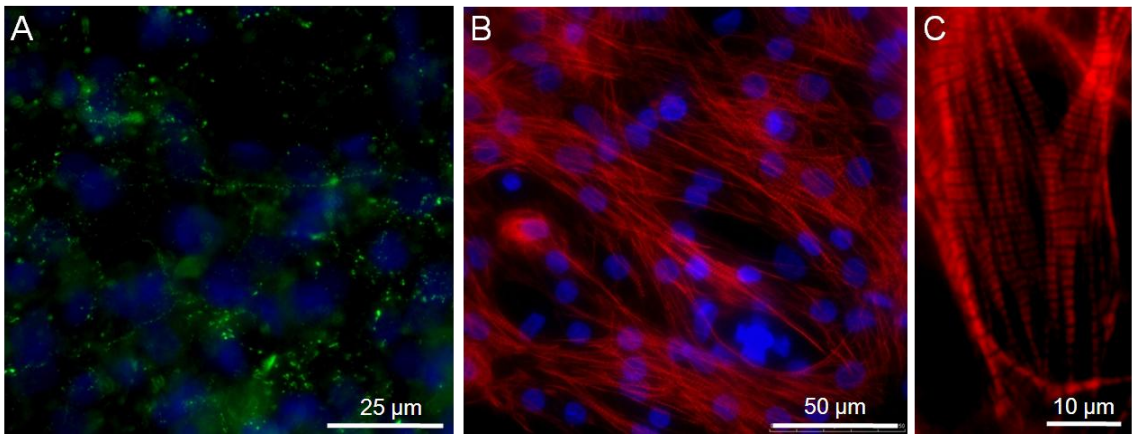

Figure 4.10. Immunofluorescence of Cx43 (A) and cardiac Troponin T(B,C). In C the sarcomeric organization of TropoinT. Nuclei are counterstained with DAPI.

4.3.2 Exogenous electric field

As discussed in paragraph 2.4, electric fields are present in many developing tissues, and have a key role in several regenerating processes[36]. Since the muscle heart is rhythmically excited by ion transfer, it is likely that electrical stimulation could play an important role in cardiomyogenic differentiation *in vitro*. Electrical stimulation has already been reported to be beneficial to primary cardiomyocytes cultured *in vitro* and to enhance the differentiation toward cardiac lineage of mESC[37]. Sauer and colleagues demonstrated that exogenous electrical stimulation induced an increment in cardiomyogenic differentiation and an increase in the generation of intracellular of Reactive Oxygen Species (ROS) in mESC-derived EBs, thus they hypothesized that ROS could be the linkage between exogenous electrical stimulation and cardiac differentiation[37]. ROS are highly reactive molecules generated during the normal metabolism of oxygen by NADPH oxidases or as side products of several enzymatic systems (e.g., cyclooxygenases, nitric oxide (NO) synthases, mitochondrial cytochromes). Although excessive concentration of ROS, such as superoxide anions (O_2^-) and hydrogen peroxide (H_2O_2), are considered destructive and results in inhibition of gene expression[38], small amounts of ROS function as intracellular second messengers and activate signaling cascades involved in growth, differentiation[39,40] and cardiogenesis[41]. The connection between ROS and cardiac differentiation is also supported by evidences that when cardiac cells are stimulated by cytokines[42], growth factors, hormones, even mechanical stress[43], they elicit a small oxidative burst and generate low concentrations of ROS. In addition, during myocardial infarction, cardiac cells generate large amounts of free radicals and ROS, which are involved in the signaling and activation of the intrinsic repair mechanisms of the damaged myocardium[44]. Sauer and colleagues showed that ROS activate the mitogen activated protein kinase (MAPK) pathways in mouse EBs[40], enhancing the angiogenesis through the activation of ERK1,2 and JNK and the cardiomyogenesis through the phosphorylation of ERK1,2, JNK and p38[43,45] (Fig. 4.11). An NADPH oxidase-like enzyme is involved in the ROS-related cardiogenesis during mESC differentiation[46].

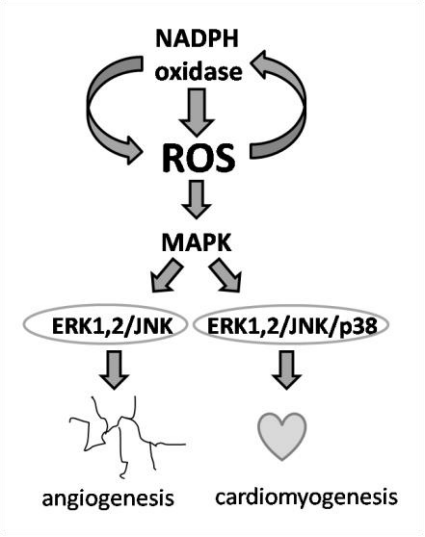

Figure 4.11. Diagram of the involvement of ROS in signaling cascades resulting in cardiovascular commitment of ES cells. ROS are generated through the activity of NADPH oxidase. ROS initiate phosphorylation of the MAPKs ERK1,2, JNK and p38. Angiogenesis requires the activation of ERK1,2 and JNK, whereas the activity of ERK1,2, JNK and p38 is necessary for cardiomyogenesis.

These findings introduce the applicability of electrical stimulation as a possible technique to control hESC differentiation and in particular to increase cardiomyogenesis.

In this study, thus, the correlation between electrical stimulation, ROS production and cardiac differentiation was investigated in hESC.

The effects of exogenous electrical stimulation (single pulse of 1 V/mm intensity and 1 or 90 s duration) on cardiomyogenesis of H13 line-derived EBs were investigated and electrodes of different materials (titanium (Ti), titanium nitride (TiN) and stainless steel (SS)) were used. The generation of intracellular ROS and the differentiation in cardiomyocytes as a consequence of electrical stimulation were analyzed. Part of this work was performed in the laboratory of Professor Vunjak-Novakovic (Columbia University, New York) and the complete manuscript is in appendix D.

It has been first established that exogenous electrical stimulation, either as single pulse or continuous stimulation, didn't compromise the EBs viability, as shown by the live and dead assay performed 2 hours after a single electrical pulse (Fig. 4.12A). The presence of dead cells (arrows in Fig. 4.12A) is negligible in a stimulated EB. Generation of intracellular ROS was measured using the fluorescent dye dichlorofluorescein diacetate (DCFH-DA), a nonpolar and nonfluorescent compound that can diffuse into the cell where it is deacetylated by cellular esterases into a nonfluorescent polar derivative 2', 7'-dichlorofluoroscein (DCFH) that is

impermeable to cell membrane. DCFH is rapidly oxidized to the highly fluorescent dichlorofluorescein (DCF) in the presence of intracellular ROS. Figures 4.11 B-C are examples of DCF fluorescence intensity of an EB before (Fig. 4.12B) and after (Fig. 4.12C) the exogenous electrical stimulation. The maximum production of ROS, corresponding to the maximum increase in fluorescence, compared to a control EB, was reached 5 minutes after the stimulus, as shown in figure 4.11D. It's known that the DCFH-DA, which have traditionally been used for detecting ROS, and in general the dihydro-compounds used for these measurements, are highly photosensitive and they tend to be autoxidized to produce a large background fluorescence, thus an increase of fluorescence is detected also in control EB[47]. The ratio between the average of fluorescence intensity at the beginning and after 5 minutes gives the amount of reactive oxygen species produced in the EB by the electrical stimulation, as summarized in Figure 4.12E.

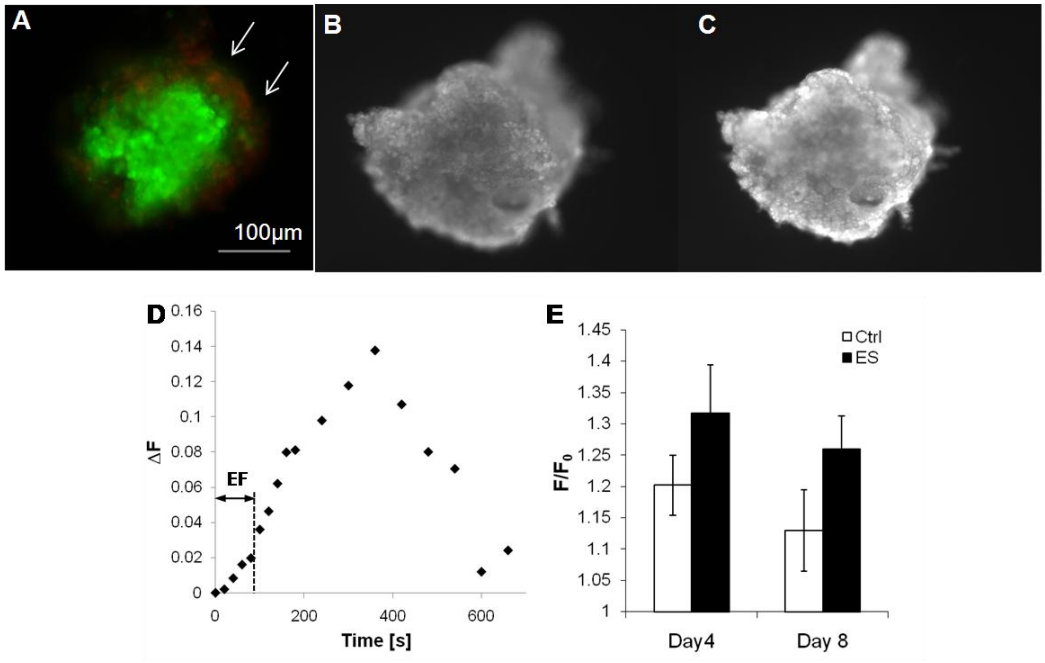

Figure 4.12. Effect of electrical stimulation on cell viability and reactive oxygen species (ROS) generation. A: Example of Live/Dead assay of an EB in suspension culture 2 hours after electrical stimulation; live cells are green, dead cells are red (arrows). B-E: Analysis of intracellular ROS generation through DCFH-DA. B-C: Fluorescence image of EB loaded with dichlorofluorescein (DCF) before (B) and 10 minutes after (C) electrical stimulations. D: An example of time course of ROS generation (DCF intensity). ΔF is the point difference in fluorescence of a stimulated and a control EB, EF = electrical field. E: ROS generation on control (Ctrl) EB and electrically stimulated EB (ES), 4- and 8-days old. The fluorescence intensity 5 minutes after electrical stimulation (F) was normalized by the intensity at time 0 (F_0).

Significant changes in ROS expression were observed with increasing durations of stimulation from 1s to 90s, as shown in figure 4.13A. All the electrodes used induced a significant increase in ROS production in stimulated EBs, if compared to control EBs, with both 1 and 90 s duration. In the case of titanium and titanium nitride, ROS generation was not significantly different when comparing stimuli of 1 and 90s duration. On the contrary, stainless steel electrodes with a stimulus of 90s duration induced an increase in ROS production statistically different in comparison to a stimulus of 1 s. This effect is due to the fact that the reactions on stainless steel electrodes provide a higher electric field when compared to other electrode materials for all 90 s of stimulation (see appendix D), inducing a significant difference between stimuli of 1s and 90s. Since human embryonic stem cells have been shown to begin differentiation toward cardiac lineage 4 days after EBs formation[48], they may show different reactivity to exogenous electric field at different stage of the development. Thus, ROS generation after electrical stimulation of 1 V/mm for 90 s was analyzed in 4- and 8 day-old embryoid bodies.

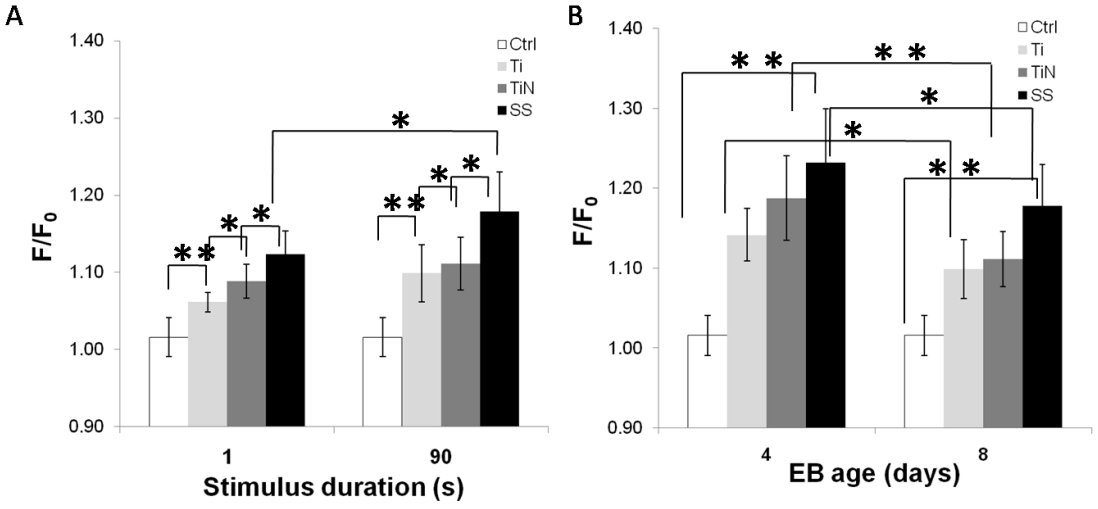

Figure 4.13. Generation of ROS in EB after electrical stimulation with different electrode materials. **A:** Effect of duration of electrical stimulation on ROS production on 6-day-old EB; **B:** Effect of EBs age on ROS generation. About 10 EBs in each of three independent experiments were used for the determination of each data point. * $p<0.01$; ** $p<0.05$.

As shown in figure 4.13B, the increase in ROS production after electrical stimulation occurred in both 4 and 8 days old EB and with all the types of electrodes (as compared to control EB). Furthermore this increase showed the same

trend observed in 6 day old EB reported in figure 4.13A. At day 8, electrical stimulation generated a lower increase in ROS, when compared to 4 day old EBs. With the aim of comparing the effects of electrical stimulation (with stainless steel electrodes) with a biochemical stimulus and to determine the amount of ROS produced as a consequence of the electrical stimulus, EBs were stimulated with increasing concentration of H_2O_2. These results are reported in figure 4.14, where ΔF is the difference between stimulated EB, either with electrical stimulation (ES) and H_2O_2, and control EB ROS generation induced in electrical field-treated EBs was equivalent to the increase observed after 15 minutes of incubation with 1 nM H_2O_2. 4 day old EBs and 8 day old EBs show statistically different in ROS increase after incubation with 10 nM H_2O_2.

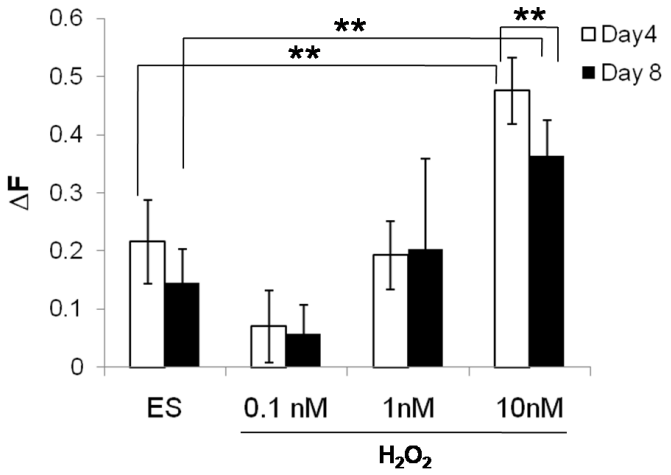

Figure 4.14. ROS generation on 4-day-old EB (open bars) and 8-day-old EBs (black bars) after electrical field (ES) and H_2O_2 treatment. H_2O_2 treated EBs were incubated for 10 min with increasing concentrations of H_2O_2: 0.1 nM, 1 nM and 10 nM. About 4 EBs in each of three independent experiments were used for the determination of each data point. About 10 EBs in each of three independent experiments were used for the determination of each data point.** $p<0.01$.

In order to evaluate if electrical field and intracellular ROS expression affect cardiac differentiation of hESC, the expression of the cardiac marker troponin T was verified. After 3 days in adhesion culture, EBs started to beat spontaneously. As shown in figure 4.15, more EBs exhibited spontaneous beating in electrically stimulated EBs. Furthermore, the expression of the cardiac marker, cardiac

Troponin T, was observed in electrically stimulated and beating EBs (Fig. 4.15B-D) and the sarcomeric organization of such marker was verified (Fig. 4.15C).

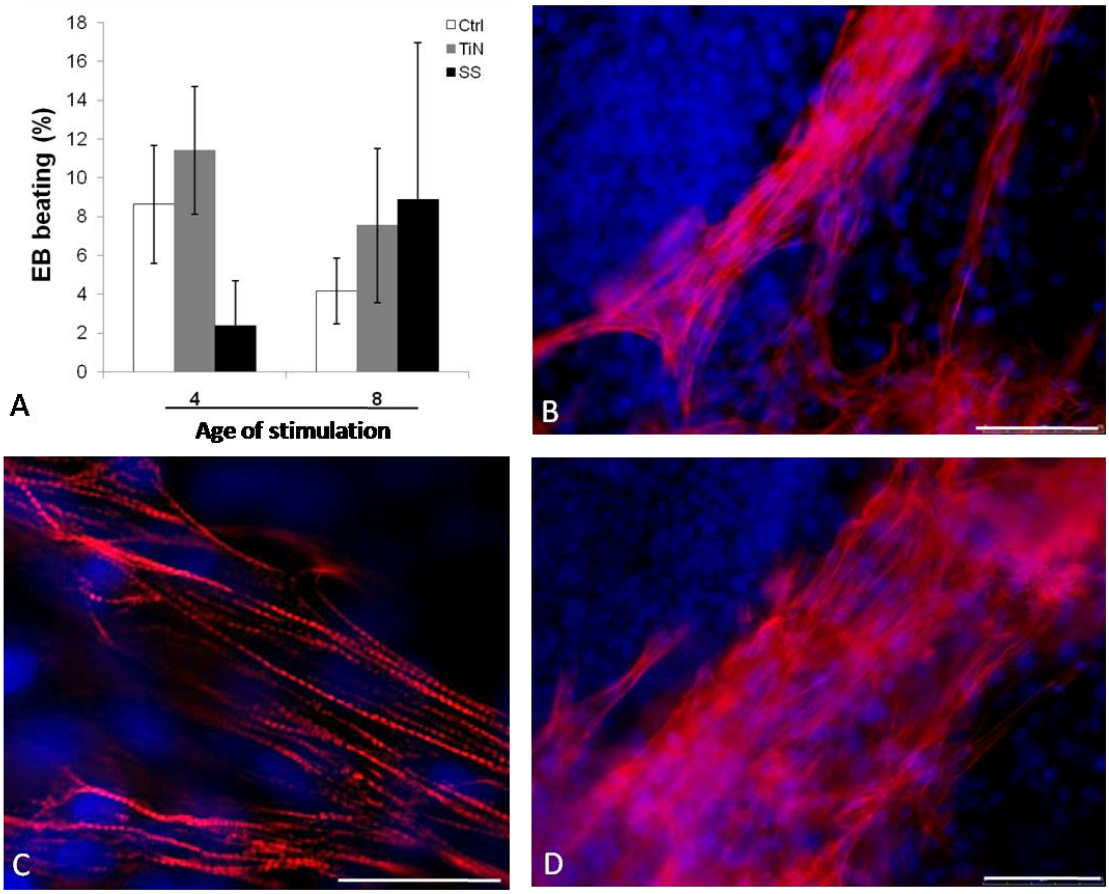

Figure 4.15. Effect of electrical stimulation on cardiomyocyte differentiation. A: The percentage of beating EBs was evaluated in 4- and 8-days-old EBs, either electrically stimulated with titanium nitride (TiN) and stainless steel (SS) electrodes or not treated (Ctrl). The evaluation was done in 19 days-old EBs. B-D: Cardiac Troponin T immunostaining of electrical field-treated representative EB. Nuclei were counterstained with DAPI. Scale bars: 75 μm in B and D, 30 μm in C.

The percentage of beating EB and cardiomyocytes obtained with this methodology is anyway low (ranging between 5 and 10%). Thus further investigations and methodology optimization are needed in order to obtain a considerable amount of cardiac cells for cell therapy or the development of an *in vitro* cardiac model.

4.4 Development of an array of human cardiomyocytes *in vitro*

The human heart is a particularly complex organ, in terms of both cell composition, it is in fact composed of cardiomyocytes and fibroblasts with a dense supporting vasculature (consisting of endothelial cells) and collagen-based ECM, and physiology, heart contractions are controlled by specialized pacemaker cardiomyocytes. Due to such a high degree of complexity, the development of an *in vitro* model of the complete human heart is challenging. A recent study succeeded in three important milestones that are required to engineer a rat bioartificial heart: engineering of a construct to provide architecture, through decellularization of a native heart, population of such a construct with an appropriate cell composition, using cardiac and endothelial cells, and maturation of this construct to develop nascent pump function, by coronary perfusion in a bioreactor that simulated cardiac physiology[49]. Anyway, no similar studies are available with human cell source and biomaterials.

The development of an *in vitro* model, reproducing at least the morphological and physiological features of human cardiomyocytes, would be of great value for physiological studies or drug and therapies development. As discussed in chapter 3 in the case of an *in vitro* model of DMD skeletal muscle, an analogous model of human functional cardiomyocytes could provide a good source of study in understanding the effects (or side effects) of new drugs on cardiomyocytes functionality, or the efficiency of a peculiar type of cell or stem cell in grafting with a preexisting functional tissue.

Is this sight, an array of hESC-derived cardiomyocytes was developed onto a poly-acrylamide hydrogel, by applying the same microscale techniques described in chapter 2 and used in chapter 3 for the skeletal muscle. The cell source used are the human cardiomyocytes derived from hESC with the protocol developed by Keller's lab (see § 4.3.1), since the high yield in cardiomyocytes cells[31]. The substrate is a poly-acrylamide hydrogel (see § 2.2.1), which mimic the correct mechanical properties of striated muscles *in vivo* (where E is ~10-15 kPa[50]). Two different geometries for protein pattern (laminin 100 μg/mL) were tested: parallel lanes, 75 μm wide and 100 μm spaced, and circular dots of 300 μm in diameter and 700 μm

center to center spaced. Once the 20-days differentiation protocol for cardiomyocytes derivation is over, almost all the obtained EBs have a dark appearance and show spontaneous contractions. In figure 4.16 are reported two images of the EB ad day 25, upon arrival from Keller's laboratory.

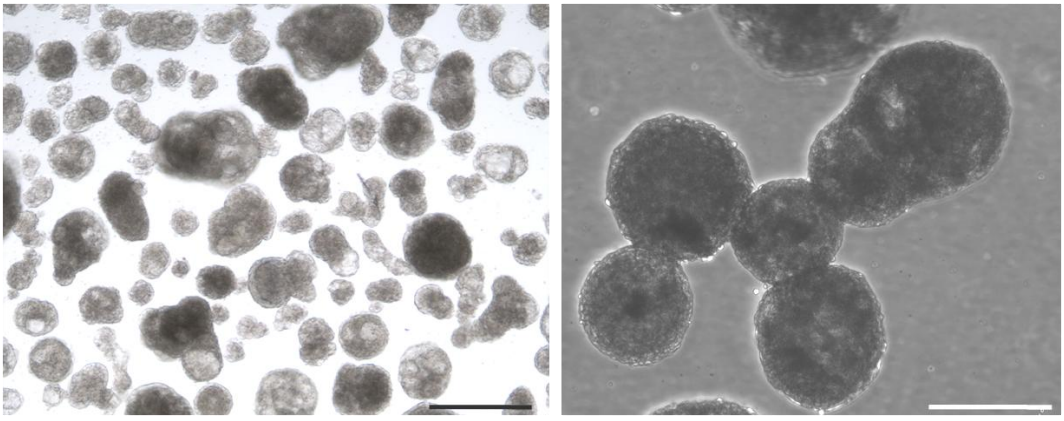

Figure 4.16. EB at day 23. The EBs have a dark appearance and they all show spontaneous contractions. Scale bar=500 μm

The cardiomyocyte seeding onto the hydrogel requires the EBs to be dissociated, in order to obtain a single cell suspension. Briefly, EBs are collected onto a 15 mL round bottom snap cap tubes and allowed to settle, the supernatant is aspirated and 2 mL of Collagenase Type I (0.2% in PBS, plus 10 μL/mL DNAse) are added. After 45 minutes of incubation at 37 °C, the collagenase is removed and followed 5 minutes of incubation with 2 mL of trypsin at 37 C. Trypsin is quenched with STOP solution (FCS plus IMDM 1:1, and 30 μL/mL DNAse) and the EBs are mechanically dissociated by resuspention through a syringe gauge. At this point the cell suspension has few cell clusters, which can be easily removed by filtration through a 40 μm cell strainer. The cells are then resuspended in plating medium (StemPro + supplement + P/S, Glutamine 10 μg/mL, Ascorbic Acid 10 μg/mL, Transferrin 5 μg/mL, MTG 3 μg/mL, VEGF 2 μg/mL, bFGF 0.5 μg/mL). The single cardiomyocytes are plated onto the patterned hydrogel at a concentration of 6,2 $\times 10^4$ cells/cm^2.

The PA hydrogel was biocompatible with regards to the hESC-derived cardiomyocytes (hESC-CM), which selectively adhered to the micropatterned substrates and maintained the correct physiologic cell behavior with respect to

cardiac Troponin T expression and the development of spontaneous contractions. Cardiomyocytes have a natural tendency to cluster and adhere on top of a lower layer (probably composed of endothelial cells) when cultured in parallel lanes (arrows in Figure 4.17).

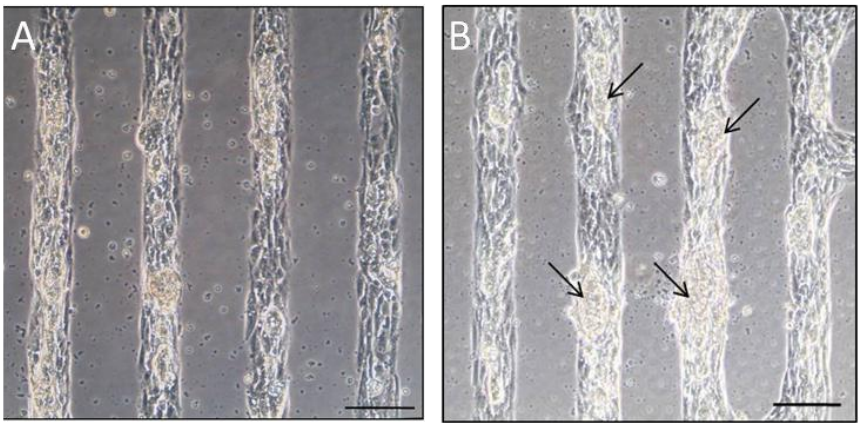

Figure 4.17. hESC-CM culture on patterning of parallel lanes 24 (A) and 48 (B) hours after seeding. At later time points is more evident how cardiac cell clusters (arrows in B) tend to adhere to the bottom layer formed by endothelial cells. Scale bar 100 μm.

Thus, the best configuration for hESC-CM is the patterning and culture in circular spots, which resulted in an homogenous array in the entire patterned surface (Fig 4.18A), and in cardiomyocytes spots maintaining the cardiac marker Troponin T even after several days of culture (Fig. 4.18B and C). Moreover, as described in paragraph 2.3, for contracting cardiomyocytes the more stable configuration is the circular dot, since the mechanical stress due to contractions are minimized and equal in all the directions, thus the risk of detachment is minimized.

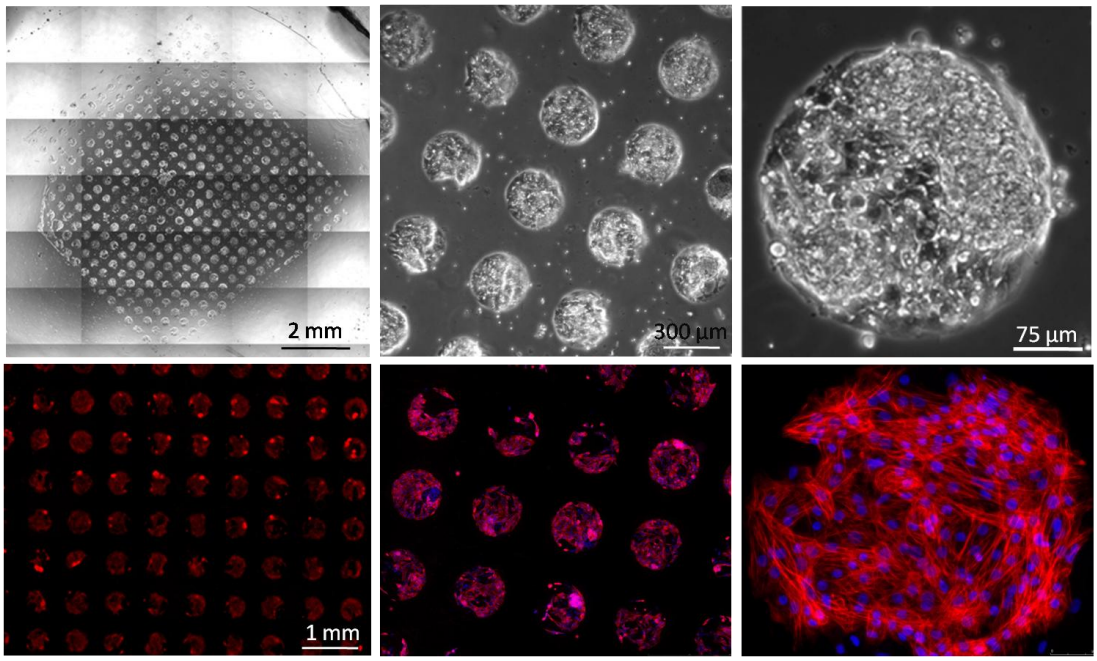

Figure 4.18. Bright field (upper panel) and cardiac Troponin T (lower panel) immunoflourescence of the developed cardiomyocytes array after 5 days of culture. Nuclei are counterstained with DAPI.

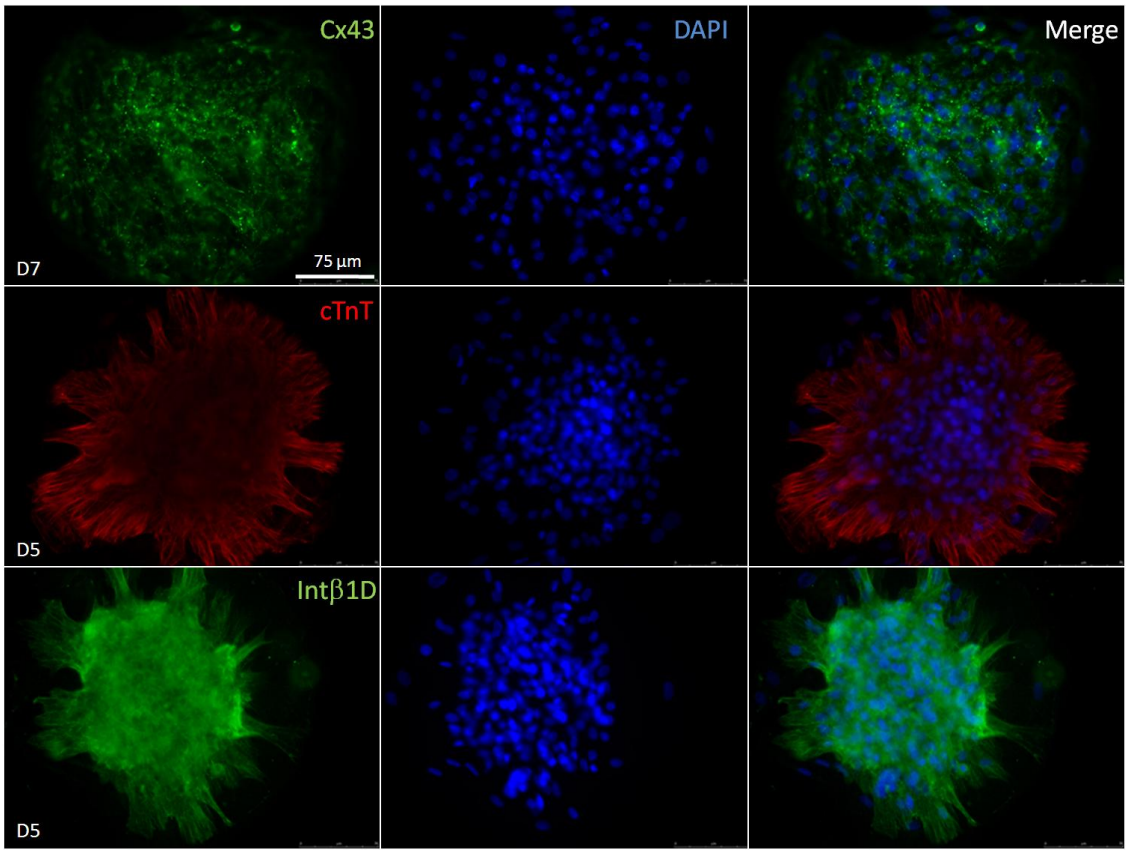

Figure 4.19. Expression of cardiac markers after 5 (D5) or 7 (D7) days of culture onto patterned hydrogel. Immunofluorescence against Connexix 43, cardiac TroponinT and IntegrinB1D are reported. Nuclei were counterstained with DAPI.

The maintenance of cardiac markers and the degree of differentiation was verified in the range of 5 and 7 days of culture. The expression of Connexin 43 (Cx43), cardiac Troponin T (cTnT) and Integrin β1D (Intβ1D) was confirmed by immunoflourescence (Fig. 4.19).

In order to verify the maintenance of hESC-CM functionality after culture onto the hydrogel, spontaneous contracting cardiomyocytes dots were electrically stimulated with the intent of inducing an excitation-contraction coupling. The contractions (before and after electrical stimulation) were recorded and the movie analyzed. Briefly, frames were obtained from the movies and the stacked images processed for image analysis. Several area of 5 μm diameter (ROIs) were positioned in appropriate regions of each cells-dot (so that their color intensity changed during contraction) and an automated routine measured the average intensity of each ROI and for all images in the stack. From the intensity values, graphs representing the cell contractions could be built (Fig. 4.20).

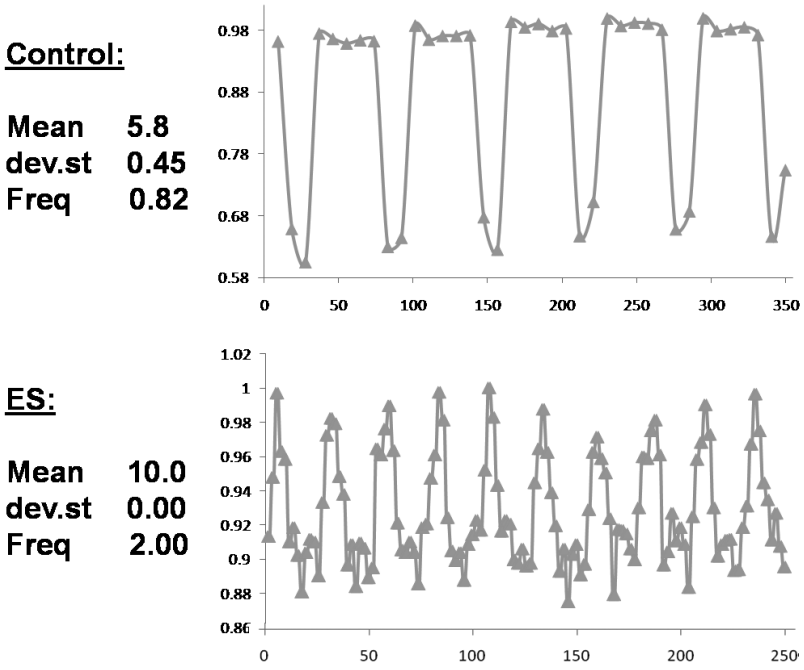

Figure 4.20. Graphs representing the contraction of control and electrically stimulated cadiomyocytes (ES). The variation of intensity is reported in function of the frame number (each frame was taken every 200ms).

The contraction frequency of control hESC-CM was relatively slow, 0.83 Hz. On the contrary, the contraction frequency of stimulated cardiomyocytes was higher

and resulted in a 2Hz frequency, matching the frequency of the applied electrical stimulus (table 4.1).

Table 4.1: The last two columns respectively report: the applied stimuli frequency, the measured contraction frequency averaged on 5 dots within one observation field.

	Electrical stimulus characteristics				**hESC-CM contraction**
	Voltage (mV)	**Duration (ms)**	**Interval (ms)**	**Frequency (Hz)**	**Frequency (Hz)**
Control	/	/	/	/	0.83±0.06
ES	5000	10	500	2	2±0.00

4.5 Conclusions and future prospective

During this thesis, the protocol and methodologies for hESC culture were acquired. In spite of the time- and labor-demanding procedures, two cell lines were successfully cultured for more than 15 passages. The procedure for EBs derivation and dissociation to single cell was established and hESC differentiation towards the cardiomyogenic lineage was studied.

One of the major issue in heart cell therapy is the survival of grafted cardiomyocytes to form enough new myocardium in order to replace the tissue lost to infarction[4]. The death of transplanted cells are slowing research progress in cell therapy for several diseases (diabetes[51], Parkinson's disease[52] and muscular dystrophy[53]). Diseased or injured tissues in fact, are generally characterized by an adverse environment (inflammation, scar tissue formation, high level of pro-inflammatory cytochines and reactive oxygen species, hypoxia,…), which weaken the transplanted cells and lead to their death. This research field would thus greatly benefit from the development of an *in vitro* model reproducing the peculiar conditions that closely match human diseased heart. The diseased factors causing cell death could be identified *in vitro* and several strategies for lowering cell death could be tested. For instance, Laflamme and colleagues identified a cocktail of pro-survival factors that limits hESC-derived cardiomyocytes death after transplantation. They demonstrated that all of the hearts that received cardiomyocytes plus pro-survival cocktail showed

hESC–derived cardiac implants after 4 weeks, and, in some cases, the grafts had remuscularized a significant portion of the infarct zone[4]. The same type of experimentation could be carried in an *in vitro* model system, being much more easy and economic to perform and requiring a lower number of animals to be treated. The array of functional contracting hESC-CM, organized in independent and aligned dots, presented in paragraph 4.4, can be designed and coupled with particular features mimicking a diseased heart, such as stiffer substrate, mimicking the formation of scar tissue, increased ROS concentration, and addition of cytokines of the inflammatory state. A further development, is the coupling of the array of human cardiomyocytes with a microfluidic platform (see § 2.5). The aligned and parallel hESC-CM dots could be easily combined to microfluidic channels (see § 2.5.1), which can stimulate each individual lane of cardiomyocytes with different conditions: cytokines, cocktail of factors, increasing concentrations of ROS. The following analysis on cell viability could give precious information for the development of efficient cell therapy. The microfluidic platform compatible with the array of cardiomyocytes described in this work has already been developed in Elvassore's laboratory; preliminary experiments and its optimization are ongoing studies[54].

Taken together, these considerations confirm that the developed array of human beating cardiomyocytes could be use for *in vitro* screenings, for example for the estimate of the average mortality of implanted cells before performing expensive and time demanding *in vivo* studies and at the same time it could give an approximate estimate of the required cell number for a successful therapy. This work thus represent a step forward in the obtainment of human cardiomyocytes from human embryonic stem cells and in the development of an *in vitro* model of human myocardium.

4.6 References

1 Engler, A. J. et al., Embryonic cardiomyocytes beat best on a matrix with heart-like elasticity: scar-like rigidity inhibits beating. *Journal of Cell Science* **121** (22), 3794 (2008).

2 MacKenna, D. A., Dolfi, F., Vuori, K., and Ruoslahti, E., Extracellular signal-regulated kinase and c-Jun NH2-terminal kinase activation by mechanical stretch is integrin-dependent and matrix-specific in rat cardiac fibroblasts. *Journal of Clinical Investigation* **101** (2), 301 (1998).

3 Gerecht-Nir, S. et al., Biophysical regulation during cardiac development and application to tissue engineering. *International Journal of Developmental Biology* **50** (2-3), 233 (2006).

4 Laflamme, M. A. et al., Cardiomyocytes derived from human embryonic stem cells in pro-survival factors enhance function of infarcted rat hearts. *Nature Biotechnology* **25** (9), 1015 (2007).

5 Cohn, J. N. et al., Report of the National Heart, Lung, and Blood Institute Special Emphasis Panel on Heart Failure Research. *Circulation* **95** (4), 766 (1997).

6 Habib, M., Caspi, O., and Gepstein, L., Human embryonic stem cells for cardiomyogenesis. *Journal of Molecular and Cellular Cardiology* **45** (4), 462 (2008).

7 Murry, C. E., Field, L. J., and Menasche, P. , Cell-based cardiac repair: reflections at the 10-year point. *Circulation* **112** (20), 3174 (2005).

8 Laflamme, M. A. and Murry, C. E. , Regenerating the heart. *Nature Biotechnology* **23**, 845 (2205); Dimmeler, S., Zeiher, A. M., and Schneider, M. D., Unchain my heart: the scientific foundations of cardiac repair. *Journal of Clinical Investigation* **115** (3), 572 (2005).

9 Segers, V. F. and Lee, R. T., Stem-cell therapy for cardiac disease. *Nature* **451** (7181), 937 (2008).

10 Thomson, J. A. et al., Embryonic Stem Cell Lines Derived from Human Blastocysts. *Science* **282** (5391), 1145 (1998).

11 Laflamme, M. A. and ., et al., Formation of human myocardium in the rat heart from human embryonic stem cells. *American Journal of Pathology* **167** (3), 663 (2005); Kehat, I. and al., et, Electromechanical integration of cardiomyocytes derived from human embryonic stem cells. *Nature Biotechnology* **22** (10), 1282 (2004); Xue, T. and al., et, Functional integration of electrically active cardiac derivatives from genetically engineered human embryonic stem cells with quiescent recipient ventricular cardiomyocytes: insights into the development of cell-based pacemakers. *Circulation* **111**, 11 (2005).

12 Leobon, B. and al., et, Myoblasts transplanted into rat infarcted myocardium are functionally isolated from their host. *Proceedings of the National Academy of Sciences of the United States of America* **100** (13), 7808 (2003).

13 Evans, M. J. and Kaufman, M. H., Establishment in culture of pluripotential cells from mouse embryos. *Nature* **292** (5819), 154 (1981); Martin, G. , Isolation of a pluripotent cell line from early mouse embryos cultured in medium conditioned by teratocarcinoma stem cells. *Proceedings of the National Academy of Sciences of the United States of America* **78** (12), 7634 (1981).

14 Reubinoff, B. E. et al., Embryonic stem cell lines from human blastocysts: somatic differentiation in vitro. *Nature Biotechnology* **18** (4), 399 (2000).

15 Thomson, J. A. and Marshall, V. S. , Primate embryonic stem cells. *Current Topics in Developmental Biology* **38**, 133 (1998).

16 Hoffman, L. M. and Carpenter, M. K., Characterization and culture if human embryonic stem cells. *Nature Biotechnology* **23** (6), 699 (2005).

17 Amit, M. et al., Clonally derived human embryonic stem cell lines maintain pluripotency and proliferative potential for prolonged periods of culture. *Developmental Biology* **227** (2), 271 (2000).

18 Itskovitz-Eldor, J. et al., Differentiation of human embryonic stem cells into embryoid bodies compromising the three embryonic germ layers. *Molecular Medicine* **6** (2), 88 (2000).

19 Andrews, P.W. et al., The International Stem Cell Initiative: toward benchmarks for human embryonic stem cell research. *Nature Biotechnology* **23** (7), 795 (2005).

20 Initiative, The International Stem Cell, Characterization of human embryonic stem cell lines by the International Stem Cell Initiative. *Nature Biotechnology* **27** (7), 803 (2007).

21 Draper, J. S., Séguin, C. A., and Andrews, P. W., in *Human Embryonic Stem Cells The Practical Handbook*, edited by S. Sullivan, C. A. Cowan, and K. Eggan (John Wiley & Sons Ltd, 2007), pp. 93.

22 Reubinoff, B. E., Pera, M. F., Fong, C. Y., and al., et, Embryonic stem cell lines from human blastocysts: somatic differentiation in vitro. *Nature Biotechnology* **18** (4), 399 (2000).

23 Améen, A. et al., Human embryonic stem cells: Current technologies and emerging industrial applications. *Critical Reviews in Oncology/Hematology* **65** (1), 54 (2008).

24 Ludwig, T.E. et al., Feeder-independent culture of human embryonic stem cells. *Nature Methods* **3** (8), 637 (2006).

25 Itskovitz-Eldor, J. et al. *Mol. Med.* **6**, 88 (2000).

26 Dang, S.M. et al., Controlled, scalable embryonic stem cell differentiation culture. *Stem Cells* **22** (3), 275 (2004).

27 Gerecht-Nir, S. and Itskovitz-Eldor, J., pp. 260.

28 Murry, C. E. and Keller, G., Differentiation of Embryonic Stem Cells to Clinically Relevant Populations: Lessons from Embryonic Development. *Cell* **132** (4), 661 (2008).

29 Kehat, I., Kenyagin-Karsenti, D., Snir, M., and al., et, Human embryonic stem cells can differentiate into myocytes with structural and functional properties of cardiomyocytes. *Journal of Clinical Investigation* **108** (3), 407 (2001); He, J. Q., Ma, Y., Lee, Y., and al., et, Human embryonic stem cells develop into multiple types of cardiac myocytes: action potential characterization. *Circulation Research* **93** (1), 32 (2003); Xue, T., Cho, H. C., Akar, F. G., and al.., et, Functional integration of electrically active cardiac derivatives from genetically engineered human embryonic stem cells with quiescent recipient ventricular cardiomyocytes: insights into the development of cell-based pacemakers. *Circulation* **111** (1), 11 (2005).

30 Mummery, C. and al, et, Differentiation of human embryonic stem cells to cardiomyocytes: role of coculture with visceral endoderm-like cells. *Circulation* **107** (21), 2733 (2003).

31 Yang, L et al., Human cardiovascular progenitor cells develop from a KDR1 embryonic-stem-cell-derived population. *Nature* **453** (7194), 524 (2008).

32 Goh, G. et al., Molecular and phenotypic analyses of human embryonic stem cell-derived cardiomyocytes. Opportunities and challenges for clinical translation. *Thrombosis Haemostasis* **94** (4), 728 (2005).

33 Heng, B. C. et al., Strategies for directing the differentiation of stem cells into the cardiomyogenic lineage in vitro. *Cardiovascular Research* **62** 34 (2004); Puceat, M., Protocols for cardiac differentiation of embryonic stem cells. *Methods* **45** (2), 168 (2008).

34 Tam, P.P. and Behringer, R.R. , Mouse gastrulation: the formation of a mammalian body plan. *Mechanisms of Development* **68** (1-2), 3 (1997).

[35] Kattman, S. J., Huber, T. L., and Keller, G. M., Multipotent Flk-1+ Cardiovascular Progenitor Cells Give Rise to the Cardiomyocyte, Endothelial, and Vascular Smooth Muscle Lineages. *Developmental Cell* **11** (5), 723 (2006).

[36] Jaffe, L. F. and Nuccitelli, R. , Electrical Controls of Development. *Annual Review of Biophysics and Bioengineering* **6** (1), 445 (1977).

[37] Sauer, H., Rahimi, G., Hescheler, J., and Wartenberg, M., Effects of Electrical Fields on Cardiomyocyte Differentiation of Embryonic Stem Cells. *Journal of Cellular Biochemistry* **75** (4), 710 (1999).

[38] Puceat, M., Role of Rac-GTPase and Reactive Oxygen Species in Cardiac Differentiation of Stem Cells. *Antioxidants & Redox Signaling* **7** (11-12), 1435 (2005); Puceat, M., Travo, P., Quinn, M.T., and Fort, P., A Dual Role of the GTPase Rac in Cardiac Differentiation of Stem Cells. *Molecular Biology of the Cell* **14** (7), 2781 (2003).

[39] Rhee, S.G., Redox signaling: hydrogen peroxide as intracellular messenger. *Experimental and Molecular Medicine* **31** (2), 53 (1999); Shah, Ajay M. and Sauer, Heinrich, Transmitting biological information using oxygen: Reactive oxygen species as signalling molecules in cardiovascular pathophysiology. *Cardiovascular Research* **71** (2), 191 (2006); Sun, Yi and Oberley, Larry W., Redox regulation of transcriptional activators. *Free Radical Biology and Medicine* **21** (3), 335 (1996).

[40] Sauer, Heinrich, Rahimi, Gohar, Hescheler, Jurgen, and Wartenberg, Maria, Role of reactive oxygen species and phosphatidylinositol 3-kinase in cardiomyocyte differentiation of embryonic stem cells. *FEBS Letters* **476** (3), 218 (2000).

[41] Sachinidis, A. et al., Cardiac specific differentiation of mouse embryonic stem cells. *Cardiovascular Research* **58** (2), 278 (2003).

[42] Sauer, H. et al., Involvement of reactive oxygen species in cardiotrophin-1-induced proliferation of cardiomyocytes differentiated from murine embryonic stem cells. *Experimental Cell Research* **294** (2), 313 (2004).

[43] Schmelter, Maike et al., Embryonic stem cells utilize reactive oxygen species as transducers of mechanical strain-induced cardiovascular differentiation. *FASEB Journal* **20** (8), 1182 (2006).

[44] Sorescu, D. and Griendling, K. K. , Reactive oxygen species, mitochondria, and NAD(P)H oxidases in the development and progression of heart failure. *Congestive Heart Failure* **8** (3), 132 (2002).

[45] Lev, S., Kehat, I., and Gepstein, L., Differentiation Pathways in Human Embryonic Stem Cell-Derived Cardiomyocytes. *Annals of the New York Academy of Sciences* **1047** (1), 50 (2005); Li, Jian et al., The NADPH Oxidase NOX4 Drives Cardiac Differentiation: Role in Regulating Cardiac Transcription Factors and MAP Kinase Activation. *Molecular Biology of the Cell* **17** (9), 3978 (2006).

[46] Chen, K., Wu, L., and Wang, Z. Z., Extrinsic Regulation of Cardiomyocyte Differentiation of Embryonic Stem Cells. *Journal of Cellular Biochemistry* **104** (1), 119 (2008).

[47] Setsukinai, K. et al., Development of Novel Fluorescence Probes That Can Reliably Detect Reactive Oxygen Species and Distinguish Specific Species. *The Journal of Biological Chemistry* **278** (5), 3170 (2003).

[48] Mummery, C. et al., Cardiomyocyte differentiation of mouse and human embryonic stem cells. *Journal of Anatomy* **200** (3), 233 (2002).

[49] Ott, H. C. et al., Perfusion-decellularized matrix: using nature's platform to engineer a bioartificial heart. *Nature Medicine* **14** (2), 213 (2008).

[50] Berry, M. F. et al., Mesenchymal stem cell injection after myocardial infarction improves myocardial compliance. *American Journal of Physiology-Heart Circulatory Physiology* **290** (6), H2196 (2006).

[51] Nakano, M. and al., et, Caspase-3 inhibitor prevents apoptosis of human islets immediately after isolation and improves islet graft function. *Pancreas* **29** (2), 104 (2004).

[52] Emgard, M. et al., Both apoptosis and necrosis occur early after intracerebral grafting of ventral mesencephalic tissue: a role for protease activation. *Journal of Neurochemistry* **86** (5), 1223 (2003).

[53] Skuk, D. et al., Resetting the problem of cell death following muscle-derived cell transplantation: detection, dynamics and mechanisms. *Journal of Neuropathology and Experimental Neurology* **62** (9), 951 (2003).

[54] Cimetta, E., Design and development of microscale technologies and microfluidic platforms for the in vitro culture of stem cells. PhD Thesis, University of Padova, 2009.

Chapter 5

Conclusions

Skeletal and cardiac muscles suffer from a variety of myopathies or diseased condition, whose multifactorial nature hinder the development of efficient drugs and therapies. Examples are the Duchenne Muscular Dystrophy, in the case of skeletal muscles, and heart failure, for the myocardium. The molecular defects causing the pathology or the cause inducing the illness condition have been investigated so far through the use of traditional systems: cell culture *in vitro* and animal experimentation *in vivo*. What is now required is the development of efficient therapies able to face and overcome several and different aspects of the disease. DMD patients need the efficient restoration of dystrophin expression, the re-establishment of a pool of stem cells for following muscle regeneration cycles, the reduction of the inflammation, the substitution of fibrous tissue with functional muscle; an infarcted heart has similar needs: it requires the replacement of scar tissue with functional cardiomyocytes, the re-establishment of efficient blood circulation. For this type of studies, the standard methodologies are not sufficient. What is missing in standard *in vitro* cell culture is biomimesis; the regular Petri dish lacks of physiological stimuli reproducing the correct cell microenvironment, while *in vivo* animal models are not representative of the human physiology. The field of tissue engineering, which is traditionally inspired by the concept of biomimesis and in the last years has developed several strategies and tools in this perspective, is now driven by this great need and its final products (engineered tissue) are finding an alternative application as *in vitro* model.

In this scenario, this PhD thesis aimed at the development of *in vitro* human functional skeletal and cardiac tissues, for a possible use as *in vitro* models . The philosophy underneath this work is based on the interaction between the use of human cells, the choice of a biomimetic environment for cell culture and the use of microscale techniques for reproducing the major cues that *in vivo* guide cell differentiation (Fig. 5.1). In particular, human primary myoblasts or cardiomyocytes derived from human embryonic stem cells were cultured onto a biocompatible hydrogel, mimicking the mechanical properties of the striated muscles *in vivo*. Cell differentiation and tissue maturation were enhanced by the application of microscale techniques: i) control of the mechanical cues exerted to the culture, in order to investigate the role of mechanical properties of the substrate; ii) protein micropatterning, with the aim of imposing a spatial organization to the culture for maximize myoblasts differentiation and cardiomyocytes beating performance; iii) electrical stimulation, in order to mimic part of the neuronal or electrical activity of striated muscles; iv)generation of a cell array in sight of coupling the tissue with a microfluidics platform for the development of highthroughput assay.

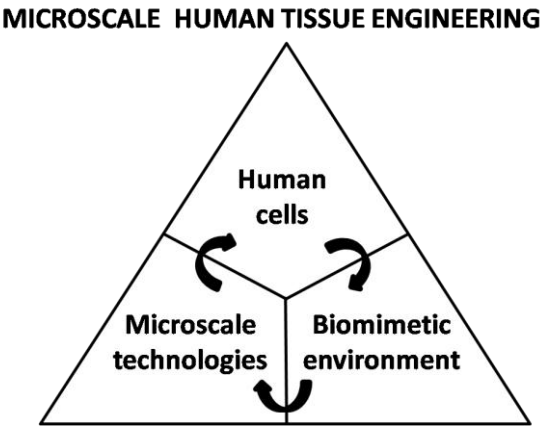

Figure 5.1. Schematic representation of the approach underneath this PhD thesis work: the biomimetic environment controlling human cells fate *in vivo* inspired microscale technology development, in order to reproduce the biophysical cues that guide human cell differentiation *in vitro* with a precise and defined control.

The microscale technologies used in this thesis are easy to reproduce, inexpensive and extremely versatile. They were designed and developed with the intent of being used in the development of an *in vitro* model, able to lower cost and time of drug

and therapy development, which could be easily used by researcher with biological (and not engineering) background.

Cell topology is particularly important in tissues with a defined and hierarchical organization such as skeletal muscles. The topological orientation *in vitro* of human myoblasts, imposed through micropatterning, has greatly reduced the time required for myoblasts fusion (few myotubes were observed 72 hours after seeding, without switching to a differentiative medium) in comparison to conventional substrates and has lead to the obtainment of parallel oriented and independent myotubes. The emerging research field of mechanobiology attempts to determine the role of mechanical and physical cues in cell behavior[1]. The use of an hydrogel with tissue-like mechanical properties in this thesis allowed the efficient formation of the functional unit of skeletal muscle, the sarcomere. The rate of sarcomere formation and the extent of myotube striations were much higher in comparison to conventional stiff substrates (glass or polystyrene). Moreover the control over the mechanical properties of the cell substrate, allowed to demonstrate the strong dependence of sarcomere formation to substrate stiffness. These results confirm the findings of Engler and colleagues[2], in primaty mouse myoblasts; so far no results were reported for human cell primary culture. It has been hypothesized that the higher efficiency in sarcomere formation in myotubes cultured onto an hydrogel is possibly due to the higher motility of membrane and ECM proteins. The hydrogel is a polymeric network, which allow a certain degree of motility and conformational adaptation, while proteins liked to the glass are almost completely immobilized. The process of myofibrillogenesis, both in skeletal and in cardiac muscles, is a highly orchestrated process whose assemble the filaments of sarcomeres and myofibrils in a precise and defined manner, giving then rise to the mature structure of the myofibril. One candidate mechanoreceptor is N-RAP, which appears at the appropriate place and time for myofibrillogenesis to be sensitive to substrate elasticity. N-RAP is a multidomain, nebulin-related, actin-binding protein critical for myofibrillogenesis. N-RAP also binds α-actinin and filamin and is thought to form a membrane-bound scaffold for nucleating actin filament growth[3]. The supposed higher motility of N-RAP allowed by the hydrogel network, or other proteins which

control the sarcomere assembly, such as integrins, could possibly explain the rapid and more efficient process of sarcomere formation in myotubes cultured onto the hydrogel surface.
The obtained human skeletal muscle tissue could be coupled to other experimental strategies and technologies for further maturation, such as three dimensional substrate architecture, electrical stimulation, culture in a perfusion bioreactor, which have already and successfully been applied to murine myoblasts (Appendix B and C).

The first critical step in cardiac muscle *in vitro* development is the choice of an adequate cell source. Human embryonic stem cells have been selected, due to their high proliferative and differentiation potential. Actually, they represent the best cell source for the obtainment of an elevated number of cardiomyocytes. Despite their high sensitivity to environmental conditions and their time-demanding cell culture, human embryonic stem cells were successfully cultured and expanded during this study. The following differentiation in cardiomyocytes was achieved both by a standardized protocol based on hESC stimulation with a defined temporal sequence of soluble factors[4], which gave an extremely high yield in cadiomyocytes (more than 50% of cells were positive to cardiac Troponin T) and by an innovative protocol based on the application of electrical stimulation, which gave a lower amount of cardiomyocytes in comparison to the first protocol, but whose potentiality could be increased by optimization of the applied stimulus. This type of studies, aiming at control the differentiation pathway of hESC, are nowadays one of the most important challenge in hESC research, since this is the major prerequisite for clinical application of hESC.
The cardiomyocytes derived from hESC were then used to verify the feasibility of the development of an *in vitro* array of functional cardiomyocytes. Independent and spatially organized circular spots of contracting cardiomyocytes were obtained onto an hydrogel. The culture conditions, for up to 7 days, did not alter the expression of cardiac markers and did not affect the presence of spontaneous contractions. Moreover, the excitation-contraction coupling was achieved by the application of

exogenous electrical stimuli; 2Hz of synchronous contractions were observed for all the cardiomyocytes spots within the array.

The advent of human embryonic stem cells opened new and exciting prospective in the field of tissue engineering and regenerative medicine. The possibility of deriving all the types of cells composing human body holds the potential of healing and defeat those diseases based on cellular disfunction and of generating artificial organs for the replacement of the failure tissue. Such a scenario is obviously a long-term prospective, but it rises from a reasonable enthusiasm for the latest results obtained in the field. The control over both hESC expansion and differentiation *in vitro* towards specific lineages for clinical application is still a long way to cover, but important steps forward have been accomplished. The coupling of biological science with engineering offer new possibilities, as demonstrated by the promising results obtained in this thesis. Novel bioengineering technologies should be integrated into the cell biology as they evolve to further enhance control of cell product identity, reproducibility, and efficacy. Cellular systems biology-based tools will likely play an important role as a strategy to address both unresolved regulatory and engineering challenges[5].

The 2008 most relevant scientific discovery, according to Science[6], is the development of induced Pluripotent Stem cells (iPS)[7]. The iPS are adult somatic cell reprogrammed to an embryonic state, which can then be differentiate to any cell type (such as hESC) but overcomes the ethical issues involving the use of embryos (Appendix E). This discovery open the possibility of creating patient-specific stem cell lines to study different disease mechanisms in the laboratory, to increase the efficiency of drug discovery and to provide valuable tools for toxicology testing. Furthermore, this reprogramming system could make the idea of customized patient-specific screening and therapy both possible and economically feasible.

It is important to underline that the use of iPS with the microscale technologies presented in this thesis is straightforward. iPS culture are fundamentally based on knowledge and protocols established for hESC.

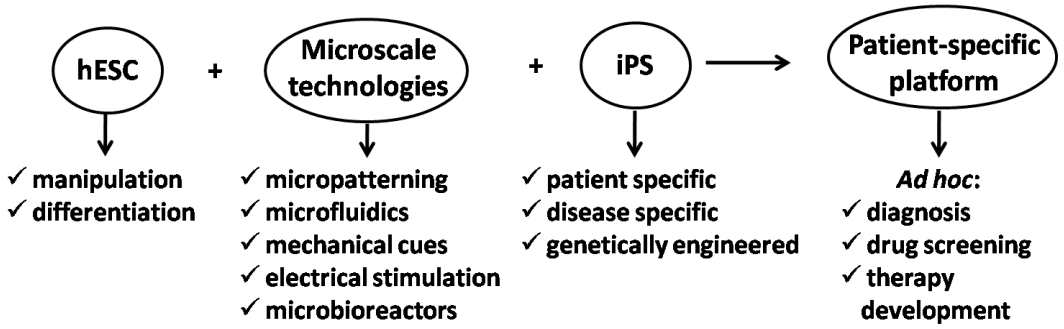

Figure 5.2. The medicine of the future: patient-specific platform. All the actual efforts in hESC culture and manipulation, development of microscale technologies to control the cell microenvironment and iPS derivation would lead to the generation of patient-specific platform, used in diagnosis, screening or therapy development.

The medicine of the future will be founded on patient-specific platforms obtained from patient-derived cells for *ad hoc* drug screening and therapy development (Fig. 5.2).

5.1 References

1 Hoffman, B. D., Massiera, G. , Van Citters, K. M., and Crocker, J. C., The consensus mechanics of cultured mammalian cells. *PNAS* **103** (27), 10259 (2006); Engler, A. J., Sen, S., Sweeney, H. L., and Discher, D. E., Matrix Elasticity Directs Stem Cell Lineage Specification. *Cell* **126**, 677 (2006).

2 Engler, A. J. et al., Myotubes differentiate optimally on substrates with tissue-like stiffness: pathological implications for soft or stiff microenvironments. *J. Cell Biol.* **166** (6), 877 (2004).

3 Carroll, S., Lu, S., Herrera, A. H., and Horowits, R., N-RAP scaffolds I-Z-I assembly during myofibrillogenesis in cultured chick cardiomyocytes. *Journal of Cell Science* **117** (1), 105 (2004).

4 Yang, L et al., Human cardiovascular progenitor cells develop from a KDR1 embryonic-stem-cell-derived population. *Nature* (2008).

5 Kirouac, D. C. and Zandstra, P. W., The Systematic Production of Cells for Cell Therapies. *Cell Stem Cell* **3**, 369 (2008).

6 Vogel, G., Reprogramming Cells. *Science* **322** (5909), 1766 (2008).

7 Takahashi, K. et al., Induction of pluripotent stem cells from adult human fibroblasts by defined factors. *Cell* **131** (5), 861 (2007).

Appendix A

Production of arrays of cardiac and skeletal muscle myofibers by micropatterning techniques on a soft substrate

Elisa Cimetta[1], Sara Pizzato[1], Sveva Bollini[2], Elena Serena[1], Paolo De Coppi[2], Nicola Elvassore[1]*

[1] Department of Chemical Engineering, University of Padua, Via Marzolo, 9 Padua, Italy

[2] Department of Pediatrics, University of Padua, Via Giustiniani, 3, Padua, Italy

*Corresponding author

Biomedical Microdevices

DOI 10.1007/s10544-008-9245-9

Keywords: micro-patterning, soft substrate, hydrogel, cardiomyocytes, satellite cells, cell array.

Abstract

Micropatterning and microfabrication techniques have been widely used to pattern cells on surfaces and to have a deeper insight into many processes in cell biology such as cell adhesion and interactions with the surrounding environment. The aim of this study was the development of an easy and versatile technique for the in vitro production of arrays of functional cardiac and skeletal muscle myofibers using micropatterning techniques on soft substrates. Cardiomyocytes were used for the production of oriented cardiac myofibers whereas mouse muscle satellite cells for that of differentiated parallel myotubes. We performed micro-contact printing of extracellular matrix proteins on soft polyacrylamide-based hydrogels photopolymerized onto functionalized glass slides. Our methods proved to be simple, repeatable and effective in obtaining an extremely selective adhesion of both cardiomyocytes and satellite cells onto patterned soft hydrogel surfaces. Cardiomyocytes resulted in aligned cardiac myofibers able to exhibit a synchronous contractile activity after 2 days of culture. We demonstrated for the first time that murine satellite cells, cultured on a soft hydrogel substrate, fuse and form aligned myotubes after 7 days of culture. Immunofluorescence analyses confirmed correct expression of cell phenotype, differentiation markers and sarcomeric organization. These results were obtained in myotubes derived from satellite cells from both wild type and MDX mice which are research models for the study of muscle dystrophy. These arrays of both cardiac and skeletal muscle myofibers could be used as in vitro models for pharmacological screening tests or biological studies at the single fiber level.

A.1 Introduction

The major advantage introduced by high-throughput technology resides in the possibility of simultaneously acquiring vast amounts of information (Kozarova et al. 2006; Chen et al. 2006). Recently, protein microarrays (Brueggemeier et al. 2005), tissue microarrays (Chen et al. 2004) and living cell microarrays (Albrecht et al.

2005) have been developed. Living cell-arrays offer unique advantages when used as the sensing element for biological assays or in drug development and differentiation studies (Flaim et al. 2005). Two-dimensional arrays of single cells or clusters of cells can provide appropriate culture conditions for adherent cells, however, the lack of structural and topological cues may alter cell behavior and phenotype expression. Mammalian cells integrate and respond to a combination of factors in the micro-scale environment, such as chemical and mechanical properties, shape, organization and cell-cell interactions (Albrecht et al. 2006; Jang et al. 2006; Kaplan et al. 2005; Vunjak-Novakovic et al. 1998). These aspects are particularly important for cell phenotypes such as cardiac, skeletal, and smooth muscular, which are highly dependent on three-dimensional (3D) cell organization (Motlagh et al. 2003). For instance, in the heart, cardiomyocytes are organized in interconnected cardiac myofibers that contract synchronously, whereas skeletal muscle is formed by parallel multinucleate myofibers. In addition, surface mechanical properties are of particular relevance for the functionality of contractile cells (Engler et al. 2004a; Ingber2002; 2005; Khatiwala et al. 2006), and this translates into the coupling to a soft or stiff substrate. In muscle tissue, contractions are transmitted through cell-cell and cell-matrix interactions. and in a recent study, Engler and colleagues proved that myotube differentiation and the development of myosin/actin striations necessary for functional muscle activity occurs preferentially on substrates with tissue-like stiffness (Engler et al. 2004a).

To guide cell adhesion, many patterning techniques have been proposed and widely reviewed over the last few years (Falconnet et al. 2006; Xia et al. 1998). Various lithographic techniques have been used to guide cell adhesion and orientation onto different substrates (Karp et al. 2006; Rohr et al. 1991; Suh et al. 2004) while microfluidics have been employed to pattern cardiomyocites on PDMS or glass substrates (Gopalan et al. 2003; Khademhosseini et al. 2007). Muscle cells have been studied on surfaces comprising nanopatterned gratings, microgrooves and microtextures (Motlagh et al. 2003; Vernon et al. 2005; Yim et al. 2005). Patterns of proteins have been created on glass or polystyrene surfaces via micro-contact printing (μCP) (Ruiz et al. 2007) and laminin lanes have been patterned using the

same technique on polimeric films for the subsequent adhesion of cardiomyocytes (McDevitt et al. 2003; McDevitt et al. 2002).

The major limitations of the enumerated techniques are related to the stiffness of the substrates used - gold, silver, metal or metal-oxide, glass and polystyrene - on the one hand and to the difficulties encountered while producing controlled patterning on soft materials on the other.

Among soft substrates, hydrogels have recently captured attention in the field of tissue engineering because of their high water content, biocompatibility and elastic properties, resembling those of native tissues. In recent years many kinds of hydrogels, especially poly(ethylene glycol) (PEG) and derivatives (Britton-Keys et al. 1998; Burdick et al. 2004; Lin-Gibson et al. 2005), have been widely used for encapsulating living cells or as substrates for cell culture. A wide variety of copolymers, composed of a synthetic backbone and grafted biomolecules (or vice versa) such as fibrinogen (Almany et al. 2005) and hyaluronic acid (Leach et al. 2003; Leach et al. 2005) or short peptides sequences such as RGD (Hern et al. 1998), was proposed and tested to develop substrates with the biological cues required for cell attachment. In addition, the elastic properties can be controlled and modulated by changing the amount of polymer and crosslinker, thus obtaining stiff or soft gels with a different influence on cell behavior at the cytoskeletal level (Engler et al. 2004b; Peyton et al. 2005).

Thus, an advisable approach is the production of arrays of isolated and independent cellular aggregates in a fiber-like fashion in which cells can align, express their phenotype, eventually fuse and differentiate or show contractile activity. In this perspective, an array of fibers able to reproduce these particular features and maintain the functionality of natural tissues can potentially become a good alternative to animal models for high-throughput pharmacological screenings. In addition, fiber arrays with the capacity of mimicking and reproducing the structural cues of native muscular tissue could represent an in vitro model resembling more closely the in vivo responses than the conventional cell cultures.

To achieve this goal we needed: 1) to spatially organize cells and drive their alignment, 2) to allow cells to differentiate and express their correct phenotype, and

3) to ensure that cells fully develop the functionality peculiar to their native tissue (i.e. contractile activity).

A poly-acrylamide (PA) based hydrogel was used as the substrate for cell culture because of its elastic properties, which are particularly suitable for muscle cell culture (Engler et al. 2004a). Moreover, this hydrogel is easy to produce, inexpensive, biocompatible ,and optically transparent; the latter being an important prerequisite for performing optical image analyses. PA hydrogel can be produced as a thin film and covalently bonded to a functionalized glass slide showing long term stability in culture.

As PA hydrogel is a non-fouling material, an adhesion-protein pattern was micro-contact printed onto the PA surface; this technique was chosen for being a simple and versatile method to pattern adhesion proteins with a resolution of ~1 μm. The immobilization on the surface occurred through physical adsorption and allowed proteins to maintain their activity without suffering from major denaturation phenomena. In addition, patterning proteins on hydrogel films enabled microscope observations on the same focal plane of the substrate.

We developed arrays of cardiac and skeletal muscle fibers on soft substrates that are potentially able to provide independent responses to different stimuli. The techniques here proposed open new and important perspectives in the field of pharmacological screening and drug testing, in order to achieve accurate biological and physiological *in vitro* studies.

A.2 Material and Methods

A.2.1 Cell isolation and culture

C2C12

The murine skeletal muscle immortalized cell line C2C12 (ATCC) was grown in Dulbecco's modified Eagle's medium (DMEM, Sigma-Aldrich) supplemented with 10% foetal bovine serum (FBS, Gibco-Invitrogen), 1% penicillin-streptomycin and

1% L-glutamine (all from Invitrogen), on standard 100 mm Petri dishes, in a 95% humidified and 5% CO_2 atmosphere at 37ºC and maintained at low confluence.
Subconfluent plates of C2C12 cells were detached on day 0 using trypsin/EDTA (Sigma-Aldrich), pelleted by centrifugation for 5 min at 1200 rpm and counted.
Cells were resuspended in DMEM and 300 µl, of the cell suspension was deposited on the hydrogel surface at 104 cells/cm² and incubated for 2 hours. After that, the culture medium and the cells that had not yet adhered were removed. The hydrogels were then gently rinsed, by first adding and then immediately removing 300 µl of DMEM. Seeded hydrogels were then incubated for one week replacing culture medium once a day.

Cardiomyocytes

Rat neonatal cardiomyocytes (CM) cultures were obtained by enzymatic digestion of newborn rat hearts. Neonatal (2-3 days-old) Sprague-Dawley rats were provided by the Department of Sperimental Surgery of the University of Padua.
The hearts were washed with ice-cold, sterile HBBS (Hank's Balanced Salt Solution, Worthington Biochemical Corporation), trimmed of auricles and excess connective and adipose tissue, and minced with sterile scissors. Myocardial tissue was then dissociated to release ventricular CM by an enzymatic isolation procedure first using a trypsin solution (50 µg/ml), incubating overnight at 4°C, and then a collagenase solution (300 units/ml, Worthington Biochemical Corporation) at 37°C for 45 minutes (Pedram et al. 2005; Speicher et al. 1974; Xiao et al. 1997). CM were then collected by centrifugation and non-myocytes cells were removed by preplating on culture dishes.
Enriched CM were seeded on the hydrogels at a density of $1.6 \cdot 10^5$ cells/cm² in plating medium (DMEM –Sigma-Aldrich, enriched with 5% FBS, 10% Horse Serum – all from Biochrom Ag., 1% L-Glutamine 1% Penicillin and Streptomicin - all from Gibco, and medium M199 17% -Biochrom Ag.) and cultured in a 95% humidified incubator 5% CO_2 at 37°C.
At day one after seeding, hydrogels were rinsed with culture medium to remove non adhering cells. The culture medium was replaced once a day.

Satellite cells

Primary myoblasts were obtained from the expansion of satellite cells isolated from single-muscle fibers adjusting the protocol previously described by Rosenblatt (Rosenblatt et al. 1995). For this reason, we refer to our myoblast culture as satellite cells. Briefly, flexor digitorum brevis from C57BL/6J mouse muscles were removed and enzimatically digested with 0,2% collagenase type I (Sigma-Aldrich). The single fibers obtained were selected on an inverted microscope (Olympus IX71) and plated on Petri dishes pre-coated with Matrigel® (BD Bioscience). Myofibers were maintained in a humidified tissue culture incubator. On day three, the plating medium, which consisted of DMEM (Sigma-Aldrich), 20% horse serum (Gibco-Invitrogen), 1% chicken embryo extract (MP-Biomedicals), and 1% penicillin-streptomycin (Gibco-Invitrogen), was added to the Petri dishes. Released and proliferated cells were detached from the plate with trypsin (Gibco-Invitrogen) before fusion into myotubes occurred, and cultured with proliferating medium (DMEM, 20% foetal bovine serum, 10% horse serum, 0.5% chicken embryo extract and 1% penicillin streptomycin).

300 μl of cell suspension in proliferating medium were seeded at a density of $3 \cdot 10^4$ cells/cm^2 on the hydrogel surfaces. After approximately 5 hours, cells that had not adhered to the surface were removed by gently rinsing the hydrogel films with proliferating medium. Satellite cells were kept in culture for one week, replacing the culture medium every two days.

A.2.2 Glass slide functionalization

Glass slides surfaces were chemically modified creating a hydrophobic layer of methacrylate groups to ensure covalent binding of the hydrogel films. Briefly, slides were washed in ethanol and rinsed with distilled water, dried at 110°C and treated with air-plasma (Plasma Cleaner PDC-002, Harrick Plasma) for 5 minutes at 0,5 mbar. A few drops of 3-(trimethoxysilyl)propyl methacrylate (Sigma-Aldrich) were deposited on the glass slides which were then stacked and after 1 hour dried in oven at 100°C for 10 minutes.

A.2.3 Hydrogel preparation

Hydrogel films

Hydrogels were prepared optimizing previously developed procedures (Flaim et al. 2005). Briefly, acrylamide/bis-acrylamide 29:1 40% solution (Sigma-Aldrich) was diluted in phosphate-buffered saline (PBS, Sigma-Aldrich) to the final concentrations of 8, 10, 15 and 20%. The photoinitiator (Irgacure 2959; Ciba Specialty Chemicals), was initially dissolved in methanol at 200 mg/ml and then added to the acrylamide/bis-acrylamide solution in order to obtain a final concentration of 20 mg/ml, and mixed thoroughly.

Three individual 20 μl volumes of the prepolymer solution were dropped over the functionalized glass surface and a glass coverslip was floated over each drop. Hydrogel polymerization occurred by exposing the prepolymer solution to UV light for 3 minutes. Irradiation was provided by a high-pressure mercury vapor lamp (Philips HPR 125W) emitting at 365 nm with an incident light intensity of 20 mW/cm^2. Selective photo-polymerization of acrylamide solutions on the glass surface was achieved by interposing a photomask with the desired geometry between the light source and the glass slide. Non-exposed regions were washed using distilled water to remove the non-polymerized solution. Such procedures resulted in homogeneous hydrogel films with an average thickness of 40 μm.

Mechanical test

The hydrogel samples for the compression tests were realized using different acrylamide/bis-acrylamide solutions (29:1) at 5, 10, 15 and 20% (v/v) in PBS. The photoinitiator Irgacure 2959, previously dissolved in methanol (200 mg/ml), was added to the prepolymer solution to achieve the final concentration of 20 mg/ml. Hydrogel samples, shaped as 60 mm diameter disks, were obtained photopolymerizing 20 ml of the prepolymer solution under UV light (λ=365 nm).

Young's modulus of the hydrogel was determined by a uniaxial compression test, performed at room temperature using the Sun 2500 Galdabini testing machine. Hydrogel disks were placed between two parallel plates and compressed at the constant rate of 1 mm/min, until a final deformation of 120% was reached. The

Young's modulus for each composition of the PA hydrogel was measured on 5 replicates.

A.2.4 Hydrogel sterilization and cytotoxicity assay

Glass slides with covalently bonded hydrogel films were immersed in ultra-pure distilled water for 48 hours to ensure complete removal of the un-reacted monomeric units or photoinitiator and then soaked in a 70% ethanol solution. After rinsing with ultra-pure distilled water, hydrogels were allowed to dry completely overnight; final sterilization occurred after 20 minutes exposure to UV light under a sterile hood.

Cell viability was assessed with Live/Dead® Viability Cytotoxicity Assay (Invitrogen) based on calcein and etidium homodimer (EthD-1) dyes, following and optimizing the supplied protocol. After mounting on microscope slides, samples were analyzed using a Leica CTR6000 fluorescence microscope.

A.2.5 Array design and realization

The desired array design was realized in digital form with Adobe Illustrator and consisted of 400 lanes 100 μm wide and 1 mm long, horizontally spaced by 100 μm and 300 μm vertically.

This pattern was printed onto an overhead transparency and used as a photomask. A standard photolithographic technique was employed for the fabrication of the master using an SU-8 photoresist (MicroChem Corporation). Briefly, the SU-8 was spun over a silicon wafer, which was thermally treated, selectively polymerized by interposing the patterned photomask, and exposed to UV light (λ=365 nm) for 50 seconds. It was finally developed with 1-methoxy-2-propanol acetate (Sigma-Aldrich).

The PDMS stamp was obtained via replica molding, curing Sylgard 184 (Dow Corning) on the patterned silicon master.

Laminin lanes (100 μm wide) were printed on smooth hydrogel surfaces via μCP technique using the PDMS stamp just described. Specifically, the stamp was inked in the protein solution (mouse-laminin 100 μg/ml in PBS) for a few seconds, and then

the excess solution was removed. Conformal contact between the dry hydrogel surface and the stamp was then achieved by applying a gentle pressure, thus transferring the desired protein micropattern on the substrate.

A.2.6 Immunostaining analyses

Cardiomyocytes-troponin I

After 4 or 7 days of culture, cells on patterned hydrogel were fixed with 2% paraformaldeyde (PFA; Carlo Erba) for 20 minutes at 4°C and permeabilized with a 0.1% Triton X-100 solution (Sigma-Aldrich) at room temperature. CM were then incubated for 25 minutes at 37°C with primary antibodies specific for cardiac troponin I (mouse IgG 1:1000, Chemicon) and diluted in a 1% PBS/BSA solution. Alexa Fluor 594-conjugated goat anti-mouse IgG (Molecular Probes) was diluted 1:150 in a 1% BSA/PBS. Human serum solution (1:100) was used as secondary antibody and incubated for 25 minutes at 37°C. Cell nuclei were then stained for 5 minutes at room temperature with a 1:5000 Hoechst solution (Sigma-Aldrich) in PBS. After mounting the samples with Elvanol® (DuPont), immunofluorescence analyses were performed using a fluorescence microscope (Leica CTR6000).

C2C12-desmin

After 4 or 7 days of culture, cells on patterned hydrogel were fixed with 2% PFA for 7 minutes at room temperature. After permeabilization with a 0.5% Triton X-100 solution (Sigma-Aldrich) for 8 minutes at room temperature, samples were blocked with a 10% FBS/PBS solution for 45 minutes at room temperature. The samples were treated with primary rabbit polyclonal antibody for desmin (AbCam) diluted 1:100 in a 3% BSA/PBS solution, and incubated for 1 hour at 37°C; then, incubation with a secondary antibody Cy™3-conjugated anti-rabbit IgG (Jackson) diluted 1:200 in a 3% PBS/BSA for 45 minutes at 37°C followed. Nuclei were counterstained with a 1:5000 Hoechst solution (Sigma-Aldrich) in PBS for 5 minutes at room temperature; the samples were then mounted with Elvanol® and analyzed with a fluorescence microscope.

Satellite cells-desmin, myosin heavy chain and troponin I

Immunofluorescence analyses were performed on patterned cells after 4 or 7 days in order to detect desmin and troponin I. The cells were fixed with 2% PFA for 7 minutes at room temperature and permeabilized with 0.5% Triton X-100 solution (Sigma-Aldrich). Patterned cells were blocked in PBS-2% horse serum (HS) for 45 minutes at room temperature. Desmin primary antibody (AbCam), rabbit polyclonal, was diluted 1:100 in PBS-3% BSA; troponin I primary antibody (Chemicon), mouse monoclonal, was diluted 1:100 in PBS-3% BSA; Myosin Heavy Chain primary antibody, mouse monoclonal, was diluited 1:50 in PBS-3% BSA. Each antigen was individually applied for 1 hour at 37 °C. the secondary antibody Cy™3-conjugated anti-rabbit IgG was diluted 1:200 in PBS-3% BSA and FITC-conjugated anti-mouse IgG (Jackson) was diluted 1:250 in PBS-3% BSA and applied for 45 minutes at 37°C. Finally, cells were incubated in 1:5000 Hoechst solution at room temperature for 10 min. Samples were mounted with Elvanol®, and viewed under a fluorescence microscope.

A.3 Results

With the aim of mimicking as close as possible the in vivo muscular microenvironment, the substrate was designed to reproduce the mechanical properties of natural tissue. With this in mind, we produced a polyacrylamide based hydrogel and quantitatively measured its elastic properties through standard compression tests (Galdabini, Sun 2500), determining the bulk Young's modulus (E).

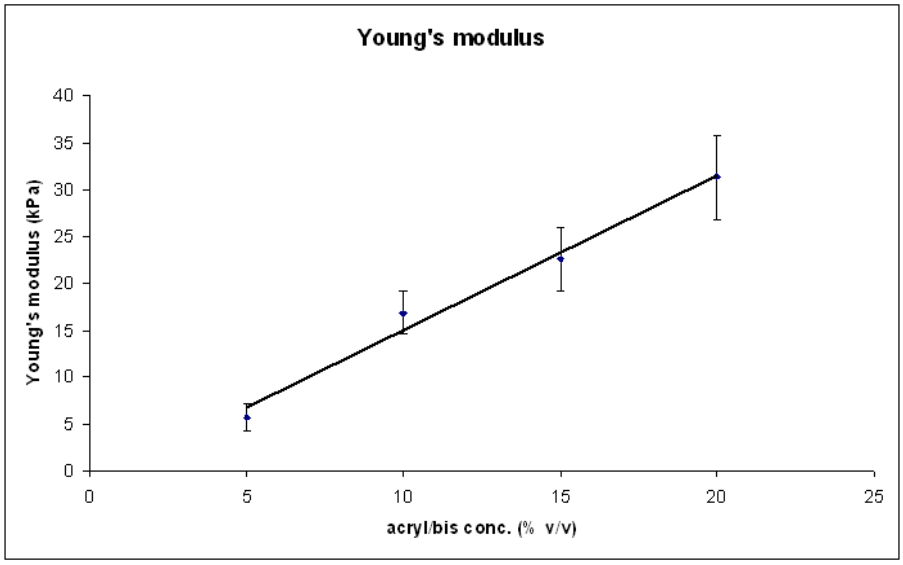

Figure 1. Young's modulus of PA hydrogel. Elastic moduli were quantitatively measured through standard compression tests for four different hydrogel compositions, i.e. 5-10-15-20% (v/v) acrylamide/bis-acrylamide 29:1 mixture in the prepolymer solution.

Figure 1 shows the result of mechanical tests performed on hydrogel samples taking in account four different concentrations of polymer (5, 10, 15 and 20% v/v of acrylamide/bis-acrylamide 29:1 mixture) in the prepolymer solution. Young's modulus increases as the acrylamide/bis-acrylamide concentration increases. A linear interpolation of the data was used to determine the optimal hydrogel compositions, which fairly approximate the elastic modulus of mouse muscle (Engler et al. 2004a). For instance, hydrogels with 8.2±2.5% (v/v) acrylamide/bis-acrylamide may reproduce the values of the elastic modulus of normal mice (En=12±4 kPa) whereas hydrogels with 12.0±3.7% reproduce that of dystrofin-deficient mice (Ed=18±6 kPa) (Engler et al. 2004a). It is worth noting that hydrogels with any bulk elastic modulus in the range of 5-30 kPa can be easily fabricated by adjusting the hydrogel composition (5-20 % v/v). If not otherwise indicated, hydrogels derive from a 10% (v/v) acrylamide/bis-acrylamyde 29:1 solution.

PA hydrogels were homogenously photopolymerized and covalently bonded to a functionalized glass slide; with the aim of selectively guiding cell adhesion on the non-fouling hydrogel surfaces, we created protein patterns using a micro-contact printing technique (Figure 2). The protein deposition procedure, involving the

pressing of a microstructured PDMS stamp, previously inked in the protein solution, allowed us to reproduce the desired pattern with high spatial resolution, virtually allowing us to create arrays of any geometry on the hydrogel surface.

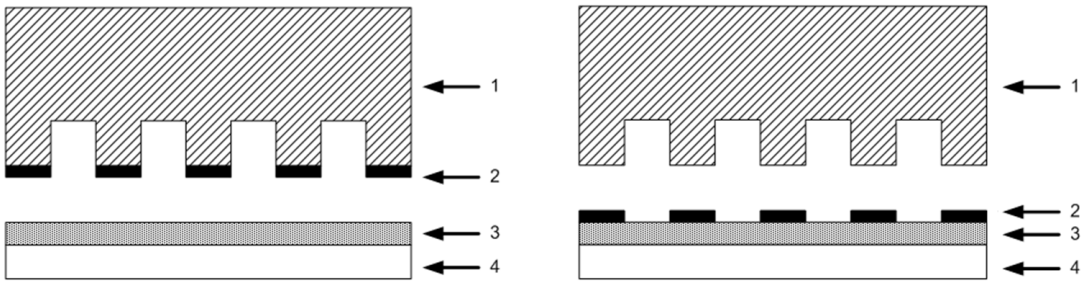

Figure 2. Schematic representation of the micro-contact printing (μCP) technique. Panel A exemplifies the microstructured PDMS stamp (1) with a monolayer of laminin (2) adsorbed on its surface. A thin film of PA hydrogel (3) is covalently bonded to a glass slide (4). Panel B schematically represents the result of the protein printing: the laminin (2) previously adsorbed on the PDMS stamp surface (1) has been transferred onto the hydrogel surface (3) adhered on the glass slide (4).

The evaluation of the fluorescence intensities of images obtained patterning different concentrations of BSA-FITC conjugated onto PA hydrogels (data not shown), allowed us to observe how the amount of adsorbed protein can be adjusted by changing its concentration in the solution used for inking the PDMS mold; in addition, it was proven that equal amounts of protein in the inking solution gave repeatable fluorescence signals. Moreover, the unchanged fluorescence signal of the protein, after washing with distilled water and incubation with culture medium at 37°C for two days, demonstrated that the protein was permanently adsorbed on the hydrogel surface.

A Live/Dead® Viability/Cytotoxicity assay performed on cardiomyocytes cultured on hydrogel surfaces clearly demonstrated that PA hydrogel, after the purification treatment previously described, was completely biocompatible and non-cytotoxic and allowed cells to grow and spread without affecting their viability (data not shown).

Figure 3 shows C2C12 cells cultured on laminin micro-patterned hydrogels.

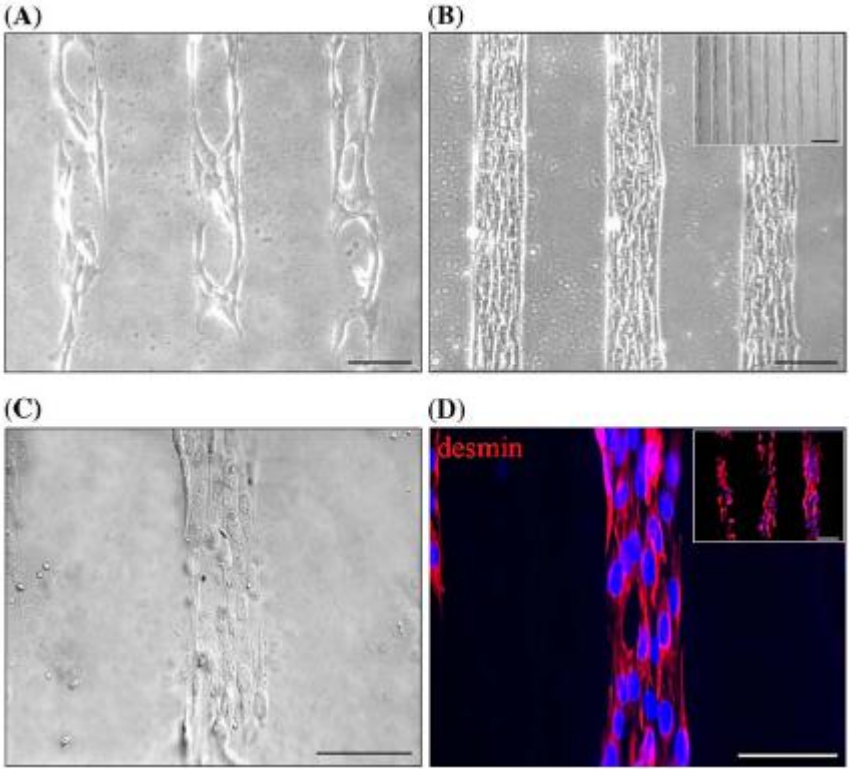

Figure 3. C2C12 cells cultured on patterned PA hydrogel at three different time points. Laminin lanes were printed on the hydrogel surface using a microstructured PDMS stamp, as described in Fig. 1A-B. The 10x (scale bar=100 μm) magnification pictures (Panels A-B) show the time course of C2C12 cells culture: 4 hours after seeding cells were spreading and attaching to the substrate (A), after 2 days they reached confluence confined inside the laminin lanes (B); the inset picture shows the high selectivity of the cell pattern on the hydrogel surface at 5x magnification (bar=300 μm). Panel C reports the bright field image at 40x magnification of C2C12 cells on which the immunofluorescence analysis to detect desmin was performed (Panel D, 40x). Cell nuclei were counterstained with Hoechst (blue). (scale bar=75 μm).

Figures 3A and 3B show the time course of adhesion, spreading, and proliferation at 4 hours and 2 days after seeding, respectively. Four hours after seeding, cells were attaching to the patterned regions and after two days reached confluence inside the protein coated lanes. Changes in cell morphology became noticeable a few hours after seeding; both the hydrogel properties and the high affinity towards laminin allowed and induced cells to spread and acquire an elongated shape. After 7 days of culture, the construct appeared perfectly organized with cells aligned and oriented along the main axis of the arrayed protein-patterned lanes (inset of Figure 3B). Optimization of the seeding protocol with the addition of a gentle rinsing 5 hours after deposition of the cell suspension, led to an increased selectivity because of the removal of unattached cells. An immunostaining for desmin, a typical muscle cell

marker, confirmed the correct expression of cell phenotype, which was neither affected by the supporting hydrogel nor by the morphological constraints created by the laminin lanes (interferential image in 3C, fluorescence image in 3D). The inset of Figure 3D shows again that both the nuclei position and the elongated cell shape was oriented in accordance with the underlying protein pattern.

Figure 4 reports extensive studies performed seeding satellite cells onto hydrogels of varying stiffness.

The histogram in panel 4A shows the results of cell counts after three and five days form seeding; it demonstrates how softer hydrogels allow the attachment of a statistically significant ($p<0.005$) higher cell number. No significant differences emerge either comparing 8% and 10% hydrogels or the two time points, this last is due to the fact that the patterned lanes readily reach a confluent state and thus inhibiting proliferation. The polar diagrams in panel B quantify the extent of organized orientation of the cells seeded in uniformly patterned (B1) and micro-patterned (B2) hydrogels; more than 90% of the cells adhering on the micropatterned lanes fall on an angle range between -10 and +10° from the longitudinal direction. Respecting the need for the optimal range of elastic modulus and following from the cell counts-observations, we chose to realize hydrogels with a 10% of acrylamide/bis-acrylamide in the prepolymer solution.

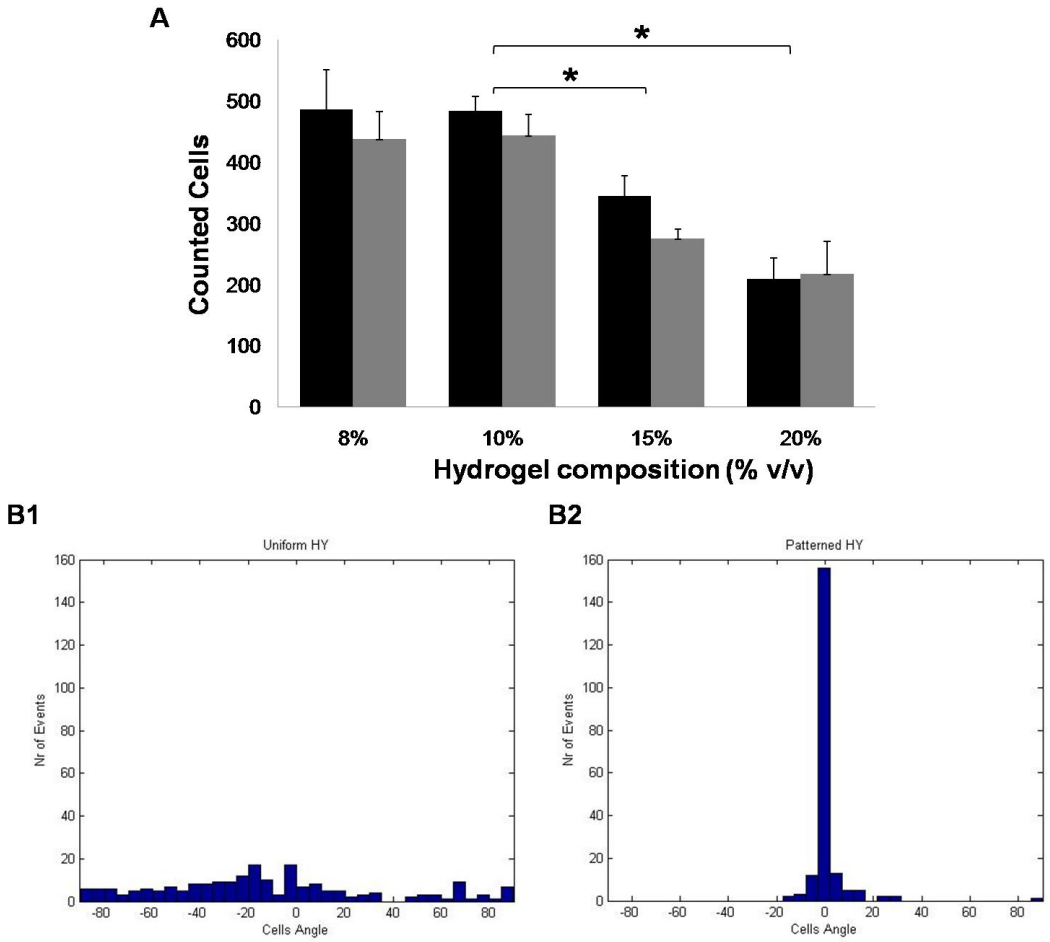

Figure 4. Satellite cells on hydrogels: counts and orientation. The histogram of panel A represents cell counts at two time points: 3 and 5 days (in black and gray, respectively) after seeding. The number of cells adhered to softer (8 and 10%) hydrogels is significantly higher than that on stiffer (15 and 20%) hydrogles ($p<0.005$). The polar diagrams in panel B quantify the extent of organized orientation of the cells seeded in uniformly patterned (B1) and micro-patterned (B2) 10% composition hydrogels; more than 90% of the cells adhering on the micropatterned lanes fall on an angle range between -10 and +10° from the main direction of the micropatterned lanes.

Figure 5 shows the results of the micro-patterning of satellite cells.

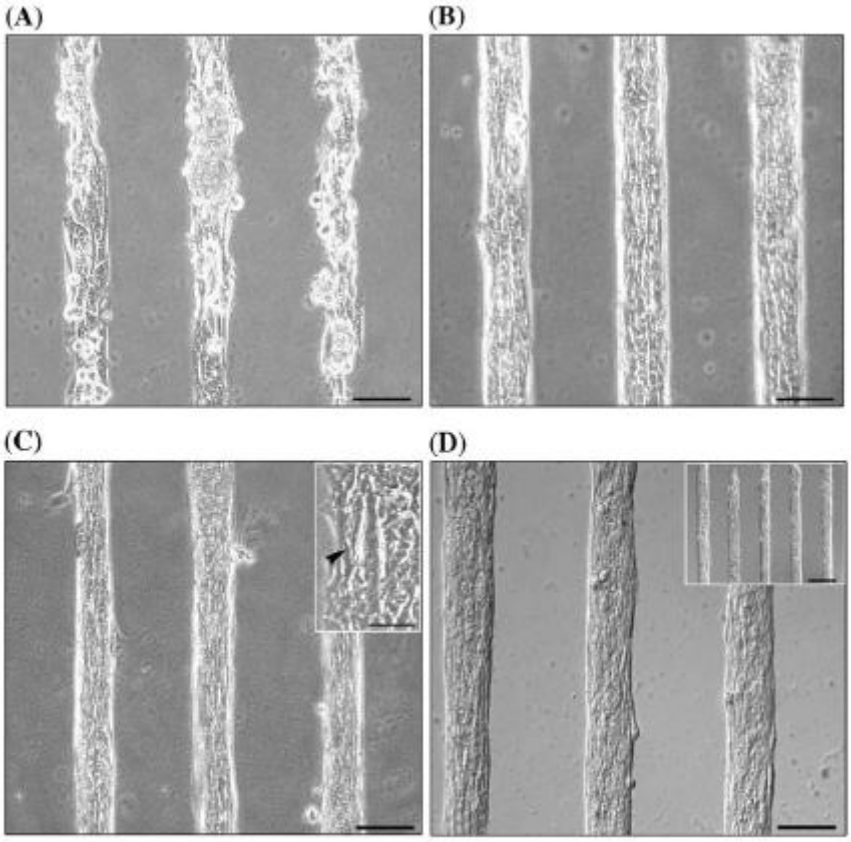

Figure 5. Satellite cells on hydrogels: counts and orientation. The histogram of panel A Satellite cells cultured on patterned PA hydrogel. Laminin lanes were printed on the hydrogel surface using a microstructured PDMS stamp, as described in Fig. 1. Mouse satellite cells attached in correspondence of the laminin lanes, as shown in A, 5 hours after seeding, and aligned following the underlying protein pattern, as shown in B and C after 3 and 7 days in culture, respectively (scale bar=100 μm). The inset in Panel C shows the occurred fusion into myotubes at 40x magnification (scale bar=37.5 μm). Panel D (10x, scale bar=100 μm) and the inset picture (5x, scale bar=300 μm) report interference microscope images showing aligned satellite cells after 7 days in culture, proving the efficiency of the patterning technique and the durability of the fiber array.

As the myogenic potential of satellite cells strongly depends on the number of passages of the expansion, we used early passages (first and second) and noticed that the results were similar in both cases in terms of cell adhesion. Figures 5A-C show the temporal evolution of satellite cell cultures on Matrigel 2.5% patterned hydrogels respectively at 5 hours, 4 days and 7 days from seeding. The Matrigel pattern and the early removal of non-adherent cells by rinsing led to a great efficiency in the selective adhesion of satellite cells. After 4 and 7 days of culture, cells proliferated extensively and aligned significantly along the direction of the lanes. Confluence was usually reached after 2 days of culture; after 7 days, satellite

cells fused to give myotubes (inset of Figure 5C). Figure 5D demonstrates the high specificity of the patterned substrate and shows the elongated cell morphology within the lanes.

Figures 6A-C show immunofluorescence analyses for three specific myogenic markers, desmin, troponin I and Myosin Heavy Chain (Myhc) on satellite cells after 4 days of culture.

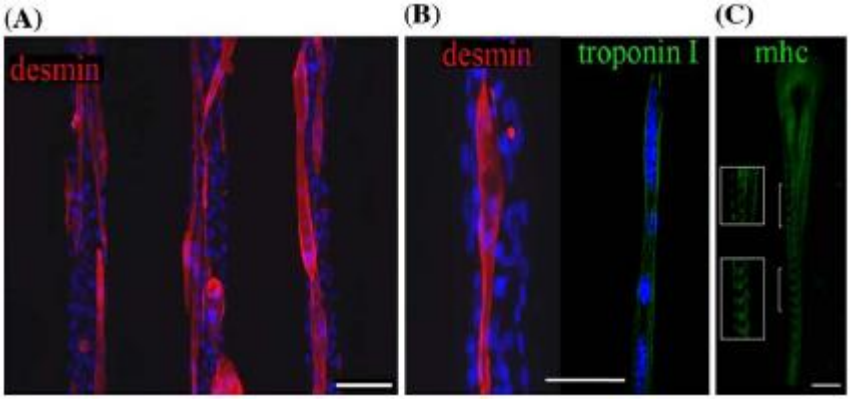

Figure 6. Satellite cells cultured on patterned PA hydrogel. Immunofluorescence analyses reported in panel A (10x, scale bar=100 μm; inset: 5x, scale bar=300 μm) and B (40x, scale bar=75 μm) assessed the correct phenotype expression in the newly formed myotubes, positively stained for desmin, red, and troponin, green. Cell nuclei were counterstained with Hoechst (blue). Panel 6C demonstrates the correct expression of Myhc and its organization in regular and uniform striations, also highlighted on the two insets (63x, scale bar=25 μm).

Immunofluorescence analyses for desmin (Figure 6A), clearly demonstrate the presence of newly formed and aligned myotubes. Figure 6B shows detailed images of the immunofluorescence analyses for desmin and troponin I on a single myotube, correctly resulting from the fusion of a large number of satellite cells as can be seen by the presence of many nuclei along each myotube. Figure 6C shows that myotubes cultured on hydrogel express Myhc and, more interestingly, that it is organized in regular and uniform striations. Satellite cells-derived myotubes exhibited fast spontaneous contraction, quantified and discussed in Figure 8.

Figure 7 shows cardiomyocytes seeded at a density of $1.6 \cdot 10^5$ cells/cm^2 and underlines the extreme selectivity obtained in cell adhesion.

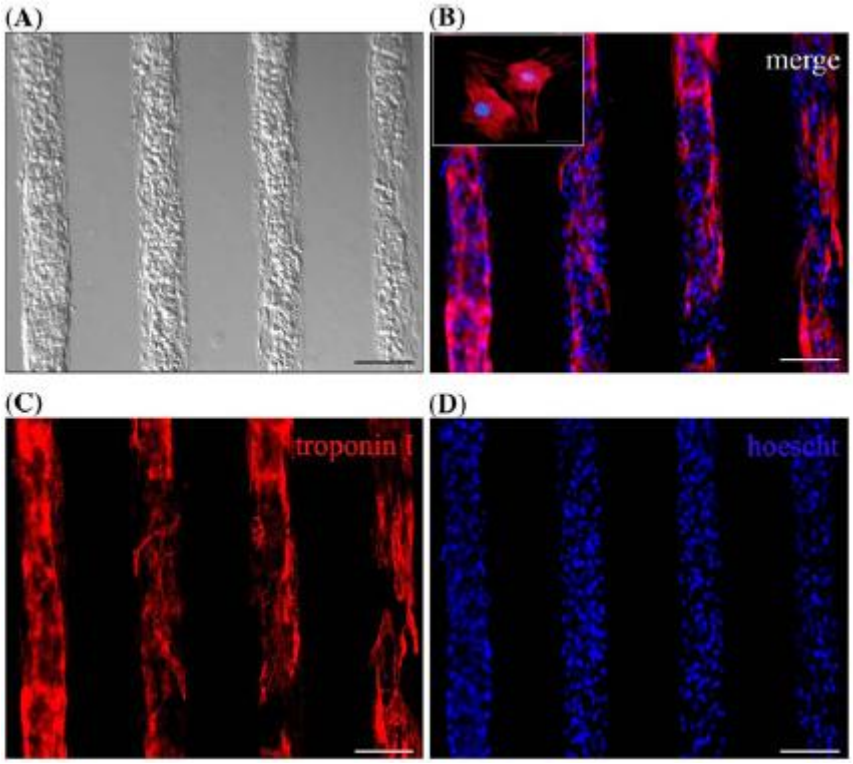

Figure 7. Cardiomyocytes cultured on patterned PA hydrogel. Images were taken at 10x magnification. (A): bright field image of cardiomyocytes after 4 days in culture; (B): cultured cardiomyocytes express troponin I (red), a typical cardiomyocytes marker; nuclei were counterstained with Hoechst (blue). Unmerged images are reported in panels C and D (bars=100μm). Immunostaining for troponin I represented in the inset of picture B shows at higher magnification (40x) a developed contractile apparatus. (scale bar=75 μm).

Four days after seeding, cardiomyocytes created aligned and organized cardiac myofibers expressing peculiar functional properties, i.e. synchronous contractile activity; the culture was maintained up to 10 days. Cell cultures (interferential image in Figure 7A) were stained for troponin I (Figure 7B-C) and the nuclei were marked with Hoechst (Figure 7B and 7D): troponin was uniformly expressed and, as it was noticeable at higher magnification (inset picture of Figure 7B), a contractile apparatus was observable.

Figure 8 reports diagrams quantifying the contractions of the myofibers obtained through image analyses of representative movies. Panel 8A refers to satellite cells-derived fibers while 8B refers to cardio-myofibers. The measured mean extents of contraction and frequency are 1.6 μm, 2 Hz and 7.1 μm, 0.3 Hz respectively.

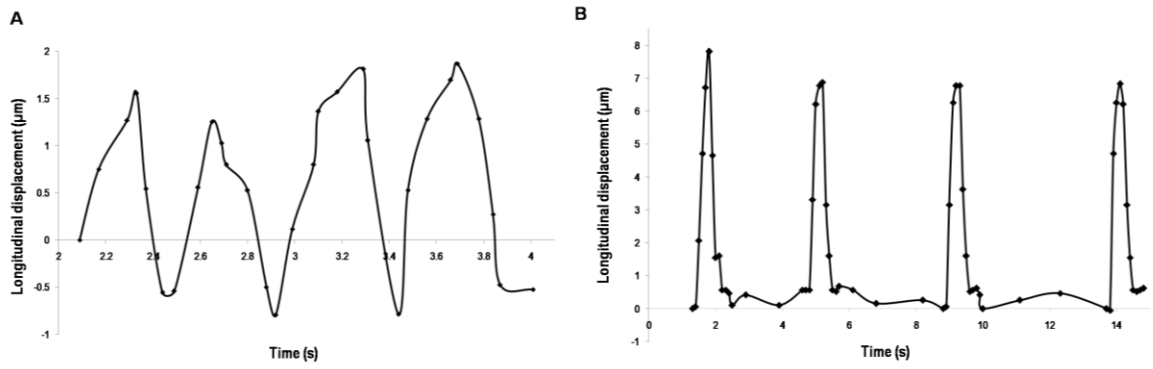

Figure 8. Fibers contraction. The reported diagrams derive from image analyses of representative movies. Panel 8A refers to satellite cells-derived fibers while 8B refers to cardio-myofibers. The measured mean extents of contraction and frequency are 1.6 μm, 2 Hz and 7.1 μm, 0.3 Hz respectively. The longitudinal displacement is evaluated in the direction of the micropatterned lanes.

A.4 Discussion

The objective of this study was to fabricate an in vitro model for cardiac and skeletal muscle fibers arranged in a high-throughput fashion for biological or physiological studies as well as for pharmacological screening tests. The essential pre-requisites to successfully achieve this goal can be summed up in two major issues: i) the fabrication of muscle substitutes that express correct markers and functional activity; and ii) the replication of this single muscle fiber in a large number of identical samples that can be used for high-throughput analyses.

In order to produce aligned muscle fibers we developed the μCP technique on soft substrates. Among many other possibilities, this technique couples simplicity and rapid realization timings with high accuracy and selectivity. Other techniques, such as micro-transfer molding (Suh et al. 2004) or the direct photo-lithography of hydrogels (Karp et al. 2006), can guide cell alignment through physical barriers and not through a functionalized area where cells can selectively adhere; thus, a potential limitation can be represented by the non-proper control over cell-surface interactions. In addition, microfluidic patterning of hydrogel surfaces proved to be successful for long-term cell adhesion only for collagen, that gelates under particular

conditions (Gopalan et al. 2003) and are applicable only on geometries that show interconnected channels.

The μCP technique on soft hydrogel substrates developed here, is an easy, robust, reliable and versatile technique that enables to pattern different proteins on hydrogels with high spatial resolution.

PA hydrogels are biocompatible and non-fouling materials; the latter property allowed us to selectively drive cell adhesion on their surface by means of micro-contact printing technique used to create protein patterns. The realization of the laminin lanes by μCP led to an array of adhesive lanes, with accurate control of shape and size. Subsequent cell seeding all over the hydrogel surface resulted in an extremely selective adhesion of every cell type used, with cells only adhering to and spreading within the patterned regions.

The techniques and procedures proposed here have been demonstrated to be successful in culturing primary cell cultures as cardiomyocytes and satellite cells up to 10 days.

We showed for the first time that mouse satellite cells spread, proliferated and differentiated into aligned myotubes on a micro-patterned soft surface (Figure 5 and 6). The time required for satellite cell to fuse and differentiate into myotubes is 4-5 days, depending on the seeding density, and is completely compatible with the hydrogel structural and physical stability. Satellite cells adhered to laminin lanes, showed an elongated morphology, and a strong alignment, which is significantly different from what is observable in conventional in vitro culture (data not shown). After 4 days in culture, the newly formed myotubes show a fully developed sarcomeric structure, as Myhc is organized in the characteristic striations of the A-band of sarcomer. Moreover, they exhibited spontaneous and electrically induced contractions.

Even if newly formed myotubes were uniformly observed over the entire array of lanes, only part of the cell population possessed the potential to differentiate. The low efficiency of myotube formation is strongly related to the extraction and expansion methods of satellite cells, which cause a loss of their myogenic potential. As reported in the literature, rat satellite cells showed a decrease in the

differentiation potential from cell isolation to the third passage (from 46.7% to 12.5%) (Machida et al. 2004). To enhance myotube formation efficiency, we aim to develop and optimize a better isolation and expansion procedure resulting in a satellite cell population with a higher myogenic potential. It is worth emphasizing that the amount of myotubes obtained on our hydrogel substrates was comparable with that obtained on glass or standard Petri dishes (data not shown). Moreover, myotubes obtained on hydrogel were parallel-oriented and spatially separated, whereas those obtained on Petri dishes form a non-oriented and interconnected network. Even more significant, is the stage of differentiation that myotubes can reach on hydrogel substrate; as using a soft substrate as hydrogel enables the spatial organization of Myhc in the physiological structure of the sarcomere, the basic structural and functional contractile unit of muscle. Once again, this result is particularly significant as it opens new perspectives in developing an in vitro substitute for biological and pharmacological studies on skeletal muscle.

Cardiomyocytes were cultured on such patterned elastic substrate and guided to form aligned and organized cardiac myofibers (Figure 7). After 3 days of culture, it was demonstrated that cardiomyocytes to express the correct phenotypic markers and, after 4 days, exhibited spontaneous synchronous contractile activity. This result is particularly significant in view of the development of a model for drug testing or other biological studies.

The methodology that has been proposed shows intrinsic advantages over traditional cell arrays, which lack the typical and basic features of complex tissues such as heart and skeletal muscle. Those functional fibers can now be analyzed simultaneously and/or differentially, marking a step further in the study of the actual morphology, structure, behaviour, and responses to determined stimuli.

A.5 Conclusions

In our work, we produced an array of contractile cardiac myofibers and skeletal muscle myotubes starting from primary cells supported on protein patterned soft

PA hydrogels. Both cardiac myofibers and skeletal muscle myotubes were part of an array composed of independent, spatially, and dimensionally controlled individual fibers. These array of fibers can reproduce the particular features and maintain the information related to the functionality and structure of cardiac tissue and skeletal muscle more closely than the traditional in vitro cultures or cell array approaches, potentially becoming a useful candidate for accurate biological and physiological studies and opening new perspectives in the field of high-throughput pharmacological screenings.

A.6 Acknowledgments

This work was supported by MIUR, University of Padua, Regione Veneto (Azione biotech II), Città della Speranza.

A.7 References

1. Kozarova, A.; Petrinac, S.; Ali, A.; Hudson, J. W., Array of informatics: applications in modern research. *J Proteome Res* **2006,** 5, (5), 1051-1059.
2. Chen, D. S.; Davis, M. M., Molecular and functional analysis using live cell microarrays. *Curr Opin Chem Biol* **2006,** 10, (1), 28-34.
3. Brueggemeier, S. B.; Wu, D.; Kron, S. J.; Palecek, S. P., Protein-acrylamide copolymer hydrogels for array-based detection of tyrosine kinase activity from cell lysates. *Biomacromol* **2005,** 6, 2765-2775.
4. Chen, D. S.; Soen, Y.; Davis, M. M.; Brown, P. O., Functional and molecular profiling of heterogeneous tumor samples using a novel cellular microarray. *J Clin Oncol* **2004,** 22, 9507.
5. Albrecht, D. R.; Tsang, V. L.; Sah, R. L.; Bathia, S. N., Photo- and electropatterning of hydrogel-encapsulated living cell arrays. *Lab Chip* **2005,** 5, 111-118.
6. Flaim, C. J.; Chien, S.; Bhatia, S. N., An extracellular matrix microarray for probing cellular differentiation. *Nature Methods* **2005,** 2, 119-125.
7. Albrecht, D. R.; Underhill, G. H.; Wassermann, T. B.; Sah, R. L.; Bhatia, S. N., Probing the role of multicellular organization in three-dimensional microenvironments. *Nat Methods* **2006,** 3, (5), 369-375.
8. Jang, J. H.; Schaffer, D. V., Microarraying the cellular microenvironment. *Mol Syst Biol* **2006,** 2, (39).
9. Kaplan, D.; Moon, R. T.; Vunjak-Novakovic, G., It takes a village to grow a tissue. *Nat Biotechnol* **2005,** 23, (10), 1237-1239.

10. Vunjak-Novakovic, G.; Freed, L. E., Culture of organized cell communities. *Adv Drug Deliv Rev* **1998,** 33, (1-2), 15-30.
11. Motlagh, D.; Senyo, S. E.; Desai, T. A.; Russell, B., Microtextured substrata alter gene expression, protein localization and the shape of cardiac myocytes. *Biomaterials* **2003,** 24, (14), 2463 76.
12. Engler, A. J.; Griffin, M. A.; Sen, S.; Bönnemann, C. G.; LeeSweeney, H.; Discher, D. E., Myotubes differentiate optimally on substrates with tissue-like stiffness: pathological implications for soft or stiff microenvironments. *J Cell Biol* **2004a,** 166, 877-887.
13. Ingber, D. E., Mechanical signaling and the cellular response to extracellular matrix in angiogenesis and cardiovascular physiology. *Circ Res* **2002,** 91, (10), 877-887.
14. Ingber, D. E., Mechanical control of tissue growth: function follows form. *Proc Natl Acad Sci U S A* **2005,** 102, (33), 11571-11572.
15. Khatiwala, C. B.; Peyton, S. R.; Putnam, A. J., Intrinsic mechanical properties of the extracellular matrix affect the behavior of pre-osteoblastic MC3T3-E1 cells. *Am J Physiol Cell Physiol* **2006,** 290, (6), C1640-1650.
16. Falconnet, D.; Csucs, G.; Grandin, H. M.; Textor, M., Surface engineering approaches to micropattern surfaces for cell-based assays. *Biomat* **2006,** 27, 3044-3063.
17. Xia, Y.; Whitesides, G. M., Soft lithography. *Angew Chem Int Ed* **1998,** 37, 550-575.
18. Karp, J. M.; Yeo, Y.; Geng, W.; Cannizarro, C.; Yan, K.; Kohane, D. S.; Vunjak-Novakovic, G.; Langer, R. S.; Radisic, M., A photolithographic method to create cellular micropatterns. *Biomat* **2006,** 27, 4755-4764.
19. Rohr, S.; Scholly, D. M.; Kleber, A. G., Patterned growth of neonatal rat heart cells in culture. Morphological and electrophysiological characterization. *Circ Res* **1991,** 68, 114-130.
20. Suh, K. Y.; Seong, J.; Khademhosseini, A.; Laibinis, P. E.; Langer, R., A simple soft lithographic route to fabrication of poly(ethylene glycol) microstructures for protein and cell patterning. *Biomat* **2004,** 25, 557-563.
21. Gopalan, S. M.; Flaim, C.; Bhatia, S. N.; Hoshijima, M.; Knoell, R.; Chien, K. R.; Omens, J. H.; McCulloch, A. D., Anisotropic stretch-induced hypertrophy in neonatal ventricular myocytes micropatterned on deformable elastomers. *Biotechnol Bioeng* **2003,** 81, (5), 578-587.
22. Khademhosseini, A.; Eng, G.; Yeh, J.; Kucharczyk, P. A.; Langer, R.; Vunjak-Novakovic, G.; Radisic, M., Microfluidic patterning for fabrication of contractile cardiac organoids. *Biomed Microdevices* **2007,** 9, 149-157.
23. Vernon, R. B.; Gooden, M. D.; Lara, S. L.; Wight, T. N., Microgrooved fibrillar collagen membranes as scaffolds for cell support and alignment. *Biomat* **2005,** 26, 3131-3140.
24. Yim, E. K. F.; Reano, R. M.; Pang, S. W.; Yee, A. F.; Chen, C. S.; Leon, K. W., Nanopattern-induced changes in morphology and motility of smooth muscle cells. *Biomat* **2005** 26, 5405-5413.
25. Ruiz, S. A.; Chen, C. S., Microcontact printing: A tool to pattern. *Soft Matter* **2007,** 3, 1–11.
26. McDevitt, T. C.; Woodhouse, K. A.; Hauschka, S. D.; Murry, C. E., Spatially organized layers of cardiomyocytes on biodegradable polyurethane films for myocardial repair. *J Biomed Mater Res* **2003,** 66A, 586-595.
27. McDevitt, T. C.; Angello, J. C.; Whitney, M. L.; Reinecke, H.; Hauschka, S. D.; Murry, C. E.; Stayton, P. S., In vitro generation of differentiated cardiac myofibers on

micropatterned laminin surfaces. *Journal of biomedical materials research* **2002,** 60, 472-479.

28. Britton-Keys, K.; Andreopoulos, F. M.; Peppas, N., Poly(ethylene glycol) star polymer hydrogels. *Macromolecules* **1998,** 31, 8149-8156.
29. Burdick, J. A.; Khademhosseini, A.; Langer, R., Fabrication of gradient hydrogels using a microfluidics/photopolymerization process. *Langmuir* **2004,** 20, 5153-5156.
30. Lin-Gibson, S.; Jones, R. L.; Washburn, N. R.; Horkay, F., Structure-property relationships of photopolymerizable poly(ethylene glycol) dimethacrylate hydrogels. *Macromolecules* **2005,** 38, 2897-2902.
31. Almany, L.; Seliktar, D., Biosynthetic hydrogel scaffolds made from fibrinogen and polyethylene glycol for 3D cell cultures. *Biomat* **2005,** 26, 2467-2477.
32. Leach, J. B.; Bivens, K. A.; Patrick, C. W.; Schmidt, C. E., Photocrosslinked hyaluronic acid hydrogels: natural, biodegradable tissue engineering scaffolds. *Biotechnol Bioeng* **2003,** 82, 578-5.
33. Leach, J. B.; Schmidt, C. E., Characterization of protein release from photocrosslinkable hyaluronic acid-polyethylene glycol hydrogel tissue engineering scaffolds. *Biomat* **2005,** 26, 125-135.
34. Hern, D.; Hubbell, J. A., Incorporation of adhesion peptides into nonadhesive hydrogels useful for tissue resurfacing. *J Biomed Mater Res* **1998,** 39, 266-276.
35. Engler, A.; Bacakova, L.; Newman, C.; Hategan, A.; Griffin, M.; Discher, D., Substrate compliance versus ligand density in cell on gel responses. *Biophys J* **2004b,** 86, 617-628.
36. Peyton, S. R.; Putnam, A. J., Extracellular matrix rigidity governs smooth muscle cell motility in a biphasic fashion. *J Cell Physiol* **2005,** 204, 198-209.
37. Pedram, A.; Razandi, M.; Aitkenhead, M.; Levin, E. R., Estrogen inhibits cardiomyocyte hypertrophy in vitro. Antagonism of calcineurin-related hypertrophy through induction of MCIP1. *J Biol Chem* **2005,** 280, (28), 26339–26348.
38. Speicher, D. W.; McCarl, R. L., Pancreatic enzyme requirements for the dissociation of rat hearts for culture. *In Vitro* **1974,** 10, 30-41.
39. Xiao, Y. F.; Gomez, A. M.; Morgan, J. P.; Lederer, W. J.; Leaf, A., Suppression of voltage-gated L-type Ca2+ currents by polyunsaturated fatty acids in adult and neonatal rat ventricular myocytes. *Proc Nat Acad Sci U S A* **1997,** 94, (8), 4182–4187.
40. Rosenblatt, J. D.; Lunt, A. I.; Parry, D. J.; Partridge, T. A., Culturing satellite cells from living single muscle fiber explants. *In Vitro Cell Dev Biol Anim* **1995,** 31, 773-779.
41. Machida, S.; Spangenburg, E. E.; Booth, F. W., Primary rat muscle progenitor cells have decreased proliferation and myotube formation during passages. *Cell Prolif* **2004,** 37, 267-277.

Appendix B

Electrophysiological stimulation improves myogenic potential of muscle precursor cells grown in a 3D collagen scaffold

Elena Serena[1], Marina Flaibani[1], Silvia Carnio[2], Luisa Boldrin[3], Libero Vitiello[2], Paolo De Coppi[3], Nicola Elvassore[1]*

[1] Department of Chemical Engineering, University of Padua, Via Marzolo, 9 Padua, Italy

[2] Department of Biology, University of Padova, Via Bassi, 58 I-35131 Padova, Italy

[3] Department of Pediatrics, University of Padua, Via Giustiniani, 3, Padua, Italy

[*]Corresponding author

Neurological Research

Vol. 30 / no. 2, 2008 / pp. 207-214

Keywords: satellite cell; ex vivo expansion, myogenicity; electrical stimulation; three-dimensional culture; collagen sponges.

Abstract

The production of engineered three-dimensional (3D) skeletal-muscle grafts holds promise for treatment of several diseases. An important factor in the development of such approach involves the capability of preserving myogenicity and regenerative potential during ex vivo culturing. We have previously shown that electrical stimulation of myogenic cells grown in monolayer could improve the differentiation process. Here we investigated the effect of exogenous electric field, specifically designed to mimic part of the neuronal activity, on muscle precursor cells (mpcs) cultured within 3D collagen scaffolds. Our data showed that electrical stimulation did not affect cell viability and increased by 65.6% the release rate of NO_x, an early molecular activator of satellite cells in vivo. NO_x release rate was decreased by an inhibitor of NO-synthase, both in stimulated and non-stimulated cultures, confirming the endocrine origin of the measured NO_x. Importantly, electrical stimulation also increased the expression of two myogenic markers, MyoD and Desmin. We also carried out some preliminary experiments aimed at determining the biocompatibility of our seeded collagen scaffolds, implanting them in the tibialis anterior muscles of syngeneic mice. Ten days after transplant, we could observe the formation of new myofibers both inside the scaffold and at the scaffold-muscle interface. Altogether, our findings indicate that electrical stimulation could be a new strategy for the effective 3D expansion of muscle precursor cells in vitro without loosing myogenic potential and that 3D collagen matrices could be a promising tool for delivering myogenic cells in recipient muscles.

B.1 Introduction

The reconstruction of skeletal muscle tissue, either lost because of traumatic injury or surgical ablation or functionally damaged due to congenital myopathies, is limited by the lack of availability of functional substitutes of this native tissue[1]. In the past few years, different approaches to recreating skeletal muscle tissue in vitro and in vivo have been proposed[1, 2]: from myoblast injection for cell therapy[3] or gene

therapy[4],to muscle tissue engineering[5]. All these therapeutic strategies for skeletal muscle reconstruction would require an efficient and robust procedure for the expansion of muscle precursor cells in vitro in order to obtain an adequate cell number for subsequent autologous transplantation[6]. Moreover, it would be of fundamental importance that the ex vivo expansion of myogenic (stem) cells could preserve their differentiative and regenerative potential upon *in vitro* expansion. At present there are evidences that traditional techniques for *in vitro* expansion of muscle precursor cells cause loss of myogenicity. Montarras and colleagues demonstrated that the in vitro 2D culture of mouse satellite cells strongly reduces their regenerative efficiency in vivo[7]. The loss of myogenic potential in rat satellite cells has been correlated by Machida and colleagues with the number of cell passages: from isolation through third passage, there was a decline in the percentage of cells with myogenic/satellite cells markers (from 90% to 55%), in proliferation rates and in differentiation potential (from 46.7% to 12.5%)[6]. In general, the design of a culture system capable of recreating in vitro the spatio-temporal evolution of the main environmental cues that regulate the stem cell fate *in vivo*[8, 9] would be highly desirable. In the case of muscle, 3D cultures and exogenous electrical stimulation have been proposed as tools for successfully expand skeletal muscle[10] and cardiac tissues culture[11]. The architecture of the in situ environment of a cell in a living organism is three-dimensional, and muscle satellite cells are no exception[12]. In traditional 2D cell culture cells alter their gene expression patterns and their production of extracellular matrix proteins; cells in 3D environment follow chemical and molecular gradient that are impossible to establish in 2D culture[13]. So far, only few studies on differentiation of myoblasts within 3D scaffold have been reported[14, 15] and most of the studies that used primary cultures of mouse myoblasts focused on in vivo implantation and not on in vitro culture[16, 17]. In addition, we also recently showed how 3D culture of satellite cells on collagen scaffolds could benefit in terms of cell viability using a perfusion bioreactor[15, 4] Electrical stimulation is fundamental in controlling several aspects of tissue formation[18]. Few articles report the effects of electrical stimulation on skeletal muscle precursor cells in vitro and most of them employed 2D cell culture methods[19]. To our knowledge, only two previous studies

investigated the effects of electrical stimuli on 3D myoblasts culture[10, 14]. Niklason and colleagues showed an increase on cell proliferation of adult rabbit myoblasts due to electrical stimulation[14], but they reproduced the environment of an infarcted heart, which does not correspond to the physiological stimulus of skeletal muscle tissue. On the other hand, Stern-Straeter and colleagues observed a negative impact of electrical stimulation on the myogenic differentiation process[10]. However, the choice of the wave form of electrical stimuli could strongly affect cell behavior; in fact, in a previous study we showed that for 2D cultures exogenous electrical stimulation increased the differentiative potential of rat mpcs[16]. In this work we wanted to take a step forward, coupling 3D culture with electrical stimulation. Our data indicated that collagen scaffold is a good substrate to culture satellite cells and that electrical stimulation increases the secretion of a mediator involved in myogenesis, NO_x as well as the expression of myogenic markers MyoD and Desmin. We propose the coupling of 3D cell culture with electrical stimulation as new strategy for the maintenance of myogenic potential of muscle precursor cells during their in vitro expansion. Our biomimetic approach provides an environment more similar to the in vivo tissue, by using electrical stimulation to mimic part of the neuronal activity, and it allows the development of implantable grafts.

B.2 Material and Methods

B.2.1 Isolation and culture of muscle precursor cells

Mpcs were obtained following the protocol previously described 20. Briefly, flexor digitorum brevis (FDB) and extensor digitorum longus (EDL) from C57BL/6J mouse muscles were removed and enzymatically digested with 0.2% Collagenase Type I (Sigma-Aldrich, USA). Fibers were individually harvested, plated on Petri dishes previously coated with 10% Matrigel (BD Bioscience, USA) and maintained in a humidified tissue culture incubator in plating medium, consisting of Dulbecco Modified Eagle's Medium (DMEM) (Sigma-Aldrich, USA), 10% horse serum (Gibco-Invitrogen, Italy), 1% chicken embryo (MP-Biomedicals, Italy), 1%

penicillin-streptomycin (Gibco-Invitrogen, Italy). After 72 hours, culture medium was switched to proliferating, consisting of DMEM, 20% foetal bovine serum, 10% horse serum, 0.5% chicken embryo and 1% penicillin-streptomycin. Cells were kept in culture with proliferating medium and detached from plate with 0.5% Trypsin-EDTA (Gibco- Invitrogen, Italy) before fusion in myotubes occurred. Cells were then re-plated and expanded. For in vivo experiments, cells were derived from C57BL/6-TgnEGFP transgenic mice.

B.2.2 Cell seeding on collagen scaffolds

3D scaffold of porous bovine collagen sponges (Avitene® UltrafoamTM Collagen Hemostat. Davol Inc., USA) was used. Before seeding, scaffolds (sized 5×10×3mm) were conditioned for 12h at 37°C in proliferating medium. At passage 2 or 3, satellite cells were detached from the plates using 0.5% trypsin-EDTA and seeded onto the scaffolds at the concentration of 3.3×10^6cells/cm^3. 50µl of medium were then added every hour. After 4 hours, seeded scaffolds were covered with 5mL of medium. Scaffolds were maintained in culture in a Petri dish for 7days, at 37°C and 5% CO_2. Medium was changed every day.

B.2.3 Electrical stimulation of cell culture

The apparatus for electric stimulation (Figure 1) was composed of two stainless steel electrodes, 0.8 cm in height and 1 cm in length, which were placed at 14 mm distance (Figure 1A). A poly(dimethylsiloxane) (PDMS, Sylgard 184, Dow Corning, MI, USA) holder was specifically designed to fit a 35 mm Petri dish and to keep the electrodes in a position perpendicular to the collagen scaffold immersed in the culture medium during the culture (Figure 1A–C). The holder had a central hole of 26×6×6 mm, which allowed to keep the scaffold in a position parallel to the electrical field (Figure 1A,C). The electrodes were connected to a NI 6035E I/O terminal interfaced with NI LabView software (National Instruments Corporation, Austin, TX, USA). LabView was programmed to produce a square wave with a 0 V baseline and impulses of 70 mV/cm for 3 ms with frequency of 33.3 mHz (Figure 1D). The amount of current flowing between the electrodes was measured by monitoring the potential drop across a 50 V resistor placed in series with the culture

chamber. Electrical stimuli were applied starting 3 days after cell seeding on collagen scaffold.

B.2.4 Cell viability

The Cell viability was measured by the MTT test (Sigma-Aldrich, USA). Briefly, a 0.5mg/mL solution of the tetrazolium salt MTT in phosphate buffer solution (PBS) was added to the cell samples, which were then incubated for 3h at 37°C. After the removal of the dye solution, cells were lysed in a 10% DMSO, 90% isopropanol solution, which also dissolved the formazan crystals. Samples were placed again at 37°C allowing complete dissolution and then centrifuged at 1200rpm for 5min to precipitate cell debris. Clear solutions were then processed for absorbance readings at 580nm with a spectrophotometer, the recorded optical density (OD) being directly proportional to the number of viable cells. Cell survival after seeding was evaluated with the LIVE/DEAD® assay (Invitrogen, Italy). Briefly, 150μL of Calcein 3.5μM and Ethidium Bromide 3.0μM in D-PBS (Gibco-Invitrogen, Italy) were added to the seeded scaffold and incubated for 45min at room temperature. Following incubation, the scaffold was washed with PBS and labeled cells were observed under fluorescence microscope.

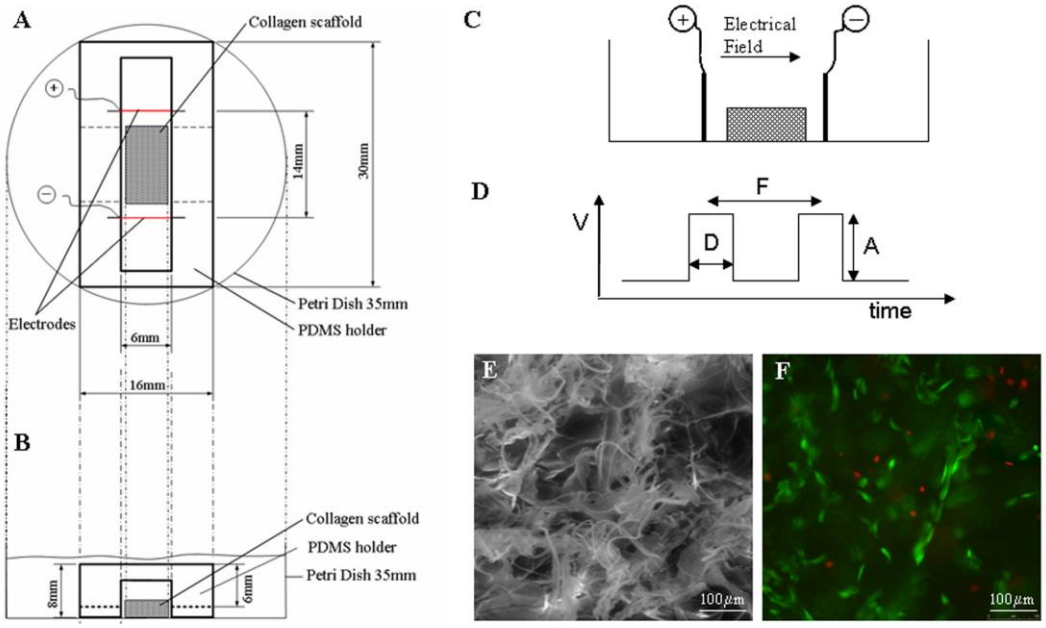

Figure 1. Schematic of experimental set-up used for electrophysiologic stimulation. (A and B) Top and front view of electrical stimulation apparatus: 35 mm Petri dish, PDMS holder, stainless steel parallel plate electrodes placed at 14 mm separation distance and collagen scaffold. Symbols 'z' and '–' show connections to the electric field function generator. (C) Schematic view of lateral prospective of 3D scaffold between two electrodes. (D) Square pulsed electric potential (V) applied to the cells within 3D scaffold: A: amplitude (70 mV/cm); D: duration (3 ms); F: 1/frequency (33.3 mHz). (E) SEM image of collagen scaffold. (F) Live and dead assay performed on scaffold 24 hours after cell seeding (cytoplasm of living cells are stained in green and nuclei of dead cells are stained in red).

B.2.5 NO_x concentration

NOx released by satellite cells in the medium culture were measured, as nitrite (NO_2^-), using Griess reagent (Fluka-Aldrich, Italy). The medium was collected every 24h. Briefly, the culture medium was mixed with Griess reagent 3:1 v/v. After 10 to 15min the absorbance at 524nm was measured at UV spectrophotometer, using non-conditioned medium as the baseline. A standard calibration curve, obtained from known concentration of sodium nitrite in non-conditioned culture medium, was used to determine 2 NÕ concentration. The total amount of nitrite released in the medium during the culture and the release rate were calculated.

To study the inhibition of Nitric Oxide Synthase (NOS), 100µl of 0.1mM L-Nitroarginine methil ester (L-NAME) (Sigma-Aldrich, USA), an analogous of its substrate, were added to the culture medium every day.

B.2.6 Immunostaining

3D scaffolds were harvested at 7 days, embedded in OCT (Sigma-Aldrich, USA) and snap-frozen in liquid nitrogen. Section of 10μm were fixed with PFA 2% for 7min. Desmin primary antibody, rabbit polyclonal, (AbCam, United Kingdom) was diluted 1:200 in PBS-3% BSA (Sigma-Aldrich, USA); GFP primary antibody, rabbit polyclonal, (Molecular Probes, Invitrogen, Italy) was diluted 1:100 in PBS-3% BSA. Each antibody was individually applied for 1h at 37°C. MyoD primary antibody, rabbit polyclonal, (Santa Cruz, Germany), was diluted 1:10 in PBS-3% BSA and applied over night at 4°C. Secondary antibody, Cy™3-conjugated anti-rabbit IgG (Jackson, UK) was diluted 1:250 in PBS-3% BSA and applied for 45min at 37°C. Secondary antibody Alexa Fluor 488-conjugated anti-rabbit IgG (Chemicon, UK) was diluted 1:100 in PBS-3% BSA and applied for 45min at 37°C. After treatment with fluorescent secondary antibodies, cells were counterstained with DAPI and mounted in fluorescent mounting medium (DakoCytomation, Italy).

B.2.7 Protein isolation

Satellite cells on collagen scaffold were placed in sample buffer (12.5 % upper-tris (Tris 0.5M, SDS 0.4%), 10% glycerol, 30% SDS10%, 0.025% bromophenol blue, 5% β-mercaptoethanol) for 20min. Cell lysates were then collected into microfuge tubes and centrifuged at 5000rpm for 1min to eliminate cell debris.

B.2.8 Western blot analysis

A volume of 20 μl was loaded per lane for all protein samples and gels were run at 100V in running buffer (Tris-HCl 25mM, glycine 192mM and 0.1% SDS). Proteins in the gels were transferred to PROTRAN nitrocellulose membranes (Schleicher & Schuell GmbH, Germany) in blotting buffer (Tris-HCl 25mM and glycine 192mM) 300mM for 2 hours at +4°C. Membranes were rinsed three times in TBS (Tris-HCl and NaCl 0.02M) for 5 min each at room temperature, blocked for 1h with 6% non-fat dry milk in TBS-T (TBS, 01.% Triton X100), and rinsed with TBS-T two times. Membranes were then incubated with primary antibody ON at 4°C, rinsed with TBS-T three times, incubated with a secondary antibody for 1h, and rinsed with

TBS-T three times. Protein expression signals were visualized by incubating each membrane with 5mL SuperSignal West Pico Chemiluminescent Substrate (Pierce, USA) for 4min, and then exposing membranes to HyperFilm ECL (Amersham) for up to 5min. The primary antibodies used for Western blot analysis were mouse anti-myosin (1:1000; Sigma-Aldrich, USA), mouse anti-desmin (1:2000; Sigma-Aldrich, USA), rabbit anti-MyoD (1:2000; Sigma-Aldrich, USA), mouse anti-actin (1:800; Sigma-Aldrich, USA). The secondary antibodies used were goat anti-mouse horseradish peroxidase (1:2000; Pierce, USA) and goat anti-rabbit horseradish peroxidase (1:400; Pierce, USA). Quantitative analysis of the western blot lane were performed with image program "ImageJ".

B.2.9 *In vivo* experiments

We used 4 to 6 months-old C57BL/6 wild-type mice and C57BL/6-Tg(ACTBEGFP) 1Osb/J transgenic mice from Jackson Laboratories. In transgenic animals, the GFP transgene was under the control of the cytoplasmic beta actin promoter. The animals were housed and operated onto at the Animal Colony of the "Centro Interdipartimentale Vallisneri", University of Padova, following all relevant bylaws issued by the Italian Ministery of Health. Animals were anesthetized with isoflurane; post-op care included three-days analgesic treatment (tramadol 10mg/kg). Scaffolds seeded with GPF positive satellite cells were implanted into the tibialis anterior (TA) muscles of C57BL/6 wild-type mice. Approximately 25% of muscle mass was removed from the central core of the muscle and scaffolds were inserted inside the pocket, which was then closed with non-absorbable sutures. At the indicated time, muscles were harvested and snap frozen in isopentane pre-cooled in liquid nitrogen. 10μm cryosections were then used for immunohistochemical analyses, using the same protocols described above.

B.2.10 Statistical analysis

One-way ANOVA test was used. $p<0.01$ and $p<0.05$ were considered statically significant.

B.3 Results

Cell characterization

Single muscle fibers were successfully isolated from skeletal muscle of adult mice. Once seeded on matrigel-coated dishes, fibers originated a rather homogeneous population of satellite cells. In each experiment, part of the cells was used for the characterization analyses. Flow cytometric analysis (data not shown) were consistent with our previously reported data[21].

Live&Dead assay showed that 24 hours after seeding almost all satellite cells attached to the collagen scaffold were alive (Fig. 1F). We also assessed the efficiency of our seeding procedure, by counting the number of cells that had not attached to the matrix (i.e., that were still in suspension or had adhered to the plate). These measurements showed that after 24 hours approximately 85% of the seeded cells were indeed attached to the scaffold. To monitor how cell viability evolved with time, MTT test was performed at 1, 4 and 7 days of culture. MTT test confirmed a good viability 24 hours after seeding (Abs580nm=0.77); an increased absorbance value at day four (Abs580nm=0.95) indicated that seeded cells had undergone some divisions. After 7 days of culture the viability remains similar to initial values (Abs580nm=0.62). Electrophysiological coupling Stainless steel electrodes have been chosen for their combination of good electrical conductibility and resistance to galvanic corrosion. Stainless steel is an inert material commonly used for clinical tools, i.e. syringe needles, and suitable for fabrication of electrodes for bio-medical application 22. The application of an electric potential difference at the electrodes induces the migration of small and large electrolytes (medium conductance was estimated to be 22mS/cm), causing charge redistribution within the media and related phenomena such as changes in trans-membrane potential and charges flow through the membrane. The current flowing through the culture chamber during electrode charging and discharging periods was monitored and showed a 10-5s duration of this transient regime. The total current flowing during the charging period was equal to the discharging current, confirming the absence of non-reversible faradaic reaction on the electrode surface. This behavior ensured the

absence of toxic electrolytic reactions, electrode oxidation and, in general, of harmful temporal changes of culture conditions due to the imposed electrical potential 16. Moreover, the flat shape of the electrodes ensured the generation of an uniform electric field, capable to homogeneously influence the whole 3D cells environment.

Effect of electrical stimulation on NO_x release

Being that it has been demonstrated on satellite cells that NO_x mediates injury-induced activation in vivo[23] and stimulation-induced in vitro 16, in this study we investigated NO_x release in mouse satellite cells and the effect of electrical stimulation on NO_x release rate. The application of electrical stimulation enhanced the total amount of NO_x released in the medium in comparison to non-stimulated culture (Fig. 2A, full symbol). Specifically, the release rate was increased by 65.6%, from 0.12 d-1 to 0.19 d-1. We performed the electrical stimulation of scaffolds not seeded with cells to verify the negligible presence of NO_x produced by electrochemical oxidation of medium components. In this case, the values of NO_x were extremely low and almost constant, thereby indicating that the increase in NO_x release rate we observed in electrically stimulated satellite cells was cell specific and not due to electrochemical oxidation of components of the medium (Fig. 2A, open symbol).

Furthermore we verified that the measured NO_x were a cell endogenous product and did not derive from oxidation of other released molecules. With this aim, we inhibited the nitric oxide synthase (NOS), which is responsible for NO_x production, using an analogous of its substrate: L-Nitroarginine methyl ester (L-NAME)[24]. In the presence of 0.1mM L-NAME, the NO_x release rate was drastically reduced, both in stimulated and non-stimulated cultures (Fig. 2B). Lastly, we assessed cell viability of the cultures treated with L-NAME (using MTT assay); no toxicity was caused by the inhibitor and the consequent lack of NOS (data not shown).

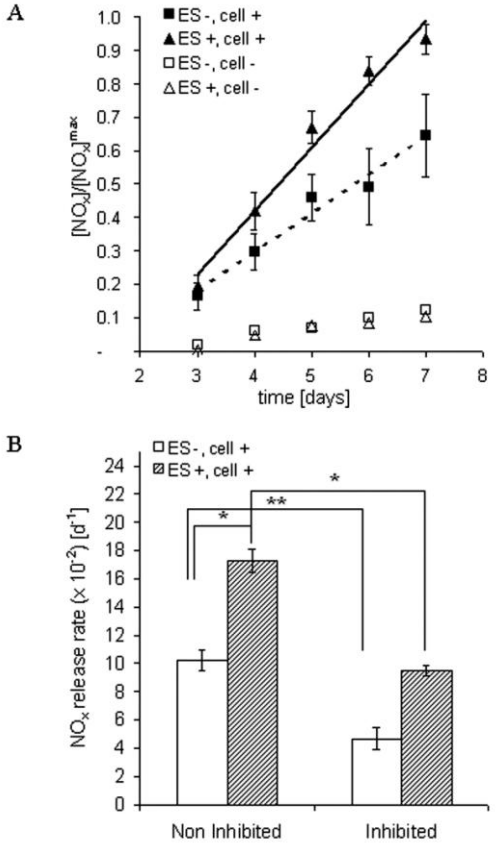

Figure 2. NO_x release in the culture medium at different time points for electrically stimulated 3D culture (ES +, cell +) and non-electrically stimulated 3D culture (ES -, cell +). Negative controls are represented by not-seeded 3D scaffold (ES ±, cell -). (A) NO_x release in the culture medium normalized by the maximum value measured: full symbols refer to 3D cell culture, open symbols are negative control. Electrical stimulation (ES) starts at day 3 (arrow). (B) The release rate of NO_x obtained by linear correlation of data in (A), and analogue ones, for stimulated and non stimulated cells, with and without 0.1 mM of L-NAME, the inhibitor of NO-synthase. *p,0.01; **p,0.

Effect of electrical stimulation on muscle marker expression

Considering the enhanced release of NO_x, we investigated the effect of electrical stimulation on the expression of three specific muscle markers, Desmin, MyoD and Myosin, trough immunohystochemistry and western blot. Immunostaining on seeded scaffolds showed that our mpcs expressed Desmin and MyoD after 7 days of *in vitro* culture (Fig. 3A and 3B), both in stimulated and non-stimulated condition. In order to better evaluate the difference in marker expression we performed semi-quantitative western blot analysis of MyoD, Desmin and Myosin (Fig. 3D and 3E). We observed that satellite cells cultured in electrically stimulated scaffold had a higher expression of MyoD ($p<0.01$) and Desmin ($p<0.05$), while Myosin expression was not significantly affected by electrical stimulation (Fig. 3E).

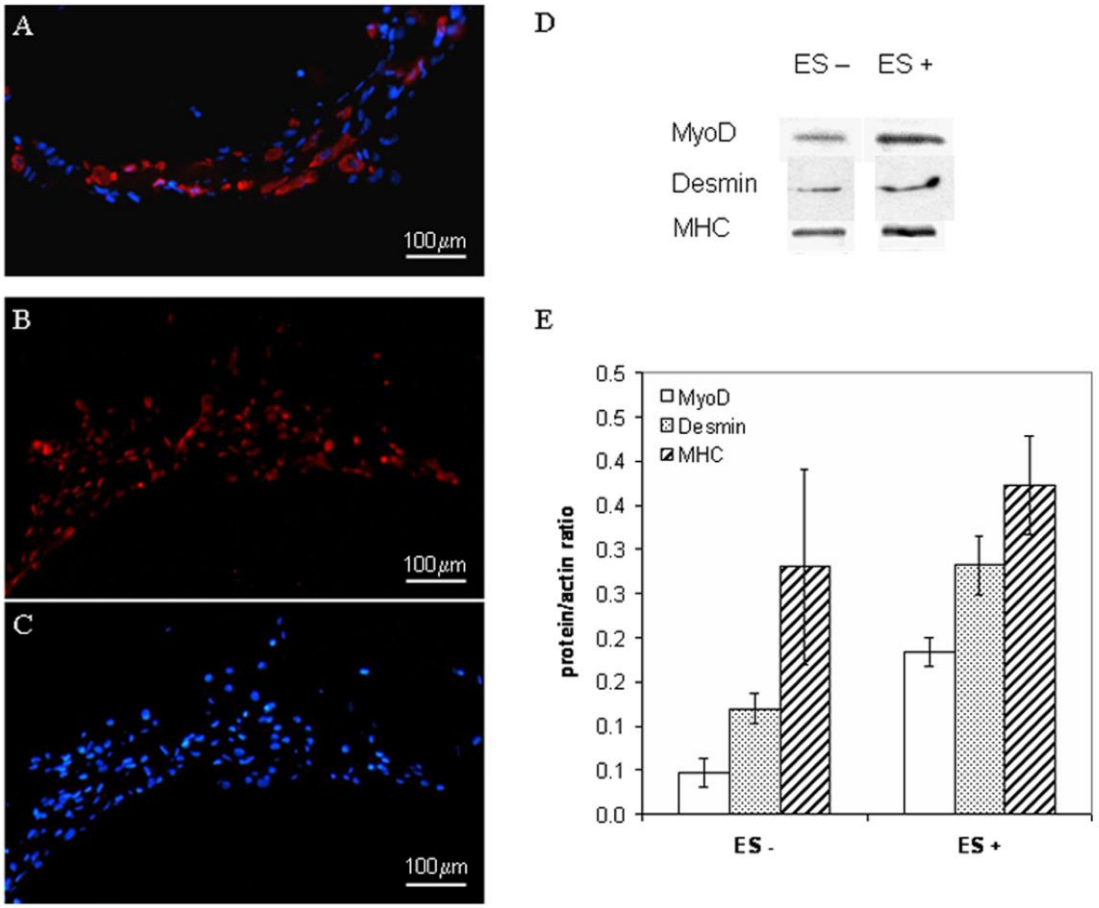

Figure 3. Analysis of muscle skeletal marker expression after 7 days of in vitro culture. (A–C) Immunofluorescence analyses: scaffold sections were stained for desmin (A) and MyoD (B), and nuclei were counterstained with DAPI (A and C). (D) Images of Western blot analysis on MyoD, desmin and myosin heavy chain (MHC) of non-electrically stimulated scaffold (ES -) and electrically stimulated scaffold (ES +). (E) Quantification of protein expression based on intensity of lanes in D normalized for intensity of the respective actin lane. *p,0.01; **p,0.05. Bar=100 mm

In vivo implantation

We performed *in vivo* preliminary analyses in order to verify collagen scaffold biocompatibility and cell response upon in vivo implant. Figure 4 shows sections of tibialis anterior muscles 10 days after implantation. GFP satellite cells were clearly visible within both stimulated (Fig 4A) and nonstimulated (Fig 4B) scaffolds; no evident differences in cell number and/or distribution could be seen between the two conditions. Importantly, at this early time point mpcs inside the implanted scaffold were still desmin positive (Fig. 4C) and there were some newly formed myotubes inside the implanted scaffold (Fig. 4C, magnification).

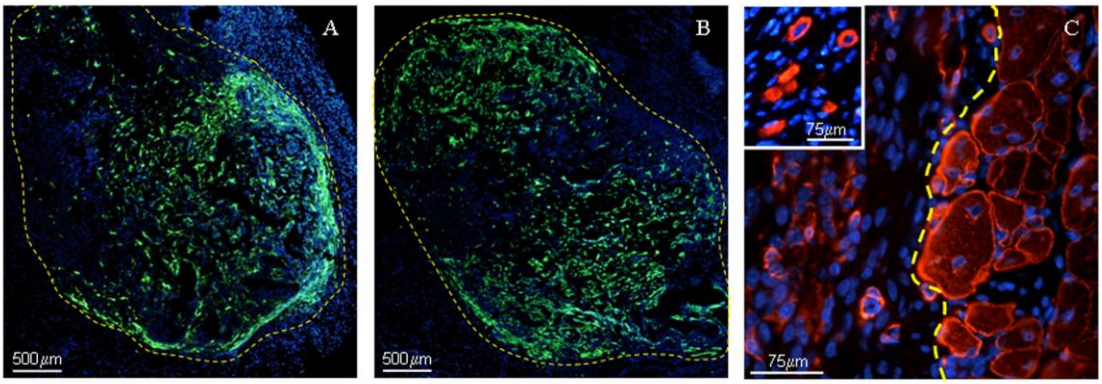

Figure 4. Immunofluorescence analysis of *in vivo* implant of cellularized 3D scaffold in syngeneic mice 10 days after the surgery. A and B show muscle section stained for GFP, while C shows staining for desmin. Nuclei were counterstained with DAPI. Dashed lines represent the interface muscle/scaffold. (A) Section of tibialis left muscle implanted with non-electrically stimulated scaffold; (B) section of tibialis right muscle implanted with electrically stimulated scaffold; (C) particular of the interface between muscle (right) and implanted scaffold (left); magnification: newly formed myotubes inside the implanted scaffold. Bar=500 μm in A and B; bar=75 μm in C

B.4 Discussion

Tissue engineering aims to reconstitute functional tissues starting from two major components: cells and scaffolds. With regards to skeletal muscle, several types of scaffold have already been tested, from synthetic polymers[15, 21] to natural scaffolds[25]; besides, several biomimetic approaches have been developed in order to increase scaffold biocompatibility. In this work we used a 3D porous collagen scaffold, characterized by biochemical and mechanical properties similar to those of *in vivo* tissues. We had already tested this kind of substrate for *in vitro* cell cultures, finding it particularly well suited for cultures of muscle precursor cells[15]. The choice of an appropriate cellular source is also fundamental for the generation of a functional homogeneous tissue *in vitro*. Satellite-derived muscle precursor cells can be an appealing solution, as they are relatively easy to isolate and represent the direct precursor of myoblasts. We previously used these cells for in vivo implants and proved that they display a high regenerative potential[21]. When it comes to clinical application of mpcs, the first issue to overcame is their *in vitro* expansion. This is one of the most critical steps, since cell proliferation and differentiation capacity can be greatly influenced by external stimuli derived by the culture environment. In

particular, it has already been demonstrated that the 2D expansion of primary myoblasts in Petri dishes leads to a loss of their potential to differentiate in myotubes[6]. The aim of this work was the development of a biomimetic culture environment capable of preserving the myogenic potential of mpcs during in vitro expansion, in sight of their in vivo implantation. For this purpose, we coupled 3D culture and electrical stimulation. Electrical stimulation plays an important role in muscle; we thus re-created in vitro an electrical field capable of influencing the distribution of ions, small peptides and proteins without being cytotoxic or affecting the cell viability. It has been shown that the application of an exogenous electrical stimulus enhances the expression of specific skeletal muscle, such as MyoD and Desmin. The not relevant effect of electric filed on Myosin suggests the hypothesis of a stronger influence of electrical stimuli in the early stages of satellite cell differentiation, in agreement with our previous work[16]. This suggests that our system could be used for preventing loss of cell myogenicity during *in vitro* expansion. Interesting results were obtained studying NO_x. Anderson and colleagues demonstrated that NO_x are one of the first activation markers of satellite cells *in vivo*[23]. In this work we observed that electrical stimulation enhances the total amount and the release rate of NO_x in culture medium. We verified that the observed increase in NO_x release rate was effectively due to cell release and not to galvanic oxidation of some medium components: not only stimulated scaffolds without cells showed negligible NO_x release but also inhibition of NOS by an analogous of his substrate causes a drastic decrease in the release rate. Recent findings on NO and HGF effects on satellite cells activation showed that NO concentration regulates a balance between quiescence and activation on fibers[23] but NO pathway has still many dark connections to by clarified. A step further could be the study of electrical stimulation on HGF signaling and coupling with stretching. The in vivo study was performed in order to obtain preliminary data on the feasibility of the surgery and on the scaffold biocompatibility. During the operation, collagen scaffolds were easily manipulated

and fitted in the injury site. Our preliminary results showed that the scaffold did not hinder the muscle regeneration, since a lot of neo-formed myofibers were observed

in the muscle-scaffold interface. The collagen scaffold can act as myogenic cells reservoir, since 10 days after the implantation we observed GFP positive cells and the formation of small myotubes inside it. Further investigation at longer time points is required to confirm these promising results. With our preliminary study we explored the effect of an alternative in vitro culture system based on coupling of culture systems already verified and tested (3D collagen scaffold and electrical stimulation); such system can be upgraded and upscaled with dynamic cell culture system, such as a perfusion bioreactor coupled with electrical stimulation. This could lead to a great improvement regarding cell proliferation, survival and cell distribution along the scaffold that could result in a more uniform and functional implantable graft. In our work, muscle precursor cells are seeded into the scaffold and then cultured in that environment (more similar to the physiological tissue), instead of being expanded in vitro using traditional Petri dishes and then seeded into the scaffold just before implantation, resulting in a reduced manual intervention by the operators. Further and exhaustive studies are needed to elucidate the effect of electrical stimulation on muscle precursor cells, however, we believe that this could be a promising approach for in vitro muscle precursor cell expansion offering new therapeutic tools. Moreover, our methodology represents a very flexible and versatile culture system: knowing cell excitability properties and scaffold dielectric properties, our culture system could be easily adapted to several cell type and different culture substrate or scaffold.

B.5 Conclusions

Here we describe for the first time a novel biomimetic tissue-engineering approach that can improve the efficacy of muscle precursor cell expansion in vitro and consequently the efficiency of cell delivery after in vivo implantation. In particular, we developed a culture methodology to reproduce in vitro the best conditions for satellite cell expansion and maintenance of their myogenicity. Our biomimetic approach is based on the coupling of 3D cell culture on a collagen scaffold, which

provides an environment more similar to the in vivo tissue, to electrical stimulation, which mimics part of the neuronal activity.

B.6 Acknowledgments

We would like to thank Dr. A. Chiavegato for her collaboration in the western blot analyses. This work was supported by grants from Citta' della Speranza, AFM, University of Padova (Progetto di Ateneo) and Regione Veneto (Azione Biotech II).

B.7 References

1. Bach AD, Beier JP, Stern-Staeter J, et al. Skeletal muscle tissue engineering. Journal of Cell. Mol. Med 2004; 8: 413-422.
2. Deasy B, Li Y and Huard J. Tissue engineering with muscle-derived stem cells. Current Opinion in Biotechnology 2004; 15: 419–423.
3. Menaschè P. Skeletal myoblast for cell therapy. Cor Art Dis 2005; 16: 106-110.
4. Urish K KY, Huard J. Initial failure in myoblast transplantation therapy has led the way toward the isolation of muscle stem cells: potential for tissue regeneration. Current Topics in Developmental Biology 2005; 68: 263-280.
5. Levenberg S, Rouwkema J, Macdonald M, et al. Engineering vascularized skeletal muscle tissue. Nature Biotechnology 2005; 23: 821-823.
6. Machida S, Spangenburg E and Booth F. Primary rat muscle progenitor cells have decreased proliferation and myotube formation during passages. Cell Prolif 2004; 37:
7. Montarras D, Morgan J, Collins C, et al. Direct isolation of satellite cells for skeletal muscle regeneration. Science 2005; 309: 2064-2067.
8. Freed LE and Vunjak-Novakovic G. Culture of organized cell communities. Advanced Drug Delivery Reviews 1998; 33: 15-30.
9. Powell K. Stem-cell niches: it's the ecology, stupid! Nature 2005; 435: 268-270.
10. Stern-Straeter J, Bach A, Stangenberg L, et al. Impact of electrical stimulation on three dimensional myoblast cultures – a real-time RT-PCR study. J. Cell. Mol. Med 2005; 9: 883-892.
11. Radisic M, Park H, Shing H, et al. Functional assembly of engineered myocardium by electrical stimulation of cardiac myocytes cultured on scaffolds. Proc Natl Acad Sci U S A 2004; 101: 18129-18134.
12. Partridge TA. Cells that participate in regeneration of skeletal muscle. Gene Therapy 2002; 9: 752-753.
13. Zhang S, Gelain F and Zhao X. Designer self-assembling peptide nanofiber scaffolds for 3D tissue cultures. Seminars in Cancer biology 2005; 15: 413-420.
14. Pedrotty D, Koh J, Davis B, et al. Engineering skeletal myoblasts: role of 3D culture and electrical stimulation. Am J Physiol Heart Circ Physiol 2005; 288: H1620-H1626.
15. Cimetta E, Flaibani M, Mella M, et al. 3D culture of muscle precursors stem cells in a perfusion bioreactor. International Journal of Artificial Organs 2007; 30: 415-428.

16. Flaibani M, Boldrin L, Cimetta E, et al. Muscle precursor cells differentiation and myotubes alignment by micro-patterned surfaces and exogenous electrical stimulation. submitted;
17. Hill E, Boontheekul T and Mooney D. Regulating activation of transplanted cells controls tissue regeneration. Proc Natl Acad Sci U S A 2006; 103: 2494-2499.
18. McCaig C, Rajnicek A, Song B, et al. Controlling cell behaviour electrically: current views and future potential. Physiol Rev 2005; 85: 943-978.
19. Naumann K and Pette D. Effects of cronic stimulation with different impulse patterns on the expression of myosin isoforms in rat myotubes cultures. Differentiation 1994; 55: 203-211.
20. P De Coppi, S Bellini, M Conconi, et al. Myoblast-acellular skeletal muscle matrix constructs guarantee a long-term repair of experimental full-thickness abdominal wall defects. Tissue Eng 2006; 12: 1929-1936
21. Boldrin L, Elvassore N, Malerba A, et al. Satellite cells delivered by micro-patterned scaffolds: a new strategy for cell trasplantation in muscle diseases. Tissue Engineering 2007; 13: 253-262.
22. Cannizzaro C, Tandon N, Figallo E, et al. Practical aspects of cardiac tissue engineering with electrical stimulation. Methods in molecular medicine: Tissue engineering, 2007.
23. Wozniak A and Anderson J. Nitric Oxide-Dependence of Satellite Stem Cell Activation and Quiescence on Normal Skeletal Muscle Fibers. Developmental Dynamics 2007; 136: 240-250.
24. Zhang J, Kraus W and Truskey G. Strech induced mitric oxide modulates mechanical properties of skeletal muscle cells. Am J Physiol 2004; 287: 292-299.
25. Borschel GH, Dennis RG and Kuzon WM. Contractile skeletal muscle tissue-engineered on an acellular scaffold. Plast Reconstr Surg 2004; 113: 595-602.

Appendix C

Enhancement of viability of muscle precursor cells on 3D scaffold in a perfusion bioreactor

Elisa Cimetta[1], Marina Flaibani[1], Marco Mella[1], Elena Serena[1], Luisa Boldrin[2], Paolo De Coppi[2], Nicola Elvassore[1]*

[a] Department of Chemical Engineering, University of Padua, Via Marzolo, 9 Padua, Italy

[a] Department of Pediatrics, University of Padua, Via Giustiniani, 3, Padua, Italy

*Corresponding author

The International Journal of Artificial Organs

Vol. 30 / no. 5, 2007 / pp. 415-428

Keywords: bioreactor, perfusion, dynamic culture, C2C12, satellite cells, skeletal-muscle precursor cells, three dimensional culture.

Abstract

The aim of this study was to develop a methodology for the in vitro expansion of skeletal-muscle precursor cells (SMPC) in a three dimensional (3D) environment in order to fabricate a cellularized artificial graft characterized by high density of viable cells and uniform cell distribution overall the 3D domain. Cell seeding and culture within 3D porous scaffolds by conventional static techniques can lead to a uniform cell distribution only on the scaffold surface, whereas dynamic culture systems have the potential of allowing a uniform growth of SMPCs within the entire scaffold structure.

In this work, we designed and developed a perfusion bioreactor able to ensure long term culture conditions and uniform flow of medium through 3D collagen sponges. A mathematical model to assist the design of the experimental set-up and of the operative conditions was developed. The effects of dynamic vs static culture in terms of cell viability and spatial distribution within 3D collagen scaffolds were evaluated at 1, 4 and 7 days and for different flow rates of 1, 2, 3.5 and 4.5 mL/min using C2C12 muscle cell line and SMPCs derived from satellite cells. C2C12 cells, after 7 days of culture in our bioreactor, perfused applying a 3.5 mL/min flow rate, showed a higher viability resulting in a three-fold increase when compared with the same parameter evaluated for cultures kept under static conditions. In addition, dynamic culture resulted in a more uniform 3D cell distribution. The 3.5 mL/min flow rate in the bioreactor was also applied to satellite cells derived SMPCs cultured on 3D collagen scaffolds. The dynamic culture conditions improved cell viability leading to higher cell density and uniform distribution through the whole 3D collagen sponge for both C2C12 and satellite cells.

C.1 Introduction

The *in vitro* reconstruction of engineered skeletal-muscle grafts holds the potential of becoming a new means for treating muscular diseases such as dystrophy and traumatic injuries (1), by improving muscle regeneration and overcoming the

limitations of direct myoblast transplantation (2, 3). For these cell-mediated therapies, the engineered skeletal muscle graft must meet specific requirements such as high cell density and uniform cells distribution (4, 5). These new therapeutic strategies are limited by the lack of automatic, efficient and robust culture systems able to expand small biopsy-derived cells populations up to the large number of cells required for an in vivo implantation.

To date, for this expansion procedure, conventional culture systems such as Petri dishes and tissue culture flasks, are usually employed. Even if many studies on two-dimensional (2D) culture systems helped improving general knowledge on culture techniques and cells behaviour, 2D cultures show a poor efficiency and expensive implementation of cell expansion process at clinical level. In addition, 2D cultures cannot fully replicate the natural in vivo microenvironment affecting the viability, proliferation and functional differentiation of most types of cells (6). On the other hand, 3D cell culture methods using scaffolds as supporting materials can generate a micro-environment better resembling the in vivo conditions, improve cell survival and proliferation (7) and offer a means for potentially obtaining high cell density constructs. Scaffolds must respond to many specific requirements such as biocompatibility, adequate mechanical, physical and chemical properties and proper conformational structure. However, static 3D cultures face problems such as the inadequate mass transfer of nutrients and the limited gas species diffusion which, in vivo, are overcome by the functionality of the capillary net, the means by which gases and nutrients are exchanged, wastes removed and biochemical signals transported (8, 9). Thus, the supply of oxygen and nutritive elements to the in vitro growing grafts can be a strong limitation in their functionality and size (10). In order to overcome such limitations, new scaffold materials and geometries, combined with dynamic perfusion culture methods in different types of bioreactors have been developed (11-13).

Bioreactors have the purpose of granting the culture of cells in sterile, physiological and controlled conditions while ensuring, through the dynamic regime, a more efficient mass transfer of nutrient and gases between the cellularized scaffold and the culture medium and removal of debris. These specific features co-operate to

obtain a more uniform cell distribution through the entire 3D structure of the supporting material (14, 15). Bioreactors have already proved useful in improving the quality of in vitro skin and cartilage, the main commercially available 3D tissue-engineered products (16, 17). In addition, the study of dynamic culture systems lead to the development of many different devices including: rotating vessels (18, 19), spinner flasks (20) and perfusion bioreactors (21, 22). Bioreactor designs can differ depending on the cell source and the aim of the study; and indeed many works have dealt with the optimization of the dynamic culture for cartilage, bone, cardiac and vascular tissues and liver (23). Only a limited number of studies involved the 3D culture of muscle cells in a bioreactor. Some of these works, for example, are focused on cell differentiation under mechanical stimuli using myoblasts seeded on microcarrier beads (24), on the improvement of the architecture of engineered cardiac tissues (25) or on smooth muscle cells cultured on stretched scaffolds (26). All these works do not deal nor overcome the limitations related to the expansion of muscle precursor cells and the realization of an uniform density of undifferentiated cells in a 3D structure and aimed to be used for cell-mediated therapy. In none of these studies, to our knowledge, have muscle precursor satellite cells been used. Satellite cells are a pluripotent population of muscle progenitor cells located, in their quiescent phase, beneath the basement membrane of myofibers. Upon activation due to muscle damage and fibre injury, satellite cells begin to proliferate and can both differentiate into newly formed multinucleated myotubes and fuse with pre-existing damaged fibers repairing them (27-30). For these reasons, the satellite-derived muscle cells are good candidates for being used as a source for cell-mediated therapy (31).

The aim of this work was to design and develop a perfusion bioreactor studied to maintain high viability and proliferation of skeletal muscle precursor cells (SMPCs) seeded on three-dimensional scaffolds in sight of their employment in clinical cell therapies. We compared static and dynamically perfused cultures and, in optimizing operating conditions for our bioreactor, we evaluated the effects of different medium flow rates and culture time points on both cells viability and cells spatial distribution inside the scaffold. Preliminary investigations sought use of the C2C12

skeletal muscle immortalized cell line; and subsequently, the entire culture procedure has then been tested on satellite cells. In particular, being oxygen a strong limiting factor in the development of a 3D cellularized construct and in particular for muscular cells (32), we employed the use of a mathematical model to assist in the design and development of our bioreactor. In particular, this mathematical model describes the oxygen concentration at the outlet of the culture chamber as a function of the cell density and medium flow rates. The model simulations aided the choice of the optimal operating parameters and assessed the maintenance of the proper physiological condition, in terms of minimum concentration of oxygen in the culture chamber, during the entire culture time.

In this study, we have demonstrated how our bioreactor has succeeded in maintaining sterile culture conditions, efficient nutrients and gases transfer, a more uniform 3D cell distribution and a higher cell density when compared with static cultures. These results open a new perspective for the development of robust and automatic systems capable of expanding the small population of SMPCs harvested from a biopsy up to the suitable number of cells required for any biomedical use.

C.2 Material and Methods

C.2.1 Cell isolation and culture

C2C12.

The murine skeletal muscle immortalized cell line C2C12 (ATCC, USA) was grown in Dulbecco's modified Eagle's medium (DMEM, Sigma-Aldrich, Milano, Italy) supplemented with 10% foetal bovine serum (FBS, Gibco-Invitrogen, Milano, Italy), 1% penicillin-streptomycin solution (1000U/mL) and 1% L-glutamine (all from Invitrogen), on standard 100 mm Petri dishes, in a 95% humidified and 5% CO2 atmosphere at 37ºC and maintained at low confluence. The medium was regularly changed every three days.

Satellite cells

Pure satellite cells cultures were obtained following the protocol previously described by Rosenblatt et al. in 1995, and performed in Stem Cell Processing Laboratory, Department of Pediatrics, University of Padua.

Briefly, *flexor digitorum brevis* mouse muscles were removed and enzymatically digested with 0.2% Collagenase Type I (Sigma-Aldrich). The single fibers were selected on an inverted microscope (Olympus IX71, Japan) and plated on Matrigel coated (BD Bioscience, California, USA) Petri dishes. Myofibers were maintained in a humidified tissue culture incubator. On day three, plating medium consisting of DMEM, 10% horse serum (Gibco-Invitrogen), 1% chicken embryo extract (MP-Biomedicals, Verona, Italy), 1% penicillin-streptomycin solution (1000U/mL), was added to the Petri dishes. After 72 more hours, culture medium was switched to proliferating, consisting of DMEM, 20% foetal bovine serum, 10% horse serum, 1% chicken embryo extract and 1% penicillin-streptomycin solution (1000U/mL). Cells were kept in culture with proliferating medium and detached from the plates with Trypsin (Gibco-Invitrogen) before fusion in myotubes occurred. Cells were then re-plated and expanded.

C.2.2 Scaffold characterization

The morphology of collagen sponges (Avitene® UltrafoamTM Collagen Hemostat. Davol inc., Cranston, USA) was analyzed using an Environmental Scanning Electron Microscope (ESEM, model XL30, Philips). Briefly, dried collagen sponges were gold sputtered under high vacuum (0.05 mTorr) and photographs were taken at different magnifications ranging from 300x to 10,000x. The mean pore diameter R of 75 μm was estimated using a imaging software (Image Tool 3.0).

In order to evaluate the hydrodynamic conditions within the 3D collagen sponge, measurements of the scaffold void fraction and head loss through the scaffold were performed. The void fraction was roughly evaluated by gravimetrical measurements; the weight difference between a wetted and dry scaffold giving the amount of water filling the scaffold porosity.

Pressure drops through the scaffold were measured as a function of the medium flow rate ranging from 0.5 to 4.5 mL/min using a differential manometer. It is worth noting, that in this range of flow rates the collagen scaffold integrity and morphology were not altered. The experimental data were correlated by the following equation:

$$\Delta P = K \cdot Q \tag{1}$$

where ΔP is the pressure drop (Pa), Q the flow rate (mL/min) and K is a constant evaluated to be 7.4 (Pa min/mL).

Using this data, the scaffold permeability coefficient, k_s, was calculated from the Darcy's law for Newtonian fluid in a laminar flow regime through a porous media (33):

$$k_s = \frac{L_{sc} \cdot \mu}{A_{sc} \cdot K} = 30.54\ \mu m^2 \tag{2}$$

where $\mu = 0.80\ cP$ (34, 35) is the medium dynamic viscosity and $L_{sc} = 3mm$ and $A_{sc} = 177\,mm^2$ are length and cross section area of scaffold, respectively.

Assuming that the collagen sponge can be represented as a package of tangled micro-channels, the mean-velocity can be approximately considered uniform through the entire scaffold cross-section (33). Under these hypothesis and approximating our scaffold to a package of micro-channels with a radius corresponding to the mean pore radius $R = 75\,\mu m$, the maximum value of shear stress (τ_w) acting on the surface of a cell attached on the collagen tube wall can be estimated using the following empirical correlation (36):

$$\tau_w = \left(\frac{4\mu}{\pi}\right) \cdot \frac{Q_{ch}}{R^3} \tag{3}$$

where Q_{ch} is the volumetric flow rate in a single micro-channel.

C.2.3 Cell seeding

As the scaffold wettability can affect cell adhesion, the dry scaffolds (16 mm diameter and 3mm height cylinders) were pre-treated with 500 µl of culture medium

inside standard 35 mm Petri dishes and incubated for 12 hours. Before cell seeding, the exceeding medium was removed by absorption with a sterile gauze.

Subconfluent plates of C2C12 and satellite cells were detached on day 0 using trypsin/EDTA, pelletted by centrifugation for 5 min at 1200 rpm and counted. In the experiments performed for the viability analyses 10^5 cells were suspended in 150 μl of culture medium and deposed over the scaffolds upper surfaces and incubated for 2 hours. In the experiments performed for the histological analyses, 10^6 C2C12 and $5 \cdot 10^5$ satellite cells were seeded following the same procedure. After the first incubation phase, 200 μl of medium were added at aliquots of 50 μl per hour. 2 mL of medium were finally added to the seeded scaffolds before the final incubation of 12 hours.

Considering the screening experiments done using the C2C12 cell line, we performed a total of 27 static cultures distributed in the different time points as follows: 4 at 1 day, 11 at 4 days and 12 at 7 days; the effect of different flow rates applied during dynamic culture (see Results) was evaluated on at least 2 replicas of the same experimental conditions at a 7 days time point. Finally, using the optimized flow rate, 14 dynamic runs were distributed in the different time points as: 4 at 1 day, 6 at 4 days and 4 at 7 days. Concerning satellite cells we ran 5 dynamic cultures and 4 static controls, all at a 7 day time point.

C.2.4 Bioreactor

The main requisites of the bioreactor can be summed as follows: i) homogeneous culture condition within the 3D domain; ii) a high cell density; iii) steady-state long-term cell culture. To achieve these objectives we needed to design a system in which the metabolites are evenly distributed within the entire 3D domain, the cells' uptake rate of metabolites are not limited by transport phenomena, and, in particular, the metabolite concentration must not change with time due to the increasing number of cells.

For these reasons, the design and development of the bioreactor was assisted by a mathematical modelling describing the time evolution of the oxygen concentration

at the inlet and outlet of the culture chamber unit. Oxygen was chosen as it represents the most important metabolite for skeletal muscle precursor cells.

Experimental set up

Our dynamic culture system (Figure 1a) was composed of four units: a cell culture chamber, a gas-exchange unit, a medium reservoir and a peristaltic pump. The culture chamber was assembled with four Teflon (PTFE) parts and EPDM O-rings were used to prevent medium leaking as shown in Figure 1b. The seeded scaffold was positioned inside the cylindrical chamber between two 70 μm mesh stainless steel nettings. In order to have a simple and easily cleanable set up, the gas-exchange unit was made of a tubular non-porous permeable membrane (platinum cured silicone tubing, Vetrotecnica, Padova, Italy) wrapped around a custom made INOX-Teflon support. The medium reservoir was composed by a 200 mL Pyrex® glass laboratory bottle whose stopper was modified with the insertion of a PTFE block hosting the connections with the bioreactor and the gas exchanger and ensuring aseptical sealing. We used a Watson-Marlow peristaltic pump (314D model) to ensure stable and controllable flow of medium through the entire apparatus. The culture medium hold up of the system was approximately of 80 mL.

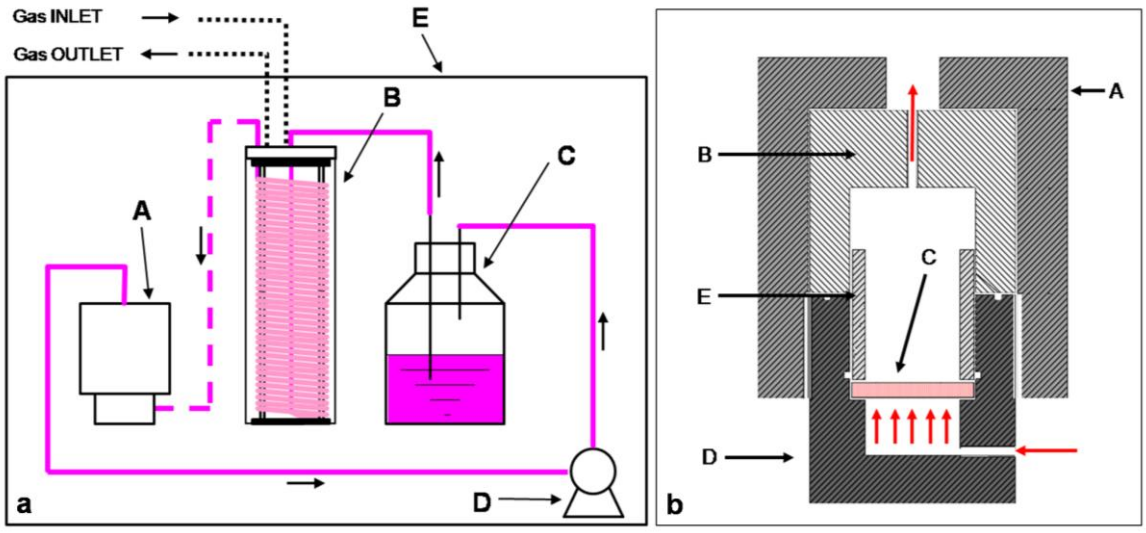

Figure 1. Schemes of the experimental set up. Figure 1a shows culture apparatus scheme: A) culture chamber; B) Gas exchange unit; C) medium reservoir; D) peristaltic pump; E) air thermostatic bath. ▪▪▪) air tubing; - - -) tubing for oxygenated medium; ——) tubing from the bioreactor. The culture medium was withdrawn from the reservoir, fed into the gas exchange unit and, successively, into the culture chamber by a peristaltic pump.

All connections were made by 1/8" INOX 316 junctions and platinum-cured silicone tubing with an internal diameter of 3.2 mm and 1.6 mm wall thickness (Vetrotecnica, Padova, Italy).

The materials used ensured biocompatibility, non-reactivity and allowed the use of repeated autoclave sterilization cycles.

C.2.5 Model assisted design

As previously underlined, for muscular cells and skeletal muscle precursor cells in particular, oxygen is one of the most critical metabolites and has thus been chosen as the reference metabolite for the development of the mathematical model.

The bioreactor model framework can be reduced to a closed loop, shown in Figure 2, composed of two units: the cell-culture chamber and the membrane gas-exchanger. Inside the culture chamber, the oxygen level decreases as a function of both the increasing number of cells and the decreasing medium flow rate, whereas it rises in the membrane gas-exchange units as function of the flow rate.

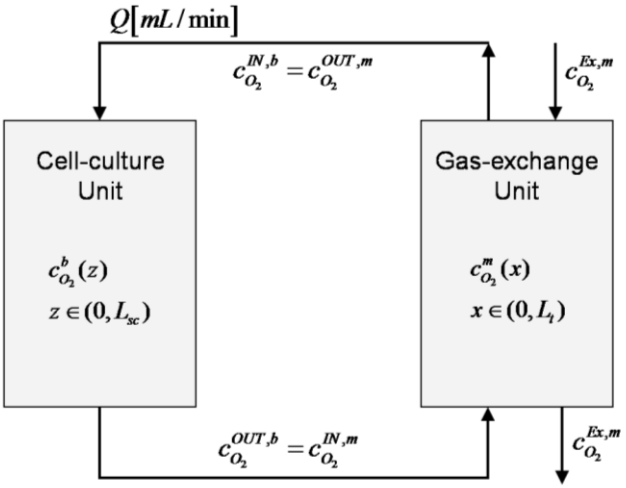

Figure 2. Bioreactor model framework. The bioreactor apparatus, for modelling purposes, was reduced to a closed loop composed of two units: the cell-culture chamber and the membrane gas-exchanger. The variables and their dependences are explicitly listed. $c_{O_2}^{b}\ z$ and $c_{O_2}^{m}\ x$ are the oxygen concentration at a given axial coordinate z and x within the scaffold and the gas exchange unit, respectively. L_{sc} and L_t are the high of the scaffold and the length of the tubing of the membrane exchange unit, respectively. The superscripts OUT and IN refer to the and inlet section of both units. $P_{O_2}^{Ex,m}$ is the oxygen partial pressure in the atmosphere on the external side of the gas-exchange unit. Q is the flow rate of the recirculated medium.

The mathematical model was obtained by simultaneously solving the steady-state mass balance equations governing the oxygen uptake rate in the cell culture chamber and the oxygen transfer rate in the membrane gas-exchange units. The results of the simulation gave the oxygen concentration at the outlet of the culture chamber as a function of the medium flow rate and the cell density.

The cell culture chamber.

The model considered a homogeneous oxygen uptake within the perfused 3D scaffold. We assumed the collagen scaffold to be a cylinder with a geometry which didn't change nor degrade during the experiments. The oxygen consumption rate was assumed to follow a zero-order kinetic as oxygen profiles obtained using higher-order kinetics doesn't differ significantly (37). In particular, the oxygen uptake rate of a single cell in a resting muscular tissue is: $R_{O_2,tissue} = 4 \cdot 10^{-4}\ cm^3_{O_2} / cm^3_{tissue} \cdot s$ (38). This uptake rate can be approximated to $R_{O_2,cell} = 0.21 \cdot 10^{-9}\ \mu L/s$ (μL at 298K and 0.1 MPa) or $R_{O_2,cell} = 8.59 \cdot 10^{-18}\ mol/s$ per cell, considering a cellular density of 1.06 gr/cm^3 (39) and an average cell diameter of 10 μm. In order to over-dimension our system, we referred our calculations to a maximum oxygen uptake rate of $R_{O_2} = 5 \cdot 10^{-9}\ \mu L/s$ or equivalently $R_{O_2} = 2.04 \cdot 10^{-16}\ mol/s$ per cell.

The culture medium was considered as an incompressible Newtonian fluid and its flow was oriented along the reactor length (z-direction) from the bottom to the top. The hydrodynamic regime was laminar and the calculated Reynolds number was *Re=5.9* for the flow rate of 3.5 mL/min. We have also evaluated (basing our calculations on formulations cited by Fournier (36)) that the hydrodynamic flow was fully developed in a laminar profile at any axial position before permeating the scaffold for any of the flow rates tested (data not shown).

Under the considerations listed above, the steady-state mass balance for the oxygen within the scaffold is:

$$-Q \frac{\partial c^b_{O_2}\ z}{\partial z} - R_{O_2} \rho_{cell} A_{sc} = 0 \qquad (4)$$

where $c_{O_2}^{b}\ z$ is the oxygen concentration at the generic cross section of the scaffold along the z coordinate, R_{O_2} is the oxygen uptake rate, ρ_{cell} the cell density, A_{sc} the scaffold cross section area and Q the medium flow rate.

Eq. (4) can be integrated from the inlet (z=0) to the outlet (z= L_{sc}) sections yielding to:

$$c_{O_2}^{OUT,b} = c_{O_2}^{IN,b} - R_{O_2}\rho_{cell}A_{sc}L_{sc}/Q = c_{O_2}^{IN,b} - A_2 \quad (5)$$

where superscripts OUT and IN refer to the corresponding bioreactor sections, L_{sc} is the scaffold length and A2 is a non-dimensional constant equal to $R_{O_2}\rho_{cell}A_{sc}L_{sc}/Q$.

Membrane gas-exchange unit.

The gas exchanger is a 10 m long silicone platinum cured tubing. The steady state mass balance of oxygen species, hypothesizing the concentration profile to be uniform in the radial direction and to vary along the tubing length is:

$$-Q\frac{\partial c_{O_2}^{m}\ x}{\partial x} + N_{O_2}\ x = 0 \quad (6)$$

where $c_{O_2}^{m}\ x$ is the oxygen concentration along the tubing length coordinate x, varying from 0 to L_t, and Q is again the medium flow rate. The oxygen flux per unit length, N_{O_2}, can be expressed as:

$$N_{O_2} = K_0 2\pi R^{\text{int}}\left[P_{O_2}^{Ex,m} - Hc_{O_2}^{m}\ x\right] \quad (7)$$

Where K_0 is the global exchange coefficient, $R^{\text{int}} = 1.6\cdot10^{-3}m$ is the tubing internal radius, $p_{O_2}^{Ex,m} = 20.22kPa$ is the oxygen partial pressure in the atmosphere and H the Henry's constant for oxygen in the medium ($H = 9,457\cdot10^{4}\ Pa\cdot m^3/mol$ (40)). Oxygen exchange can be seen as a three-step process: diffusion through the gas-phase, through the tubing walls and through the liquid phase. Assuming no-

resistance in the gas phase, the global exchange coefficient, K_0, is expressed as follows:

$$\frac{1}{K_0} = \frac{H}{K_L} + \frac{1}{K_M} \tag{8}$$

Where $K_M = P_m/\delta$ (40) and K_L are the mass transfer coefficient in the membrane and in the liquid phase, respectively; $\delta = 1.6 \cdot 10^{-3}\, m$ is the tubing wall thickness and P_m is the oxygen permeability ($P_m = 2{,}84 \cdot 10^{-13}\, mol \cdot m/m^2 \cdot s \cdot Pa$ (41)). K_L is evaluated considering that, for fluids under a laminar flow regime inside a cylindrical duct of length L and internal diameter, d_{ti} , we have (42):

$$K_L = \frac{D_{O_2}}{d_{ti}} 1{,}62 \left(\frac{d_{ti}^{\,2} \cdot \nu}{L_t \cdot D_{O_2}} \right)^{1/3} \tag{9}$$

where $D_{O_2} = 3.29 \cdot 10^{-9}\, m^2/s$ (43) is the oxygen diffusion coefficient in the culture medium and $\nu = 8.6 \cdot 10^{-7}\, m^2/s$ is the cinematic viscosity of culture medium (44).

Being that $c_{O_2}^{IN,b} = c_{O_2}^{OUT,m}$ and $c_{O_2}^{OUT,b} = c_{O_2}^{IN,m}$, substitution of Eq. 7 in Eq. 6 and integration of Eq.6 yields:

$$\frac{c_{O_2}^{IN,b} - P_{O_2}^{Ex,m}/H}{c_{O_2}^{OUT,b} - P_{O_2}^{Ex,m}/H} = \exp(-A_1) \tag{10}$$

Where A_1 is a non-dimensional constant equal to $K_0 2\pi R^{\text{int}} HL/Q$.

Rearranging Eq. (5) in Eq. (10) we obtain:

$$c_{O_2}^{IN,b} = \frac{P_{O_2}^{Ex,m}/H - A_2 + P_{O_2}^{Ex,m}/H}{1 - \exp(-A_1)} \tag{11}$$

$$c_{O_2}^{OUT,b} = c_{O_2}^{IN,b} - A_2 \tag{12}$$

Using Eq. 11-12 we evaluated oxygen concentration values at the inlet and outlet section of the cell culture chamber for the different flow rates of 0.01, 0.1, 1 and 10

cm3/min and different cell densities of 10^5, 10^6 and 10^7 per cm^3. We calculated the ratios of the variation of oxygen concentration between the two sections and the initial concentration at the inlet section.

C.2.6 Dynamic culture protocol

The start up operations of the dynamic culture system were the following: under a sterile hood the medium reservoir was filled with culture medium and sealed, the bioreactor chamber was opened and the first netting allowed in place using sterile tweezers. Twelve hours after seeding, the collagen scaffold was moved from the Petri dish and placed above the supporting netting with the seeded surface upside down; the second netting was then placed upon the collagen sponge. The culture chamber was then sealed and the entire apparatus moved to the thermostatic air bath where the gas exchange unit was connected to the gas cylinder supplying air-5% CO_2 and the tubing ducting the culture medium was connected to the peristaltic pump. Finally, the pump was allowed to operate at a voltage corresponding to the desired flow rate.

For each scaffold kept under dynamic culture, at least one static control culture was performed following the same seeding procedure and incubated at 37°C, 95% humidity and 5% CO_2. Culture medium was changed every other day.
The culture time points for both dynamic and static controls have been 1, 4 and 7 days; the samples were then carefully removed from the bioreactor culture chambers or Petri dishes and processed for histological and viability assessment.

C.2.7 Cell viability

Cellular viability was measured with the MTT test (Sigma-Aldrich, St.Louis, USA): 300 μL of the dye solution containing 5 mg/mL of the tetrazolium salt MTT in PBS was diluted to a final volume of 3 mL with fresh PBS and added to the samples; 3 hours incubation at 37°C followed. After the removal of the dye solution, 3 mL of a solubilization solution made with 10% DMSO and 90% Isopropanol was added to lyse the cells and dissolve the formazan crystals. The samples were then placed

inside the incubator at 37°C for a time allowing the complete dissolution and then centrifuged at 1200 rpm for 5 minutes to precipitate wastes. Clear solutions were processed for absorbance readings at 580 nm with an UV500 spectrophotometer, Spectronic Unicam (Cambridge, UK). In our range of absorbance, the recorded optical density (OD) was directly proportional to the number of viable cells.

C.2.8 Histological analysis

The samples were fixed in 4% PFA for 1 hour, rinsed thrice with PBS for 10 min and kept at +4°C covered by a thin layer of PBS. Before sectioning, fixed tissue specimens were dehydrated and embedded in paraffin. Sectioning was performed with a microtome and 7 μm thick sections of the cultured collagen matrices were analyzed both by Hematoxylin-Eosin (H-E) staining and Masson's trichrome staining using phosphomolybdic acid. Cell density and distribution within the scaffold were then assessed by microscope observations (inverted microscope Olympus IX51 Tokjo, Japan); images were captured and acquired using a JVC KY-F30 3-CC camera supported by Pinnacle, DVTools – Capture & Playback Application software.

C.2.9 Statistical analysis

Data are presented as histogram when only three replicates were available, whereas box plots are used in case of higher number of data. Briefly, box plots are statistical graphs in which the lower and upper lines of each box stand for the 1st and 3rd percentiles of the represented sample. The distance between the top and bottom of the box is the interquartile range. The middle line is the sample median, which is the 50th percentile of a given sample. The median is a robust estimate of the centre of a sample of data since it is affected very little by outlying points. A median not centred in the box is an index of skewness for the data. The vertical lines extending above and below the boxes show the distribution of the data falling outside the ranges cited above. Assuming no outliers, the maximum of the sample is the top of the upper whisker while the minimum is the bottom of the lower one. Values

exceeding 1.5 times the interquartile range are represented with plus signs (+) and can be considered as outlier data.

One-way ANOVA test was used and $p<0.01$ was considered statically significant.

C.3 Results

A representative image of 3D collagen scaffold is reported in Figure 3, showing its high porosity; mean pore diameter estimated at 150±10μm, and void fraction evaluated by gravimetric analysis at approximately ε=97%. These properties ensured the availability of a high specific surface for cell adhesion within the 3D scaffold and consequently, the potential for obtaining a high cell density. However, as transport phenomena can be strongly limited by slow diffusion processes, we needed to develop dynamic culture conditions contributing to recreating a suitable microenvironment for cell adhesion, spreading and proliferation within the entire 3D domain of the scaffold.

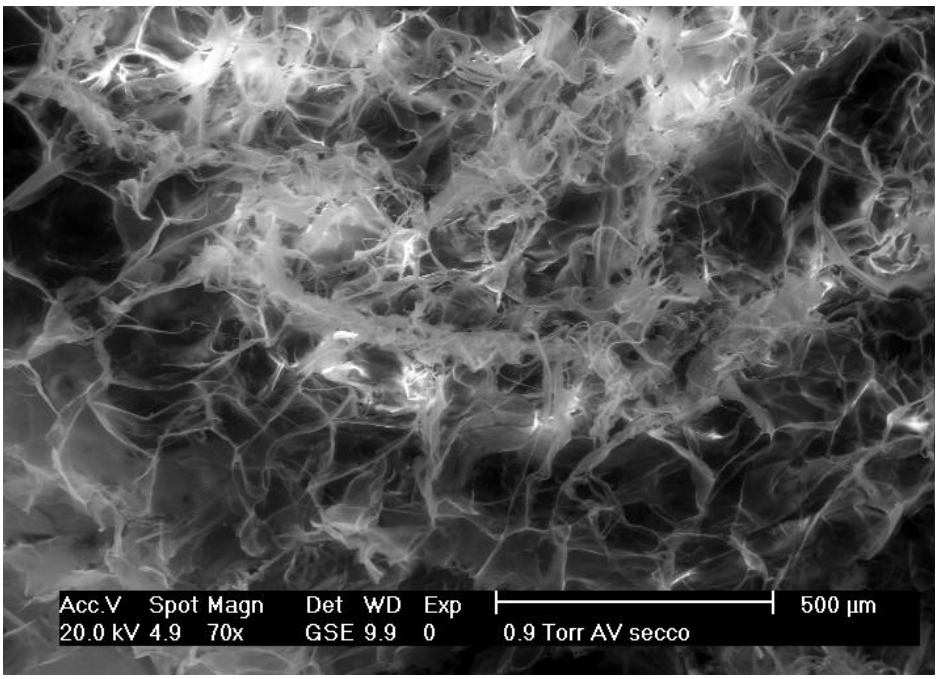

Figure 3. ESEM micrograph of dry collagen scaffold at 70x magnification.

The seeding procedure was optimized in order to achieve high cell adhesion on 3D collagen sponges for both C2C12 and satellite stem cells. The pre-treatment of the collagen scaffolds with culture medium helped in creating a more suitable environment for cells adhesion, such that the pre-wetted sponge was able to uniformly adsorb the 150 μL cell suspension used for seeding without showing preferential sites of adhesion. This seeding protocol valuably succeeded in granting cell adhesion without Matrigel coating, as its use, similarly of other chemically undefined reagents, may represent a limit for clinical applications.

For an *a priori* choice of medium flow rate we evaluated the oxygen concentrations at the inlet and outlet sections of the bioreactor culture chamber for the different flow rates of 0.01, 0.1, 1 and 10 cm3/min at the different cell densities of 10^5, 10^6 and 10^7 cell/cm^3. Figure 4 shows the fractional variation of oxygen concentration which is calculated as the oxygen concentration difference between the inlet and outlet sections normalized by the initial inlet concentration.

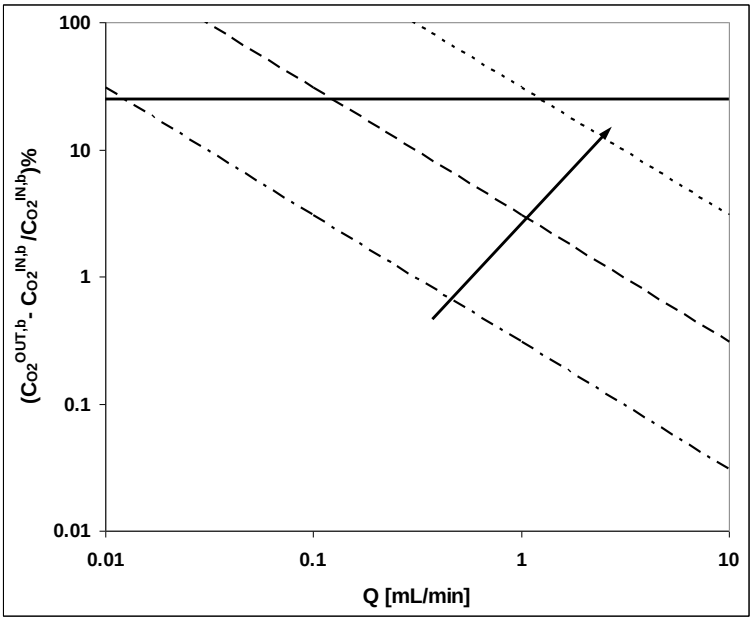

Figure 4. Profiles of the variation of oxygen concentration from the inlet to the outlet section of the culture chamber normalized with respect to the inlet concentration, as a function of the medium flow rate calculated from Eq (11) and (12). Profiles are parametric in the cell density (cell/cm^3): ▪—▪) 10^5; — —) 10^6; ▪▪▪) 10^7. Upper horizontal line represents the threshold level of oxygen concentration that ensures a physiological value throughout the scaffold This value corresponds to the 40 mmHg partial pressure of oxygen in the interstial fluid, thus being the 26% of the initial saturation value. The parameters characterizing the graph region above such threshold assess proper physiological conditions for cells cultures during the perfusion experiments. Arrow indicates the direction of increasing cell density.

Figure 4 shows that: 1) increasing the flow rate at constant cell density leads to a decrease in the percent variation of the oxygen concentration between the inlet and the outlet sections of the culture chamber; 2) increasing the cell density (see arrow) the curve shifts up, so that at the same flow rate, a higher cell density corresponds to higher variation of oxygen level between the inlet and the outlet sections.

The diagram shown in Figure 4 can prove very useful in verifying whether the operative variables in the culture chamber ensured viable cell culture conditions within the entire 3D domain of the scaffolds. For instance, the medium flow rate with a given cell density should yield to oxygen concentration at the outlet section higher than the physiological limit at any moment. The horizontal line, shown in Figure 4, represents the threshold of the physiological oxygen level (the partial pressure level of oxygen in the interstitial fluid of a resting tissue(36)) which is cautiously set to 5.33 KPa representing the 26% of the oxygen concentration value at the inlet section of the culture chamber. This latter value was verified to fairly approximate to the partial pressure of oxygen in the atmosphere.

Figure 5 shows a comparison between viabilities of C2C12 cells seeded on collagen sponges and cultured for 7 days in dynamic conditions at different medium flow rates ranging from 1 mL/min to 4.5 mL/min. A control is represented by C2C12 cells seeded onto identical collagen scaffolds at the same density and statically cultured changing media every other day.

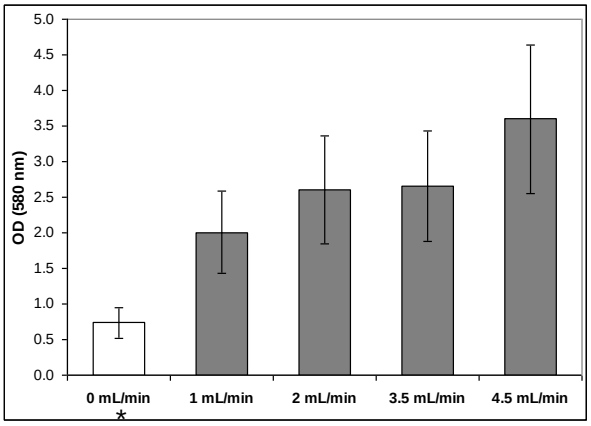

Figure 5. Influence of medium flow rate ranging between 1mL/min and 4.5mL/min on C2C12 viability measured after 7 days of continuous culture in the bioreactor. (*) The column labelled "0mL/min" is an internal control which shows the viability of C2C12 cell statically cultured in 3D collagen sponges in standard Petri dishes.

Figure 5 shows the significant differences between static and dynamic culture conditions, however there aren't noticeable differences between the various flow rates tested. Error bars are reported as 29% of mean values and represent an average of the measured errors on all the independent tests.

Considering the non-significant influence of the flow rate value, we chose to use 3.5mL/min in all following experiments. For this flow rate we calculated the mean perfusion velocity of medium through the scaffold being $330\,\mu m/\sec$ and the shear stress being $0.14\,dyne/cm^2$. Literature reports *in vivo* shear stress values ranging between 1 and 100 $dyne/cm^2$ and a threshold of 10 $dyne/cm^2$ for the in vitro loosening of intercellular interactions (45).

Comparison between static and dynamic culture of C2C12 cells (Figure 6) showed how, at the earlier time points of 1 and 4 days, there were no significant differences in mean culture viabilities. Evaluating the 7th day results, we noticed how static culture viabilities were comparable with those measured at 4 days, while dynamic conditions gave rise to a three-fold increment ($p = 4.3 \cdot 10^{-4}$). Moreover, viabilities of dynamic cultures measured at day 7 were significantly higher than the static ones at the same time point ($p = 8.3 \cdot 10^{-6}$).

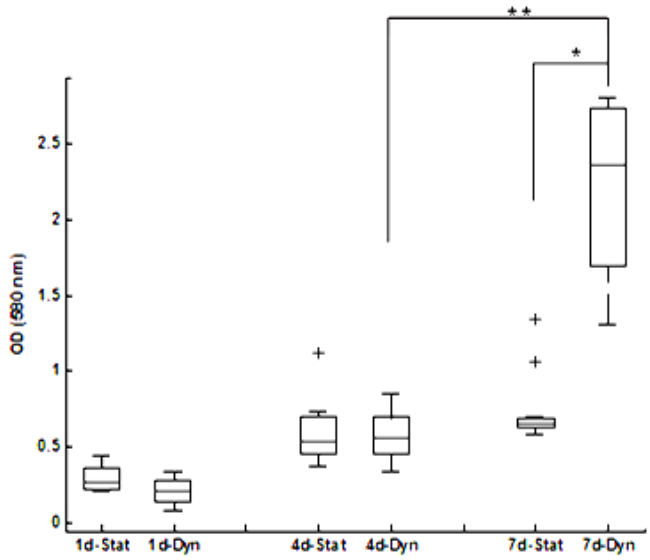

Figure 6. Box plot graph shows the comparison between C2C12 cell viabilities cultured in static (Stat) and dynamic (Dyn) conditions after 1, 4 and 7 days. Values exceeding 1.5 times the interquartile range are represented with plus signs (+) and can be considered as outlier data. * $p = 8.3 \cdot 10^{-6}$; ** $p = 4.3 \cdot 10^{-4}$.

The MTT semi-quantitative assay demonstrated a significant increment in cells viability after 7 days of dynamic culture but it was histological analysis which revealed the most interesting effect of the application of a perfusion bioreactor (Figure 7): statically cultured scaffolds resulted in a thick, high density layer of cells on the seeded surface (7a) while few or no cells at all could be seen in the core and bottom sections of the collagen sponge (7c and 7e respectively); on the contrary, histologies related to dynamic culture showed an uniform, high density cells distribution in the sequence of pictures covering the entire three-dimensional structure of the scaffold. Last, microscope observation of the culture medium performed after scaffold removal, proved that no cells detached during perfusion.

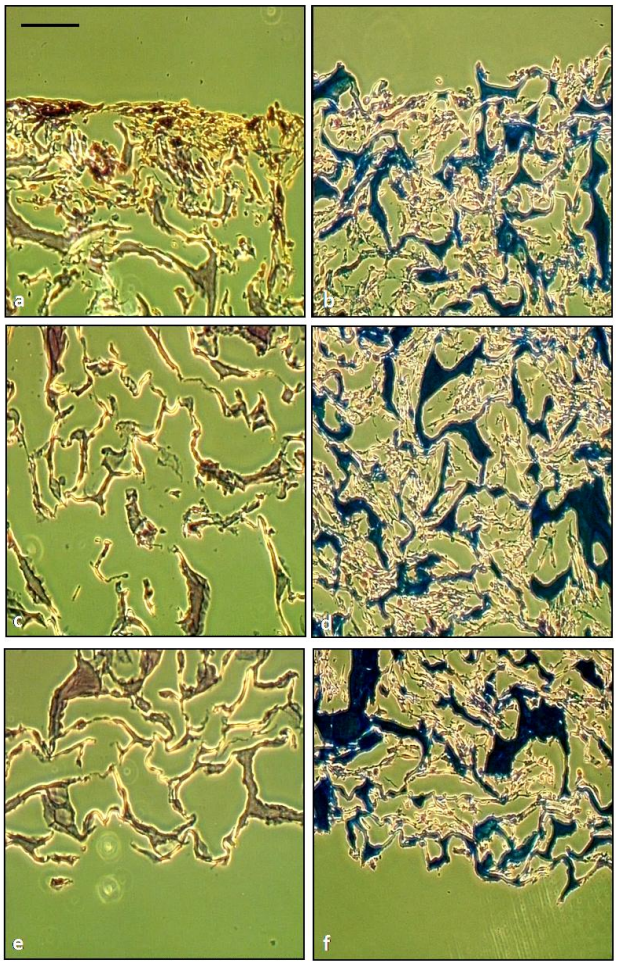

Figure 7. Histology on 7μm thick cross sections of collagen sponges cultured with C2C12 cells stained with Masson's trichrome. The collagen matrix is stained blue, the nuclei are stained black and the cytoplasm is stained red. Left column (a; c; e) refers to a static control culture while right column (b; d; f) refers to a 7 days dynamic culture at a flow rate of 3.5mL/min. Picture a and b represent the seeded surface; c and d the central volume of the sponge; e and f the surface opposite to initial seeding. Magnification x100. Scale bar = 200 μm.

Our experiments on C2C12 cells allowed individuation of the optimal operating conditions in terms of seeding protocol, imposed medium flow rate and culture time points; with these data we undertook a preliminary study on satellite cells.

Figure 8 represents box plots showing the comparison between viabilities of satellite cells cultured in static and dynamic conditions using a medium flow rate of 3.5mL/min evaluated after 7 days of culture.

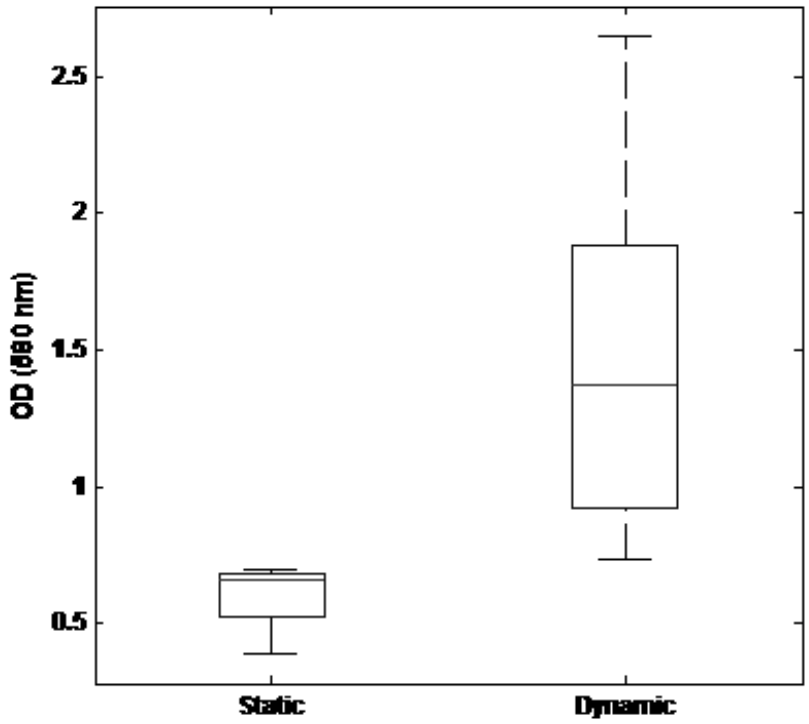

Figure 8. Box plot graph shows the comparison between viabilities of satellite stem cell cultured in static and dynamic conditions (flow rate of 3.5mL/min) after 7 days ($p<0.06$).

When cultured in our bioreactor, satellite cells expressed a 2.4 fold increase in their metabolic activity. Dynamic culture resulted again in a 3D construct with improved characteristics in terms of uniformity of cellular density (Figure 9).

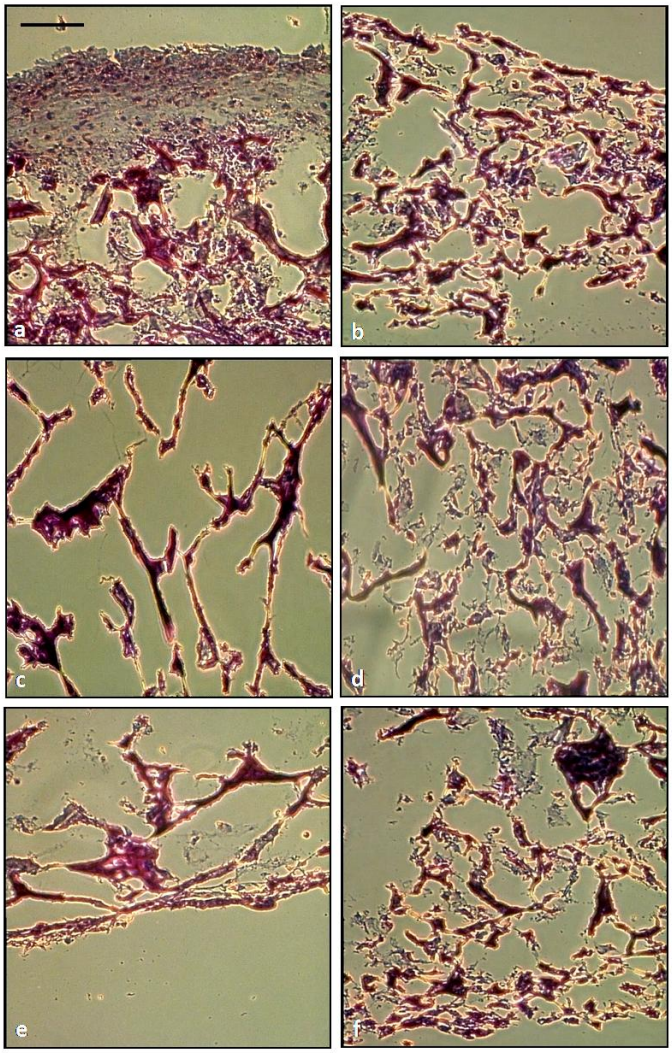

Figure 9. Histology on 7μm thick transversal sections of collagen sponges cultured with satellite stem cells in static (a; c; e) and dynamic (b; d; f) conditions stained with Hematoxylin-Eosin. Nuclei are stained "blue" with hematoxylin. Cytoplasm, connective, and all other tissues are counterstained "red" with eosin. Pictures a and b represents the seeded surface; c and d the central volume of the sponge; e and f the surface opposite to initial seeding. Magnification x100. Scale bar 200 μm.

C.4 Discussion

The development of a 3D cellular construct engineered starting from stem cell cultures becomes necessary in sight of possible future clinical application. The homogeneity of a 3D construct, in terms of cell density and cell phenotype, is fundamental to improve the success of skeletal muscle grafts. Focused on that aim, we recognize the importance of properly choosing all the materials involved in cell culture, of optimizing the seeding protocols and, last but not least, finding and

pointing the optimal values of the operating variable conditions at which the culture should be lead.

In this study we tested the properties of collagen scaffold: a natural and biocompatible material, relatively simple to process and with a high potential in sight of an in vivo utilization. Collagen scaffolds were confirmed to be appropriate for supporting 3D cultures because of its their diameter, high porosity and permeability(46).

Collagen proved to be a good support for cell growth also in granting a solid structure not suffering from the prolonged permanence under total perfusion culture conditions. The high material porosity did not hinder the flow of nutrients and gases and promoted cell diffusion thus resulting in a complete cellularization of the 3D sponge when cultured in dynamic conditions.

The cell seeding protocol has been optimized, in terms of timing and volume of medium, which yields an initially uniform cell distribution over the entire scaffold surface and reduces cell losses during all the operations up to the bioreactor start up. We showed that all of the materials used to fabricate the bioreactor apparatus responded to our needs of biocompatibility, reliability, resistance to repeated high thermal stress due to autoclave sterilizations (thus avoiding employment of potentially toxic chemicals for sterilization) and prolonged usage.

Profiles of oxygen concentration variation from the inlet to the outlet sections of the bioreactor, normalized over the inlet concentration were calculated from Eq (11) and (12) (Figure 4). This graph confirms that the flow rates used in this study ensured physiological oxygen concentration in the outlet scaffold section for cell densities up to an approximated value of 108cell/cm3. Considering this finding and the low value of shear stress evaluated with equation (3), results reported in Figure 5 are not surprising. The flow rates tested are in a range that does not allow observation of significative differences in viability.

A relevant increase in viability of dynamically cultured cells compared with static control is noticeable after 7 days of culture while at earlier time points medium perfusion does not seem to have the same effect. This result can evidence of an

initial "adaptative phase" which could be needed for cells cultured under dynamic conditions to adhere on the scaffold and start to proliferate.

We have demonstrated that dynamic conditions resulted in improved characteristics of the final cellularized construct not only in terms of cellular viability, but also of density and spatial distribution through the whole 3D scaffold. Histological analyses (Figure 7) proved that perfusion can promote cell diffusion through the scaffold layers thus allowing a complete coverage of the sponge volume. Static culture, on the contrary, resulted in the formation of a thick layer of cells located on the seeding surface which constitutes a barrier hindering the further migration of proliferating cells inside the 3D construct. In addition, diffusion alone cannot fulfill nutrient demands of the growing cells without cooperation of the convective flow deriving from medium perfusion. We thus unequivocally demonstrated how dynamic culture assured a more efficient mass transfer leading to cellular constructs with improved properties. In our previous work (47), we have shown through a mathematical modeling of 3D cell cultures in perfusion bioreactors the fundamental role of metabolite mass transport on cell growth and proliferation.

Finally, preliminary experiments demonstrated how our culture system proved to be reliable in granting suitable conditions for the survival and proliferation even of a primary cell culture such as that of satellite cells. Nevertheless, in underlining the increased variability of the resulting data we note that operative conditions tested with the C2C12 cell line does not necessarily correspond to an optimum for satellite cells. Consequently, a further step will be a deeper insight in monitoring satellite cells' behavior under dynamic culture conditions and their response in terms of viability following variations in culture parameters such as medium flow rate and culture time point. Our 3D collagen scaffolds recreated a microenvironment which was suitable for satellite cells, promoting adhesion, maintaining viability and proliferation. Dynamic culture served the purpose of increasing viability and giving rise to a uniformly and densely cellularized 3D construct. A recent work confirms how transplantation of muscle precursor cells seeded on a scaffold improves muscle regeneration more than direct cell injection (48). In addition, the efficacy of other cell therapy approaches employing different cell sources and interacting factors(49,

50) could be improved and increased by the usage of 3D scaffolds and the dynamic perfusion conditions developed in bioreactors. Interesting future directions would involve the use of oriented scaffolds in sight of the obtainment of an aligned structure and a network of microchannels mimicking the vascular network existing in vivo, an essential feature for a capillary delivery of metabolites and for a more efficient waste removal. Combining all these fundamental issues highlights how the employment of dynamically cultured 3D scaffolds for in vivo transplantation seeded with muscle precursor cells could highly increase and help natural host tissue repair and regeneration.

C.5 Acknowledgement

We would like to thank Dr. G. Abatangelo and Dr. B. Zavan for their collaboration in histological analyses and MIUR, University of Padova and Fondazione Città della Speranza for financial support.

C.6 References

1 Bach AD, Beier JP, Stern-Staeter J and Horch RE. Skeletal muscle tissue engineering. Journal of Cell. Mol. Med 2004; 8(4):413-422

2 Partridge TA. Invited review: myoblast transfer: a possible therapy for inherited myopathies? Muscle Nerve 1991; 14(3):197-212

3 Huard J LY, Fu F. H. Muscle Injuries and Repair: Current Trends in Research. J. Bone Joint Surg. Am. 2002; 84(822-832

4 Carrier RL, Papadaki M, Rupnick M, Schoen FJ, Bursac N, Langer R, et al. Cardiac tissue engineering: Cell seeding, cultivation parameters, and tissue construct characterization. Biotechnology and Bioengineering 1999; 64(5):580-589

5 Okano T and Matsuda T. Muscular tissue engineering: capillary-incorporated hybrid muscular tissues in vivo tissue culture. Cell Transplantation 1998; 7(5):435-442

6 Freed LE and Vunjak-Novakovic G. Culture of organized cell communities. Advanced Drug Delivery Reviews 1998; 33(1-2):15-30

7 Hill E, Boontheekul T and Mooney D. Designing Scaffolds to Enhance Transplanted Myoblast Survival and Migration. Tissue Engineering 2006; 12(5):1295-1304

8 De Coppi P, Delo D, Farrugia L, Udompanyanan K, Yoo JJ, Nomi M, et al. Angiogenic Gene-Modified Muscle Cells for Enhancement of Tissue Formation. Tissue Engineering 2005; 11(7-8):1034-1044

9 Nomi M, Atala A, De Coppi P and Soker S. Principals of neovascularization for tissue engineering. Molecular Aspects of Medicine 2002; 23(6):463-483
10 Lewis MC, MacArthur BD, Malda J, Pettet G and Please CP. Heterogeneous proliferation within engineered cartilaginous tissue: the role of oxygen tension. Biotechnology and Bioengineering 2005; 91(5):607-615
11 Figallo E, Flaibani M, Zavan B, Abatangelo G and Elvassore N. Micropatterned Biopolymer 3D Scaffold for Static and Dynamic Culture of Human Fibroblasts. Biotechnol Prog 2007; 23(1):210-6
12 Cha JM, Park S-N, Park G-O, Kim JK and Suh H. Construction of Functional Soft Tissues From Premodulated Smooth Muscle Cells Using a Bioreactor System. Artificial Organs 2006; 30(9):704-707
13 Marolt D, Augst A, Freed LE, Vepari C, Fajardo R, Patel N, et al. Bone and cartilage tissue constructs grown using human bone marrow stromal cells, silk scaffolds and rotating bioreactors. Biomaterials 2006; 27(36):6138-6149
14 Papadaki M, Bursac N, Langer R, Merok J, Vunjak-Novakovic G and Freed LE. Tissue engineering of functional cardiac muscle: molecular, structural, and electrophysiological studies. Am J Physiol Heart Circ Physiol 2001; 280(1):H168-178
15 Radisic M, Park H, Shing H, Consil T, Schoen FJ, Langer R, et al. Functional assembly of engineered myocardium by electrical stimulation of cardiac myocytes cultured on scaffolds. Proc Natl Acad Sci U S A 2004; 101(52):18129-34
16 Kuo CK, Li W-J, Mauck RL and Tuan RS. Cartilage tissue engineering: its potential and uses. Current Opinion in Rheumatology 2006; 18(1):64-73
17 Mansbridge J. Commercial considerations in tissue engineering. Journal of Anatomy 2006; 209(4):527-532
18 Freed LE, Hollander AP, Martin I, Barry JR, Langer R and Vunjak-Novakovic G. Chondrogenesis in a Cell-Polymer-Bioreactor System. Experimental Cell Research 1998; 240(1):58-65
19 Gooch KJ, Blunk T, Courter DL, Sieminski AL, Bursac PM, Vunjak-Novakovic G, et al. IGF-I and Mechanical Environment Interact to Modulate Engineered Cartilage Development. Biochemical and Biophysical Research Communications 2001; 286(5):909-915
20 Vunjak-Novakovic G, Obradovic B, Martin I, Bursac PM, Langer R and Freed LE. Dynamic Cell Seeding of Polymer Scaffolds for Cartilage Tissue Engineering. Biotechnol. Prog. 1998; 14(2):193-202
21 Bancroft GN, Sikavitsas VI and Mikos AG. Technical Note: Design of a Flow Perfusion Bioreactor System for Bone Tissue-Engineering Applications. Tissue Engineering 2003; 9(3):549-554
22 Cartmell SH, Porter BD, Garcia AJ and Guldberg RE. Effects of Medium Perfusion Rate on Cell-Seeded Three-Dimensional Bone Constructs in Vitro. Tissue Engineering 2003; 9(6):1197-1203
23 Bilodeau K and Mantovani D. Bioreactors for Tissue Engineering: Focus on Mechanical Constraints. A Comparative Review. Tissue Engineering 2006; 12(8):2367-2383
24 Torgan C, Burge S, Collinsworth A, Truskey G and Kraus W. Differentiation of mammalian skeletal muscle cells cultured on microcarrier beads in a rotating cell culture system. Med Biol Eng Comput 2000; 38(5):583-590
25 Carrier R, Rupnick M, Langer R, Schoen F, Freed L and Vunjak-Novakovic G. Perfusion Improves Tissue Architecture of Engineered Cardiac Muscle. Tissue Engineering 2002; 8(2):175-188

26 Cha J, Park S-N, Park G-O, Kim J and Suh H. Construction of Functional Soft Tissues From Premodulated Smooth Muscle Cells Using a Bioreactor System. Artificial Organs 2006; 30(9):704-707

27 Asakura A, Komaki M and Rudnicki M. Muscle satellite cells are multipotential stem cells that exhibit myogenic, osteogenic, and adipogenic differentiation. Differentiation 2001; 68(4-5):245-253

28 Conconi MT, Coppi PD, Bellini S, Zara G, Sabatti M, Marzaro M, et al. Homologous muscle acellular matrix seeded with autologous myoblasts as a tissue-engineering approach to abdominal wall-defect repair. Biomaterials 2005; 26(15):2567-2574

29 De Coppi P, Bellini S, Conconi MT, Sabatti M, Simonato E, Gamba PG, et al. Myoblast-Acellular Skeletal Muscle Matrix Constructs Guarantee a Long-Term Repair of Experimental Full-Thickness Abdominal Wall Defects. Tissue Engineering 2006; 12(7):1929-1936

30 Partridge TA. Cells that participate in regeneration of skeletal muscle. Gene Therapy 2002; 9(11):752-753

31 Boldrin L, Elvassore N, Malerba A, Flaibani M, Cimetta E, Piccoli M, et al. Satellite Cells Delivered by Micro-Patterned Scaffolds: A New Strategy for Cell Transplantation in Muscle Diseases. Tissue Eng 2006;

32 Portner R, Nagel-Heyer S, Goepfert C, Adamietz P and Meenen N. Bioreactor Design for Tissue Engineering. Journal of Bioscience and Bioengineering 2005; 100(3):235-245

33 Bird RB, Stewart WE and Lightfoot EN. Transport Phenomena. Second John Wiley & Sons, inc.; 2002

34 Bacabac RG, Smit T-H, Cowin SC, Loon JJWAV, Nieuwstadt FTM, Heethaar R, et al. Dynamic shear stress in parallel-plate flow chambers. Journal of Biomechanics 2005; 38(159-167

35 Gosgnach W, Messika-Zeitoun D, Gonzalez W, Philipe M and Michel J-B. Shear stress induces iNOS expression in cultured smooth muscle cells: role of oxidative stress. Am J Physiol Cell Physiol 2000; 279(6):C1880-1888

36 Fournier RL. Basic Transport Phenomena in Biomedical Engineering. Lillington, NC: Edwaed Brothers; 1998

37 Chow DC, Wenning LA, Miller WM and Papoutsakis ET. Modeling pO(2) distributions in the bone marrow hematopoietic compartment. II. Modified Kroghian models. Biophys J. 2001; 81(2):685-96

38 Salathe EP and Gorman AD. Modelling oxygen concentration in skeletal muscle. Mathematical computing modelling 1997; 26(4

39 Richardson RS. Oxygen transport and utilization: an integration of the muscle system. Advances in physiology education 2003; 27(4):183-191

40 Perry RH and Green DW. Perry's chemical engineers' handbook. Seventh Mc Graw-Hill International; 1998

41 Brandrup J, Immergat EH and Grulke EA. Polymer handbook. IV Wiley Interscience publication; 1999

42 Cussler EL. Diffusion: Mass Transfer in Fluid System. Second Cambridge University Press; 1997

43 Zhao F, Pathi P, Grayson W, Xing Q, Locke BR and Ma T. Effects of Oxygen Transport on 3-D Human Mesenchymal Stem Cell Metabolic Activity in Perfusion and Static Cultures: Experiments and Mathematical Model. Biotechnol. Prog. 2005; 21(4):1269-1280

44 Sen A, Kallos MS and Behie LA. Expansion of mammalian neural stem cells in bioreactors: effect of power input and medium viscosity. Developmental Brain Research 2002; 134(103-113
45 Reutelingsperger CPM, Van Gool RGJ, Heijnen V, Frederik P and T. L. The rotating disc as a device to study the adhesive properties of endothelial cells under differential shear stresses. J. Matr Sci.: Mater. In Medicine 1993; 5(6-7):361-367
46 Desai TA. Micro- and nanoscale structures for tissue engineering constructs. Medical Engineering & Physics 2000; 22(9):595-606
47 Coletti F, Macchietto S and Elvassore N. Mathematical modeling of three-dimensional cell cultures in perfusion bioreactors. Industrial & Engineering Chemistry Research 2006; 45(24):8158-8169
48 Hill E, Boontheekul T and Mooney D. Regulating activation of transplanted cells controls tissue regeneration. Proc Natl Acad Sci U S A 2006; 103(8):2494-2499
49 Deasy B M LYaHJ. Tissue engineering with muscle-derived stem cells. Current Opinion in Biotechnology 2004; 15(419–423
50 Urish K KY, Huard J. Initial failure in myoblast transplantation therapy has led the way toward the isolation of muscle stem cells: potential for tissue regeneration. Current Topics in Developmental Biology 2005; 68(263-280

Appendix D

Effect of electrode material on ROS expression of human embryonic stem cell

Elena Serena[1,2], Elisa Figallo[1,3], Christopher Cannizzaro[3], Sharon Gerecht-Nir[3], Nina Tandon[2], Nicola Elvassore[1], Gordana Vunjak-Novakovic[2]*

[1]Department of Chemical Engineering, University of Padua, Via Marzolo, 9 Padua, Italy

[2]Department of Biomedical Engineering, Columbia University, New York, USA

[3]Division of Health Sciences and Technology and Bioengineering departments, Massachusetts Institute of Technology, Cambridge, USA

[*]Corresponding author, gv2131@columbia.edu

To be submitted

Keywords: human embryonic stem cells; human embryoid body; electrical field; reactive oxygen species; cardiac differentiation.

Abstract

The emerging alternatives to traditional therapies for cardiac diseases, cardiac tissue engineering and cell transplantation, require a cell source with great proliferation and differentiation potential, such as human embryonic stem cells (hESCs). Because reactive oxygen species (ROS) have been implicated in the regulation of mouse embryonic stem cell differentiation toward cardiac lineage, in this study, we exposed embryoid bodies derived from human embryonic stem cells to an exogenous electric field. We applied fields of 1 V/mm in order to increase the generation of ROS and tested for consequent cardiac differentiation. In this study, we varied electrode material (stainless steel, titanium and titanium nitride), age of EB (4 and 8 days) and length of stimulus (1 and 90 s). We characterized electrode materials by electrochemical impedance spectroscopy (EIS) and analysis of currents. The ROS generation showed a high dependence on electrode material, age of EB and length of stimulus. In particular, stainless steel yielded the best results, with a higher response for 90s stimulation. The magnitude of this increase was correlated with EB age (either 4- and 8-days old) with a maximum occurring at 4 days. A comparable increase in the generation of ROS was achieved by an incubation for 15 minutes with 1 nM H2O2. Cardiac differentiation was verified by detection of the specific cardiac marker Troponin T, showing a remarkable sarcomeric organization, and spontaneous contractions. These results imply that electrical stimulation could play an important role in hESC cardiac differentiation, through the intracellular generation of ROS.

D.1 Introduction

The true utility of human embryonic stem cells (hESC) will only be realized when they may be safely differentiated into cell lines of clinical importance [1-3]. Heart disease and stroke, the principal components of cardiovascular disease, are the first and the third leading cause of death in the U.S., accounting for nearly 40% of all deaths, more than all cancer combined [4]. Because cardiomyocytes are unable to

regenerate in the adult heart, cell-based therapy of transplantation provides a potential alternative approach to replace damaged myocardial tissue and restore cardiac function. A major limitation toward this goal is the lack of donor cells: although human embryonic stem cells have enormous potential as a source of therapeutic tissues (including cardiovascular cells), the regulatory elements mediating their differentiation to cardiomyocytes are largely unknown [5].

Numerous studies have demonstrated the importance of chemical and/or mechanical stimuli in directing stem cell differentiation [6-9]. And although the presence of endogenous electrical fields and currents in the developing vertebrate embryo has been widely documented, the role of electrical fields and currents during tissue development and stem cell differentiation is unclear. Endogenous electromagnetic fields (EF) are present in developing and regenerating tissues, usually in the extracellular space, but sometimes within the cytoplasm of a single cell or a group of cells, and they range in strength from a few to hundreds of mV/mm [10, 11]. The magnitude of these electrical fields can directly guide cell movement and growth [12]. They may also generate chemical gradients of charged macromolecules [13] that can be present for hours, days, or even weeks during both development and regeneration [14]. At the site of an injured epithelium a substantial electrical field is instantly generated and may extend over many cell diameters and persist for hours [15, 16]. Combined with diffusible chemical gradients, electric fields lead to the polarization and the formation of spatial patterns in developing embryo [17-19] creating directional signals necessary for the proper placement of the components of the organism. In the laboratory, exogenous electrical fields have been shown to influence cell behavior and differentiation [20]. Several studies have reported galvanotaxis in a variety of cells cultured in vitro after stimulation with a constant direct current (DC) field comparable with those detected in vivo [21]. The cell responds to an externally applied electric field with specific mechanism, including the passive and active intracellular influx of ions, such as calcium and sodium [22, 23], or the localization of lipid and epithelial growth factor (EGF) receptors in the membrane [13]. The equilibrium between these processes determines the reorganization of the cytoskeleton and the migration towards one of

the two electrodes. It has been shown that the exposure to electric fields promotes mouse embryonic stem cell (mESC) cardiomyogenic [24] and angiogenic [25, 26] differentiation and mouse N1E-115 neuroblastoma neuronal [27] and MG63 osteogenic [28, 29] differentiation. However, the course of action of electrical stimulation on the activation of differentiative pathways are still unclear. One possible mechanism involves the generation of reactive oxygen species (ROS) within the cell [24, 30]. Sauer and colleagues demonstrated that stimulation with an exogenous electric field increases intracellular ROS production in mouse EBs [24]. ROS are highly reactive molecules generated during the normal metabolism of oxygen by NADPH oxidases or as side products of several enzymatic systems (e.g., cyclooxygenases, nitric oxide (NO) synthases, mitochondrial cytochromes). Although excessive concentration of ROS, such as superoxide anions (O2-) and hydrogen peroxide (H2O2), is considered destructive and results in inhibition of gene expression [31, 32], small amounts of ROS function as intracellular second messengers and activate signaling cascades involved in growth and differentiation of many cell types [33-36]. ROS are known to be involved and regulate cardiogenesis [37]. When cardiac cells are stimulated by cytokines [38], growth factors, hormones, even mechanical stress [39], they elicit a small oxidative burst and generate low concentrations of ROS. During myocardial infarction, cardiac cells generate large amounts of free radicals and ROS, which are involved in the signaling and activation of the intrinsic repair mechanisms of the damaged myocardium [40, 41]. Sauer and colleagues demonstrated that ROS activate the mitogenactivated protein kinase (MAPK) pathways in mouse EBs [35], enhancing the angiogenesis through the activation of ERK1,2 and JNK and the cardiomyogenesis through the phosphorylation of ERK1,2, JNK and p38 [42-44]. An NADPH oxidase-like enzyme is involved in the ROS-related cardiogenesis during mESC differentiation [5].

These studies introduce the applicability of electrical stimulation as a possible technique to control hESC differentiation and to increase their differentiation towards the cardiac lineage. In this study, we thus investigate, for the first time to our knowledge, the effects of an exogenous electric field on hESC.

In order to control cell behavior through the efficacious application of electric fields, it is necessary to characterize the stimulation at the electrical level and understand its mechanisms of action at the biological level. To enable an efficacious in vitro stimulation it is necessary to control the intensity, duration and frequency of the stimulus on the cell. If the stimulation is given applying a constant voltage between the working and counter electrodes, for example, the geometry of the system and the properties of the electrode determine the duration of the stimulation. When a couple of electrodes are introduced in an electrolyte and the potential across the electrodes is set, the ions in the medium will be redistributed by the electrostatic forces creating, in a very narrow volume at the interface called electrical double layer, a plane of charge that shields the charges on the electrode surface. The movement of ions determines the transient presence of current in the system. At the steady state, in absence of chemical reactions, the potential drop is concentrated in the double layer and the current in the system is absent. If a cell is placed between the electrodes in a steady condition, it will not be affected by any electrical stimulation because the electric field across it will be negligible [45]. In the presence of reactions, the equilibrium condition is characterized by a small current in the system due to the charge-transfer on the electrode-electrolyte interface [46]. The time necessary to reach a steady state condition is dependent on the properties of the electrolyte and the amount of charge accumulated on the electrode surface. The amount of charge accumulated on the electrode surface is in turn dependant on the voltage applied between the electrodes and the properties of the electrode material, such as its surface area, capacitance, and chemical properties. For biological applications, additional requirements are the electrode material to be biocompatible and to not alter the biochemical properties of the culture medium. Herein lies the necessity to characterize accurately the system before performing biological experiments.

In this study the electrical properties of electrodes of varying material and identical geometry have been evaluated through electrochemical impedance spectroscopy (EIS). The electrode-electrolyte interface has been modeled by Randles cell equivalent circuit, evaluating capacitance and polarization resistance of titanium,

titanium nitride and stainless steel electrodes. The evolution of the stimulation has been monitored measuring the current in the system. The effectiveness of the electrode material has been evaluated through the expression of intracellular ROS in hESC. Different stages of EB differentiation have been investigated to examine the possibility that the EB differentiation stage could influence the intracellular production of ROS,. The percentage of beating EBs in presence of electrical stimulation has also been compared with the basal condition in absence of stimulation.

D.2 Material and Methods

D.2.1 Human Embryonic Stem Cells culture

Undifferentiating hESCs (H13 line, National Stem Cell Bank, Madison, WI) were grown on mouse embryonic fibroblasts (MEF, Chemicon) inactivated with mitomycin C (Sigma-Aldrich) in growth medium consisting of 80% KnockOut DMEM (Gibco), supplemented with 20% KnockOut Serum Replacement (Invitrogen Corporation, Carlsbad, CA), 4 ng/ml basic Fibroblast Growth Factor (Invitrogen Corporation, Carlsbad, CA), 1 mM L-glutamine (Gibco), 0.1 mM □–mercaptoethanol (Gibco), 1% non-essential amino acid stock (Invitrogen Corporation, Carlsbad, CA). hESCs were passaged to new feeder using 1mg/ml type IV collagenase (Invitrogen Corporation, Carlsbad, CA). To induce the formation of human embryoid bodies (EBs), the undifferentiated hESCs were treated with 1 mg/mL collagenase (Gibco), and then transferred to low attachment plates containing EB medium: 80% knockout- Dulbecco´s modified Eagle medium (Gibco Invitrogen Co.) supplemented with 20% defined fetal bovine serum (Hyclone), 1mM L-glutamine, and 1% nonessential amino acid stock (Gibco). Human EBs were cultured at 37 ºC, and 5% CO2 in a humidified atmosphere, with changes of media every 3 days. In order to check the influence of electrical stimulation in cardiac differentiation, 4 and 8 days-old EBs were stimulated in the electrical stimulation system described below in presence of "pulsing buffer". The

EBs were then cultured in suspension culture and three days after stimulation they were transferred to adhesion culture. Media was replaced daily.

D.2.2 Electrical stimulation system

EBs were electrically stimulated within a bioreactor built exclusively for this purpose in poly(dimethylsiloxane) (PDMS). The bioreactor is characterized by an array of 4 by 4 wells as showed in Figure 1. Electrodes of 1.3 mm of diameter can be inserted in both sides of each row.

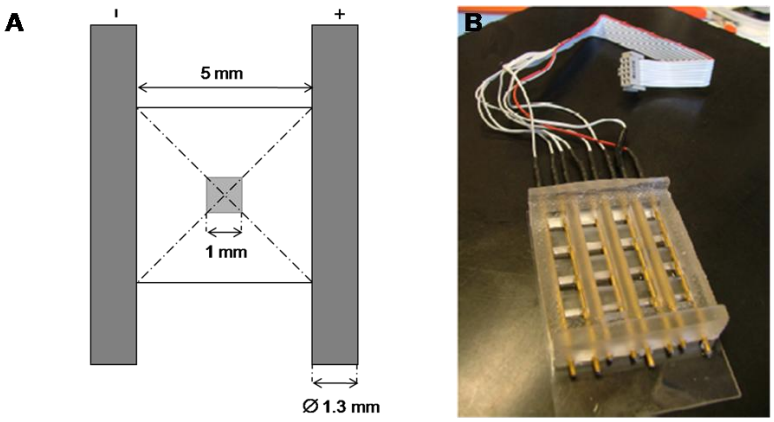

Figure 1. Bioreactor for electrical stimulation. A: Schematic representation of the bioreactor. B: Schematic representation of a single chamber of stimulation (25 mm^2). The electrodes are 5 mm spaced and the EB placed in the gray area (1 mm^2). C: Image of the bioreactor.

Independent stimulation of each row was guaranteed by PDMS insulation. The device was fabricated with stereolithographic method curing PDMS in a mold-fabricated by QuickParts, reproduced with a precision of 50 μm the original drawing. The 10:1 mixture of PDMS and initiator (Dow Corning) was poured in the mold where the electrodes were already inserted in specific holes. The inlet and outlet holes of the electrodes were designed slightly smaller of the electrodes dimension in order to seal them. The PDMS bioreactor was attached directly to a 75 × 25 mm glass slide via plasma (Plasma Cleaner PDC-002, Harrick Plasma) treatment. The optical transparency of the glass slide allowed the EB observation during the stimulation. EBs were suspended in a bioreactor well (gray area in Figure 1B) in a low ionic content "pulsing buffer" which contained 255 mM sucrose, 1 mM CaCl2, 1 mM MgCl2, and 5 mM HEPES (pH 7.2) (Sigma-Aldrich, St. Louis, MO)

and had a conductivity of 500 μS/cm. The electrodes were connected to electrical stimulator generating square-wave electric pulses (Astro-Med, Inc., West Warwick, RI). A single electrical field pulse with a field strength of 1 V/mm and duration of 1 and 90 s was applied to embryoid bodies.

D.2.3 Electrode material characterization

The electrode/electrolyte interface was characterized as previously published [47, 48] through electrochemical impedance spectroscopy (EIS) and charge injected measurements for different electrode materials. Electrodes (10 cm length x 1.3 mm diameter) were fabricated from 304 stainless steel and titanium rods (McMaster-Carr, Atlanta, GA). Some of these titanium rods were sent Eclat Industries Inc. (Levittown, NY) where they were coated with titanium nitride. EIS measurements were performed with an electrochemical interface (Solartron 1287) and a frequency response analyzer (FRA, Solartron 1250) controlled by a computer with ZPlot software (Solartron Analytical, Oak Ridge, TN). The system was set up as the equivalent circuit shown in Figure 2A and associated parameters were determined using ZView 2.5b. The Nyquist and Bode plots were calculated for each condition. The EIS spectra were acquired for the electrodes in pulsing buffer over a frequency range from 1 x 106 to 1 x 10–2 Hz with perturbation amplitude of 10 mV, 100 mV and 1 V. The current profile in the system during 90 s stimulations was measured by the potential drop profile across a 330 ohm resistor placed in series in the stimulation loop. The current value was calculated by dividing the potential measured across the resistor (with an oscilloscope) by the value of the resistor (Ohm's law). Since the current across the system was low enough to reach the 10 mV lower limit of the oscilloscope, at least 11 measurements were taken for each material.

D.2.4 Cell Viability

The cell viability after 4 days of continuous electrical stimulation was studied in EBs through live/dead assay (Molecular Probes, Eugene). The 4 days old EBs were stimulated continuously at 1 V/mm for 5ms at the frequency of 1Hz. This

fluorescence based method detects live and dead cells using 3mM calcein-AM and 3mM ethidium homodimer-1 (EthD-1) dye. The calcein-AM is retained within live cells and converted enzymatically in green fluorescent calcein (ex/em ~495 nm/~515 nm). EthD-1 enters cells with damaged membranes where it binds to nucleic acids, thereby producing a bright red fluorescence in dead cells (ex/em ~495 nm/~635 nm). Prior to and after staining, the EBs were washed with DPBS, to minimize serum esterase activity present in serum-supplemented growth medium and wash out the excess of dyes. Each well was covered by 250 μL of the combined solution of calcein-AM and ethidium. The cells were incubated for 90 minutes at room temperature. The labeled cells were analyzed using fluorescence microscope Zeiss inverted microscope.

D.2.5 H_2O_2 stimulation

4- and 8-days old EBs were treated for 15 minutes with 0.1 nM, 1 nM and 10 nM H_2O_2 (Sigma Aldrich, St. Louis, MO); in order to understand the amount of H_2O_2 giving an intracellular ROS generation comparable to the one determined by electrical stimulation.

D.2.6 Reactive Oxygen Species generation

Generation of intracellular reactive oxygen species (ROS) was measured using the fluorescent dye dichlorofluorescein diacetate (DCFH-DA) (Sigma Aldrich, St. Louis, MO). DCFH-DA was stored at -20 °C at a concentration of 10 mg/mL in methanol. DCFH-DA is a nonpolar and nonfluorescent compound that can diffuse into the cell where it is deacetylated by cellular esterases into a nonfluorescent polar derivative 2',7'-dichlorofluoroscein (DCFH) that is impermeable to cell membrane. DCFH is rapidly oxidized to the highly fluorescent dichlorofluorescein (DCF) in the presence of intracellular ROS. Embryoid bodies were incubated in Knockout medium containing 20 μM DCFH-DA in dark conditions for 30 minutes at room temperature. Embryoid bodies were then washed twice with pulsing buffer and transferred to the bioreactor. Fluorescence images were taken with excitation wavelength of 488 nm and emission wavelength of 530 nm every 20 s for three

minutes and every minute after that. The fluorescence variation was calculated by normalization of fluorescence intensity at each time point after stimulation (F) to the initial value (F_0).

D.2.7 Cardiac TroponinT immunoflourescence

Electrically stimulated and control EBs were cultured for 19 days and then fixed with 2% PFA for 7 minutes. Cardiac TroponinT primary antibody, mouse monoclonal, (NeoMarkers, USA) was diluted 1:100 in PBS–3% BSA (Sigma-Aldrich, USA) and applied for 1 hour at 37°C. Secondary antibody, Alexa Fluor 594-conjugated anti-mouse IgG (Invitrogen, Italy) was diluted 1:250 in PBS–3% BSA and applied for 45 minutes at 37°C. Cells were counterstained with DAPI and mounted in fluorescent mounting medium (DakoCytomation, Italy).

D.2.8 Statistical Analysis

Significance of each data point was determined by Anova test, where a value of $p < 0.05$ was considered significant.

D.3 Results

Bioreactor characterization

In order to evaluate the influence of different electrode materials on effectiveness of EBs stimulation, the bioreactor was characterized through electrochemical impedance spectroscopy (EIS). Fixing the type of stimulation, the current profile in the system depends on the geometry of the system and properties of electrode materials, such as effective surface area or polarization resistance. Bode and Nyquist plots, obtained by EIS analysis with a perturbation of 10 mV, are shown in Figure 2B for Stainless Steel (SS), titanium (Ti) and titanium nitride-coated (TiN) electrodes. The equivalent circuit shown in Figure 2A was used to fit the spectra and model the electrode-electrolyte interface. The interfacial capacitance and

polarization resistance were obtained by this fitting and are summarized in the table in Figure 2.

Material	Perturbation Voltage	CPE, F/cm² (% error)	Rp, Ω/cm² (% error)	η (% error)
Stainless steel	10 mV	3.17E-06 (0.28%)	1.68E+06 (2.50%)	0.71 (0.71%)
	100 mV	6.28E-06 (0.81%)	8.76E+05 (10.00%)	0.66 (0.36%)
	1000 mV	3.02E-05 (4.61%)	1.87E+04 (10.26%)	0.53 (3.33%)
Titanium nitride	10 mV	3.27E-06 (0.63%)	6.86E+06 (10.00%)	0.77 (1.85%)
	100 mV	4.51E-06 (0.64%)	3.18E+06 (18.40%)	0.76 (0.29%)
	1000 mV	1.23E-05 (1.04%)	1.78E+05 (5.42%)	0.73 (0.57%)
Titanium	10 mV	1.61E-06 (0.53%)	4.78E+06 (7.28%)	0.80 (0.65%)
	100 mV	1.60E-06 (0.66%)	4.05E+06 (7.28%)	0.79 (0.29%)
	1000 mV	3.02E-05 (4.61%)	1.87E+04 (10.26%)	0.53 (3.33%)

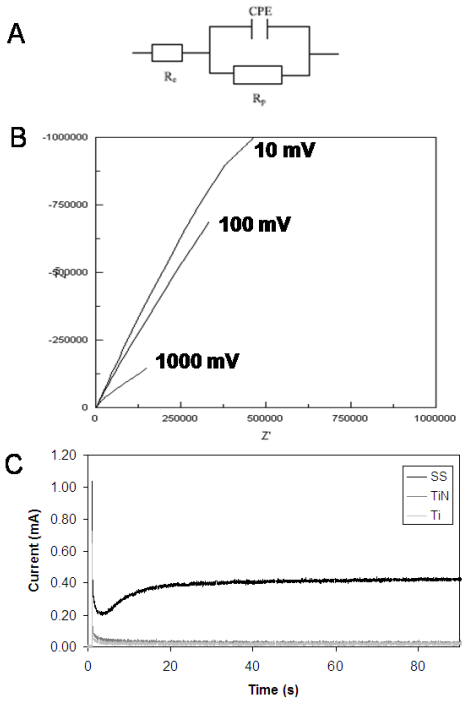

Figure 2. In the table. Constant phase element (CPE), polarization resistance (Rp) and capacitance dispersion (h) calculated fitting the equivalent circuit of the electrode/electrolyte systems (A), where Re is the resistance of the electrolyte. B: Nyquist plot of stainless steel electrodes at increasing perturbation voltage. C: Effect of electrode material on effectiveness of electrical stimulation (10 V/cm 90 s). Current vs time profile in the system during stimulation with stainless steel, titanium nitride and titanium electrodes.

The tested electrodes showed similar interfacial capacitance of the order of 10-6 F/cm² whereas the polarization resistance (Rp) for titanium and titanium nitride is an order of magnitude higher than for the stainless steel. This more accentuated curvature in the Nyquist plot gives a visual confirmation of this calculation.

Increasing the amplitude of the stimulus up to 1 V, the capacitance increases whereas the resistance to the reactions becomes up to two orders of magnitude lower. These results agree with the changing on the Nyquist plot shape that becomes more and more curved, as shown in Figure 2B.

The amount of charge injected was calculated for stimulations of 50 ms, 1 s and 90 s. The current-time plots show an initial increasing of the current (and thus the potential applied to the cells) followed by a rapid decrease due to the polarization of the medium and the shielding of charges on the electrode, as shown in Figure 2C.

However the current reaches values close to zero only for titanium and titanium nitride, whereas for stainless steel electrodes the reactions that occur in the electrode-electrolyte interface keep the potential higher up to saturation in around 5s.

Cell viability and ROS expression

Exogenous electrical stimulation, either as single pulse or continuous stimulation, didn't compromise the variability of the embryoid bodies, as shown by the live and dead assay performed 2 hours after a single pulse (Fig. 3A) and after 4 days of stimulation (Fig. 3B-C).

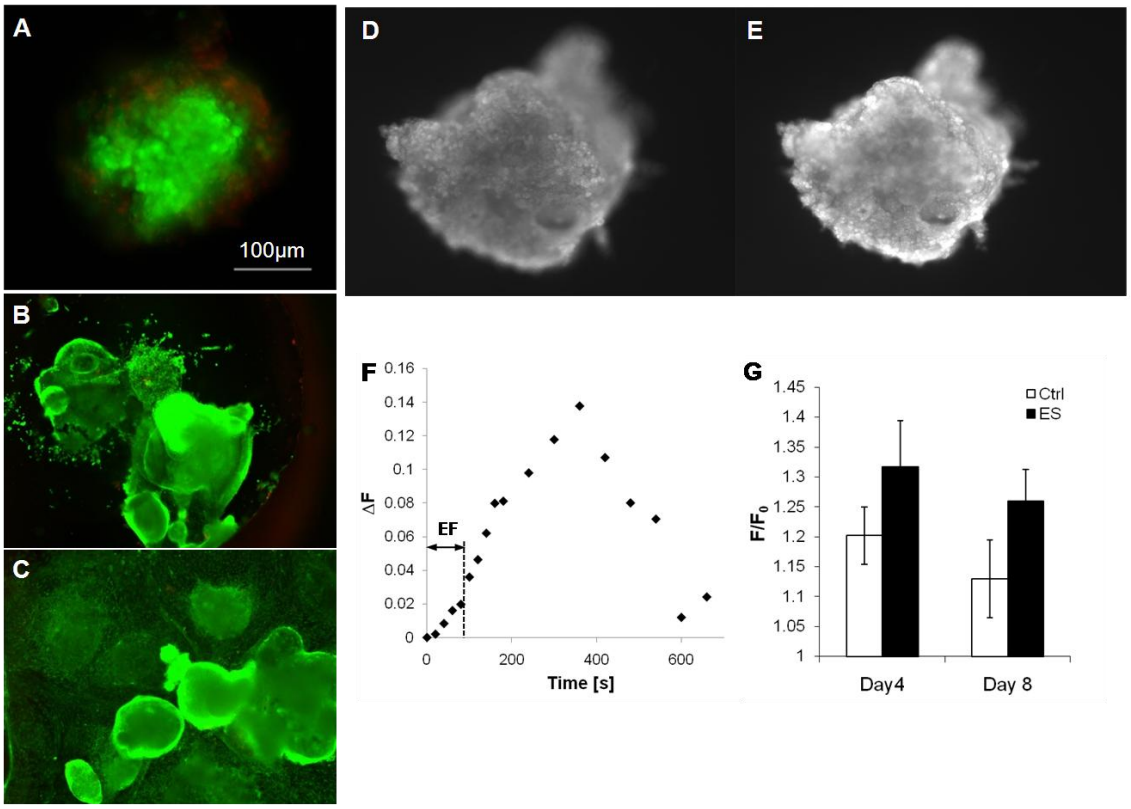

Figure 3. Effect of electrical stimulation on cell viability and reactive oxygen species (ROS) generation. Fig (A-C): Live/Dead assay, living cells are green, while dead cells are red. (A) EB in suspension culture 2 hours after a single pulse of electrical stimulation, (B) non stimulated adherent EBs, (C) adherent EBs after 4 days of continuous stimulation. Fig. D-G: Analysis of intracellular ROS generation through DCFH-DA. (D-E): Fluorescence image of EB loaded with DCF before (D) and 10 minutes after (E) electrical stimulations (90s, SS). F: An example of time course of ROS generation (DCF intensity). ΔF is the point difference in fluorescence of a stimulated and a control EB. (G) ROS generation on control (Ctrl) EB and electrically stimulated EB (ES) (90s, SS), 4- and 8-days old. The fluorescence intensity after 5 minutes of electrical stimulation, F was normalized by the intensity at time 0, F_0.

As shown in Figure 3A-C, the presence of dead cells is negligible in stimulated and unstimulated EBs. Figure 3D and E are examples of DCF fluorescence intensity of an EB before (Fig. 3D) and after (Fig. 3E) the exogenous electrical stimulation. We verified that the maximum increase of fluorescence, compared to a control EB, is reached 5 minutes after the stimulus, as shown in figure 3F. It's in fact known that the DCFH-DA, which have traditionally been used for detecting ROS, and in general the dihydro-compounds used for these measurements, are highly photosensitive and they tend to be autoxidized to produce a large background fluorescence, thus an increase of fluorescence is detected as well in control EB[49]. The ratio between the average of fluorescence intensity at the beginning (F0) and after 5 minutes (F) gives the amount of reactive oxygen species produced in the EB by the electrical stimulation, as summarized in Figure 3G.

Significant changes in ROS expression were observed with increasing durations of stimulation from 1s to 90s, as shown in Fig 4A.

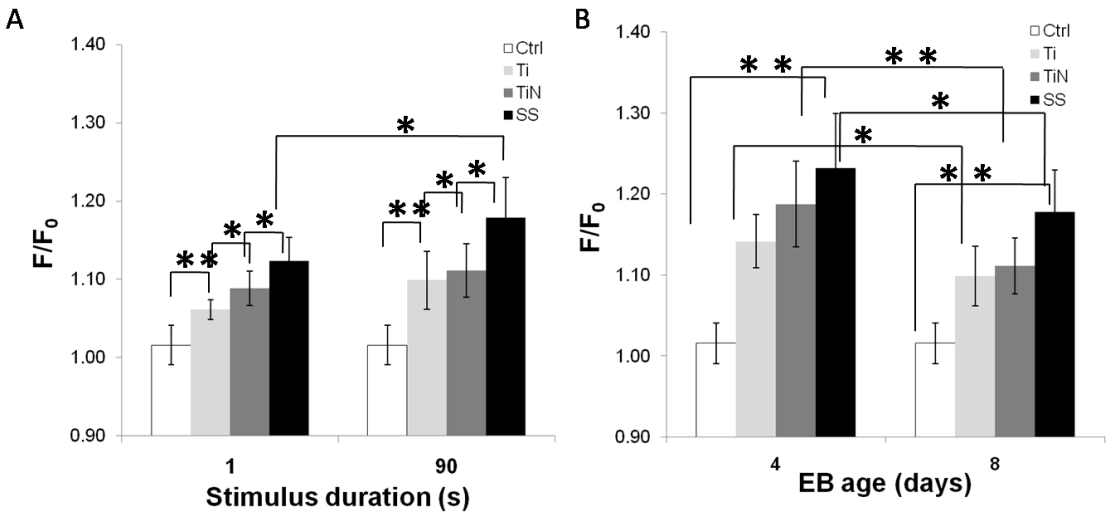

Figure 4. Generation of ROS in EB after electrical stimulation with different electrode materials. A: Effect of duration of electrical stimulation on ROS production on 6-day-old EB; B: Effect of EBs age on ROS generation. About 10 EBs in each of three independent experiments were used for the determination of each data point. * $p<0.01$; ** $p<0.05$.

All the electrodes used induced a significant increase in ROS production after electrical stimulation, if compared to control, with both 1 and 90 s duration. In the case of titanium and titanium nitride ROS generation was not significantly different when comparing stimuli of 1 and 90s duration.. On the contrary, stainless steel

electrodes with a stimulus of 90s duration induce an increase in ROS production statistically different in comparison to a stimulus of 1 s. This increase suggests the dependence of the ROS production on the duration of the stimulation. The reactions on stainless steel electrodes provide a higher electric field when compared to other electrode materials for all 90 s stimulation, increasing the final expression of ROS.

Since human embryonic stem cells have been shown to begin differentiation toward cardiac lineage 4 days after EBs formation [50] and they may show different reactivity to exogenous electric field at different stage of the development, it seemed interesting to analyze the ROS generation after electrical stimulation of 1 V/mm for 90 s of 4- and 8 day-old embryoid bodies. As shown in Figure 4B, the increase in ROS production after electrical stimulation occurs in both 4 and 8 day-old EBs and with all the types of electrodes (as compared to control EBs). Furthermore, this increase showed the same trend observed in 6 day-old EBs reported in figure 4.A. At day 8, electrical stimulation generated a lower increase in ROS, when compared to 4 day-old EBs.

With the aim of comparing the effects of electrical stimulation (with stainless steel electrodes) with a biochemical stimulus and to determine the amount of ROS produced as a consequence of the electrical stimulus, EBs were stimulated with increasing concentration of H_2O_2. These results are reported in figure 5, where ΔF is the difference between stimulated EB, either with electrical stimulation (ES) and H_2O_2, and control EB. Figure 5 shows that ROS production increased with H2O2 concentration. These results suggests that the ROS generation induced in electrical field-treated embryoid bodies was equivalent to the increase of ROS generation observed after 15 minutes of incubation with 1 nM H_2O_2. 4 day-old EBs and 8 day-old EBs show statistically different ROS increase after incubation with 10 nM H_2O_2.

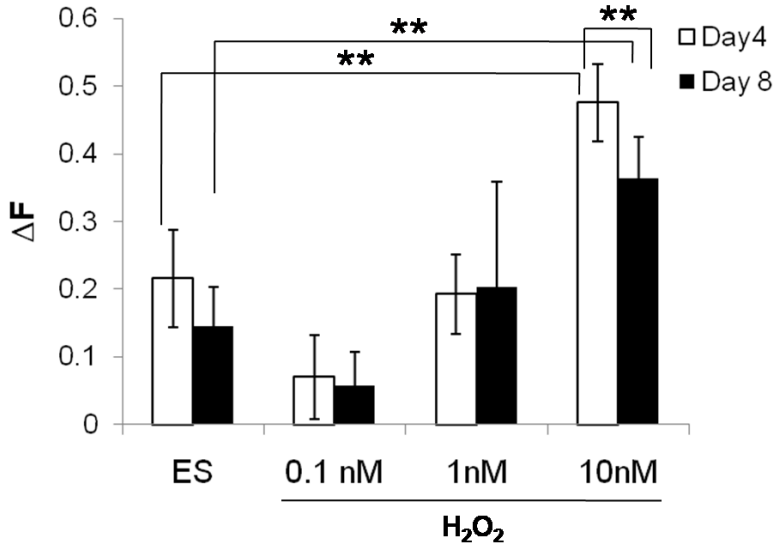

Figure 5. ROS generation on 4-day-old EB (open bars) and 8-day-old EBs (black bars) after electrical field (ES) and H_2O_2treatment. H_2O_2 treated EBs were incubated for 10 min with increasing concentrations of H_2O_2: 0.1 nM, 1 nM and 10 nM. About 4 EBs in each of three independent experiments were used for the determination of each data point. About 10 EBs in each of three independent experiments were used for the determination of each data point.** $p<0.01$

Cardiac differentiation

To evaluate whether electrical field and intracellular ROS expression affect cardiac differentiation of hESC, 4- and 8-day-old EBs were electrically stimulated, plated 3 days later and analyzed at 19 days. After 3 days in adhesion culture, embryoid bodies started to beat spontaneously. The percentage of beating EBs is summarized in Figure 6A. We observed that more EBs exhibited spontaneous beating in electrically stimulated EBs. Furthermore, the expression of the cardiac marker, cardiac Troponin T, was observed in electrically stimulated and beating EBs (Fig. 6B-D) and the sarcomeric organization of such marker was verified (Fig. 6C).

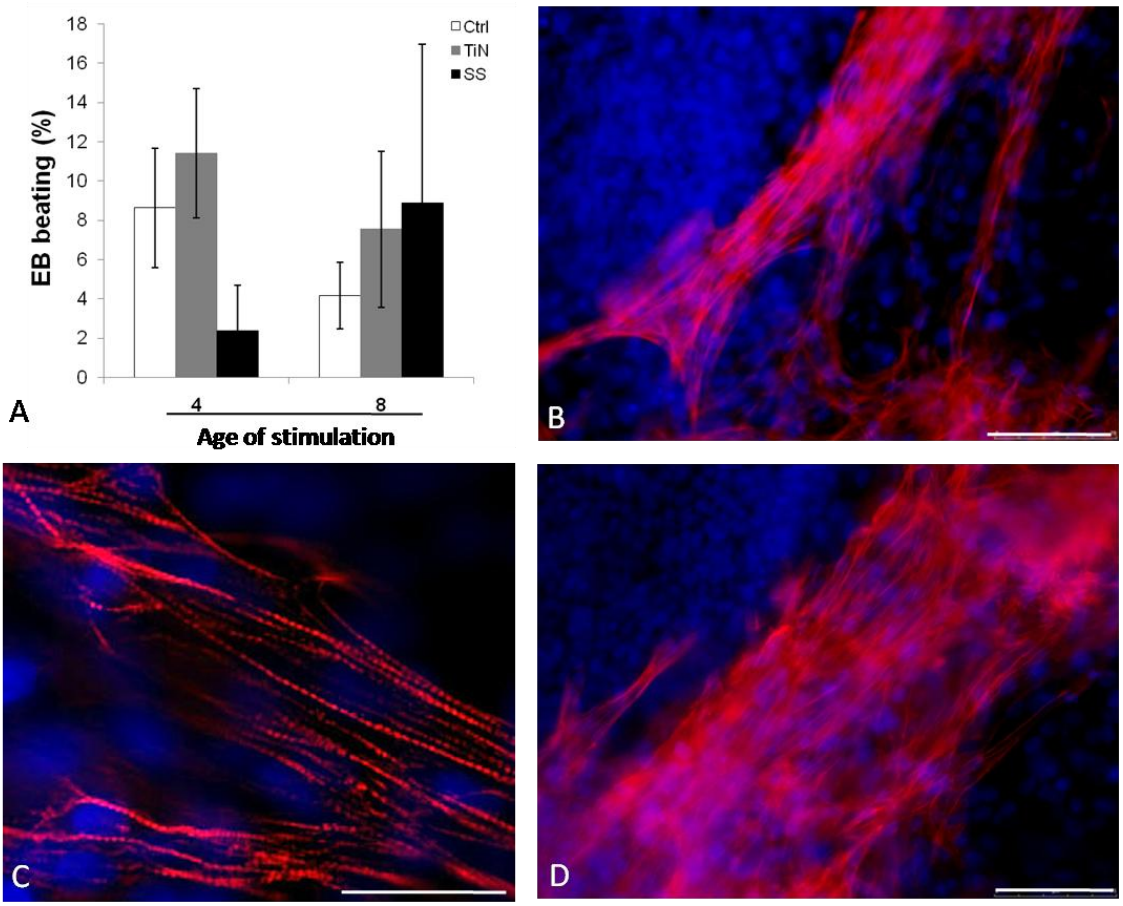

Figure 6. Effect of electrical stimulation on cardiomyocyte differentiation. A: The percentage of beating EBs was evaluated in 4- and 8-days-old EBs, either electrically stimulated with titanium nitride (TiN) and stainless steel (SS) electrodes or not treated (Ctrl). The evaluation was done in 19 days-old EBs. B-D: Cardiac Troponin T immunostaining of electrical field-treated representative EB. Nuclei were counterstained with DAPI. Scale bars: 75 μm in B and D, 30 μm in C.

D.4 Discussion

The existence of endogenous electric fields during the embryonic development as well as certain effects of exogenous fields for different cell types have been already reported in several studies [10, 51]. However the interpretation of the cellular response to such fields is complicated by inadequate characterization of the systems used for stimulation. Uncertainties about the type and magnitude of field hinder the interpretation of the biophysical and biochemical mechanisms implicated in the considered biological system. Here we report differences in intracellular ROS generation solely due to choice of electrode material. In biological applications,

material selection for electrodes is a complex issue. The ideal material for electrode fabrication must be biocompatible, have stable characteristics during the stimulation and should not alter the chemical and biological properties of the medium. The effects of electrical stimulation are strongly dependent on the electrode geometry and material properties. The charge-transfer at the electrode-electrolyte interface happens through three mechanisms: (i) non-faradaic charging/discharging of the electrochemical double layer, (ii) reversible faradaic reactions, and (iii) non-reversible faradaic reactions [45, 52]. Electrochemical impedance spectroscopy (EIS) gives information about the relative presence of each mechanism, determining the value of capacitance and resistance to reactions for each specific electrode. This method was used here to characterize electrodes in stainless steel, titanium and titanium nitride. The data shows mainly differences in polarization resistance (Rp) value, which is much lower for stainless steel. In agreement with this result, the current-time plot for stainless steel plateaus at a value of 0.4 mA after ~20 ms by the presence of reactions on its surface during the stimulation. For titanium and titanium nitride we have instead an initial increasing of the current profile followed by a rapid decrease up to a value close to zero due to the polarization of the medium and the shielding of charges on the electrode. Previous studies have shown the correlation between electrical stimulation and ROS expression in different kind of cells, including murine embryonic stem cells [24, 53]. Here we show that the applied electric field lead to generation of intracellular ROS in human embryonic stem cells. The EIS results were useful to evaluate the correlation between duration of a stimulation and ROS expression on human EBs. In agreement with these results, the use of stainless steel electrodes in addition to lengthening the stimulation duration to 90 s enhanced the intracellular ROS expression. Due to the enhanced benefits of lengthened stimuli, it may be more useful when optimizing electric field stimulus parameters to move to current-controlled systems (as opposed to the voltage controlled-system presented here). Developing such stimulator systems and corresponding bioreactors are part of our ongoing work.

Since mouse embryonic stem cells have shown a reduction of the intracellular ROS production during development [35], it was interesting to check the response of

human embryonic stem cells at different time points. When we stimulated human EBs of different stages of development (4- and 8-day-old), we observed a maximum expression of ROS for 4 day-old EBs. The decay of ROS generation may be likely due to down regulation of NADPH oxidase activity during the development, as already shown for mESC [35]. The active role of NADPH oxidase in differentiation, already shown in other cell type [44], may suggest the higher predisposition of the hESC to a cardiac differentiation and a more efficacious electrical stimulation at earlier stage of development. The ROS increase after electrical stimulation, was correlated to a stimulation with about 1nM of H_2O_2, indicating a possible correlation between electrical stimulation and ROS signaling pathway, involved in cardiac differentiation of hESC.

Even if the role of ROS in the cardiac lineage differentiation in human embryonic stem cell has still not been investigated, these results seems promising in the final propose of enhancing the number of cardiac-differentiated human embryonic stem cell through electric stimulation.

D.5 References

1. Lovell, M.J. and A. Mathur, *The role of stem cells for treatment of cardiovascular disease.* Cell Proliferation, 2004. **37**(1): p. 67-87.
2. Fukuda, K. and S. Yuasa, *Stem Cells as a Source of Regenerative Cardiomyocytes.* Circ Res, 2006. **98**(8): p. 1002-1013.
3. Murry, C.E. and G. Keller, *Differentiation of embryonic stem cells to clinically relevant populations: Lessons from embryonic development.* Cell, 2008. **132**(4): p. 661-680.
4. *American Heart Association 2008 Update At-a-Glance.* Heart Disease and Stroke Statistics, 2008.
5. Chen, K., L. Wu, and Z.Z. Wang, *Extrinsic Regulation of Cardiomyocyte Differentiation of Embryonic Stem Cells.* Journal of Cellular Biochemistry, 2008. **104**: p. 119-128.
6. Passier, R. and C. Mummery, *Cardiomyocyte differentiation from embryonic and adult stem cells.* Current Opinion in Biotechnology Tissue and cell engineering/Biochemical engineering, 2005. **16**(5): p. 498-502.
7. Heng, B.C., et al., *An overview and synopsis of techniques for directing stem cell differentiation in vitro, Cell and Tissue Research.* Cell Tissue Res, 2004. **315**(3): p. 291-303.
8. Hong Wei, O.J., Jinliang Li, Yelena S. Tarasova, Kenneth R. Boheler, *Embryonic stem cells and cardiomyocyte differentiation: phenotypic and molecular analyses.* J. Cell. Mol. Med., 2005. **9**(4): p. 804-817.
9. Heng, B.C., et al., *Strategies for directing the differentiation of stem cells into the cardiomyogenic lineage in vitro.* Cardiovascular Research, 2004. **62**(1): p. 34-42.

10. Jaffe, L.F. and R. Nuccitelli, *Electrical Controls of Development.* Annual Review of Biophysics and Bioengineering, 1977. **6**(1): p. 445-476.
11. Robinson, K., *The responses of cells to electrical fields: a review.* J. Cell Biol., 1985. **101**(6): p. 2023-2027.
12. Joshua Rutenberg, S.-M.C.M.L., *Early embryonic expression of ion channels and pumps in chick and <I>Xenopus</I> development.* Developmental Dynamics, 2002. **225**(4): p. 469-484.
13. Zhao, M., et al., *Membrane lipids, EGF receptors, and intracellular signals colocalize and are polarized in epithelial cells moving directionally in a physiological electric field.* FASEB J., 2002. **16**(8): p. 857-859.
14. McCaig, C.D., et al., *Controlling Cell Behavior Electrically: Current Views and Future Potential.* Physiol. Rev., 2005. **85**(3): p. 943-978.
15. Pullar, C.E. and R.R. Isseroff, *Cyclic AMP mediates keratinocyte directional migration in an electric field.* J Cell Sci, 2005. **118**(9): p. 2023-2034.
16. Song, B., et al., *Electrical cues regulate the orientation and frequency of cell division and the rate of wound healing invivo.* PNAS, 2002. **99**(21): p. 13577-13582.
17. Richard Nuccitelli, *Endogenous ionic currents and DC electric fields in multicellular animal tissues.* Bioelectromagnetics, 1992. **13**(S1): p. 147-157.
18. Lodish, Berk, and Matsudaira, *Molecular Cell Biology.* fifth ed. 2003, New York: W.H Freeman and Company.
19. Kenneth R. Robinson, M.A.M., *Left/right, up/down: The role of endogenous electrical fields as directional signals in development, repair and invasion.* BioEssays, 2003. **25**(8): p. 759-766.
20. Zhao, M., J.V. Forrester, and C.D. McCaig, *A small, physiological electric field orients cell division.* PNAS, 1999. **96**(9): p. 4942-4946.
21. Mycielska, M.E. and M.B.A. Djamgoz, *Cellular mechanisms of direct-current electric field effects: galvanotaxis and metastatic disease.* J Cell Sci, 2004. **117**(9): p. 1631-1639.
22. Donna R. Trollinger, R.R.I.R.N., *Calcium channel blockers inhibit galvanotaxis in human keratinocytes.* Journal of Cellular Physiology, 2002. **193**(1): p. 1-9.
23. Djamgoz, M.B.A., et al., *Directional movement of rat prostate cancer cells in direct-current electric field: involvement of voltagegated Na+ channel activity.* J Cell Sci, 2001. **114**(14): p. 2697-2705.
24. Sauer, H., et al., *Effects of Electrical Fields on Cardiomyocyte Differentiation of Embryonic Stem Cells.* Journal of Cellular Biochemistry 1999. **75**: p. 710-723.
25. Sauer, H., et al., *Redox control of angiogenic factors and CD31-positive vessel-like structures in mouse embryonic stem cells after direct current electrical field stimulation.* Experimental Cell Research, 2005. **304**(2): p. 380-390.
26. Zhao, M., et al., *Electrical stimulation directly induces pre-angiogenic responses in vascular endothelial cells by signaling through VEGF receptors.* J Cell Sci, 2004. **117**(3): p. 397-405.
27. Mie, M., et al., *Induction of neural differentiation by electrically stimulated gene expression of NeuroD2.* Journal of Biotechnology, 2003. **100**(3): p. 231-238.
28. Walter Hong-Shong Chang, et al., *Effect of pulse-burst electromagnetic field stimulation on osteoblast cell activities.* Bioelectromagnetics, 2004. **25**(6): p. 457-465.
29. C. H. Lohmann, et al., *Pulsed electromagnetic field stimulation of MG63 osteoblast-like cells affects differentiation and local factor production.* Journal of Orthopaedic Research, 2000. **18**(4): p. 637-646.
30. Sauer, H. and M. Wartenberg, *Reactive Oxygen Species as Signaling Molecules in Cardiovascular Differentiation of Embryonic Stem Cells and Tumor-Induced Angiogenesis.* Antioxidants & Redox Signaling, 2005. **7**(11-12): p. 1423-1434.
31. Puceat, M., et al., *A Dual Role of the GTPase Rac in Cardiac Differentiation of Stem Cells.* Mol. Biol. Cell, 2003. **14**(7): p. 2781-2792.
32. Puceat, M., *Role of Rac-GTPase and Reactive Oxygen Species in Cardiac Differentiation of Stem Cells.* Antioxidants & Redox Signaling, 2005. **7**(11-12): p. 1435-1439.

33. Rhee, S.G., *Redox signaling: hydrogen peroxide as intracellular messenger.* Experimental and Molecular Medicine, 1999. **31**(2): p. 53-59.
34. Sun, Y. and L.W. Oberley, *Redox regulation of transcriptional activators.* Free Radical Biology and Medicine, 1996. **21**(3): p. 335-348.
35. Sauer, H., et al., *Role of reactive oxygen species and phosphatidylinositol 3-kinase in cardiomyocyte differentiation of embryonic stem cells.* FEBS Letters, 2000. **476**(3): p. 218-223.
36. Shah, A.M. and H. Sauer, *Transmitting biological information using oxygen: Reactive oxygen species as signalling molecules in cardiovascular pathophysiology.* Cardiovascular Research, 2006. **71**(2): p. 191-194.
37. Sachinidis, A., et al., *Cardiac specific differentiation of mouse embryonic stem cells.* Cardiovasc Res, 2003. **58**: p. 278-291.
38. Sauer, H., et al., *Involvement of reactive oxygen species in cardiotrophin-1-induced proliferation of cardiomyocytes differentiated from murine embryonic stem cells.* Exp Cell Res, 2004. **294**: p. 313-324.
39. Schmelter, M., et al., *Embryonic stem cells utilize reactive oxygen species as transducers of mechanical strain-induced cardiovascular differentiation.* Faseb J., 2006. **20**: p. 1182-1184.
40. Sorescu, D. and K.K. Griendling, *Reactive oxygen species, mitochondria, and NAD(P)H oxidases in the development and progression of heart failure.* . Congest Heart Fail, 2002(8): p. 132-140.
41. Heng, B.C., et al., *Strategies for directing the differentiation of stem cells into the cardiomyogenic lineage in vitro.* Cardiovasc Res, 2004. **62**: p. 34-42.
42. Schmelter, M., et al., *Embryonic stem cells utilize reactive oxygen species as transducers of mechanical strain-induced cardiovascular differentiation.* FASEB J., 2006. **20**(8): p. 1182-1184.
43. LEV, S., I. KEHAT, and L. GEPSTEIN, *Differentiation Pathways in Human Embryonic Stem Cell-Derived Cardiomyocytes.* Ann NY Acad Sci, 2005. **1047**(1): p. 50-65.
44. Li, J., et al., *The NADPH Oxidase NOX4 Drives Cardiac Differentiation: Role in Regulating Cardiac Transcription Factors and MAP Kinase Activation.* Mol. Biol. Cell, 2006: p. E05-06-0532.
45. Merrill, D.R., M. Bikson, and J.G.R. Jefferys, *Electrical stimulation of excitable tissue: design of efficacious and safe protocols.* Journal of Neuroscience Methods, 2005. **141**(2): p. 171-198.
46. Norlin, A., J. Pan, and C. Leygraf, *Investigation of interfacial capacitance of Pt, Ti and TiN coated electrodes by electrochemical impedance spectroscopy.* Biomolecular Engineering, 2002. **19**(2-6): p. 67-71.
47. Cannizzaro, C., et al., *Practical Aspects of Cardiac Tissue Engineering With Electrical Stimulation*, in *Tissue Engineering*. 2007. p. 291-307.
48. Tandon, N., et al., *Electrical stimulation systems for cardiac tissue engineering.* Nat. Protocols, 2009. **4**(2): p. 155-173.
49. Setsukinai, K., et al., *Development of Novel Fluorescence Probes That Can Reliably Detect Reactive Oxygen Species and Distinguish Specific Species.* The Journal of Biological Chemistry, 2003. **278**(5): p. 3170-3175.
50. Mummery, C., et al., *Cardiomyocyte differentiation of mouse and human embryonic stem cells.* Journal of Anatomy, 2002. **200**(3): p. 233-242.
51. Nuccitelli, R., *Endogenous electric fields in embryos during development, regeneration and wound healing.* Radiat Prot Dosimetry, 2003. **106**(4): p. 375-383.
52. Cannizzaro, C., et al., *Practical aspects of cardiac tissue engineering with electrical stimulation.* Methods in molecular medicine, 2006.
53. Wartenberg, M., J. Hescheler, and H. Sauer, *Electrical fields enhance growth of cancer spheroids by reactive oxygen species and intracellular Ca2+.* Am J Physiol Regul Integr Comp Physiol, 1997. **272**(5): p. R1677-1683.

Appendix E

"Financing for research on embryonic stem cells: The situation in Italy and its origins"

3rd Italian National Congress of the Group of Italian Researchers on Embryonic Stem Cells (IES Group)

Rome, 1st July 2008

Report by E. Serena, E. Cimetta and M. Zagallo (University of Padua)

Published on:

"Notizie di Politeia. Rivista di Etica e Scelte Pubbliche"

Vol. 91/Anno XXIV, 2008, pp. 110-113

"*Opened up to this vast and most excellent science, of which my work is mere the beginning, ways and means by which other minds more acute than mine will explore in remotest corners*"

These are the words of Italian astronomer and physicist Galileo Galilei, who was sentenced to indefinite prison in San Macuto Palace, on which site the Group of Italian Researchers on Embryonic Stem Cells (IES Group) organized its 3rd National Congress on "Research on Embryonic Stem Cells" (1 July 2008). These scientists strongly believe in the potential of human embryonic stem cells (hESCs), which are already the main focus of their research. A parallel thus emerges, as innovative and revolutionary scientific issues are discussed once again in this place.

In the magnificent structure of the Refectory Room of the Chamber of Deputies, IES scientists presented their research and discussed ethical aspects of its implications.

The elegant Refectory Room of the Deputy Chamber at San Macuto Palace. In this site Galileo Galilei (1564-1642) was tried by the Inquisition for his advocacy of Copernican theory, which held that the Earth revolves around the sun. Since 1974 the Palace is an official site of the Italian Chamber of Deputies.

The main aim of the Congress was to highlight the need for an immediate and tangible opening to research on hESC in Italy. In fact, even while it is legally allowed to work on established hESC lines, it is prohibited to derive new lines from embryos; and even more limiting is the lack of funding from the Government. Consequently, a first and most crucial step is to improve the dialogue between science and both society and politics, in order to make known the potential, in terms of therapeutic outcomes, of hESC research. Opening speakers of the congress were Elena Cattaneo, pioneer of hESC research in Italy, and Andrew Smith, project manager from ESTOOLS. Cattaneo's speech highlighted the main aims of the meeting, to identify the role of the IES group and to inform the audience on the research carried by its members. Since 2002, the interest of the international scientific community in hESCs has strongly increased, shown by the augmented financial investment and by the number of participants at specific conferences. In this scenario, IES scientists must create a solid network in order to facilitate

financial and practical aspects of their research (training of personnel, development of protocols, reporting of results, etc) and to sensitize the public towards the relevant ethical aspects of their research. In underlining the tremendous potential of hESCs as tools for studying human physiology, disease and new therapies development, she stated that IES researchers do not exclusively work on embryonic but also believe in the potential of adult stem cells. Prof. Cattaneo focused the attention on the nr.1 scientific discovery of 2007 (according to The Times): induced pluripotent stem cells[1] now receiving much interest by some Italian laboratories. This discovery, overcoming the ethical issues involving the use of embryos, would have never been possible without preceding research on hESCs.

Last but not least she expounded the chronic problem of fund-raising in Italy and Europe, and of the long and laborious iter leading to a project approval by the EU.

Taking a look outside academia, Andrew Smith described how the ESTOOLS consortium endorses lab research but at the same time tries to make it accessible to the public. Rescaled on an European level, with their 21 labs in 10 countries, the main targets of ESTOOLS resemble those listed by Cattaneo with regard to IES. In particular, ESTOOLS focuses on four different areas of activity: research and technology development (integration of funding and projects), dissemination of results (website, international public symposia), training (fellowships, lab staff exchanges, videos of lab techniques, and media training) and outreach (newsletters, trans-Europe telescope, ethic workshops). Most importantly, ESTOOLS promotes the development of integrated projects involving both academics and industrial partners: successful scientists should thus possess the skills of a good researcher and a good manager, be able to communicate with the public, be open minded and flexible.

After the welcome note of Carlo Flamigni, chairman of the session, Marisa Jaconi and Tiziano Barberi, top Italian scientists working on hESC outside Italy presented the results of their research on cardiac and skeletal muscle, respectively. Jaconi (University of Geneve, Switzerland), in particular, is working to develop animal free protocols and GMP-grade cell lines and to understand and control hES differentiation process for possible clinical applications. She also pointed put the

pros and cons of iPS: no embryos are involved and no immune response is elicited but, on the contrary, a strong teratogenic effect would be possible due to their derivation through viral infection. Barberi (Beckman Research Institute of the City of Hope, Duarte, California) works on mesodermal progenitors isolation from pluripotent stem cells; he reported his latest achievements that follow his previous results on skeletal muscle[3]. The major efforts of his lab are directed on the development of more solid and reproducible protocols in order to take a step further towards clinical applications in general.

E.1 Research activities inside the IES

Research on hESC is applied in three different directions: studying embryonic development, controlling the differentiation in specific lineages, and clinical applications (e.g. drug screening and therapy development). All these research themes are equally important and tightly related, each of them needing the knowledge derived from the others to proceed; the IES group has competencies to over them all.

IES new members

During the last year, four more research labs (Elvassore, Bianco, Gambari, Mantovani) joined the IES ranks and thus had the chance to present their projects to the audience and to the other members. Nicola Elvassore, Chemical Engineer from Padova University, supported the idea of coupling engineering and biotechnology skills to develop technologies serving biology. His laboratory already established hESC culture, and is currently developing devices (e.g. substrates, micro and macro-scaled bioreactors, ..) for the control of the culture microenvironment and thus of the cellular differentiation process. Bianco and Gambari's labs are studying two specific genetic diseases: McCune-Albright syndrome and β-Thalassemia respectively. In particular, Riminucci (Bianco's lab) explained that such syndrome is caused by a mutation occurring in embryonic cells and Gambari underlined the importance of studying the activation of fetal γ-globin in thalassemic patients. For these reasons, they now both aim at using hESC for developing therapeutic strategies as they represent the closest in vitro human model.

Mantovani, studying the transcription factors regulating stemness, recognizes how this research would greatly benefit from the use of hESC.

IES senior members

Cardiac differentiation is the leading theme for research by Condorelli and Cerbai. The first aims at reproducing the protocols for cardiomyocytes derivation from hESCs developed by Keller[2] and showed interest in adopting iPS cells cultures. The second is studying cardiac functionality and physiology in diseased heart in vitro, in vivo and in silico, using hESC as a cellular model. The teams led by Brevini and Oliviero focus on deriving new cell lines not originating from human embryos and thus overcoming the possible ethical issues. Brevini's group works on human parthenogenetic stem cell, which possess all of the main features of hESC but their potential for clinical application has yet to be tested. Riding the clamor of iPS cells, Oliviero succeeded in inducing iPS and obtaining a 100-fold increased yield by adding myc transcription factor to the original Yamanaka recipe (Takahashi et al., Cell, 2007). Another important application of hESC is gene therapy; the Sangiuolo group works on this application with regards to spinal muscular atrophy and cystic fibrosis. Elena Cattaneo and her prominent team working on neural differentiation have derived a population of neural crest precursors from hESC and are currently testing its differentiation potential, in vitro and in vivo, with a view to possible clinical application. Italian scientists here gathered, unequivocally demonstrated how their research hold an enormous social relevance and all expressed hope in the future possibilities deriving from their integration within the IES and in the common efforts in remodeling the Italian scenario.

E.2 Round table discussion: financing research on hESC

Why use embryos and why finance hESC-based research? These two major issues emerged during the meeting and the final discussion. In the near future there may no longer be the need for to discuss the rightness of using embryos for progressing science and research, said Neri, followed by Corbellini who underlined that it would

be desirable that prejudices should not hinder successful research. In addition, besides the lack of funding for research in general and on hESCs in particular, it is clear that Italy needs deeply to reform its financing mechanisms. Even Senator Ignazio Marino, Deputy at the Italian Parliament and invited participant to the meeting, expressed his opinion firmly in these terms. It is unfortunately clear that government does not recognize science as crucial for the future of the country's economy. Mindful of his past experience as a scientist in the US, Senator Marino affirmed how Italy should not pose any ideological barrier to scientific research and, most important, should adopt absolutely new project-evaluation criteria. To date, only 10% of the research investments are allocated through peer review; the remaining 90% through unclear top-down methods. A reform of the entire system must thus be done, basing the entire distribution of funding on the mechanism of peer review in order to enhance meritocracy and transparency in the selection of projects. Barberi, active participant in the discussion, finally stated that there's no need for further speculation on the validity of peer review as it must be the sole and only method for a meritocratic evaluation of research projects. With a favourable legislative and financial environment supporting all areas of human embryonic stem cell research, the future promises to be very exciting for scientists interested in this field, and crucial for progress in clinical applications.

E.3 References

1. Takahashi K, Tanabe K, Ohnuki M, Narita M, Ichisaka T, Tomoda K, Yamanaka S. "Induction of pluripotent stem cells from adult human fibroblasts by defined factors". Cell. 2007 Nov 30;131(5):861-72.

2. Barberi T, Bradbury M, Dincer Z, Panagiotakos G, Socci ND, Studer L. "Derivation of engraftable skeletal myoblasts from human embryonic stem cells". Nat Med. 2007 May;13(5):642-8.

3. Yang L, Soonpaa MH, Adler ED, Roepke TK, Kattman SJ, Kennedy M, Henckaerts E, Bonham K, Abbott GW, Linden RM, Field LJ, Keller GM. "Human cardiovascular progenitor cells develop from a KDR+ embryonic-stem-cell-derived population". Nature. 2008 May 22;453(7194):524-8.

Ringraziamenti

3 anni "improvvisamente" materializzati in una tesi, completa, impaginata, stampata…incredibile!
Incredibile perché sembra sempre tutto difficile ed in salita, ed invece un po' alla volta si raggiunge il cucuzzolo e se ne gode il panorama. Ed è subito una sensazione di pienezza, soddisfazione felicità; pronti a ripartire!
Grazie di cuore a Nicola, per aver sempre creduto in me (più di me stessa??), per avermi insegnato a fare ricerca, per aver fatto chiarezza mille volte nei miei pensieri auto-incasinanti, per tutti gli imput a ripartire, per lo scale-up delle mie conoscenze e possibilità ;-) e per il suo costante lavorare "last-second", che ha nettamente migliorato il mio self-control. Grazie a Gordana, per la magnifica opportunità offertami, per la chiarezza scientifica che ha dei progetti e dei risultati e la comprensione e umanità che ha dimostrato nei miei momenti di sconforto.
BioERA! Mi guardo spesso attorno, a volte mi lamento perché non sono abbastanza bio, conosco poco di molecolare!!, ma tornando indietro rifarei le stesse scelte e continuerò a il lavorare, perché altri bio, ing e scienziati dei materiali abbiano la mia stessa possibilità. Grazia ad Elisa, che in questi anni di "simbiosi" mi ha sempre spronato ad andare avanti con il suo enorme entusiasmo per le celluline!, grazie anche per i momenti di incomprensione, dai quali ho imparato più che da una risata. Maraina! Una certezza, c'è sempre una risposta alle mie domande! Grazia a Silvia, F!..no non intendo formattare! La prima bio con cui ho condiviso questo viaggio, tante chiacchiere e condivisione e quante risate in queste ultime settimane??????
Un grazie particolare va ai laureandi che hanno avuto la pazienza di sopportare la mia inesperienza e senza i quali questa tesi sarebbe sicuramente meno bella! Grazie ad Elena, Susi, Andrea!
Un grazie al gruppo embryo (Monica, so sempre che nel tuo quaderno troverò una risposta, grazie dottoressissima), a Camilla per la determinazione e sicurezza che sa trasmettere e in generale a tutto il lab! GRAZIE!

Un grazie enorme, gigante, infinito alla mia famiglia!! Ai miei genitori che mi hanno insegnato la coerenza alle scelte prese, il rispetto per il prossimo ed a sapersela cavare con le proprie forze. Senza il vostro aiuto non avrei potuto fare questo dottorato e l'esperienza a NY. Grazie alle mie sorelle per i consigli e le tante risate e a Paolo e Michel che le

rendono felici [mi raccomando eh!]!! Grazie di cuore a Claudio, per il suo costante supporto e incoraggiamento, per la pazienza nei miei attacchi di angoscia e gli orari non proprio ortodossi! E, relativamente alla tesi, le referenze avrebbero qualche errore in più senza il suo aiuto!

Alle mie amiche grazie perché mi fate sempre sentire a casa e perché vi adattate sempre ai miei spostamenti pd-monte! Grazie a Lisa, amica sincera e sempre presente, John e il bagigetto!!, che mi danno ogni volta una ventata di amicizia con la A maiuscola e integrità. Grazie ad Augusta, che manca tantissimo a tutti e non vedo l'ora ritorni…ritornerai vero??? Beh, spero intanto di venire io a trovarti prima!! Grazie a Marisa e Giada, con le quali mi sento sempre tanto puffa, ma non rinuncerei mai alla vs compagnia, risate e chiacchierate! Grazie! Ad Elisa, sono contenta di averti "ritrovata" adesso posso dire che la tua tazza ha fatto tutto il suo dovere!
Grazie a Donatella e Giuly, mi fate proprio sentire in famiglia!!! GRAZIE!!
Grazie agli amici di SanBe!! Siete veramente unici, un gruppo aperto (anche alle campagnole!!hehe) e coinvolgente. Grazie per aver allietato questi tre anni!! In particolare grazie al mitico ed unico Checco! Per le grasse risate, le cene a postazioni fissate!, il tuo altruismo sconvolgente e l'accoglienza sempre festosa! Ad Albe e Stefy per le mille proposte alternative e l'entusiasmo nel fare le cose. A Flevour che ha sempre un pensiero attento nel momento giusto (e Checco) per "I miss a miss", mi ha fatto moltissima compagnia a NY. A Maria Paola ed Enri, mitici, non posso aggiungere altro! Ad Ila, Giulia, Lidya, Alessandra, Cristina, che risate!! Grazie!

Grazie a Michy e Samchy!!! La ns casetta era proprio un disastro, ma al tempo stesso stupenda e piena di calore familiare. GRAZIE! Grazie per il sostegno nei momenti difficili e le lunghissime chiacchierate sul mondo! Grazie ad Anna, per la sua dolcezza e determinazione, ad Erika, per la sua encomiabile organizzazione e simpatia, ed a JC, senza di voi NY non avrebbe gli stessi ricordi ed emozioni! Grazie per l'aiuto, le grasse risate, le code da Grom, i viaggi, le mille cose esplorate assieme! Grazie a Nina, per le levatacce a orari impossibili e l'aver risolto ogni dubbio su NY!

…..insomma, grazie a tutti coloro che hanno contribuito alla buona riuscita di questa tesi, sia dal punto di vista scientifico che umano!!

Elena